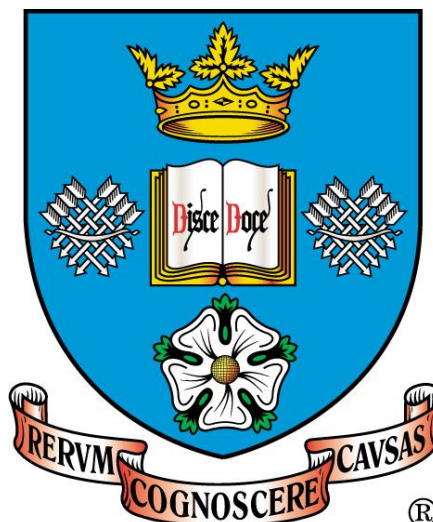


Cloning and Analysis of Thyroid Stimulating Hormone Antibodies



Salema R. M. Qowaider

Department Of Human Metabolism

(Academic Unit of Endocrinology)

Faculty of Medicine Dentistry & Health

University of Sheffield

Thesis submitted for the degree of Doctor

Philosophy

May 2014

Declaration

I hereby declare that this thesis has been composed by myself and has not been accepted in any previous application for a higher degree. The work reported in this thesis has been carried out by me and all sources of information have been specifically acknowledged by means of references.

Salema

May, 2014

DEDICATION

I would like to dedicate this thesis to:

The loving memory of my dear father, who has always been an inspiration to me through his loving care, patience and loving sacrifice and who is forever in my prayers.

My mother for her Love, Support and Encouragement

My husband for his Love, Support and Encouragement

My Lovely Daughters Hala and Sarah

Acknowledgments

I thank the Almighty God for giving me the opportunity and the strength to go through the course.

I give a massive thank you to my supervisor Dr Phil Watson who have given me many a wise word and have truly been brilliant supervisor. Thank you for all your time, effort and energy. It may be your job, but you do it very well.

I am indebted to my many colleagues who supported me: Jamila, Basma, Maha, Jehan, Najwa Muftah, Najwa, Muna and Mabrouka.

I would like to thank Dr Bouka for her constant help and advice.

I would like to thank Sue Justice and Janine for their help.

Finally I would like to thank the Libyan Arabian cultural bureau in London for funding of this work.

Summary

In this study we were able to synthesis a control TSAb monoclonal phage antibody construct and investigate binding of this and related reagents to the human TSH receptor. We are the first group to report stimulatory activity of a TSAb in scFv format, a finding that will contribute to our understanding of the mechanism of receptor stimulation by autoantibodies. We were able to demonstrate that the conformation of the native receptor rendered the target stimulatory epitope inaccessible to phage antibody constructs. This was an important finding that explained previous failed attempts, both reported and unreported, to enrich receptor antibodies by phage display. We went on to investigate this phenomenon at length and were finally able to resolve these difficulties by generating a novel cell line which expressed a receptor sub-domain (amino acids 1-260) anchored by a GPI motif. We were able to demonstrate that this receptor construct was able to specifically bind TSAb monoclonal antibody in phage form, a discovery that will open the door to future phage enrichment studies, and may contribute to the isolation of further examples of TSAb monoclonals from patient samples. Finally, we became the first research group to generate an anti-idiotypic monoclonal antibody that was able to bind and negate the antigen recognition site of the M22 TSAb antibody. This reagent should enable an entire series of novel experiments involving isolation and recovery of “M22-like” antibodies and corresponding B cells from patients samples. In addition this anti-idiotypic reagent should offer a novel selective strategy for the recovery of stimulatory antibodies from recombinant antibody libraries.

Abbreviations

α	Alpha
a.a	Amino acid
ADCC	Antibody dependent cell mediated cytotoxicity
AITD	Autoimmune thyroid disease
AH	Autoimmune hypothyroidism
Amp	Ampicillin
bp	Base pairs
β	Beta
BSA	Bovine serum albumin
Cam	Chloramphenicol
cAMP	Cyclic adenosine 3', 5'-monophosphate
cDNA	Complementary Deoxyribonucleic acid
Cfu	Colony forming unit
CGD	Chronic granulomatous disease
CHO	Chinese hamster ovary
cm	Centimetres
Da	Daltons
$^{\circ}\text{C}$	Degrees centigrade

DMSO	Dimethyl sulphoxide
DNA	Deoxyribonucleic acid
DNase	Deoxyribonuclease
dNTP	Deoxyribonucleoside triphosphate
EDTA	Ethylenediamine tetra-acetic acid
ELISA	Enzyme immune sorbent assay
Fab	Fragment of antigen binding
FACS	Fluorescence activated cell sorter
Fc	Fragment of crystallization
FCS	Fetal calf serum
FITC	Fluorescein isothiocyanate
FR	Framwork region
FSH	Follicle stimulating hormone
Fv	Variable fragment of immunoglobulin
g	Grams
γ	Gamma
GD	Graves' disease
GO	Graves' ophthalmopathy
GPI	Glycosylphosphatidyl inoisitol
×g	Gravitational accelaration

h	Hour
HBSS	Hanks' balanced salt solution
HLA	Human leukocyte antigen
HRP	Horseradish peroxidase
HT	Hashimoto's thyroiditis
IFN	Interferon
IgG	Immunoglobulin
IL	Interleukin
IMAC	Immobilised metal ion affinity chromatography
IPTG	Isopropyl β -D-thiogalactoside
κ	Kappa
kb	Kilobase pairs
Kan	Kanamycin
kDa	Kilodalton
λ	Lambda
L	Litres
LB	Luria-Bertani
LH	Luteinizing hormone
M	Molar
mAb	Monoclonal antibody

MCS	Multiple cloning site(s)
MHC	Major Histocompatibility
Min	Minute
µg	Microgram
µl	Microliter
ml	Millilitre
µM	Micromolar
Mm	Millimolar
MMLV-RT	Moloney murine leukaemia virus reverse transcriptase
mol	Moles
MOPS	4-morpholinepropanesulfonic acid
mRNA	Messenger RNA
MW	Molecular weight
NIS	Sodium iodide symporter
OD	Optical density
ORF	Open reading frame
<i>ori</i>	Origin(s) of DNA replication
PAGE	Polyacrylamide gel electrophoresis
PBS	Phosphate buffer saline
PCR	Polymerase chain reaction

PEG	Polyethylene glycol
Pfu	Plaque forming unit
RNA	Ribonucleic acid
RNAse	Ribonuclease
rpm	Revolutions per minute
Sec	Seconds
SDS	Sodium deodecyl sulphate
T3	Triiodothyronine
T4	Thyroxine
TAE	Tris-acetate EDTA buffer
TBAb	Thyroid blocking antibody
TBII	TSH binding inhibiting immunoglobulin
TBS	Tris buffer saline
TEMED	N,N,N', N'-tetramethylethylenediamine
TCR	T cell receptor
TFC	Thyroid follicular cell
TG	Thyroglobulin
TGAb	Thyroglobulin antibody
Th1	T helper type 1
Th2	T helper type 2

TNF	Tumour necrosis factor
TPO	Thyroid peroxidase
TPOAb	Thyroid peroxidase antibody
TSH	Thyroid stimulating hormones
TSHR	Thyroid stimulating hormones receptor
TSAb	Thyroid stimulating antibody
TSHRecd	Thyroid stimulating hormones extracellular domain
T6SS	Type 6 secretion system
Tween20	Polyoxyethylene sorbitan monolaurate
UV	Ultra violet (light)
V	Volts
VH	Variable heavy
VL	Variable light
v/v	Volume:volume ratio
w/v	Weight:volume ratio

Table of content

Declaration	ii
DEDICATION	Error! Bookmark not defined.
Acknowledgments.....	iv
Summary.....	v
Abbreviations	vi
Table of content.....	xii
1.1 Introduction to Autoimmune Thyroid Disease (AITD)	1
1.1.1 Autoimmune Hypothyroidism	3
1.1.2 Graves' Disease.....	3
1.1.3 Aetiology of Autoimmune Thyroid Disease.....	5
1.1.4 Genetic Risk Factors for AITD	7
1.1.5 Non-Genetic Factors.....	8
1.1.5.1 Infection and Molecular Mimicry	8
1.1.5.2 Toxins and Drugs.....	9
1.1.6 Immunopathogenesis of Graves' disease.....	11
1.1.6.1 Role of T lymphocytes.....	11
1.1.6.2 Role of B cells.....	12

1.1.6.3 Regulation of apoptosis	12
1.1.6.4 Current drugs targeting autoimmunity.....	12
1.1.7. Antigens in Autoimmune Thyroid Disease	15
1.1.7.1 Thyroglobulin.....	16
1.1.7.2 Thyroid Peroxidase	16
1.1.7.3 Thyrotropin Receptor	17
1.2 The Thyrotropin Receptor.....	17
1.2.1 TSHR Structure and Function.....	17
1.2.1.1 Thyrotropin.....	18
1.2.1.2 Structural Studies of TSHR	22
1.2.2 Recombinant Expression of TSHR.....	25
1.2.3 TSHR Autoantibodies - Discovery and Early Characterisation	27
1.2.4 TSHR Antibody Assays	28
1.2.4.1 Thyroid Stimulating Activity.....	28
1.2.4.2 Indirect TBI Assays	29
1.2.4.3 Direct Binding Assays.....	30
1.2.5 Animal Models and Isolation of TSHR Monoclonal Antibodies	31
1.2.5.1 Spontaneous Models	31
1.2.5.2 Induced Models	31
1.2.6 Cloning of TSHR Monoclonal Antibodies.....	33
1.3 Antibody Structure and Function.....	37

1.3.1 The Variable Domains of Immunoglobulin	38
1.3.2 Immunoglobulin Diversity	41
1.4 Antibody Engineering	43
1.4.1 Introduction.....	43
1.4.2 Combinatorial Antibody Library Technology	44
1.4.3 Phage Display antibody Techniques	45
1.4.4 Structure and Genetics of Filamentous Phage	47
1.4.5 Biopanning technique.....	49
1.4.6 Applications of Antibody Phage Display	49
1.4.7 Phage Display in the Analysis of Autoimmune Thyroid Disease.....	49
1.5 Hypothesis	52
1.6 Aims	52
CHAPTER 2.....	53
MATERIALS AND METHODS.....	53
2.1 Materials	54
2.1.1 Plasmids, Bacterial Strains, and Phage	54
2.1.2.1 pCOMB3.....	54
2.1.2.2 pAK100.....	56
2.1.2.3 pET21a	56
2.1.2.4 pcDNA 3.1	56

2.1.3 Bacterial Strains and Helper Phage	60
2.1.4 Media.....	61
2.1.5 Antibiotics.....	62
2.1.6 List of the cell lines and materials used in the tissue culture	63
2.1.7 Western blotting materials.....	64
2.1.8 General Laboratory Solutions and Reagents	66
2.2 Methods.....	68
2.2.1 RNA Extraction.....	68
2.2.2 Synthesis of cDNA.....	69
2.2.3 Polymerase Chain Reaction (PCR)	70
2.2.4 Agarose Gel Electrophoresis.....	71
2.2.5 Purification of DNA fragments and PCR Products	71
2.2.6 Phenol-Chloroform Extraction of DNA	71
2.2.7 Restriction Digest of DNA	71
2.2.8 Ligation of DNA.....	72
2.2.9 Heat Shock Transformation.....	73
2.2.10 Electroporation of XL-1 Blue.....	73
2.2.11 Preparation of Plasmid DNA (Miniprep Purification of DNA)	73
2.2.12 Isolation of Plasmid DNA by Midiprep Procedure	74
2.2.13 Chemically Competent Cell Preparation.....	74
2.2.14 Preparation of Bacterial Glycerol Stocks	75

2.2.15 Rescue of Library Displaying Phage	75
2.2.16 Preparation of Host Cells	75
2.2.17 Titration of Phage Library	75
2.2.18 High Level Expression of Recombinant Protein from pET21a	78
2.2.18.1 Pilot Scale Expression	78
2.2.18.2 Subcellular Fraction Solubilisation Test	78
2.2.18.3 Large Scale Expression of Recombinant Proteins	79
2.2.19 Solubilisation, Refolding and Purification of Inclusion Body Material.....	79
2.2.19.1 Inclusion Body Preparation.....	79
2.2.19.2 Solubilisation and Refolding of Inclusion Body Material	80
2.2.20 Preparation of bacterial cell extracts by using osmotic shock method.....	80
2.2.21 Protein purification.....	81
2.2.21.1 Purification of His-Tagged Recombinant Proteins by IMAC.....	81
2.2.21.2 Purification of IgG using Protein G columns	82
2.2.22 Protein Content Estimation (Bradford assay).....	82
2.2.23 SDS-PAGE.....	83
2.2.24 Western Blotting	84
2.2.25 Transfection of Mammalian Cells Using Lipofectamine	85
2.2.26 Development of Stably Transfected Mammalian Cell Lines	85
2.2.27 Flow Cytometry (FACS).....	86
2.2.28 Enzyme-linked Immunosorbent Assay (ELISA)	86

2.2.29 Cell ELISA	87
2.2.30 Preparation of Mammalian Cell Extracts	88
2.2.31 Triton X-114 Phase Partitioning of GPI-linked Proteins	88
2.2.32 TSHR Stimulation Bioassay	89
2.3.33 Immunisation	90
CHAPTER 3	91
3. Cloning of synthetic human monoclonal M22-scFv into phage display vector pAK100	92
3.1 Introduction	92
3.2 Methods and Results	93
3.2.1 Gene Synthesis of M22 VH and VL Genes	93
3.2.2 PCR Amplification of Heavy and Light Chain Genes	93
3.2.3 Assembly PCR and Cloning into PAK100 and PAK400	99
3.2.4 Expression of M22-scFv	101
3.2.5 SDS-PAGE and Western Blot Analysis of Bacterial Extracts	102
3.2.6 Purification of Histidine Tagged M22-scFv from Bacterial Periplasmic Extracts	107
3.2.7 FACS Analysis of M22-scFv	107
3.2.8 Stimulation of cAMP Production by M22 scFv	113
3.3 Discussion	115
CHAPTER 4	116
4.1 Introduction	117

4.2 Initial Phage Binding Experiments.....	119
4.2.1 Investigation of M22-scFv Phage.....	119
4.2.1.1 Methods.....	119
4.2.1.2 Results	120
4.2.2 Enrichment of Graves' Patient Antibody Library on BRAHMS Tubes	120
4.2.2.1 Methods.....	120
4.2.2.2 Results	121
4.2.3 Results Summary	125
4.3 M22 Fab Binding Experiments	128
4.3.1 Methods	130
4.3.1.1 Cloning of M22 Immunoglobulin Chains into pComb3.....	130
4.3.1.2 Expression and Purification of M22 Fab	131
4.3.1.3 FACS Analysis of M22 Fab.....	132
4.3.1.4 cAMP Bioassay of M22 Fab.....	133
4.3.1.5 Rescue of M22 Fab Phage and Binding Experiments.....	133
4.3.1.6 Panning of M22 Fab Phage	133
4.3.2 Results	134
4.3.2.1 M22 cloning into pComb3	134
4.3.2.2 Expression and Purification of M22 Fab	136
4.3.2.3 FACS Analysis of M22 Fab.....	137
4.3.2.4 cAMP Bioassay	137

4.3.2.5 M22 Fab Phage Binding	143
4.4 Construction of M22 Long Linker pComb3 Plasmid.....	145
4.4.1 Methods	145
4.4.1.1 Insertion of Peptide Linker into M22-pComb3 Construct	145
4.4.1.2 Generation of M22 Long Linker Phage	146
4.4.1.3 Phage Binding Experiments	146
4.4.2 Results	147
4.5 Triton X114 Extraction of TSHRecd-GPI	150
4.5.1 Methods	150
4.5.1.1 Detergent Extraction of TSHR Extracellular Domain.....	150
4.5.1.2 Binding of M22 Fab to Extracted TSHRecd-GPI	152
4.5.1.3 Binding of M22 Phage to Extracted TSHRecd-GPI	152
4.5.2 Results	153
4.5.2.1 Extraction of TSHRecd from GPI-95	153
4.5.2.2 Binding of M22 Fab to Extracted TSHRecd	153
4.5.2.3 Binding of M22 Phage to Extracted TSHRecd	154
4.6 Binding to GPI-95 Cells	158
4.6.1 Binding of M22 Fab to GPI95 Cells	158
4.6.1.1 Methods	158
4.6.2 Binding of M22 Phage to GPI95 Cells	159
4.6.2 Results	160

4.7 Discussion	162
CHAPTER 5	164
CONSTRUCTION OF CHO TSHR260-GPI	164
5.1 Introduction.....	165
5.2 Methods and Results.....	166
5.2.1 Cloning of TSHR 1-260 as a GPI Anchored Membrane Protein (TSHR260-GPI).....	166
5.2.2 Expression of TSHR 1-260 on CHO-K cells.....	168
5.2.2.1 Transient Expression of TSHR260 and Protein Analysis.....	168
5.2.2.2 SDS-PAGE and Western Blotting.....	169
5.2.2.3 Production of Stable CHO-K1 Transfectants	170
5.2.4 Binding of M22-Fab to CHO/TSHR260 Cells	177
5.2.5 M22 phage binding to CHO/TSHR260-GPI.....	180
5.3 Discussion	184
6.1 Introduction.....	187
6.2 Cloning of M22 scFv into pET21a (+)	188
6.3 Expression of M22 scFv	189
6.3.1 Preliminary E.coli Expression of M22-scFv Proteins	189
6.3.2 Large Scale Expression of M22 scFv Protein.....	190
6.3.3 Solubilisation of Aggregated M22 scFv Insoluble Fraction	196
6.3.4 Post- M22 scFv Solubilisation Buffer Exchange	196

6.3.5 Purification of M22 scFv Protein	196
6.4 Immunisation	199
6.5 Cloning of anti-M22-idiotype.....	199
6.5.1 Cloning of anti-M22-idiotype scFv.....	199
6.5.2 Sequence Analysis of Anti M22-scFv Library	207
6.5.3 Anti M22-scFv Library Rescue	207
6.5.4 Enrichment of anti-M22-scFv library on M22 scFv.....	207
6.5.5 M22 scFv ELISA of Selected Anti-idiotypic Phage Libraries	208
6.5.6 ELISA Analysis of Random M22 scFv Anti-Idiotypic Clones	209
6.6 Production of Anti M22 scFv protein	209
6.6.1 Cloning of anti M22 Idiotype scFv From pAK 100 to pAK 400	209
6.6.2 Expression of ID-43-scFv.....	214
6.6.3 SDS-PAGE and Western Blot Analysis of Bacterial Extracts.....	214
6.6.4 Purification of Histidine Tagged ID-43 from Bacterial Extracts	216
6.6.5 Confirmation of Binding Properties.....	216
6.6.6 Inhibitory Effect of ID-43 on M22-scFv Phage Binding to TSHR	218
6.7 Discussion	220
CHAPTER 7	222
DISCUSSION	222
7 Discussion	223

Future Work	230
8 References	231
References	Error! Bookmark not defined.

Table of Figures

Figure1.1 Pathogenesis of Graves' disease	4
Figure1.2 Immune pathogenesis of Grave's disease.	14
Figure1.3 Structure of the LRR domain of the thyrotropin receptor.	20
Figure1.4 Structure of Thyrotropin.	21
Figure1. 5: Structure of the FSHR in complex with FSH.	23
Figure1.6 Diagram showing the proposed model of TSH binding to the TSHR.	24
Figure1.7 The TSH Receptor-M22-Fab Complex Structure	36
Figure1.8 Schematic representations Structure of an immunoglobulin G (IgG)	39
Figure1.9 Schematic representation Structures of Fab, scFv and Fv fragments.	40
Figure1.10 Construction of V-region genes from gene segments.	42
Figure1.11 The structure of filamentous phage.	48
Figure1.12 Phage display cycle.	51
Figure2.1 Cloning sites of phage display vector pComb3.	55
Figure2.2 Map of pAK100 vector.	57
Figure2.3 Cloning regions of the pET21a T7 expression vector.	58
Figure2.4 Mammalian expression vector pcDNA3.	59

Figure2.5 Schematic Diagram for Panning Process.	77
Figure3.1 Sequence of Synthetic M22-VH Construct.	95
Figure3.2 Sequence of Synthetic M22-VLConstruct.	96
Figure3.3 PCR products of M22 VH and VL Regions and their Overlap Assembly.	98
Figure3.4 Schematic Diagram of Synthesis of M22-scFv Construct.	100
Figure3.5 Restriction digest screening of M22-scFv-pAK100.	103
Figure3.6 Purification of digested pAK400 and M22 scFv.	104
Figure3.7 SDS-PAGE analyses of unpurified M22 scFv periplasmic extracts.	105
Figure3.8 Western blot analysis of His-tagged purified M2 scFv periplasmic extracts.	106
Figure3.9 Elution of purified M22-scFv protein from Ni- column.	108
Figure3.11 JP09 Bioassay of TSHR Stimulation by Recombinant M22 scFv.	114
Figure 3.10.a FACS of the binding of 2c11 to CHO-K and GPI-95 cells.	109
Figure 3. 10.b FACS of the binding of A10 IgG to CHO-K and GPI-95 cells.	110
Figure 3.10.c FACS of the binding of Fab 8 to CHO-K and GPI-95 cells.	111
Figure 3.10.d FACS of the binding of Biotinylated M22-scFv to CHO-K and GPI-95 cells.	112

<u>Figure3.11 JP09 Bioassay of TSHR Stimulation by Recombinant M22 scFv.</u>	114
Figure4.1 Binding of M22-scFv to TSHR-coated BRAHMS tubes.	122
Figure 4.2 Enrichment of 127-scFv library to TSHR-coated BRAHMS tubes.	123
Figure 4.3 Enrichment of 127-scFv library to non-coated tubes.	124
Figure 4.4 Schematic diagram showing the components of phage antibody structures.	127
Figure 4. 5 Cloning sites of phage display vector pComb3.	129
Figure 4.6 PCR products of VL and VH M22 Fab.	135
Figure 4.7 Cloning of M22 VH and VL genes into pComb3.	135
Figure 4.8 Digestion and gel purification of M22-pComb3.	138
Figure 4.9 Partial sequence of the M22 VH region of construct M22-pComb3-His.	138
Figure 4.10: Non-reducing SDS-PAGE analysis of induced cultures of M22-pComb3-His.	139
Figure 4.1: SDS-PAGE analysis of purified M22 Fab.	140
Figure 4.12 Flow cytometric analysis of M22 Fab binding to TSHR expressed on GPI-95 cells.	141
Figure 4.13 JP09 Bioassay of TSHR Stimulation by Recombinant M22 scFv.	142
Figure 4.1: Binding of M22 Fab-phage to BRAHMS tubes.	144
Figure 4.15 Strategy for introducing a flexible peptide linker into M22 Fab construct.	148
Figure 4.16 Partial sequence of M22-pComb3-LL.	148
Figure 4.17 Binding of M22 LL-Fab-phage to BRAHMS tubes.	149

Figure 4.18: SDS PAGE for the GPI-anchored TSHRecd extracted by triton X-114	155
Figure 4.19 Western blot for the GPI-anchored TSHRecd extracted by triton X-114	155
Figure 4.20 Binding of M22 Fab to detergent extracts of TSHR.	156
Figure 4.21 Binding of M22 Fab-phage to detergent extracts of TSHR.	157
Figure 4.22 M22 Antibody Binding to GPI-95 cells.	160
Figure 4.23 Phage binding to GPI-95 cells.	161
Figure 5.1 PCR amplification of TSHR 1-260	173
Figure 5.2 Enzymatic digestions of the pCR3.1/GPI and the TSHR1-260 PCR products.	173
Figure 5.3 Sequencing data and translation for pTSHR260-GPI construct.	174
Figure 5.4 Western blots of TSHR260-GPI and GPI-95.	175
Figure 5.5 Flow Cytometric analysis of constructed TSHR-260.	176
Figure 5.8 Binding of Antibody Phage Constructs to TSHR260 Determined by Cell ELISA.	182
Figure 5.9 Binding of M22 phage antibody constructs to CHO/TSHR260 and GPI-95 cells determined by cell ELISA.	183
Figure 6.1: Cloning of M22 scFv into pET21a gel images	191
Figure 6.2: Flow diagram of preliminary fractionation of M22-scFv protein.	192
Figure 6.3 SDS PAGE for the induction of M22-scFv.	193

Figure 6.4	Fractionation protocol for large scale expression of M22-scFv protein.	
		194
Figure 6.5	SDS-PAGE for protein fractions of M22 scFv expression.	195
Figure 6.6	Elution of purified M22 scFv.	197
Figure 6.7	SDS-PAGE of Purified M22 scFv.	198
Figure 6.8	Western blot analysis of purified M22 scFv.	198
Figure 6.9	Post-immune mouse response to M22 scFv (first boost).	200
Figure 6.10	Post-immune mouse response to M22 scFv (final boost).	201
Figure 6.11	Total RNA of mouse spleen after immunisation with M22 scFv.	203
Figure 6.12	List of primers for cloning mouse scFv fragments.	204
Figure 6.13	Cloning of anti M22 idiotype scFv into pAK100 gel images.	205
Figure 6.14	Gel purification of digested scFv fragments of anti-M22 scFv.	206
Figure 6.15	Panning of anti-M22 scFv library to M22 scFv-coated wells.	211
Figure 6.16	Binding of selected anti-M22 idiotype scFv libraries to M22 scFv.	212
Figure 6.17	ELISA screening of random phage clones for binding to M22 scFv.	213
Figure 6.18	ELISA screening of random phage clones for binding to M22 scFv.	Error! Bookmark not defined.
Figure 6.19	SDS-PAGE analysis of purified ID-43 scFv protein.	215
Figure 6.20	Binding of anti-idiotypic mAb ID-43 to purified M22 scFv.	217
Figure 6.21	Inhibition of M22-scFv-phage binding by anti-idiotypic mAb ID-43.	219

CHAPTER 1

INTRODUCTION

1.1 Introduction to Autoimmune Thyroid Disease (AITD)

Autoimmune thyroid disease (AITD) is the most common form of organ-specific autoimmunity with a frequency in the population of 1-2% (Tunbridge, Evered et al. 1977). Historically, thyroid autoimmunity was the first human autoimmune disease to be characterised. Autoantibodies to thyroid specific antigens were observed in patients with Hashimoto's thyroiditis and hypothyroidism (Rose and Witebsky 1956). In the same year it was shown that the symptoms of Graves' disease (autoimmune hyperthyroidism) were caused by a long acting thyroid stimulator (LATS) in the patient serum (Adams and Purves 1956) and this was subsequently shown to be autoantibodies directed against the thyrotropin receptor (TSHR).

Autoimmune thyroid disease is a series of overlapping conditions including, Graves' disease (GD), Hashimoto's thyroiditis, postpartum thyroiditis (PPT), atrophic autoimmune hypothyroidism, and thyroid-associated ophthalmopathy. The conditions can be broadly classified as loss of thyroid function, hypothyroidism (the most common form), and excessive thyroid function, or autoimmune hyperthyroidism, also known as Graves' disease. The disease may shift from one form to another other as the course of the autoimmune process progresses (Swain 2005). Autoimmune hypothyroidism affects about 5 to 10% of women in middle age and older age group. In addition, many GD patients develop hypothyroidism either spontaneously after treatment with antithyroid drugs, or following radiotherapy or surgery (Rose, Bonita et al. 2002). The main feature of autoimmune thyroid disease is the development of autoantibodies to thyroglobulin (TG), thyroid peroxidase (TPO), and the TSHR (Weetman and McGregor 1984). The latter class of antibodies include a subclass that possesses bioactivity, acting as agonists, and rarely antagonists, of the thyrotropin receptor. These thyroid stimulatory antibodies represent the focus of this current study.

Table1. 1: Presentation of the main types of autoimmune thyroid diseases (AITD)

Clinical presentation	Volume of thyroid gland	Function of thyroid gland	Characteristics
Focal thyroiditis	Variable	Normal or subclinical hypothyroidism	Presence of TG-Ab and TPO-Ab May progress to overt hypothyroidism P+++
Hashimoto's thyroiditis	Nontender, firm goitre	Normal or hypothyroid	Presence of TG-Ab and TPO-Ab US: hypoechoic P+++
Atrophic thyroiditis (primary myxedema)	Atrophic	Hypothyroid	Presence of TG-Ab and TPO-Ab P+
Postpartum thyroiditis	Small	Transient hyperthyroid and/or hypothyroid	P± US: hypoechoic
Silent thyroiditis	Small	Transient hyperthyroid and/or hypothyroid	P+++ US: hypoechoic
Graves' disease	Variable	Hyperthyroid	Presence of TSAb Presence of TG-Ab and TPO-Ab Extrathyroidal manifestation P+++

P: prevalence; TG-Ab: Thyroglobulin antibody; TPO-Ab: thyroid peroxidase antibodies; TSAb

1.1.1 Autoimmune Hypothyroidism

Autoimmune hypothyroidism includes Hashimoto's thyroiditis (chronic autoimmune thyroiditis) and non-goitrous primary myxedema. The diagnosis of autoimmune hypothyroidism depends on both histochemical, and biochemical (thyroid hormone and TSH levels) abnormalities as well as the presence of high levels of circulating autoantibodies directed against TG, TPO and the TSHR. TPO and TG autoantibodies are present in the serum of more than 90% of autoimmune hypothyroidism patients. The most important mechanisms of thyroid damage are mediated by infiltrating lymphocytes and complement fixation by TPO and TG antibodies (Weetman and McGregor 1984).

1.1.2 Graves' Disease

Graves' disease is the most common cause of hyperthyroidism worldwide, with an incidence of 30 to 200 per 100,000. A diffuse bilateral goitre and eye signs such as proptosis characterise the disease. Approximately 90% of Graves' disease patients show some degree of Graves' ophthalmopathy (GO), and evidence suggests that the basis of this association is the presence of a cross-reactive antigen present in both sites, most probably the TSHR (Garrity and Bahn 2006; Franklyn and Boelaert 2012).

TSHR antibodies can be detected in almost all untreated Graves' disease patients. An important class of TSHR antibodies, thyroid stimulating antibodies (TSAb) mimic the action of TSH, activating the receptor, leading to thyroid hyperplasia, increased thyroid hormone production, and clinical thyrotoxicosis (Fig. 1.1) (Bartels 1941; Weetman and McGregor 1984; de Lloyd, Bursell et al. 2010). A distinct class of TSHR antibodies (TBAb) block binding of TSH to TSHR and can play a role in the pathophysiology of hypothyroidism. Assays are available for the different classes of TSHR antibodies. Radioligand assays based on labelled TSH measure IgG-mediated inhibition of TSH binding and are generally referred to as the TSH binding inhibiting immunoglobulin (TBII) assay. In common with other G-protein coupled receptors, TSHR stimulates the cAMP pathway when activated and TSAb activity is usually assayed by measurement of cAMP production by cultured thyrocytes or TSHR-expressing cells (Weetman and McGregor 1984; Ochi, Kajita et al. 2012).

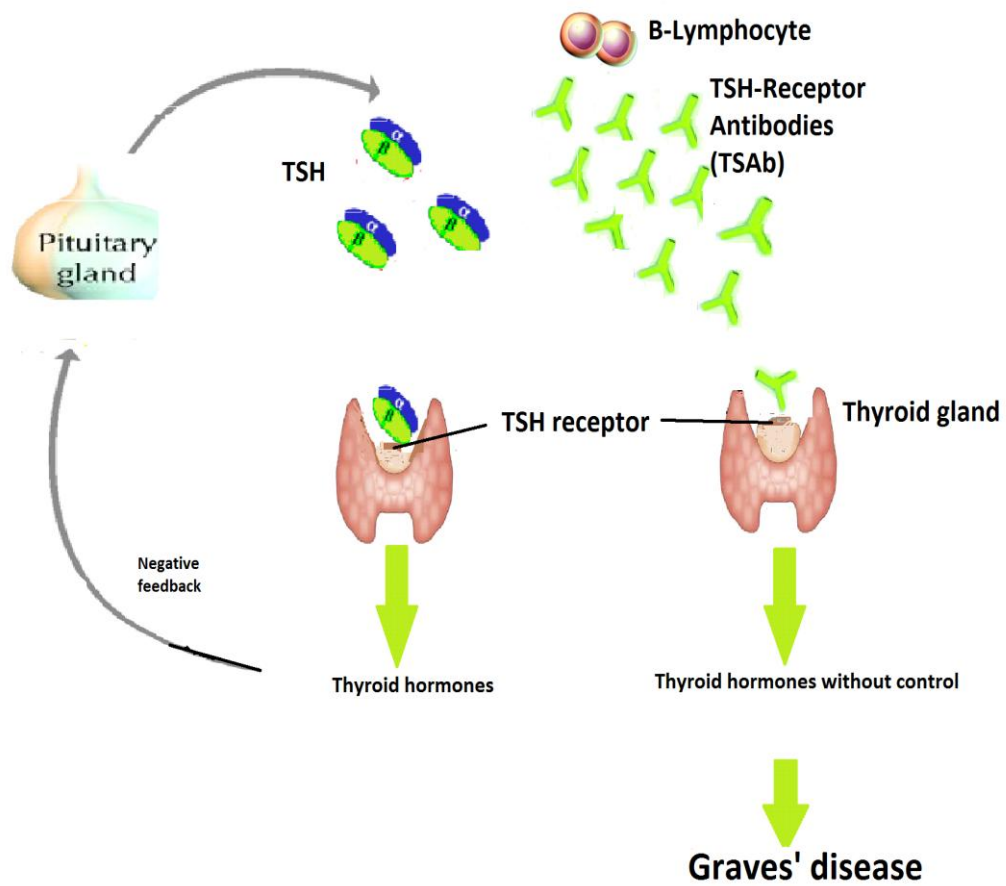


Figure1.1 Pathogenesis of Graves' disease

The thyroid gland is regulated by thyroid-stimulating hormone (TSH), which is made by the pituitary gland, TSAb mimic the action of TSH, activating the receptor, leading to de-regulated thyroid hormone production leading to Graves' disease.

1.1.3 Aetiology of Autoimmune Thyroid Disease

Susceptibility to AITD is determined by a combination of genetic and non-genetic factors. It is generally accepted that disturbance of the immune system due to environmental effects combined with genetic susceptibility leads to a breakdown in self-tolerance.

The process of autoimmunity in autoimmune thyroid disease is influenced by several factors. These include:

- Cross-reacting epitopes with thyroid antigens
- The expression of inappropriate HLA-DR
- Mutated B or T cell clones
- Failure in T cell and B cell tolerising mechanisms
- Stimulation of the thyroid by inflammatory cytokines
- Re-exposure of antigens by thyroid cell damage
- T suppressor cell malfunction
- Inheritance of HLA and other immune-response related genes

Even though, the immune system is proposed to avoid self-reactivity, low levels of reactivity to self antigen are usually present, and may have some physiological function (DeGroot and Quintans 1989). Apparently environmental and genetic factors act together to enhance self immunity, from a benign level, to a level that may cause a disease. Several contributing factors in the aetiology of GD and other AITD have been recognized. TSHR mRNAs, TG and TPO are processed in the human thymus to immunoreactive proteins (Coles, Wing et al. 1999) and other researchers have noted the same (Sospedra, Ferrer-Francesch et al. 1998). This means pre-T lymphocytes might be taught in the thymus to identify thyroid epitopes, and hence to develop tolerance against these antigens. This procedure is not complete, as cells reacting with thyroid antigens are both in the peripheral blood of normal, and in those with AITD (Spitzweg, Joba et al. 1999). In a process planned to give the maximum repertoire of lymphocytes, the lymphocytes, which recognize weakly self antigens in the context of autologous HLA, may be approved to continue in the circulation. It is not known if this differs from one individual to another and is a predisposing factor for the initiation of GD.

GD immune responses include generation of antibodies to different autoantigens (Table 1.1) and cell-mediated immune responses caused by lymphocyte reactivity, and the generation of circulating antigen/antibody complexes (Mariotti, Kaplan et al. 1980), at least for some antigens. GD is statistically linked with autoimmune diseases including pernicious anaemia, vitiligo (Ochi and DeGroot 1969), alopecia (Welti 1968), angioedema (Amoroso, Garzia et al. 1997), and myasthenia gravis (Marino, Ricciardi et al. 1997). There may be a weak link with systemic lupus erythematosus (White, Bass et al. 1961; Dalan and Leow 2012).

Table1. 2: Antibodies in Graves' disease

Antibodies in Graves' disease
Increase TSAb, TBII, and TSBAb level
Increase TPO-Ab level
Increase TG-Ab level
Increase iodide symporter antibodies level (NIS)
Increase antibodies recognizing components of fibroblasts
Increase DNA antibodies level
Increase parietal cells antibodies level (rarely)
Increase platelets antibodies level

1.1.4 Genetic Risk Factors for AITD

Research among twins and families shows the aetiology of AITD is multifactorial and involves the interplay of environmental, genetic and constitutional elements in the working of the immune system (Weetman 1991). Disturbances to the immune system from environmental effects (e.g. infection, stress, trauma, diet, drugs) combined with a background of genetic susceptibility lead to a loss of tolerance to thyroid antigens (Weetman 2003; Bogdanos, Smyk et al. 2012).

The role of heredity in Auto immune thyroid disease is well established and there is a significant concordance in family members, monozygotic twins and first-degree relatives, (Weetman and McGregor 1994; Hasham and Tomer 2012). Genes of the HLA system are major determinants of the susceptibility to some autoimmune diseases and class II MHC alleles have been the subject of a number of studies of AITD (Tomer 2010). The majority of studies have identified HLA-DR3 as a susceptibility gene for HT and GD in Caucasians, and has been shown to incur an approximately 2 fold increased risk. The researchers had shown that an amino acid substitution between glutamine or alanine and arginine at position 74 in the HLA-DR peptide is a key factor in the occurrence of AITD (Hasham and Tomer 2012). Additionally to class II MHC genes, now there are few established gene loci linked to auto immune thyroid disease, involving immune-regulatory (CD40, CTLA-4, PTPN22, CD25 and FOXP3) and thyroid-specific genes (thyroglobulin and TSHR)(Tomer 2010; Eschler, Hasham et al. 2011; Simmonds and Gough 2011; Dalan and Leow 2012; Hasham and Tomer 2012).

Many studies have been undertaken on the immunomodulatory molecule CTLA-4, which is expressed on the T cell surface and cooperates with B7 on APC to down-regulate T cell activation. Polymorphisms of CTLA-4 have been considered as a risk factor for Graves' disease and Hashimoto's thyroiditis (Yanagawa, Hidaka et al. 1995; Kotsa, Watson et al. 1997; Hasham and Tomer 2012). Many other groups have demonstrated polymorphisms in immunoregulatory cytokines IL-1 α , IL-1 receptor, TNF, antagonist that may also work as minor risk factors in AITD (Dinarello 1991; Badenhoop, Schwarz et al. 1992). Recent study shown that polymorphisms in the IL-17F gene increase the risk of AITD, therefore IL-17F considered as a superior gene for the prediction of AITD in the population of Han Chinese (Guo, Huo et al. 2013).

Recently, fine mapping of the Graves' disease locus, 14q, shown that Graves' disease phenotype has association with rs2284720 and, rs12147587 markers, present in the genes TSHR and NRXN3, consequently. These findings of new Auto immune disease susceptibility genes create a new clarification of the aetiology of AITD (Tomer, Hasham et al. 2013).

1.1.5 Non-Genetic Factors

1.1.5.1 Infection and Molecular Mimicry

The role of infectious agents in aetiology of AID has always been interesting theory. There are numerous data showed that bacteria and virus may play a role in AITD (Weetman 1996). Several mechanisms have been suggested by which infectious agent can cause the AITD. Some bacterial and viral proteins share antigenic epitopes with proteins of the host. In this method they may 'trick' the immune system into allowing them access because of the protection of self-tolerance. on the other hand, an immune response against the epitope of the bacterial and viral agent may cross-react with the mimicked host protein leading to autoimmunity. An example of this idea is cross reactivity of *Yersinia enterocolitica* with TSHR autoantibodies (Arscott, Rosen et al. 1992) (Davies 2008) . It has been found that patients with *Y. enterocolitica* infections have TSABs and that Graves' disease patient have antibodies to *Y. enterocolitica* (Gripenberg, Miettinen et al. 1978) It has also been demonstrated that thyroiditis can be induced in rats by injection of *Y. enterocolitica* membranes (Luo, Fan et al. 1993). This concept is still under review but seems unlikely to be of major importance, as most of the patients with *Y. enterocolitica* infections do not progress to GD. *H. pylori* infection of the gastric mucosa is also contributing in the development of AITD. Eighty five percentage of autoimmune atrophic thyroiditis patients have *H. pylori* infection, and this implied that *H. pylori* might be implicated in the pathogenesis of AITD (de Luis, Varela et al. 1998). This is also suggested that staphylococcal enterotoxins are highly mitogenic for T-cells and work as super antigens which stimulate the expression of T cells to certain TCR families (McIntosh, Watson et al. 1997). Viruses have been implicated as cross-reacting agents showing similarity to thyroid antigens, or as immune

system stimulators; influenza, measles, adenovirus, Coxsackie, Epstein-Barr viruses, and retroviruses are some of those suggested. Even though it has been demonstrated that GD mononuclear cells contain retroviral sequences (Ciampolillo, Marini et al. 1989) and also that HIV-1 (human immune deficiency virus-1) and TSHR have 66% similarity which could suggest molecular mimicry. These findings have not been confirmed subsequently.

An additional possible role for viral infection in autoimmune diseases is that cell damage caused by viruses can release hidden self-antigens leading to a breakdown in tolerance state or causing the development of altered self-antigens leading to an immune response (Tomer and Davies 1993). Moreover viral infections can stimulate IFN γ production, which consecutively induce HLA class expression in non-immune cells (e.g. thyrocytes).

Mechanisms of how infection may influence AITD. (Davies 2008)

- Molecular mimicry
- superantigens
- TLR activation by virus
- Increase HLA thyroid expression

1.1.5.2 Toxins and Drugs

It has been reported that the treatment by radiation predisposes people to AITD (Nagataki, Shibata et al. 1994) and as well lithium therapy can exacerbate AITD by its action on regulatory T cells (Weetman, Creagh et al. 1981; Lazarus 1998). Moreover, it was been shown that using of pro-inflammatory cytokines including IL-2, IFN- α , and GM-CSF, in the treatment, can aggravate existing AITD. Apparently these types of treatment act to increase occurrence latent immunity (Hoekman, von Blomberg-van der Flier et al. 1991). Novel therapeutic approaches to multiple sclerosis include lymphocyte depletion using T cell specific monoclonal reagents. The researchers noted

that the treatment with anti-CD52 monoclonal antibody may change the immune system from a Th1 to a Th2 type response or delete an important subset of suppressor or regulatory T cells leading to a breakdown in tolerance to thyroid antigens (Coles, Wing et al. 1999). Onset of auto immune thyroid diseases has been noted to occur after IFN- α treatment for hepatitis B and C (Preziati, La Rosa et al. 1995), or treatment with IFN- α for multiple sclerosis patients (Kreisler, de Seze et al. 2003; Prummel and Laurberg 2003).

Recently, several studies on the influence of the environmental chemicals on disruption of the thyroid function have been published. In vitro studies and animal experiments have concentrated on clarifying the mechanism of action of some chemicals. (Boas, Feldt-Rasmussen et al. 2012).

1.1.6 Immunopathogenesis of Graves' disease

Autoimmune response in Graves' disease needs a thyroid specific and non thyroid specific signal (Fountoulakis and Tsatsoulis 2004). The antigen specific signal could be exogenous (e.g. viruses or bacteria in the course of molecular mimicry) or endogenous (e.g. dying thyrocytes going through apoptosis) (Fountoulakis and Tsatsoulis 2004). Apoptosis of thyrocytes can be caused by Toxins like smoking, and drugs or lead to a modification in TSHR structure by the receptor mutation and encourage the follicular cells to generate chemokines (Yamazaki, Tanigawa et al. 2010). During the early stages, the abnormal structural of the TSHR endure spontaneous cleavage and produce free A subunit acting a vital role in the initiation of Graves' disease (Chazenbalk, Jaume et al. 1997; Nielsen, Leslie et al. 2001; Chen, Pichurin et al. 2003). Dendritic cells (antigen-presenting cells (APC)) (Chen, Pichurin et al. 2003), and thyrocytes which can act as APCs MHC class II expression, even though this cannot provoke an autoimmune attack on its own and only serves to propagate disease once it is initiated (Kimura, Kimura et al. 2005). TSHR extracellular domain epitopes must associate with MHC class II peptide, HLA-DR. Those peptides are transferred to the surface of APCs (Ghosh, Amaya et al. 1995; Posch, Araujo et al. 1995). The APCs present thyroid autoantigens to T helper cells in the draining lymph nodes of the thyroid in the early stage but later lymphoid tissue develops in the thyroid forming mainly of activated T lymphocytes, and a small number of B lymphocytes, macrophages and dendritic cells (Iyer and Bahn 2012). Even though the regional lymph nodes and bone marrow plasma cells are resources of TSHR antibodies (Weetman, McGregor et al. 1984), the thyroid is perhaps the major site of these autoantibody production (Rapoport and McLachlan 2001).

1.1.6.1 Role of T lymphocytes

Activation of T lymphocytes in Graves' disease through (TCR)-CD3 complex with CD4, TCR-CD3 complex, binds to TSHR peptides located in the binding compartment of MHC class II molecule on the APCs (signal 1). The T lymphocytes now need other co-stimulation to proliferate and produce cytokines (signal 2) (Fig. 1.2). Immature CD4⁺ T cells can differentiate into Th1, Th2, Th17 and Treg according to the cytokine.

In Graves' disease, Cell immunity usually mediating by Th1 CMI and humoral immunity mediating by Th2 (Fountoulakis and Tsatsoulis 2004).

The immune response mediated by Th1 related to CXC chemokines production of which induced by gamma interferon (Antonelli, Rotondi et al. 2005) also associated with high levels of TSHR autoantibodies (Romagnani, Rotondi et al. 2002). Recently, Th17 has been correlated to autoimmune diseases, that the quantity of Th17 cells was more during active disease (Nanba, Watanabe et al. 2009). Lack of T regs cells can induce autoimmunity, because of its suppressive roles on effector T cells.

1.1.6.2 Role of B cells

Activated T cells enhance the production of thyroid antibodies from B cells (Fig. 4). B cells regulation is affected in AITD due to defects of tolerance (peripheral and central). B cells work as Antigen presenting cells and they are essential to produce a varied T lymphocytes and maturity of memory T cells (Braley-Mullen and Yu 2000).

1.1.6.3 Regulation of apoptosis

The regulation of apoptosis in Graves' is abnormal because Th2 cytokines able to upregulate anti-apoptotic factors, including Bcl-2. This unusual apoptotic regulation suppresses the roles of cytolytic infiltrating lymphocytes whereas letting thyroid cells to endure longer than usual and become hyperplastic, thus leading to hyperthyroidism.

1.1.6.4 Current drugs targeting autoimmunity

Blocking the effects of TSHR antibodies by using monoclonal antibodies considered as possible autoimmune plan. On the other hand, although the noticed effect of TBAb of those antibodies in vitro, their effect on patients was week (Lenzner and Morgenthaler 2003). This is most likely because of the fact that a different types of thyroid antibodies are present in the Graves' disease patient sera, and the monoclonal antibodies can not bind to all TSAb epitopes (Lenzner and Morgenthaler 2003), Sanders, generated a human monoclonal antibody (5C9) which can block TSHR to the TSHR using severe

hypothyroid patients 'sera. IgG preparations of 5C9 inhibited the cAMP activities of M22, TSH, serum TSABs and mouse monoclonal TSABs (Sanders, Evans et al. 2008). On the other hand, the fact that this new mAb will be useful for Graves' patients is unclear. Those therapies which directed to B cell are hopeful for Graves' disease patients. Rituximab (RTX) is a chimeric monoclonal antibody against CD20 (Hasselbalch 2003; Edwards and Cambridge 2006). Consequently, a number of reports were on the treatment of Graves' ophthalmopathy by RTX (Nielsen, Hegedus et al. 2004; El Fassi, Nielsen et al. 2007).

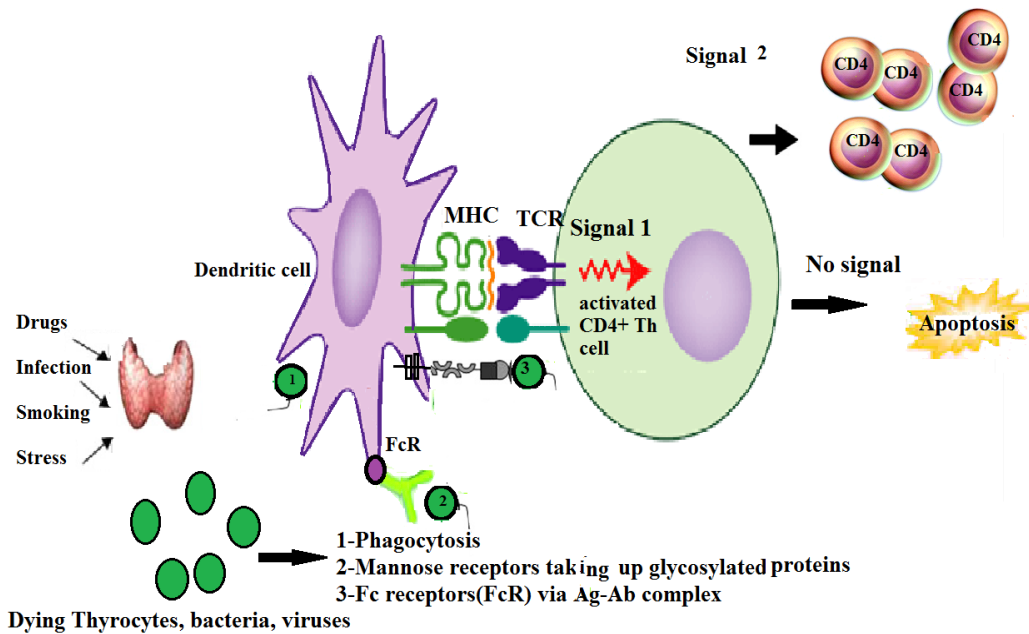


Figure 1.2 Immune pathogenesis of Grave's disease.

Due to exposure to many factors e.g. stress, drugs, infection or any environmental factors, thyrocyte undergo apoptosis and TSH parts release into the circulation, then taken in the regional lymph nodes by the dendritic cells, which deal with the antigens by many ways. The dendritic cells and B lymphocytes present the thyroid peptide which bound to class II MHC, CD4, TCR-CD3 complex, binds to the antigens located in the binding compartment of MHC class II molecule on the APCs (signal 1). The T lymphocytes with other co-stimulation proliferate and produce cytokines (signal 2). Immature CD4+ T cells can differentiate into Th1, Th2, Th17 and Treg according to the cytokine.

1.1.7. Antigens in Autoimmune Thyroid Disease

There are three major thyroid autoantigens; thyroglobulin (TG), thyroid peroxidase (TPO), and thyroid stimulating hormone receptor (TSHR). Highly specific autoantibodies against these antigens are found in autoimmune thyroid disease patients. The main properties of these major autoantigens are summarised in Table 1.2 (Paschke, Van Sande et al. 1996; Tomer, Hasham et al. 2013).

Table1. 3: The important features of the major thyroid autoantigens (Paschke, Van Sande et al. 1996).

Feature	TSHR	TPO	TG
Protein type	G protein binding receptor	Haemoprotein	Iodinated glycoprotein
Chromosome location	14	2	8
Thyroid Location	Basolateral membrane	Apical cell surface	Lumen of thyroid follicular
Function	Receptor for TSH	Iodination and coupling of tyrosine	Precursor of T3 and T4
Amino Acids	764	933	2748
Molecular weight (kDa)	87	105-110	660
Glycosylation	+	+	+

Other minor antibodies against the sodium/iodide symporter have been detected in the majority of GD sera by immunoprecipitation and immunoblotting assays, but the relevance of this to thyroid function is unclear (Ajjan, Findlay et al. 1998). Recent studies identified pendrin, a transporter mediating iodide efflux from thyroid cells into the follicular lumen, as an autoantigen (Yoshida, Hisatome et al. 2009). Antibodies that interact with thyroxine, triiodothyronine, tubulin, megalin, calmodulin, and DNA are also occasionally present in autoimmune thyroid disease (Weetman 2010).

1.1.7.1 Thyroglobulin

Historically, thyroglobulin antibodies were the first to be detected and associated with human thyroid disease. Thyroglobulin antibodies recognize a 670 kDa glycoprotein, synthesized and secreted by thyroid epithelial cells. Thyroglobulin contains 140 tyrosine residues, and some of these combined with iodine to form thyroid hormones, in a reaction catalysed by TPO. Experimental immunisation of animals has led to the identification of approximately 40 distinct TG epitopes. However, patient autoantibody recognition is restricted to only 6 major epitopes. Thyroglobulin antibodies are found in 30% of Graves' disease patients and 60% of patients with autoimmune thyroiditis (Weetman and McGregor 1984). Although not of real pathogenic importance, they may contribute to inflammatory process via antibody dependent cell mediated cytotoxicity (ADCC) (Song, Li et al. 1996).

1.1.7.2 Thyroid Peroxidase

TPO is expressed on the thyroid cell surface as well as in the cytoplasm. It is the primary enzyme involved in thyroid hormone synthesis. It catalyses the oxidative fixation of iodide during thyroid hormone synthesis. TPO autoantibodies are not known to play a role in GD, although they are thought to be cytotoxic and function in the pathology of chronic autoimmune thyroiditis, and are able to fix complement and cause antibody dependent cell mediated cytotoxicity (ADCC) (Song, Li et al. 1996).

1.1.7.3 Thyrotropin Receptor

Thyroid stimulating hormone receptor (TSHR), also known as the thyrotropin receptor, is expressed on the basal surface of thyroid follicular cells and regulates thyroid growth and function. The landmark discovery of the long acting thyroid stimulator (LATS) in the circulation of Graves' patients (Adams and Purves 1956) was the first suggestion that the TSHR may be a target for autoimmunity, though it was not until 20 years later that it was conclusively shown that autoantibodies bound to solubilised preparations of receptor (Petersen, Dawes et al. 1977). Autoantibodies directed against the thyrotropin receptor are the basis of Graves' disease and as such these antibodies belong to an important class of bioactive autoantibodies. The nature of TSHR antibodies and the particular nature of the antigen itself represent a field of study with such scope and complexity that this topic will be considered in a separate section below.

1.2 The Thyrotropin Receptor

1.2.1 TSHR Structure and Function

Evidence for a specific cell surface receptor for TSH came from studies of cAMP activation in cultured thyroid cells (Pastan, Roth et al. 1966; Yamashita and Field 1970). The structural gene was cloned in 1989 (Libert, Lefort et al. 1989; Nagayama, Kaufman et al. 1989). TSHR is a member of G protein-coupled receptor (GPCR) family, also known as seven transmembrane-spanning receptors (7TMRs). In common with other members of the receptor family, TSHR features a transmembrane domain (7TM) with 7 membrane-spanning loops, and an extracellular ligand binding domain. In TSHR the ligand binding domain contains a leucine rich repeat motif (LRR) (Latif, Michalek et al. 2010; Unal, Jagannathan et al. 2012). In contrast to other glycoprotein receptors, that are present on the surface of cells as single polypeptide chains, TSHR can be subjected to intra-molecular cleavage within its ectodomain. This cleavage leads to the removal of a 50 residue fragment between the extracellular and transmembrane

domains, forming a mature receptor composed of two subunits (A and B), attached together by disulphide bonds (Fig. 1.3) (Rapoport and McLachlan 2001). The biological role of this cleavage is still unclear (Michalek, Morshed et al. 2009; Neumann, Raaka et al. 2009; Unal, Jagannathan et al. 2012). It has been speculated that shedding of the A subunit may play a role in the breakdown of tolerance to TSHR observed in Graves' disease, and autoimmunity to other gonadotropin receptors, that do not share this subunit structure, is almost unknown or very rare (Chen, Pichurin et al. 2003). The extracellular domain of TSHR is heavily glycosylated, approximately 35% by weight as sugars (Rapoport, Chazenbalk et al. 1998). It remains a matter of debate how critical this glycosylation is for receptor function. Evidence from expression studies (discussed below) suggest that unglycosylated receptor does not bind TSH or patient antibodies (Rapoport, Chazenbalk et al. 1998) but it is not clear whether this phenomenon is the result of defective cellular processing of nascent protein or truly indicates a dependence on glycosylation for ligand binding. Structural studies of the FSH receptor show that glycosylation is not present on the ligand binding surface (Fan and Hendrickson 2005).

1.2.1.1 Thyrotropin

Thyrotropin is an approximately 30 kDa glycoprotein produced by thyrotrophs in the anterior pituitary. It belongs to the glycoprotein hormone family, that includes follicle stimulating hormone (FSH), luteinising hormone (LH), and human chorionic gonadotropin (hCG). Glycoprotein hormones are heterodimeric cystine-knot glycoproteins, comprising a common α -subunit and a unique β -subunit that determines functional specificity (Szkudlinski, Fremont et al. 2002). These glycoprotein hormones share a common structure and the crystallisation of FSH and hCG provided useful insights into the three dimensional nature of these proteins (Laphorn, Harris et al. 1994; Fox, Dias et al. 2001). The crystal structure of hCG shows that each subunit features a central cystine knot and three β -hairpin loops, two on one side of the cystine knot (L1, L3), and a large loop (L2) on the opposite side (Fig.1.4). The so-called cystine-knot is formed by a series of three disulphide bridges formed by central cysteine residues, in which one bridge reaches through a loop formed by the remaining two bonds (Laphorn,

Harris et al. 1994). This structure has also been observed in a number of growth factors, including PDGF, VEGF, and TGF- β (Sun and Davies 1995). One particular feature of hCG and other glycoprotein hormones is the "seat belt" structure, in which a loop of the beta subunit crosses over the long L2 loop of the α -subunit and is stabilised in place by a disulphide bond,

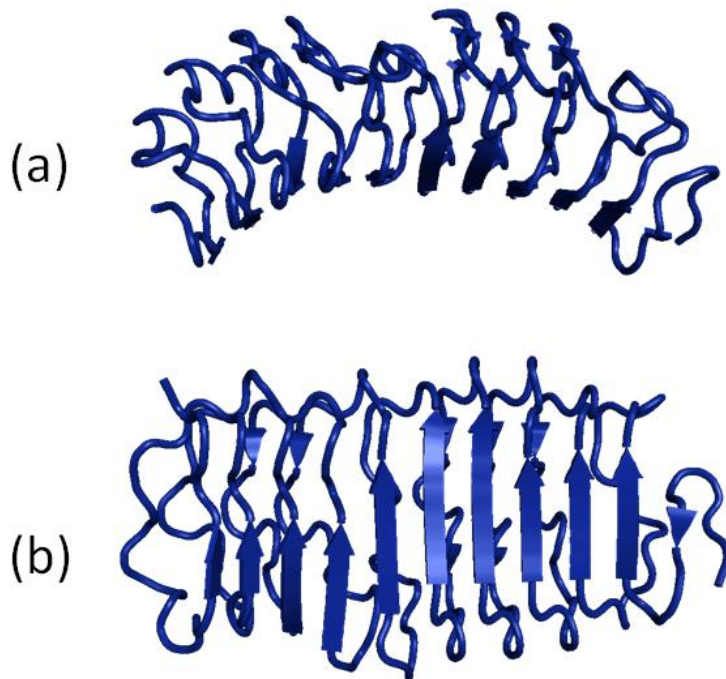


Figure1.3 Structure of the LRR domain of the thyrotropin receptor.

The diagram shows the 3-dimensional structure of the Leucine Rich Repeat (LRR) domain of the thyrotropin receptor. The side view (a) shows the concave shape of LRR ligand binding domain and the front view (b) shows the relatively planar surface presented by the arrangement of parallel beta sheets that comprise the ligand binding domain. The figure was produced using PYMOL and published X-ray data (Sanders, Chirgadze et al. 2007).

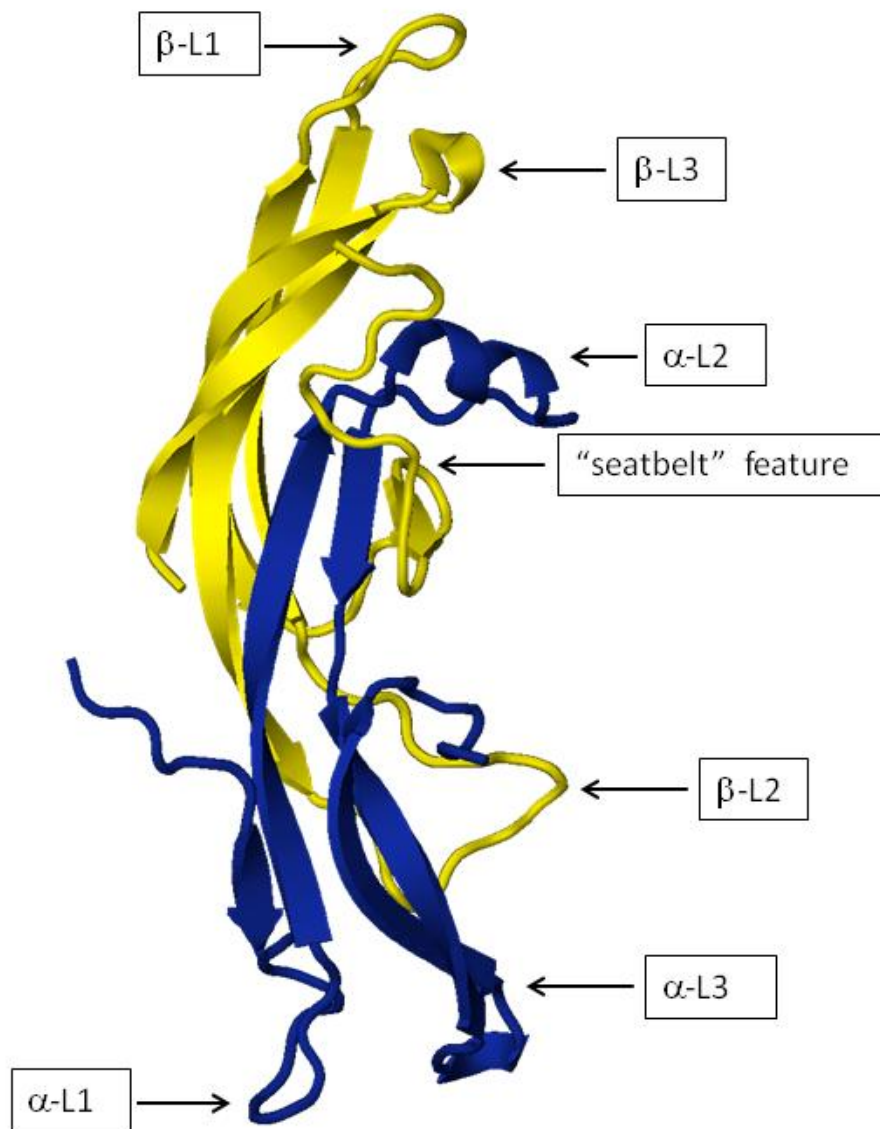


Figure1.4 Structure of Thyrotropin.

The diagram shows the proposed structure of TSH based on crystallographic analysis of human chorionicgonadotrophin (hCG) and follicle stimulating hormone (FSH) (Szkudlinski, Fremont et al. 2002). The α -chain is shown in blue and the β -chain in yellow. Critical hairpin loops are indicated and the "seatbelt" structure in which a β -chain loop crosses over and encloses part of the α -chain.

1.2.1.2 Structural Studies of TSHR

Insights into the three dimensional structure of TSHR were provided by the crystallisation of the related FSH receptor extracellular domain in complex with its ligand (Fan and Hendrickson 2005). This study showed that the conformation of the LRD resembles a slightly bent tube, in common with other LRR receptors, Fig.1.4 (Kobe and Kajava 2001). The hydrophobic leucine repeats are buried in the core of the structure, and the ligand binding site is provided by the almost flat concave surface of untwisted beta sheets. FSH is bound by the receptor with long axis of FSH perpendicular to FSHR tube structure (Fig. 1.5). The ligand binding site has a relatively large surface area ($2,600 \text{ \AA}^2$) suggesting multiple contacts between receptor and ligand. The majority of contacts come interactions between the parallel beta sheets of the TSHR and similarly planar beta sheets of TSH- α and the C-terminal 'seat belt' region of TSH- β . A key question relating to signalling is the orientation of the ligand binding domain with respect to the 7TM region. Fan and Hendrickson reasoned that as the L1 and L3 loops of the α and β subunits are antibody accessible when ligand is bound to the receptor, but the L2 tip of the α -subunit is not, then the receptor probably lies approximately parallel to the plasma membrane and holds FSH with the α -subunit tip proximal to the 7TM domain (Fig. 1.6). This arrangement is most probably common to the other glyco hormone receptors, and in the case of TSHR may be a critical factor in the binding of experimental mAbs and autoantibodies.

A major recent advance saw the publication of the three dimensional structure of the TSHR ectodomain in complex with a monoclonal thyroid stimulating antibody (Sanders, Chirgadze et al. 2007). As expected the structure of the TSHR was shown to be very similar to that of FSHR with the same arrangement of LRR domains and overall geometry. This study confirmed many hypothesised features of TSAbs, demonstrating that the antibody recognised the TSH binding site, and the molecular interactions between antibody variable regions and receptor mimicked those of thyrotropin. The features of this TSAbs monoclonal and the details of its isolation will be discussed in more detail below.



Figure1. 5: Structure of the FSHR in complex with FSH.

This diagram shows the 3-dimensional structure of the FSH receptor in complex with FSH. The concave face of the LRR domain (shown in red) presents a relatively flat surface that interacts with multiple sites on the FSH dimer (a-chain shown in blue and the b-chain in yellow). This figure was produced with PYMOL using published X-ray data (Fan and Hendrickson 2005).

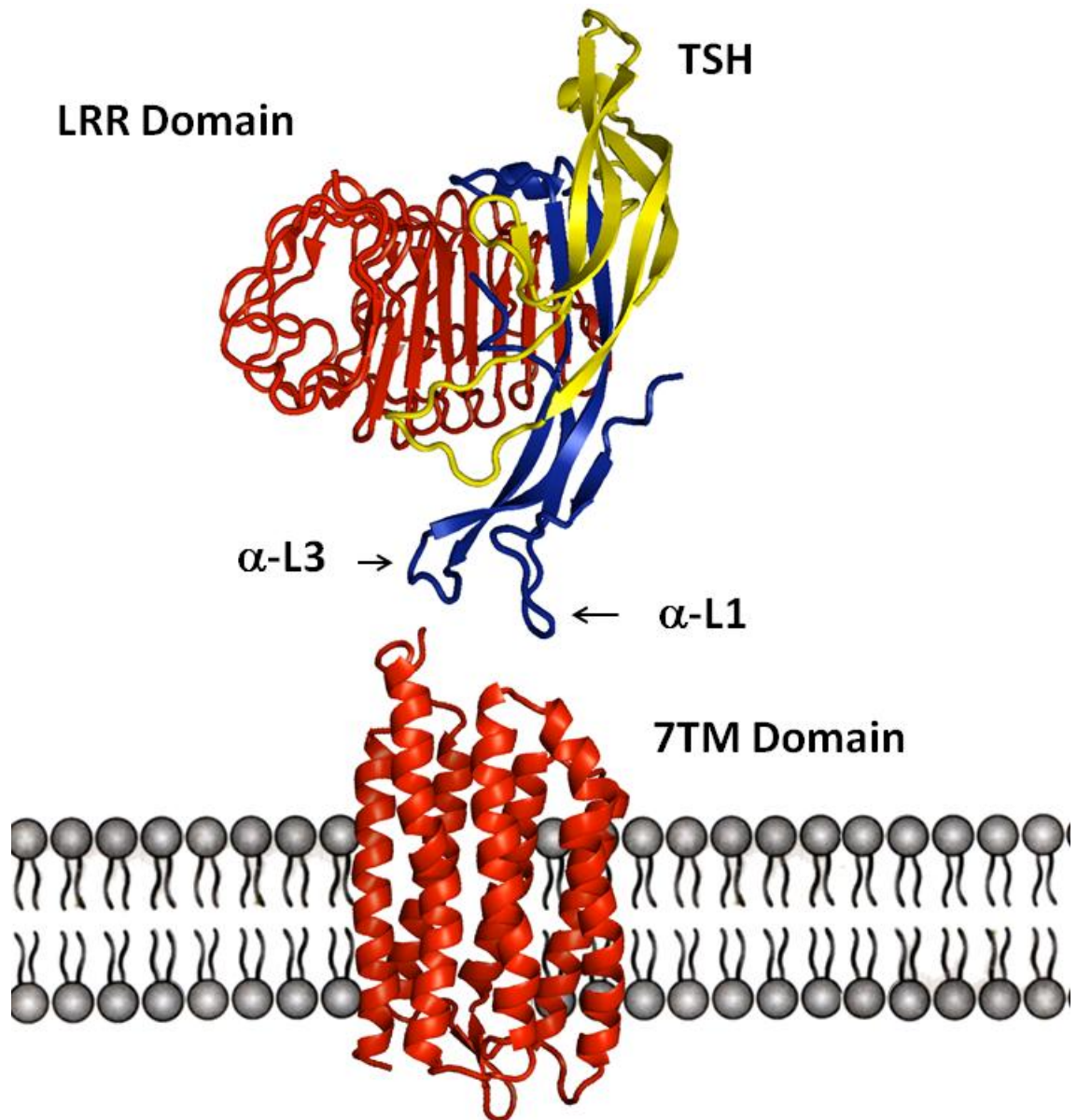


Figure1.6 Diagram showing the proposed model of TSH binding to the TSHR.

The TSHR is shown in red (the region between the LRR domain and 7TM omitted for clarity). TSH α -chain is shown in blue and the β chain in yellow. The TSH dimer is clasped by the concave face of the LRR domain, with the "seatbelt" region facing the binding site. The LRR domain is arranged approximately normal to the plasma membrane and binding of TSH brings the α -chain loops L1 and L3 into proximity with the 7TM alpha helices resulting in signal transduction. This model is based on data from structural analysis of the FSHR in complex with its ligand (Fan and Hendrickson 2005) and TSHR complexed with TSAb monoclonal M22 (Sanders, Evans et al. 2008).

1.2.2 Recombinant Expression of TSHR

Following identification of TSHR as the key autoantigen in Graves' disease it was anticipated that progress in understanding the pathology of the disease would be rapid, and in particular this discovery would enable the development of relevant animal models. This early optimism gave way to the realisation that as an autoantigen the TSH receptor presented particular difficulties. The receptor is expressed at a low level on normal thyrocytes (approx. 2000 - 5000 receptors) and this, together with the instability of TSHR during purification, meant that recombinant expression of the receptor was going to prove essential for efficient purification of native protein (Rapoport, Chazenbalk et al. 1998).

With the cloning of the human TSHR cDNA in 1989 (Libert, Lefort et al. 1989; Nagayama, Kaufman et al. 1989) it was hoped that all the tools of recombinant DNA technology could now be employed to express and fully characterise this key autoantigen. In the beginning many efforts were made to express recombinant TSHR in bacteria, and though a high level of expression of various fragments was attained, these purified proteins did not exhibit a native structure and more importantly were not recognised by the vast majority of patient sera (Takai, Desai et al. 1991; Rapoport, Chazenbalk et al. 1998). As antibodies recognise the extracellular domain attempts were made to express this region of the receptor as a soluble subunit (Rapoport, Chazenbalk et al. 1998). However, once again, the majority of patient sera did not recognise these recombinant forms of TSHR expressed in prokaryotic cells (Costagliola, Alcalde et al. 1994). Efforts shifted to the use of baculovirus vectors and expression in eukaryotic insect cells (Harfst, Johnstone et al. 1992; Huang, Page et al. 1993; Seetharamaiah, Desai et al. 1993). Attempts to express the holoreceptor all failed and expression of the extracellular domain produced a good yield of protein but it was not able to bind TSH and was not recognised by the majority of patient sera (Rapoport, Chazenbalk et al. 1998). Recombinant protein was retained in the endoplasmic reticulum, necessitating elaborate purification steps, and secondly the pattern of post-translational glycosylation in insect cells was inappropriate for patient antibody recognition (Rapoport, McLachlan et al. 1996).

Mammalian cells supply the most effective vehicle for generating conformationally native and functional TSHR. Stable expression of human TSH holoreceptor in Chinese hamster ovary (CHO) cells was reported by a number of groups (Harfst, Johnstone et al. 1992; Harfst, Ross et al. 1994; McLachlan, Nagayama et al. 2005). A stable CHO cell line expressing full-length TSHR are responded to TSH and patient autoantibodies, and are used as the basis of bioassays for thyroid stimulating antibodies. Intact cells or membrane produced from these cells can be used in a TSH binding inhibition assay for TSHR autoantibodies. A typical level of TSHR expression in stably transfected cell is approximately 90,000 receptors per cell as in the commonly used JP09 line (Ludgate, Costagliola et al. 1992). Although this level of expression is far higher than which estimated in thyroid tissue, it is still too low to make TSHR purification practical (Rapoport, Chazenbalk et al. 1998). High density surface expression of the TSHR ectodomain was achieved through the use of a glycosylphosphatidylinositol (GPI) anchor (Da Costa and Johnstone 1998), and this approach provided cell lines that were very useful for characterising patient antibody binding through techniques such as FACS.

Even though relatively high level surface expression of the TSHR extracellular domains was achieved by the use of a GPI anchor (approximately 300,000 copies per cell) (Da Costa and Johnstone 1998), this still provided too little recombinant protein to enable purification. Indeed, it has been estimated that approximately six confluent 10 cm dishes of these cells would be needed to produce 1 µg of receptor (Rapoport, Chazenbalk et al. 1998).

A significant breakthrough in expression was achieved through the use of a specialised bicistronic vector that permitted the allowed the isolation of high producing clones by neomycin selection (Costagliola, Morgenthaler et al. 1999). These cell lines produced between $1-2 \times 10^6$ copies of receptor per cell, and for the first time it became possible to mass produce recombinant TSHR in bioreactors (Stiens, Bunttemeyer et al. 2000).

1.2.3 TSHR Autoantibodies - Discovery and Early Characterisation

The discovery of the long acting thyroid stimulator (LATS) in 1956 was a landmark in our understanding of Graves' disease (Adams and Purves 1956), and by 1964 LATS had been shown to be immunoglobulin in nature, suggesting the possibility of humoral autoimmunity against a specific thyroid antigen as the basis of Graves' disease (Meek, Jones et al. 1964). The next development in the field came with the discovery of a specific thyrotropin receptor on the surface of thyroid cells (Pastan, Roth et al. 1966; Yamashita and Field 1970). Some 20 years later it was unequivocally established that the target of the LATS IgG was the thyrotropin receptor (Petersen, Dawes et al. 1977). Despite these early insights attempts to characterise these antibodies proved surprisingly difficult. Analysis of bulk sera from GD patients did provide yielded valuable data using the available technology of the period. It was shown that TSAbs are class restricted to IgG1 (Weetman, Byfield et al. 1990; Weetman, Yateman et al. 1990) and approximately one third of patients use a lambda light chain in these antibodies (Williams, Marshall et al. 1988). These findings suggested that a restricted number of B-lymphocytes are responsible for producing TSAbs. Clearly the question of oligoclonality is central to our understanding of the origins of this autoantibody response, and may highlight novel therapeutic approaches, but cannot be precisely determined through the analysis of bulk patient sera. For these reasons great effort was exerted in attempts to isolate both animal and human examples of monoclonal TSAbs and these studies, and the particular difficulties presented by the TSHR as an antigen, will be discussed in depth later in this chapter.

Interestingly, measurements of circulating levels of thyroid autoantibodies in patient sera demonstrated that although anti-TPO and anti-TG IgG are relatively abundant in the circulation, TSAbs are present at a very low level (de Forteza, Smith et al. 1994; Chazenbalk, Jaume et al. 1997), suggesting that the circulating precursor B cells would be correspondingly rare also. As will be discussed, this feature of TSAbs was to prove a significant hindrance for the isolation of patient monoclonals, and is another way in which this class of autoantibodies clearly differ from other thyroid antibodies.

1.2.4 TSHR Antibody Assays

TSH receptor autoantibodies (TRAbs) are the basis of Graves' disease and can be detected in the sera of almost all patients if the assay used is of sufficient sensitivity (Rees Smith, McLachlan et al. 1988; Rapoport, Chazenbalk et al. 1998).

1.2.4.1 Thyroid Stimulating Activity

Historically the first methods used to detect TSAb was the study by Purves and Adams in 1956, though at the time it was not known that the so-called Long Acting Thyroid Stimulator (LATS) detected in Graves' disease serum was immunoglobulin (Adams 1956). In these studies the assay was based on the stimulated release of radioiodine from guinea pig thyroids and this *in vivo* approach was subsequently developed in mice as the eponymous "McKenzie" assay for both TSH and LATS (McKenzie 1958; McKenzie 1958). Useful though these assays were they were, the use of animals was cumbersome and not accessible for all laboratories. Accordingly, significant effort was invested in the development of effective *in vitro* bioassays of thyroid stimulating activity. Attention focused initially on the use of tissue slices, with output measurements based on the production of colloid droplets or increases in cAMP production (Onaya, Kotani et al. 1973), but these and other early assays suffered from both irreproducibility or insensitivity or both. Tissue culture of human and animal thyroid cells proved a more fruitful area of study and sensitive and accurate assays of thyroid stimulatory activity, based on measurements of cAMP, were developed using cultured cell monolayers (Rapoport and Adams 1978; Toccafondi, Aterini et al. 1980). With the cloning of the human TSHR cDNA (Libert, Lefort et al. 1989; Nagayama, Kaufman et al. 1989) the use of thyroid cell lines has been almost completely replaced by stably transfected cells, offering both higher levels of receptor expression and simpler tissue culture requirements (Persani, Tonacchera et al. 1993; Michelangeli, Munro et al. 1994). It was through the use of activity assays that another class of TRAb was discovered. A studies of TSAb activity in a collection of Graves' patient sera showed that in a few patients antibodies were present that could block the activity of TSH, as measured by cAMP production (Orgiazzi, Williams et al. 1976). This finding shed new light on the range of different TRAbs present in AITD patients and this new class of autoantibodies, TSH blocking antibodies (TBAb) can play a significant role in

some cases of autoimmune hypothyroidism (Endo, Kasagi et al. 1978; Matsuura, Yamada et al. 1980). The discovery of TBAb suggested that the interaction of patient IgG and the TSH receptor was complex, with a range of different epitopes, and associated effects on thyroid function. For the field to advance it was necessary to move beyond bioassays, and to investigate the binding of IgG to the receptor directly, and it is to these assays that we will now turn.

1.2.4.2 Indirect TBI Assays

The identification of a specific thyrotropin receptor on the surface of thyroid cells was the initiating point for the development of direct binding assays for TRAb. The demonstration that some patient TRAbs could compete with TSH for binding to the TSHR was ultimately developed into an assay for characterising antibody binding characteristics. This TSH Binding Inhibition (TBI) assay is relatively easy to perform and proved a useful tool to classify different classes of receptor antibodies. The assay originally used solubilised porcine receptor (Smith and Hall 1981) and, given the difficulties of expressing and purifying human TSHR (section 1.2.1.2), this material is still in common use at present. The assay was used to show that thyroid stimulating antibodies blocked the binding of TSH to the receptor, evidence that they were likely to recognise a similar binding site on the receptor as the natural ligand. One drawback of the assay is that it does not discriminate between thyroid blocking antibodies (TBAb) and TSAbs, which limits the clinical usefulness of TBI measurements. A second problem with the original TBI assay, based on porcine receptor preparations and bovine TSH, was that it had a sensitivity of only 50-80% for the detection of TRAb from Graves' patient samples (Kamath, Adlan et al. 2012). This was improved with the introduction of so-called 'second generation' assays which used recombinant human TSHR and produced a 90-100% sensitivity for the detection of Graves' patient receptor antibodies (Costagliola, Morgenthaler et al. 1999). Interestingly, though pure recombinant human TSH is available, bovine TSH is still used as it has a higher binding activity than the human hormone (Rapoport, Chazenbalk et al. 1998). With the isolation of human monoclonal TSAbs (Sanders, Evans et al. 2003) a 'third generation' TBI assay has been developed based on the ability to compete for binding to the receptor with the stimulating IgG, and is claimed to have even greater sensitivity (Zophel, Roggenbuck et

al. 2010). The use of TBI assays has allowed TRAb to be classified accordingly to their ability to compete with TSH. The nomenclature associated with thyroid stimulating and TBI activity has been subject to both confusion and variety, and a case has made for simplifying this terminology (McLachlan and Rapoport 2013). In the case of bioassays, TSAb refers to antibodies with thyroid stimulating activity, and TSH-blocking antibodies or TBAb, inhibit signalling by TSH. Competition assays are most commonly referred to as TSH binding inhibition (TBI) assays, though TSH is no longer always used as the ligand, this term can still refer to blocking of TSAb binding.

1.2.4.3 Direct Binding Assays

Detecting binding of patient TRAbs to receptor is a technically challenging task. As discussed, patient TSHR autoantibodies are present at a very low level in sera, typically in the nanogram per ml, with rare patients exhibiting microgram levels of TSAb (Rapoport, Chazenbalk et al. 1998). Faced with such low levels of antibody, direct binding assays require a significant level of purified autoantigen to provide sufficient sensitivity. Producing significant amounts of purified TSHR, together with the strict requirement for native conformation for recognition by patient antibodies, presented a significant hurdle for the development of direct binding assays. The use of GPI anchors for surface expression of TSHR ectodomain (section 1.2.2) allowed the development of flow cytometric assays for the detection of antibody binding (Jaume, Kakinuma et al. 1997), though this approach lacked sensitivity and did not lend itself to high throughput screening.

The isolation of cell lines expressing very high ($1-2 \times 10^6$ receptors per cell) levels of TSHR (section 1.2.2) lead to the commercial development of the first true direct binding assay of TSHR antibodies, the so-called "2nd generation" assay (Costagliola, Morgenthaler et al. 1999). This assay was based on the use of tubes coated with purified human TSHR captured by a monoclonal antibody and held in a stable native conformation. This "BRAHMS" assay offered higher sensitivity and selectivity than previous assays and was estimated to offer a detection level of 70-90%.

1.2.5 Animal Models and Isolation of TSHR Monoclonal Antibodies

1.2.5.1 Spontaneous Models

Many key aspects of autoimmunity have been uncovered by the use of animal models of autoimmune disease. These models are divided into two distinct types, spontaneous and induced. Spontaneous autoimmune disease models exist as a result of deliberate inbreeding of strains for particular characteristics including the incidence of autoimmune disease. In the case of AITD, there are a limited number of spontaneous animal models. The best known are the Buffalo Breed (BB) rat, some strains of non-obese diabetic (NOD) mouse and the obese strain chicken. In all these models there is an infiltrative thyroiditis, tissue destruction, and the immune response is directed against the thyroid antigens TG (chicken and rat) and TPO (mouse). Interestingly none of these animal models exhibited the hyperthyroidism or circulating TSAb characteristic of human disease (McLachlan, Nagayama et al. 2005).

1.2.5.2 Induced Models

Since the 1950s researchers have successfully use immunisation with antigen and adjuvants to produce thyroiditis and autoantibody production in a range of species (Rose and Witebsky 1956). Immunised rabbits and mice developed serum antibodies that would recognise TSHR preparations in a range of assays including, ELISA, western blotting and immunoprecipitation (Seetharamaiah, Wagle et al. 1995). It soon became clear however that in no case did the animal sera contain thyroid-stimulating activity, and the development of an animal model of Graves' disease was going to prove more of a challenge than anticipated (McLachlan, Nagayama et al. 2005).

GD patient sera recognise conformational epitopes, thus an animal model would need to target these same epitopes in order to generate antibodies with thyroid stimulating activity. Attention turned to the expression of the native receptor.

The first successful induction of autoimmune hyperthyroidism in animals was achieved using the "Shimojo" model (Shimojo, Kohno et al. 1996). In this approach expression of native receptor was achieved by injecting mice with autologous fibroblasts stably transfected with the genes for human TSHR and murine class II MHC. The features of

this model included lymphocytic infiltration of the thyroid gland, and more importantly, the induction of stimulatory TSHR antibodies. Mice were injected six times and approximately two weeks after the final injection about 90% of mice developed antibodies against the TSHR, as determined by TBI activity. Approximately 25% of these mice went on to exhibit hyperthyroidism, and had detectable levels of TSAb activity (Shimojo, Kohno et al. 1996). This approach was extended by other groups and used to induce hyperthyroidism in hamsters (Ando, Imaizumi et al. 2003), and repeated in mice using stably transfected B cells and human embryonic kidney (HEK293) cells (Kaithamana, Fan et al. 1999).

An alternative approach was based on the induction of transient TSHR expression by naked DNA or genetic immunisation. Immunisation with DNA has shown to be an efficient method of generating an immune response, leading to antigen expression in myocytes and local antigen presenting cells (Tang, DeVit et al. 1992). It was reported that DNA immunisation of mice with TSHR DNA lead to the induction of TSHR antibodies in almost 100% of treated mice (Costagliola, Rodien et al. 1998). Interestingly, in this study TSAb activity could be detected in some mice, but none of them were thyrotoxic. Three other groups were subsequently unable to reproduce these results (Pichurin, Yan et al. 2001) and it became clear that the model was highly susceptible to the genetic background of the subject mice and sensitive to environment conditions such as animal housing and diet (Baker, Mazziotti et al. 2005).

As an alternative to transient expression by DNA immunisation a number of groups investigated the use of replication-deficient adenovirus vectors to transfect TSHR DNA into animal cells. Nagayama et al (Nagayama, Kita-Furuyama et al. 2002) injected recombinant adenovirus intramuscularly into a number of different inbred mouse strains and were able to report the induction of TSHR antibodies almost all BALB/c treated mice, with detectable TBI activity and TSAb and thyrotoxaemia in 50%. Interestingly only 25% of another strain, C57BL/6, became thyrotoxic, and some strains of mice undergoing the same treatment remained euthyroid (Nagayama, Kita-Furuyama et al. 2002). However, despite this variation, the adenovirus model has been confirmed by two other laboratories (Chen, Pichurin et al. 2003; Gilbert, Salehi et al. 2004).

Through these advances it was established that immunisation with native TSHR receptor could lead to the production of receptor antibodies that resembled those observed in human disease, and, as will be discussed below, it with the use of these new animal models that the first TSAb monoclonal antibodies were isolated.

1.2.6 Cloning of TSHR Monoclonal Antibodies

The development of methods for generating monoclonal antibodies by cell fusion (Kohler and Milstein 1975) enabled the characterisation of single antibodies of defined specificity. Theoretically it was now possible to generate monoclonal antibodies against antigen by immunisation with purified, often recombinant, antigen. This technique was soon applied to the field of autoimmunity and the generation of antibodies against known disease-related antigens. With the advent of recombinant DNA techniques and cloning of the human TSHR cDNA (Libert, Lefort et al. 1989; Nagayama, Kaufman et al. 1989) it was anticipated that rapid progress would be made in the generation of experimental antibodies by immunisation with purified recombinant protein. In the area of thyroid autoimmunity progress was initially rapid, and examples of anti-Tg and anti-TPO were soon reported (Kodama, Sikorska et al. 1984; Czarnocka, Ruf et al. 1985).

As described above, many different approaches have been taken to generate murine monoclonal antibodies to TSHR. Early studies used immunisation with thyroid membrane extracts. Antibodies from these mice failed to convincingly recognise TSHR in immunoassays. Subsequent studies using immunisation with different forms of recombinant TSHR were more successful. A series of monoclonal antibodies were generated, and evaluated using numerous criteria including immunoprecipitation, immunoblotting, and ELISA. However, with two exceptions, none of these monoclonals were shown to interact with native conformationally intact TSHR, and crucially, none possesses stimulatory activity (McLachlan, Nagayama et al. 2005). The field rapidly became rather confused, with a number of groups claiming TSAb activity for their respective monoclonals. In an effort to clarify the goal of antibody studies a set of criteria were described that authentic TSAb should meet

Despite the availability of animal models, the isolation of monoclonal TSAbs remained an insurmountable obstacle for some time. A number of particular difficulties remained

to be overcome. The choice of suitable animal donor was the first obstacle, and success was eventually achieved using spleens from rodents with very high levels of TSAb and TBII activity, and evident thyrotoxinemia. The second contributing factor was the development of a high throughput screening technique (Costagliola, Morgenthaler et al. 1999). In general, ELISA is the method of choice for screening of monoclonal antibodies as the technique lends itself to large throughput analysis necessary for the identification of specific antibody activity. The identification of TSAb clones required the use of more specific assays, such as those for TBII, or TSAb activity. Even with the use of an improved screening assay, few monoclonal TSAb have been isolated and these have been the result of tremendous effort (McLachlan, Nagayama et al. 2005).

The development of successful animal models of GD was a crucial advance in our understanding of the origin of the autoimmune thyroid disease. Perhaps the most important aspect of this breakthrough was the impact it had on the attempts to characterise the TSHR autoantibody response, in particular the nature of thyroid stimulating antibodies that are the basis of GD. The availability of animal models was an important step in an attempt to isolate monoclonal TSAb.

The experimental TSAb monoclonals described above were derived using variants of the well-established hybridoma procedure. In this approach, activated splenocytes from immunised subjects are fused with an immortal cell line such as myeloma, cultured and screened for the desired activity. The isolation of human monoclonal antibodies is in general, a much more difficult challenge, and in the case of TSHR antibodies, the difficulties were an order of magnitude greater still. The stable immortalisation of human B cells remains a technical challenge, not least due to the difficulty in developing suitable fusion partners (Smith 2003). More significantly, peripheral blood, the most accessible source of patient lymphocytes, contains few activated B cells, and booster immunisation is not an option with human subjects. The successful isolation of human TSAb mAb thus represented a major technical triumph (Smith 2003). A critical factor in this success was the selection of a patient with active GD and very high levels of TSHR antibodies, as measured by TBII and TSAb bioassay. Some insight into the magnitude of the task is provided by the fact that 16,500 culture wells needed to be screened to isolate this single clone, some 10-20 times that required in the case of

animal TSAb, and this does not take into account any unreported failed attempts. The isolation of a human thyroid stimulating monoclonal autoantibody (M22) has been a key advance for the study of the thyroid autoimmunity (Smith 2003).

The availability of monoclonal TSAb also allowed, a second major advance in the field: the crystallisation of the receptor-antibody complex (Sanders, Chirgadze et al. 2007). For the first time, structural studies could be carried out on the TSH receptor, and the stimulating antibody-binding site determined. It was shown that both the thyroid stimulating human monoclonal antibody M22 and TSH bind to the concave surface of the leucine rich domain (LRD) of the TSHR. It was also shown that M22 and TSH interact with the same or similar amino acid residues in the receptor ligand-binding domain (Sanders, Chirgadze et al. 2007; Nunez Miguel, Sanders et al. 2009; Guo, Huo et al. 2013). The light chain of M22 resembles the TSH β chain in its binding properties, while the heavy chain of M22 exhibits binding interactions similar to those of the TSH α chain (Fig. 1.7) (Sanders, Chirgadze et al. 2007; Nunez Miguel, Sanders et al. 2009; Sanders, Young et al. 2011). Recently two additional human monoclonal antibodies to the thyrotropin receptor (K1-18 with stimulating and K1-70 with blocking activity) have been isolated from a patient with hypothyroidism who previously presented with Graves' disease (Sanders, Young et al. 2011). This provides the first experimental confirmation that a patient can produce both blocking and stimulating TSHR antibodies (Sanders, Chirgadze et al. 2007; Smith, Sanders et al. 2009; Sanders, Young et al. 2011). Crystallographic analysis of the TSH blocking antibody, K1-70, complexed with the TSHR LRR domain showed that the epitope of K1-70 showed a substantial degree of overlap with that of the TSAb clone M22 (Sanders, Young et al. 2011)

Although these examples of human TSHR monoclonal antibodies have provided useful insights into the nature of TSAb, both in terms of epitope recognition and immunoglobulin gene usage, it is clear that the isolation of further examples is required to fully understand and investigate TSAb.

Analysis of TSAb monoclonal and corresponding TSHR epitopes would provide novel therapeutic strategies and diagnostic tools as well as allowing the design of specific antagonists or the development of anti-idiotypic reagents.

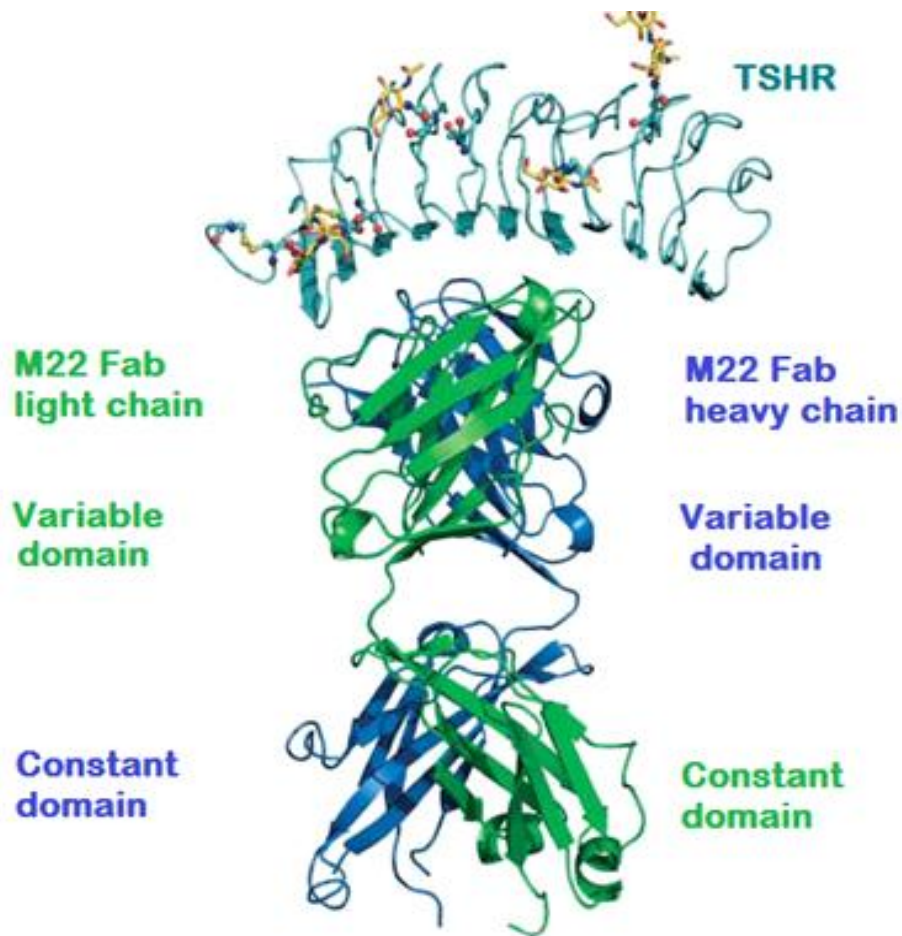


Figure1.7 The TSH Receptor-M22-Fab Complex Structure

The TSH receptor-M22 Fab complex structures are shown in differently aligned views related by 90° rotation about the vertical axis. TSH LRD is in cyan, M22 Fab light chain is in green, M22 heavy chain is in blue, the N-linked carbohydrates are in yellow and carbohydrate-bound asparagines are labelled. The amino-(N) and carboxyl-(C) termini are indicated. Disulphide bonds are shown in black (adapted from (Sanders, Chirgadze et al. 2007)).

1.3 Antibody Structure and Function

The molecule of Immunoglobulin (IgG) are made up of light (L) and heavy (H) polypeptide chains. The molecular weight of each H chain is 50-75 kDa containing about 445 residues. Whereas each L chain has a molecular weight of 25 kDa consisting of approximately 220 a.a., The antibody molecule composed of 4 polypeptide chains: 2 H chains and 2 L chains, forming Y shape (Fig 1.8). An antibody molecule always consists of identical H chains and identical L chains. Each H chain is covalently linked with an L chain by a disulfide bond and the two heavy chains are associated to each other by disulfide bonds (Paul 2003). H and L chains are subdivided into variable (V) and constant (C) domains. Most H chains consist of one variable heavy (VH) and 3 constant heavy (CH) domains, the constant heavy domain 1 (CH1), the constant heavy domain 2 (CH2), and the constant heavy domain 3 (CH3). And L chain consists of one variable light (VL) and one constant light (CL) regions. The main function for the variable domains is antigen binding, while the functions of constant regions are binding to cell surface receptors and complement activation. Each variable region contains three complementary-determining regions (CDRs) or hypervariable regions. When VH and VL are attached by coupling the light and heavy chains, CDRs form the antigen binding site (paratope), complementary in structure to epitope or the antigenic determinant and determine antibody specificity. The remarkable specificity of antibodies is due to these hypervariable regions and the immune system ability to generate high affinity antibodies to a huge array of antigens means that the diversity in variable regions encoding genes have to be very high. Two types of light chains, λ (lambda) and κ (kappa) chains are with a similar function. In human these are present in a κ : λ ratio of about 2:1, but this varies greatly between species. Both types occur in all classes of immunoglobulin (IgG, IgM, IgA, IgE and IgD), but any one immunoglobulin molecule contains only one type of L chain. The amino-terminal portion of each L chain participates in the antigen-binding site. H chains are distinct for each of the immunoglobulin classes and are designated γ (gamma), μ (mu), α (alpha), δ (delta), and ϵ (epsilon). The amino-terminal portion of each H chain participates in the antigen-binding site; the carboxy terminal forms the Fc fragment, which has the biological

activities (Paul 2003). By using enzymatic cleavage property, the antibody molecule part of different functions can be classified. Two Fab fragments, each consisting of VH, CH1, VL and CL and one Fc (crystallisable fragment) fragment can be produced by papain treatment of antibody molecule. Pepsin cleavage releases the two fragments binding domains bound together, a fragment known as (Fab)₂, which maintains the link offered by the disulphide bridge in the hinge region and thus consists of two Fab fragments. The antibody Fab or (Fab)₂ fragment of an antibody is a unit containing the antigen-binding site with high affinity to their targets. Of interest is the Fv and scFv fragments, which considered as the smallest fragment of immunoglobulin including the entire antigen-binding site, consist of only VH and VL (Fig. 1.9). Through the use of protein engineering a range of alternative immunoglobulin domain constructs are possible (Janeway and Travers 1997; Paul 2003).

1.3.1 The Variable Domains of Immunoglobulin

The variability is not in the entire variable region, but only in certain part of the domain. The less variable region of the variable domain known as framework regions (FR), and hypervariable regions (HV) considered as the most hypervariable regions present antigen epitope binding regions that are structurally complementary to their specific epitope, and they are known as CDR (complementary determining regions), which classified to CDR1, CDR2 and CDR3 (Janeway and Travers 1997; Paul 2003).

Immunoglobulin genes can be classified into families according to the similarities of the DNA sequence. Seven of them which have 80% or more homology (Janeway and Travers 1997) and the λ chain is divided into eight families. These 8 families are not evenly represented in the antibody repertoire.

The largest gene family of heavy chain is VH3, which about 50% of the collection of VH in peripheral B cells of the adults (Janeway and Travers 1997; Paul 2003).

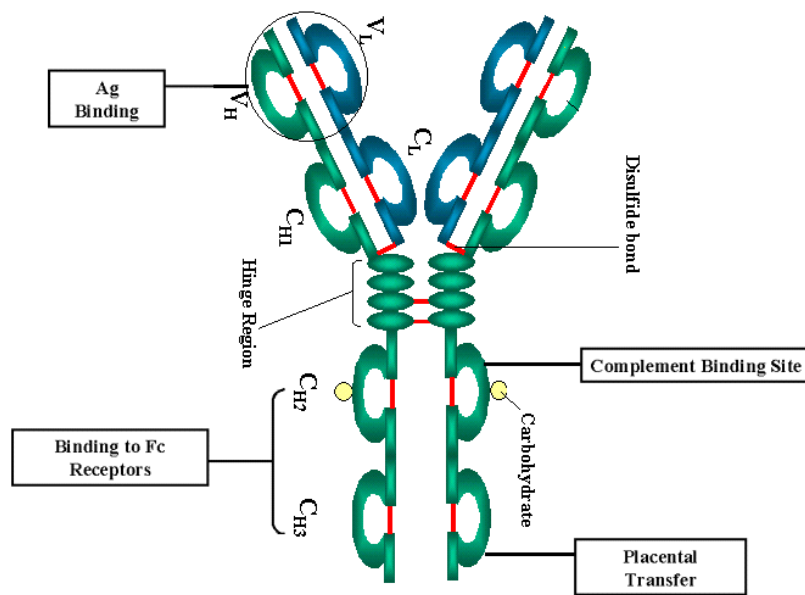


Figure 1.8 Schematic representations Structure of an immunoglobulin G (IgG)

Antibody molecule includes two identical heavy (H) chains and two identical light (L) chains are connected by disulfide bonds and each chain consists of variable and constant region. Within the variable regions, the hypervariable (complementary determining) regions comprise the actual antigen-binding sites and are responsible for the specificity of antibody.

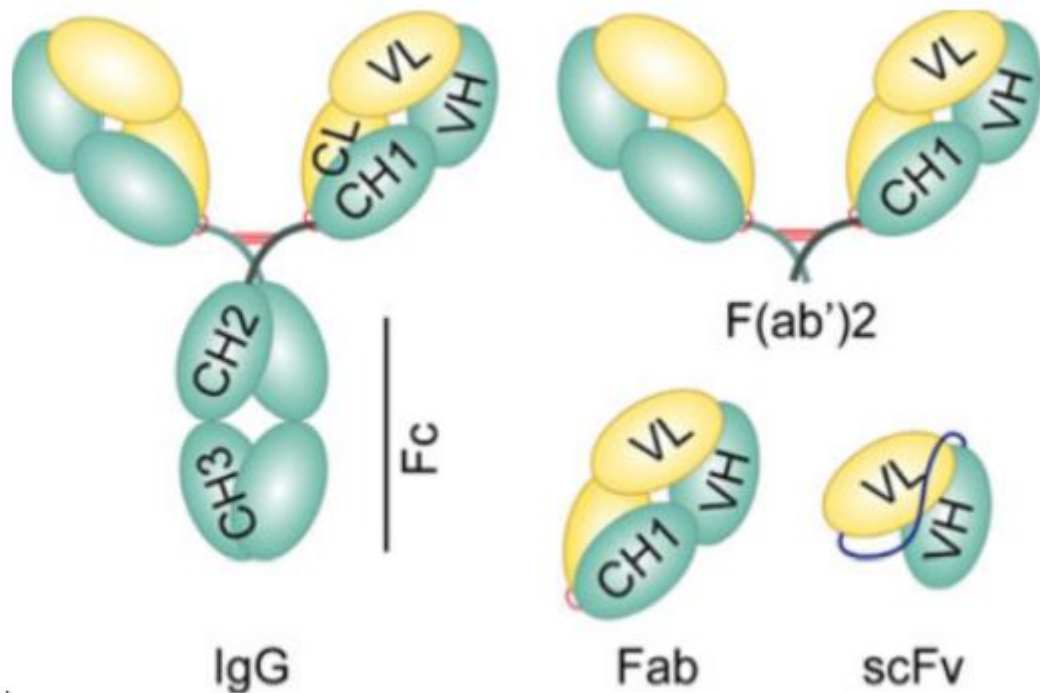


Figure1.9 Schematic representation Structures of Fab, scFv and Fv fragments.

The Fab fragment of antibody is monovalent capable of binding to antigen and contains light chain associated to variable and CH1 portions of heavy chain by disulfide bond. The scFv fragment containing the whole antigen-binding site, consist of only VH and VL covalently connected by glycine-serine linker.

1.3.2 Immunoglobulin Diversity

The DNA encoding the constant and variable regions of Ig chains are separated in the germ line. Somatic rearrangements take place during B cell development to form the genes that, expressed as surface bound and secreted Igs. The heavy chain variable domain is encoded in three different genetic elements, variable heavy (VH), diversity heavy (DH) and joining heavy (JH) gene segments. These regions are brought together to generate a functional gene by DNA rearrangement (Paul 2003; Mochizuki, Nakamura et al. 2011).

All the gene segments comprising the heavy and light chains are present in several copies, and the extensive variation observed in immunoglobulin variable regions comes from the different combinations of these multiple genes (Fig 1.10)(Christoph and Krawinkel 1989). The joining of different parts in the recombination is inaccurate, which give possibility for more variability.

The final source of variability, somatic hypermutation, takes place in secondary lymphoid organs after a given B cell has encountered antigen. Under the influence of T cell help and specific environmental conditions found in germinal centres, this process may creates point mutations at a very high rate in the rearranged V regions (Neuberger and Milstein 1995; Paul 2003; Mochizuki, Nakamura et al. 2011)

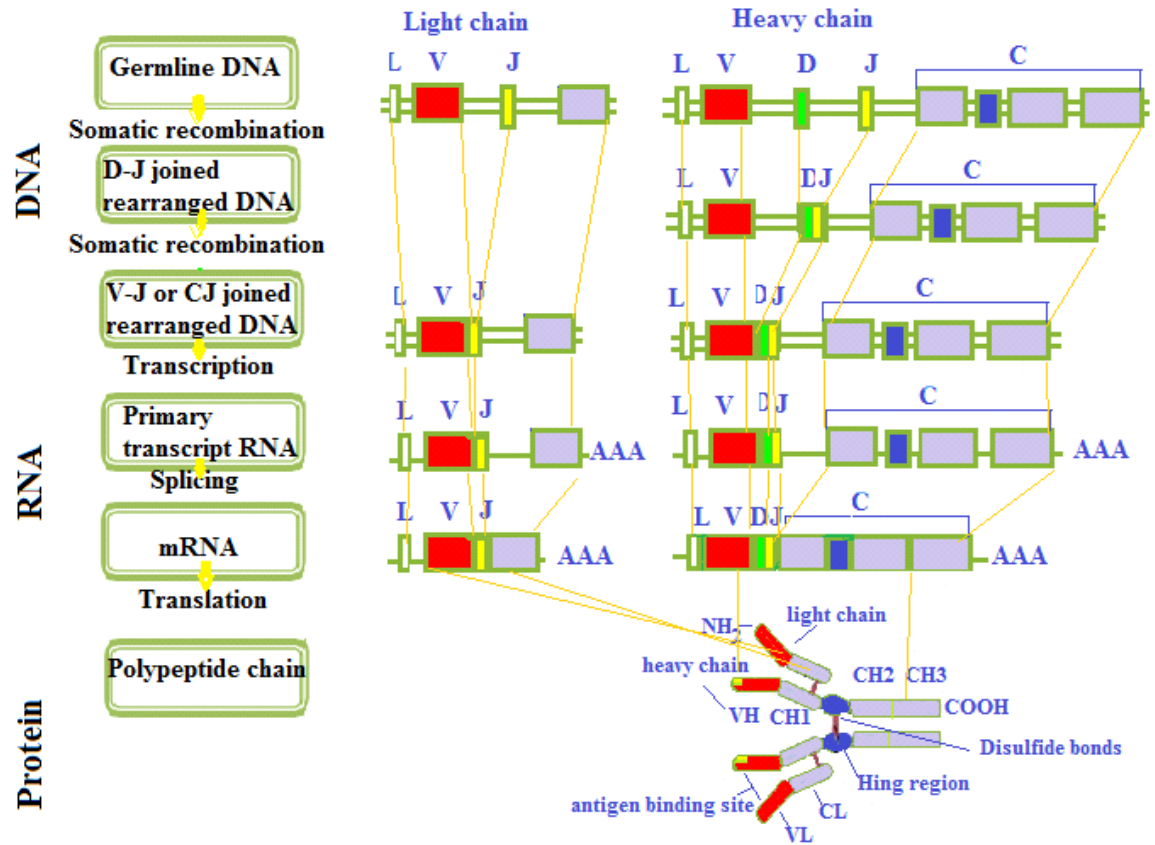


Figure 1.10 Construction of V-region genes from gene segments.

Construction of light-chain V-region genes from two segments (center panel). A joining (J) gene and variable (V) gene part in the genomic DNA are joined together to form a light-chain V-region exon.

1.4 Antibody Engineering

1.4.1 Introduction

Antibodies are used in science and medicine as marker molecules. The specific properties of antibodies binding are used for the identification of antigens under study in the laboratory and in diagnostic tests. Antibodies are also used for purification of biomolecules for both therapeutic and diagnostic application in vivo (Li, Janda et al. 1994). The low toxicity and specificity of antibodies give a hopeful innovative plan for treatment of a range of diseases (Berger, Shankar et al. 2002). The production of antibodies was a very difficult and time consuming procedure involving immunization of animal and/or generation of hybridoma. Recombinant antibodies are used in a number of applications in medicine. For a number of reasons, antibody engineering is performed including minimise immunogenicity, improving antibody generation through bacterial expression, improving pharmacokinetic profile and modifying for novel effector functions (Holliger and Bohlen 1999). A range of recombinant technologies have now assisted the genetic strategy of immunoglobulin. Three important approaches are available to the modification of antibodies for certain applications: humanization of antibodies, size reduction, and binding modulation (Hoogenboom and Winter 1992). The development of phage display vectors (Smith 1985) and successful expression of antibody fractions in *E. Coli* (Better, Chang et al. 1988) introduced the possibility of antibody engineering. The construction of phage display combinatorial libraries presenting human antibody fragments on the surface of bacteriophage as single chain Fragment variable region (scFv)(McCafferty, Griffiths et al. 1990) or Fab fragments (Barbas 1991; Barbas, Kang et al. 1991) permitted the direct selection of such libraries for antigen-binding clones. This work has stimulated interest in the production and modifications of recombinant antibodies as production of bivalent or bispecific recombinant antibody fragments, the production of antagonised antibodies (Zaghouani, Steinman et al. 1993). The selecting antibodies from phage libraries considered as the main advantages especially with the antigens that can give difficulties in the immunization e.g. unstable or auto antigens. The construction of antibody parts in *E. coli* has many advantages like, the possibility of labelling the antibody fragment for structural studies. Size reduction also has several advantages as can be seen in the

structure of the antibody molecule. The recombinant phage antibody system has been adapted to clone different fragments of antibody (e.g. scFv and Fab) and to express and detect functional antibodies.

1.4.2 Combinatorial Antibody Library Technology

With the improvement of molecular biological methods efforts were made to develop the value of monoclonal antibody reagents by the expression of modified antibody molecules in recombinant forms. In the beginning, antibody genes which obtained from hybridomas were expressed in mammalian cells as whole antibodies (Neuberger 1983) or in bacteria as antibody fragments (Cabilly, Riggs et al. 1984). A number of other systems including insect cells (Hasemann and Capra 1990), yeast (Wood, Boss et al. 1985), Chinese hamster ovary cells (Wood, Dorner et al. 1990), transgenic plants (Hiatt, Cafferkey et al. 1989) and lymphoid cells (Shu, Qi et al. 1993). Each one of those expression systems has advantages and disadvantages. Bacterial systems generally well for the expression of Fv and Fab fragments but poor in the expression of whole antibodies.

At first, the combinatorial immunoglobulin technique began by using a lambda (λ) phage vector for cloning and expression of H-chain and L-chain genes. Then this library binding a target antigen tested by plaque lift for clones (Burton and Barbas 1994). This method evolved from two key developments. Firstly, it was demonstrated that the Fv antigen binding fragments could be expressed and functionally assembled in *E. coli* (Skerra and Pluckthun 1988). Secondly, the development of the polymerase chain reaction (PCR) allowed for the rapid cloning of antibody genes from hybridomas (Orlandi, Gussow et al. 1989) and mixed populations of antibody-producing cells, even in the case of limiting cell numbers. Initially libraries were expressed in λ phage, a lytic phage that releases the periplasmically sequestered Fab into the plaque of lysed host bacteria (Huse, Sastry et al. 1989). These libraries were screened by transfer of recombinant Fab onto nitrocellulose filters, which were then probed with I¹²⁵-labelled antigen. Subsequently (Persson, Caothien et al. 1991) used human peripheral blood lymphocytes from an individual recently boosted with tetanus toxoid to construct an

IgG₁K library in a lambda vector. The antibodies generated in this case showed considerable sequence diversities and affinities in the range of 10^{-7} - 10^{-9} nM. Recent boosting proved important, as it was not possible to isolate antigen-specific Fabs from an individual with a high anti-tetanus toxoid titre who had not been boosted. This was probably related to the frequency of antigen-specific plasma cells, with their high concentration of specific mRNA, in boosted subjects (Lum, Burns et al. 1990). A significant limitation to the lambda phage screening procedure was the size of the library antibodies would require an examination of a minimum of 10,000 filter lifts (assuming 50,000 plaques per plate). It is also important to remember that the VH and VL chain permutations are randomised in the cloned library and a particular combination may be present at only a low frequency. This problem is particularly exacerbated in the absence of booster immunisation. Furthermore, the screening procedure places restrictions on the antigens which are being examined in that the native antigen must be available in significant quantities, sufficiently pure, and be amenable to labelling with I¹²⁵ or conjugation to enzymes.

1.4.3 Phage Display antibody Techniques

In general the selection is a more efficient than screening, and the next advance in the field of recombinant antibody library technology was to develop a system analogous to the B cell selection and maturation process observed in the native immune system. This was achieved by the coupling of antigen recognition and B cell selection and proliferation, or more simply, the linkage of phenotype to genotype.

It was shown in 1985, that they could incorporate short peptides into the f1 filamentous phage genome, and expressed on the phage without interference with the it's life cycle (Smith 1985) . In the beginning it was applied for mapping immunoglobulin epitopes by expression of 10^7 - 10^8 clones (large libraries) of random peptides (Parmley and Smith 1988; Scott and Smith 1990). Consequently it was established that the antibody fragments can be expressed successfully in the filamentous phage system and maintain their binding properties to the antigens (McCafferty, Griffiths et al. 1990; Barbas 1991). Unlike the λ lytic phage system, the filamentous phage life cycle allowed the use of the

biopanning technique of very large highly diverse libraries to enrich specific antibody clones.

The finding of the possibility of the expression of functional antibody fragments on the surface of filamentous phage was an important advance in recombinant antibody engineering. Derivatives such as the "single chain fragments variable" (scFv), the "fragment variable" (Fv), and the "fragment antigen binding" (Fab), can be expressed and then secreted into the bacterial periplasm of the bacteria in the oxidative environment, where they can be processed in a way that is similar to the process taking place in the endoplasmic reticulum, mainly in terms of disulfide bond formation (Skerra and Pluckthun 1988). Recombinant antibody technology developments enable fast, easy and efficient modification and expression of the antibodies.

The Fv fragment is the smallest and heterodimeric part which contains the antigen binding site, and is composed of the variable domains of the light and heavy chain (VL and VH, respectively). Variable domain is made up of a conserved β -sheet framework. The binding site is composed of the CDR regions, six in total, and three to each domain. In contrast to Fabs in which interchain disulfide bonds hold and stabilize the heterodimers together and, the Fv is unstable because the VL and VH domains are non-covalently connected (Webber, Reiter et al. 1995). VL and VH domains in synthetic single-chain fragments (scFv) are covalently bonded by a peptide linker (Webber, Reiter et al. 1995), which fuse either the N-terminus of VL and C-terminus of VH or vice versa.

1.4.4 Structure and Genetics of Filamentous Phage

The M13, f1 and fd filamentous bacteriophages having similar genomic structure (Fig 1.11). They can infect *E. coli* by a specific interaction among the phage and the bacterial pilus. In general the phage have a ssDNA genome, which about 6.4 kb, and its shape are cylindrical with a length which can differ with the size of the enclosed genome and a diameter of 650 nm (Simons, Konings et al. 1981). The coat is composed of around 2,700 copies of protein VIII which forms a shell around the genome (Simons, Konings et al. 1981). pVII, pIX, pIII and pIV present only at 3 to 5 copies per virion, (Simons, Konings et al. 1981). Coat protein III (cpIII) has two domains, a carboxyl-terminal domain that integrates into the phage structure and an amino-terminal domain which important for phage infectivity. Unlike λ phage, in which the first repertoire cloning experiments were performed, Fd phage are not assembled in the cytoplasm and are not released by cell lysis. They are instead extruded through the outer membrane leaving the cell intact. Bacteriophages are extruded as they are assembled in the bacterial membrane. Since both pIII and pVIII are secreted and anchored in the periplasmic space of *E. coli* and are assembled to form the surface of the phage, they are ideal targets for fusion with antibody domains. Several systems have now been produced for the surface expression of Fab or Fv fragments on the surface of filamentous phage. The majority of these use pIII fusions (McCafferty, Griffiths et al. 1990; Barbas, Kang et al. 1991), although pVIII fusion vectors, giving polyvalent antibody display, have also been constructed (Kang, Burton et al. 1991).

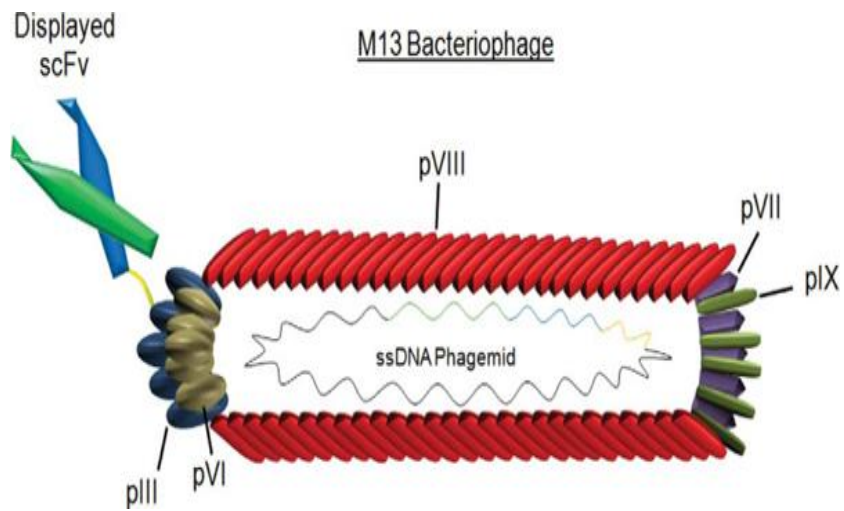


Figure 1.11 The structure of filamentous phage.

A single stranded circular genome is surrounded by ~2700 copies of the major coat protein 8, and 4 or 5 copies of each of four types of minor coat proteins, including pIII.

1.4.5 Biopanning technique

Biopanning is the process by which phage expressing desired specificities and binding characteristics are enriched from a library of phage displaying a diverse pool of biomolecules. This process usually involves a progressive reduction in diversity of phage library over repeated round of panning (Cortese, Monaci et al. 1995). The panning process generally involves immobilizing a target molecule onto a solid surface, exposing the immobilized target molecule on the phage library and eluting phage that bind (Fig 1.12). The eluted phage are usually amplified by infecting *E. coli* and again panned on the immobilized molecule, to enable further enrichment of specifically-binding phage.

1.4.6 Applications of Antibody Phage Display

These systems have provided the opportunity for production of human antibodies directly from libraries, with the possibility of mutating and then selecting for antibodies with desired properties (Winter and Milstein 1991; Burton 1993). In human organ-specific diseases, the phage display technique has been used to identify disease-associated autoantibodies in primary biliary cirrhosis, myasthenia gravis and insulin-dependent diabetes mellitus. In systemic autoimmune disease, this approach has been used successfully to clone autoantibodies against UI RNA-associated A protein in SLE by using semi-synthetic as well as patient-derived combinatorial libraries (de Wildt, Finnern et al. 1996)

1.4.7 Phage Display in the Analysis of Autoimmune Thyroid Disease

Initially, a λ library approach was used to probe the TPO autoantibody repertoire in GD. Using mRNA from thyroid-infiltrating lymphocytes, an IgG₁ library was constructed in λ phage and screened to identify Fabs with high affinities (around 0.1 nM) for TPO (Portolano, Seto et al. 1991; Portolano, Chazenbalk et al. 1992). These Fabs were able to inhibit a high proportion (36-72%) of serum TPO Abs from 11 patients with AITD, implying that the epitope recognised was of major significance. At the same time, (Hexham, Persson et al. 1991; Hexham, Furmaniak et al. 1992) utilised the same approach to construct an IgG library from the thyroid tissue of a HT patient and isolate

a high affinity TPO antibody. All the above studies were carried out using the λ phage system and screening with radiolabeled purified human TPO.

The introduction of the filamentous phage display methodology has had wide application in the analysis of human autoimmunity. In contrast to the λ phage system, in which the recombinant Fab is released into solution and not physically attached to the viral particle, highly diverse patient antibody repertoires can be readily enriched on a range of antigen preparations, including pure antigen, peptides, and even cell surfaces. Using the pComb3 phage display system three Fabs with high affinities for TPO were derived from a thyroidal library of a HT patient (Hexham, Partridge et al. 1994).

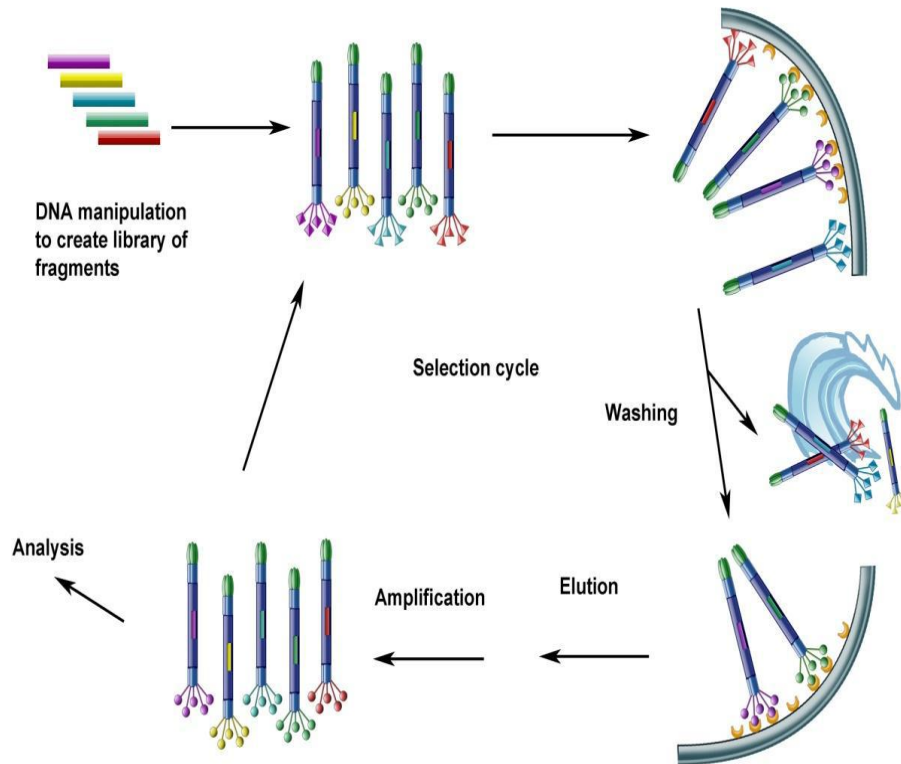


Figure 1.12 Phage display cycle.

The isolation of a specific phage for its binding to a target guides to the isolation of the corresponding gene, while the unbound clones are removed from the selection. Five rounds of selection can be made, the end result of the enrichment, production of phages that are represented in low numbers in the original library.

1.5 Hypothesis

Phage display is a powerful technique for the isolation of further examples of monoclonal antibodies to thyrotropin receptors.

1.6 Aims

- Clone the recombinant human M22 scFv into a phage vector and verify that we had synthesised the correct scFv by characterising the binding and thyroid stimulatory activities of the construct
- Investigate the binding of the M22 scFv phage construct to TSHR (BRAHMS tubes), and use the data obtained to design panning protocols to recover TSHR antibodies from phage antibody libraries.
- Clone the recombinant human M22 Fab into pComb and verify that we had synthesised the correct scFv by characterising the binding and thyroid stimulatory activities of the construct.
- Investigate the binding of the M22 Fab phage construct to TSHR (BRAHMS tubes)
- Investigate the use of different TSHR expression systems to optimise binding of phage antibodies. Finally we will use the results obtained to attempt the isolation of novel examples of TSHR antibodies and analyse the properties of these reagents.
- construct a novel cell line in which a smaller region of the TSHR.
- Production of Anti-Idiotypic Antibodies Targeted Against the M22 s Chain.

CHAPTER 2

MATERIALS AND METHODS

2.1 Materials

2.1.1 Plasmids, Bacterial Strains, and Phage

Plasmid	Source
pAK100	Prof. A Pluckthun, University of Zurich, Institute of Biochemistry
pAK400	Prof. A Pluckthun, University of Zurich, Institute of Biochemistry
pComb3	Prof CF Barbas, Scripps Research Institute, La Jolla, CA, USA
pET-21a(+)	Novagen
pcDNA3	Invitrogen

2.1.2.1 *pCOMB3*

The vector pComb3 was used in this study to clone and express Fab antibodies for phage display (Barbas, Kang et al. 1991). The plasmid expresses immunoglobulin heavy and light Fab chains from two separate lacZ promoters. Each chain is preceded by a pelB secretion leader which directs the expressed chains to the bacterial periplasm, where the redox environment favours disulphide bond formation and assembly of Fab fragments. The heavy chain is inserted upstream of the coding region for phage coat protein cpIII and is expressed as a N-terminal cpIII fusion, leading to incorporation of functional Fab onto the phage surface, Fig. 2.1.

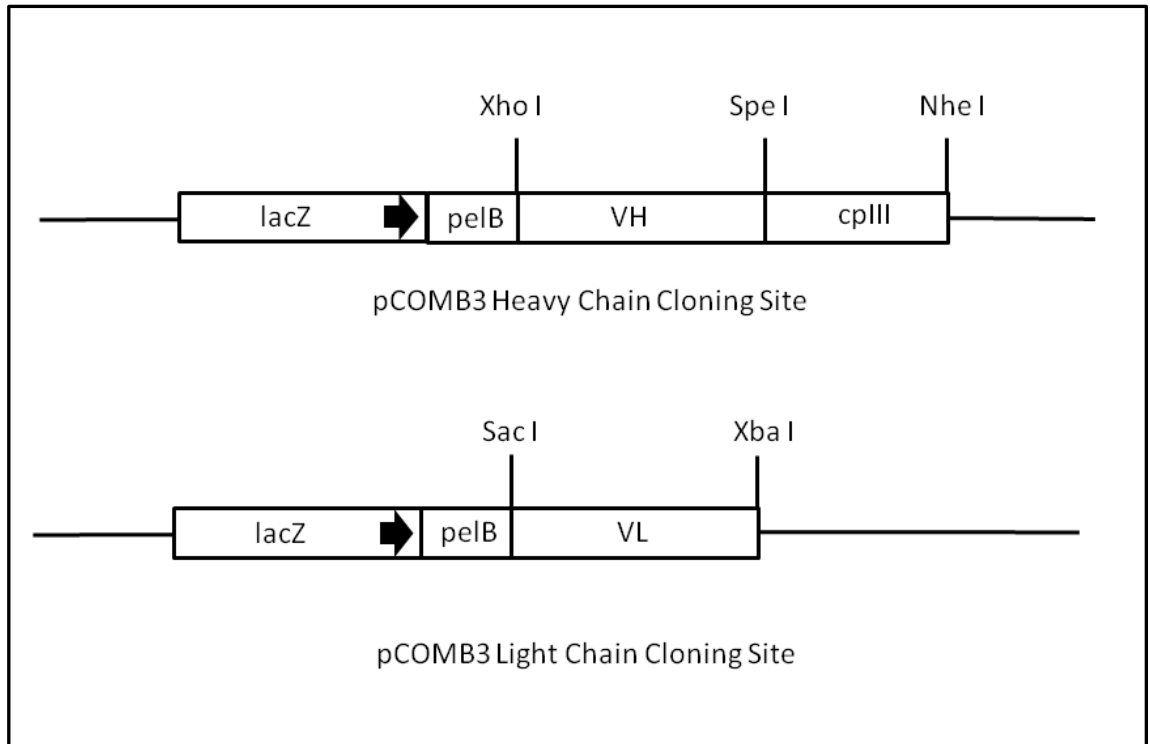


Figure 2.1 Cloning sites of phage display vector pComb3.

Immunoglobulin heavy chains are cloned into the Xho I and Spe I sites and expressed as amino terminal fusions with phage protein cpIII. Light chains are cloned into Sac I and Xba I sites. Expression of both chains is driven by a lacZ promoter and secretion into the periplasm is directed by a pelB secretion leader.

2.1.2.2 pAK100

This vector was designed to allow the expression of scFv on the surface of filamentous phage (Knappik and Pluckthun 1994). Single chain Fv fragments are expressed from a lacZ promoter as N-terminal fusions with a segment of the cpIII gene of filamentous phage. Fusion proteins are expressed into the periplasm via a pelB secretion leader and incorporated into nascent virions. Antibodies are cloned into two Sfi I restriction sites with non-complementary overhangs (Fig. 2.2). The vector features a 2 kb tetracycline resistance stuffer fragment which is inserted into the Sfi I sites and is replaced by cloned scFv genes.

2.1.2.3 pET21a

High level expression of recombinant proteins was achieved using the T7 expression vector pET21a (Novagen). The essential features of the vector are shown in Fig. 2.3.

2.1.2.4 pcDNA 3.1

Mammalian expression vector with a selectable resistance marker to ampicillin, and contains promoters for T7 and SP6 polymerases flanking a diverse multiple cloning site (Fig. 2.4).

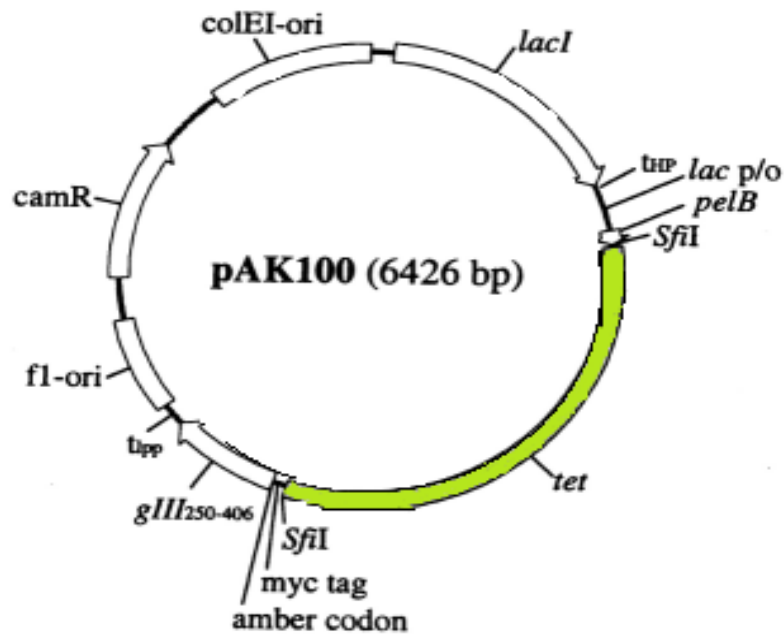


Figure 2.2 Map of pAK100 vector.

The tetracycline-resistance cassette is used as a stuffer fragment (approximately 2000 bp) that is replaced by cloned scFv genes. In pAK100 scFv genes are expressed as fused to the coding region of phage minor coat protein *cplIII*. The myc tag is expressed as a carboxy-fusion and facilitates the detection and purification of expressed scFv fragments. Between the myc tag and *cplIII* there is an amber stop codon and this allows expression of myc-tagged soluble scFv protein in a non-suppressive host. The inset shows the key differences between pAK100 and pAK400. In pAK400 the phage coat protein coding region is absent as is the myc tag. These are replaced with a carboxy-terminal 6-histidine tag for protein purification.

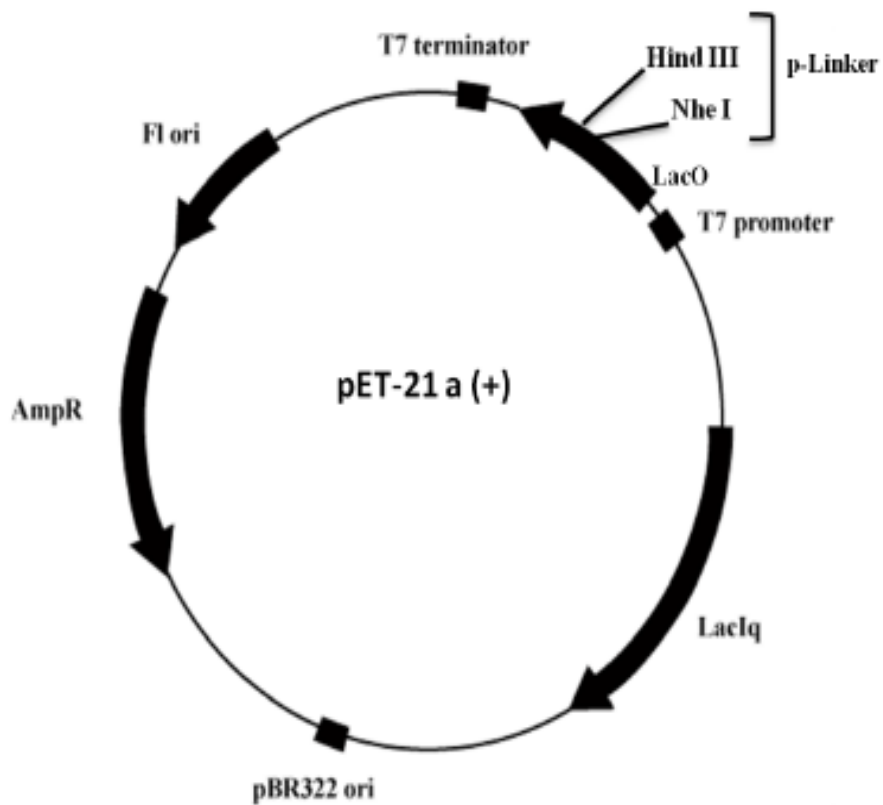


Figure 2.3 Cloning regions of the pET21a T7 expression vector.

Coding sequences are cloned into the multiple cloning sites downstream of the T7 promoter. The vector features an optional T7-tag and a [His]6 purification tag at the carboxy terminus. Expression is achieved by transformation into an appropriate host expressing T7 RNA polymerase.

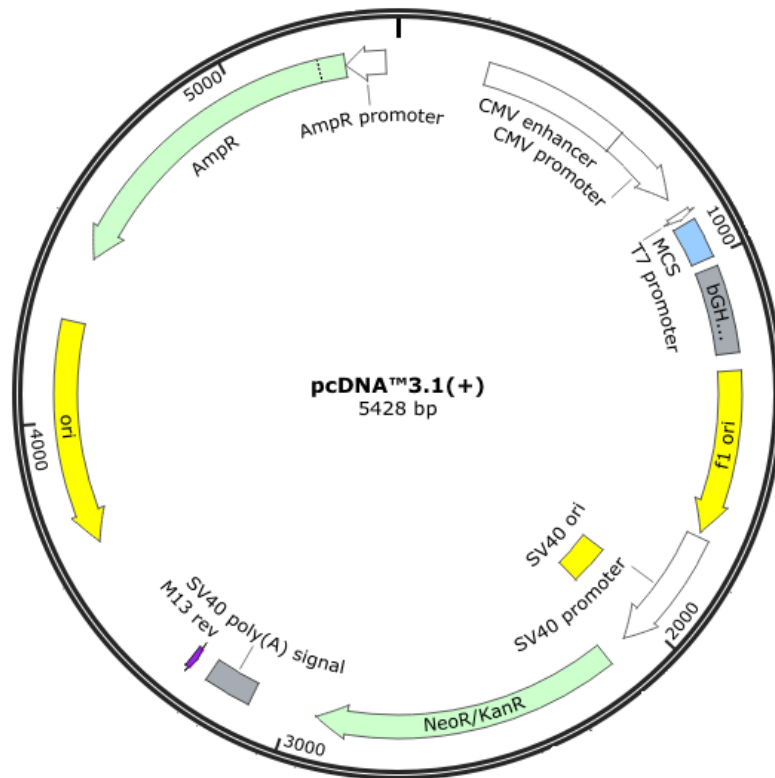


Figure 2.4 Mammalian expression vector pcDNA3.

Mammalian expression vector contains CMV promoter and allows high level transient and stable expression in mammalian cells

2.1.3 Bacterial Strains and Helper Phage

	Genotype	Source
XL1-Blue	$\Delta(mcrA)183 \quad \Delta(mcrCB-hsdSMR-mrr)173$ endA1 supE44 thi-1 recA1 gyrA96 relA1 lac[F' proAB lacI ^q Z Δ M15 Tn10(Tet ^r)]	Stratagene, La Jolla, CA, USA
VCSM13 helper phage	Kan ^r	Stratagene, La Jolla, CA, USA
BL-21(DE3)- pLysS	F ⁻ ,ompT, hsdS _B (r _B ,m _B -)dcm,gal, λ (DE3),pLys, Cm ^r	Promega

2.1.4 Media

Bacterial growth media, which we used, are shown in the following table:

Media	Content
SOC medium	0.5% (w:v) yeast extract 2% (w:v) tryptone 1mM MgSO ₄ ·7H ₂ O 10mM NaCl 1mM MgCl ₂ ·6H ₂ O 2.5mM KCl 2mM glucose
Luria-Bertani (LB) medium	1% (w:v) tryptone, 85.6mM NaCl, 0.5% (w:v) yeast extract
Luria-Bertani (LB) agar plates	0.5% (w:v) yeast extract 85.6mM NaCl 5% (w:v) agar 1% (w:v) Tryptone Selective antibiotic

2.1.5 Antibiotics

All antibiotics were prepared as 1000x stocks, sterilised by filtration (Millipore) and used in medium at the final concentrations shown below. All antibiotics were obtained from Sigma Aldrich.

Antibiotic	Diluent	Final Concentration	Source
Ampicillin	H ₂ O	100 µg/ml	Sigma-Aldrich
Tetracycline Hydrochloride	50% ethanol/ H ₂ O (v:v)	20 µg/ml	Sigma-Aldrich
Kanamycin	H ₂ O	30 µg/ml	Sigma-Aldrich
Chloramphenicol	50% ethanol/ H ₂ O (v:v)	30 µg/ml	Sigma-Aldrich

2.1.6 List of the cell lines and materials used in the tissue culture

Material	Source
Chinese hamster ovary cells(CHO-K1)	European Collection of Animal Cell Culture (ECACC), Porton Down, UK.
JP09	Prof. G Vassart, Institut de Recherche Interdisciplinaire en Biologie Humaine et Moléculaire, Faculté de Médecine, Université Libre de Bruxelles, Belgium
GPI-95	Dr. P Watson (school of medicine, University of Sheffield)
Mouse hybridoma A9 and A10	Dr. JP Banga, Guys, King's, and St Thomas' School of Medicine, London
Sterile Dulbecco's minimal essential medium (DMEM) and foetal calf serum (FCS).	Gibco BRL, Paisley, UK.
Cell dissociation solution	Gibco (Invitrogen Corp.)
Sterile trypsin (0.25%) Ethylene Di-amino Tetra Acetic acid (EDTA solution, Cat. 0180).	Sigma-Aldrich Company, Irvine, Ayrshire, UK.
T25 and T75 tissue culture flasks (Cat. Nu. 156367 and156499 respectively).	Nunc™, Roskild, Denmark.
Tissue culture sterile 6, 12, 24 and 96 well plates.	COSTAR®, Corning, USA.
Tissue culture Petri dishes (100mm, Cat. Nu. 150350).	Nunc™ (Thermo Scientific), Roskild, Denmark.

2.1.7 Western blotting materials

Material	Source
PVDF membrane (GE Healthcare, Amersham Hybond-P PVDF membrane optimized for protein transfer, pack nu. RPN1416F).	GE Health care.
TEMED	BDH, Poole, England (4430833)
Sodium dodecyl sulphate (cat. Nu. 444464T)	BDH, Poole, England.
Tris (hydroxymethyl) methylamine AnalaR® (cat Nu.	BDH, Poole, England.
Tris/glycine/SDS running buffer 10X (Cat. Nu. 161-0732).	BIO-RAD laboratories, München.
SDS-PAGE Transfer Buffer 10X	BIO-RAD laboratories, München.
Acrylamide/Bisacrylamide	BioRad
Ammonium persulphate 2% (v: w) ammonium persulphate was made in sterile deionised H ₂ O	BDH, Poole, England (443073E)

Constituents of Polyacrylamide Resolving and Stacking Gel

Running (Resolving) gel							Stacking gel 1.5%	
	10%		12%		15%		1 x	2 x
	10ml	20ml	10ml	20ml	10ml	20ml	(10 ml)	(20 ml)
Sterile H₂O	3.3 ml	6.6 ml	4.3 ml	8.6 ml	3.55 ml	7.1 ml	2.22 ml	4.45 ml
Acrylamide 40% w:v	2.3 ml	4.6 ml	3.0 ml	6.0 ml	3.75 ml	7.5 ml	375 µl	750 µl
1.5 M Tris, pH 8.8	2.5 ml	5.0 ml	2.5 ml	5.0 ml	2.5 ml	5.0 ml	0 µl	0 µl
1 mM Tris, pH 6.8	0 ml	0 ml	0 ml	0 ml	0 ml	0 ml	380 µl	760 µl
SDS - 10%	100 µl	200 µl	100 µl	200 µl	100 µl	200 µl	30 µl	60 µl
APS - 10%	100 µl	200 µl	100 µl	200 µl	100 µl	200 µl	30 µl	60 µl
TEMED	4.0 µl	8.0 µl	4.0 µl	8.0 µl	4.0 µl	8.0 µl	3 µl	6 µl

APS = Ammonium per-sulphate (Freshly prepared), TEMED = N, N, N', N'-tetramethylethylenediamine, SDS = Sodium dodecyl sulphate.

Secondary Antibodies

Anti-human IgG, (Fab specific)	Amersham Pharmacia Biotech
F (ab) ₂ rabbit anti-mouse IgG-Biotin	Serotec
Rabbit anti-mouse IgG-HRP	Amersham Pharmacia Biotech

2.1.8 General Laboratory Solutions and Reagents

	Content	
Elution Buffer	Glycine	3.755 g
	H ₂ O	500ml
	pH	adjusted to 2.7
Phage precipitation solutions		
	40% PEG	
	PEG 8000	200 g
	H ₂ O	500ml
5M NaCl	NaCl	146.1g
	H ₂ O	500ml
Coating Buffer	Na ₂ HCO ₃	2.93 g
	Na ₂ CO ₃	1.59g
	NaN ₃	0.2 g

	H ₂ O	1 L
	pH	adjusted to 9.2
Neutralizing Buffer	Tris Base	2.42 g
	H ₂ O	10 ml
Tris-HCl	Tris-HCl	60.55 g
	H ₂ O	500 ml
	pH	adjusted to 8.0
PBS (10x)	NaCl	80 g
	KH ₂ PO ₄	2.4 g
	Na ₂ HPO ₄	14.4 g
	KCl	2 g
	H ₂ O	1 L
50 X TAE buffer	EDTA	50 ml
	Tris base	121g
	Acetic acid	28.6ml
	H ₂ O	500 ml

2.2 Methods

2.2.1 RNA Extraction

Total RNA was extracted from cells using Trizol. Prior to the experiment, all pipettes to be used were incubated under a UV light for 10 min to minimize the DNA contamination. Cells were homogenized by the addition of 1 ml of Trizol and incubated at 37°C for 5 min. This was followed by the addition of 400 µl of chloroform, and centrifugation for 10 min at 8,000 g to separate the upper phase and RNA precipitated with isopropanol and pelleted by centrifugation at 13,000 g for 10 min. The supernatant was disregarded, while the pellet washed with 1 ml of 70% ethanol and centrifuged for 10 min at 8,000 g. The pellet was finally resuspended in 40 µl of DEPC-treated distilled water.

2.2.2 Synthesis of cDNA

Total RNA was used to synthesize cDNA using Moloney murine leukemia virus reverse transcriptase (MMLV-RT) (Promega) in a 60 μ l reaction containing:

RNA (approx 1 μ g)	5 μ l
dNTPs (100mM)	6 μ l
Reverse transcriptase (200 U/ μ l)	6 μ l
Reverse transcriptase buffer (5X)	12 μ l
Random oligonucleotide hexamers (0.5 μ g/ μ l)	1 μ l
DEPC-H ₂ O	30 μ l

The mixture were incubated at 37°C for 5 min and then incubated at 40°C for 1 h, followed by 75°C for 10 min incubation, cooled down to 4°C.

2.2.3 Polymerase Chain Reaction (PCR)

PCR performed on many templates depending on the DNA to amplify. Prior to the experiment, all pipettes to be used were incubated under a UV light for 10 min to minimize the DNA contamination

Each reaction contained the following (Promega):

Mg ²⁺ buffer (25 mM)	5 µl
Promega reaction buffer (10X)	10 µl
dNTPs (10 µM)	1 µl
Primer mixture (1 µM each) 0.02 µM	2 µl
Sterile distilled H ₂ O	34 µl
Tag polymerase (5 U/µl)	0.25 µl

The standard PCR parameters (unless stated in the results text) were as follows:

Event	Temperature	Time	Cycles
Initial Denaturation	95°C	5 min	1 cycle
Denaturation	95°C	30 s	n cycles
Primer annealing	x°C	30 s	
DNA extension	72°C	1-2 min	
Final extension	72°C	10 min	1 cycle
Final hold	4°C	As required	1 cycle

2.2.4 Agarose Gel Electrophoresis

Gel electrophoresis was used qualitatively to check the DNA preparations. Agarose gels (1%) was dissolved in TAE buffer and melted for 1 minute in a microwave oven. The molten agarose was cooled and ethidium bromide added. The molten agarose was poured into the casting deck, combs inserted and the agarose left to set. Once it set, the combs removed and covered with TAE buffer and 5 µl of PCR reaction was loaded into each well. A molecular weight marker lane was included; a voltage of 60-100 V was applied for 15-60 min. The agarose gel was visualized on a UV transilluminator and photographed.

2.2.5 Purification of DNA fragments and PCR Products

PCR products were extracted using the PCR Prep kit (QIAquick kit) according to the manufacturer's instructions (Qiagen). In brief, gel slices or PCR reactions were mixed with 700µl membrane binding buffer and incubated at 50°C until complete dissolving. The dissolved gel slices were passed through a column then washed with 700 µl and 250 µl of washing buffer respectively. The excess wash solution was removed by centrifugation at 8,000 g for 2 min and eluted with 60 µl of TE.

2.2.6 Phenol-Chloroform Extraction of DNA

The DNA solution was made up to 200 µl in TE buffer and 200 µl of phenol:chloroform (1:1 v:v) (Fisher scientific) was added, mixed well and centrifuged for 10 min at 13,000 g. The top layer was removed, avoiding the interface, transferred to a fresh tube and an equal volume of chloroform was added. The mixture was vortexed and then centrifuged at 8,000 g for 10 min and the top aqueous layer recovered. Purified DNA was precipitated with 2 volumes of ethanol and centrifuged at 8,000 g for 20 min. The supernatant was removed and the pellet dried and resuspended in TE buffer.

2.2.7 Restriction Digest of DNA

A typical digestion reaction is shown below:

Component	Volume
DNA	500 ng-1 µg
Restriction enzyme buffer (10x)(Promega)	2 µl
Restriction enzyme (10u/µl) (Promega)	1 µl
Sterile water to a final volume of	100 µl

For double digestion, the compatibility is checked according the manufactures' charts. If two enzymes were known to have 100-75% activity in the same buffer, then double digestion of the DNA was carried out in a single reaction. Digestion reactions were incubated according to the manufacturer's instructions. To ensure correct digestion of each reaction a sample of known volume was mixed with the appropriate volume of 6X DNA agarose gel loading buffer and analysed by agarose gel electrophoresis.

2.2.8 Ligation of DNA

A typical ligation reaction as follows:

Component	Volume
Insert	60 ng
Vector	100 ng
DNA ligase	0.5-1 µl
Ligase buffer	2 µl
Sterile water to a final volume of	20µl

Reaction was incubated at room temperature for 3 h.

2.2.9 Heat Shock Transformation

50 µl aliquot of one shot *E. coli* was thawed on ice, 3 µl of cloning reaction was added to the vial and mixed gently, incubated on ice for 5 min, then transferred the tube to a preheated water bath at 42°C for 30 s without shaking. Rapidly the vial was placed on ice and allowed to chill for 2 min. 250 µl of S.O.C media was added to the contents of the tube. The culture was incubated at 37°C with shaking for 1 hour. The transformed cells were plated out onto LB agar plate containing appropriate selective antibiotic and incubated overnight at 37°C. Random colonies were picked from the plate and sub cultured into 10ml medium containing appropriate antibiotics and incubated at 37°C in shaking incubator. DNA was extracted by miniprep and tested by sequencing analysis.

2.2.10 Electroporation of XL-1 Blue

Aliquot of electrocompetent XL1- Blue cells were thawed on ice and placed in 0.1 cm cuvette. 5-10 µl of DNA or the ligation reaction to be transformed was added to the cells and mixed gently, and the cuvette placed into the electroporation machine (*E. coli* Pulser, BioRad) and a pulse of 1700 V applied. The cuvette was washed out with 1ml SOC medium (GIBCO), and transferred to a universal container, then incubate it for one hour in a 37°C with shaking. The cells were placed on selective agar media and incubated for 18 h at 37°C.

2.2.11 Preparation of Plasmid DNA (Miniprep Purification of DNA)

A single colony was picked from freshly streaked agar plate containing appropriate antibiotics. The culture was grown at 37°C with shaking over night. Then the 10 ml cultures centrifuged at 2000 g for 10 min and the pellet resuspended in 250 µl of cell resuspension solution and transferred to microcentrifuge tube. A further addition of 250 µl cell lysis buffer and the samples gently mixed prior to incubation at room temperature for 5 min and neutralised by addition of 350 µl neutralisation buffer. The mixture was centrifuged for 5 min at 13,000 g; the supernatant was passed through a mini column then washed with 700 µl and 250 µl of washing buffer respectively. DNA eluted with 100 µl of nuclease free water.

2.2.12 Isolation of Plasmid DNA by Midiprep Procedure

The Wizard midiprep kit (Promega) was used according to the manufacturer's instructions, to purify 10 µg-200 µg of plasmid. Briefly 100 ml cultures were centrifuged at 13,000 g for 1 min and the pellet suspended in 3 ml of cell resuspension solution (50 mM Tris-HCl pH 7.5, 10 mM EDTA, 100 µg/ml RNase A) the cells were lysed by addition of 3 ml cell lysis solution (0.2 M NaOH, 1% SDS) and then neutralized by addition of 3 ml neutralization solution (1.32 M potassium acetate, pH 4.8) the solution was mixed gently and centrifuged at 13,000 g for 15 min, the supernatant was mixed with 10 ml Wizard midiprep DNA purification resin and loaded onto a Wizard midi column and washed two times with 15 ml column wash solution (80 mM potassium acetate, 8.3 mM Tris-HCl pH 7.5, 40 µM EDTA, 55% ethanol). Wizard midi column was centrifuged for 2 min at 13,000 g to remove excess column wash solution and resuspended in 400 µl of sterile H₂O.

2.2.13 Chemically Competent Cell Preparation

The chemically competent *E. coli* strain XL1-Blue cells were used to transform different plasmids and they were prepared according to the following protocol. About 10 µl of the XL1-Blue glycerol stock was streaked on a fresh LB/Tet agar plate and incubated at 37°C for overnight. Next day, one well-isolated colony was picked up from the plate and grown in 2 ml of selective LB/Tet broth media for 6 h at 37°C in an orbital shaker. The cells then seeded with 0.5ml of the bacterial culture into 50 ml LB/Tet media and returned to the 37°C shaker for overnight. Next day, 30 ml of the overnight culture were transferred into 400 ml of a pre-warmed LB/Amp media and grow until OD₆₀₀ = 0.9. The cells centrifuged at 4000 rpm for 20 min at 4°C in H6000 rotor. The pellet was resuspended in 100 ml of sterile and ice cold 0.1 M MgCl₂ solution and re-centrifuged again. The pellet resuspend in 100 ml of a sterile and ice cold 0.1 M CaCl₂ and left on ice for 1 hour before another spin. The pellet was finally resuspended in 25 ml of 85 mM CaCl₂ plus 15% glycerol and aliquoted into chilled 1.5 ml eppendorf tubes (400 µl/tube) and frozen immediately in liquid nitrogen. Cells were then stored at -80°C.

2.2.14 Preparation of Bacterial Glycerol Stocks

Glycerol stocks were prepared by mixing 1 volume of culture with 1 volume of 50% glycerol and stored at -80°C.

2.2.15 Rescue of Library Displaying Phage

Library rescue describes the process by which phage libraries are converted into phage particles prior to enrichment. 10 ml LB media contain an appropriate antibiotic inoculated with 10 µl of glycerol stock of cells that contain cloned antibody fragments (scFv or Fab) and grown at 37°C. After the culture becomes turbid, 15 µl VCMS13 helper phage (10^{11} plaque forming units (pfu)/ml) (Stratagene) was added and incubated at 37°C for 15 min. The culture was then transferred to 100 ml LB medium containing appropriate selective antibiotics and grown at 37°C overnight. The culture was centrifuged for 15 min at 2000 g. Supernatants were transferred into a 100 ml glass measuring cylinder containing 10 ml of 5 M NaCl and 10 ml of 40% PEG 4000, mixed and incubated on ice for 2 h to precipitate the phages. The mixture was centrifuged for 30 min at 2000 g to harvest the phages and the pellet resuspended in 1 ml of PBS/Tween. Stocks with titres of 10^{10} - 10^{11} colony forming units (cfu)/ml typically were obtained in this way.

2.2.16 Preparation of Host Cells

10 µl of commercial XL1-Blue glycerol stock added to 10 ml LB medium containing appropriate antibiotics. The culture was incubated at 37°C with shaking until become turbid (4-6 h).

2.2.17 Titration of Phage Library

The phage library was diluted serial dilution and 5 µl of 10^{-4} phage were used to infect 1 ml of fresh host cells at 25°C for 20 min. 10 µl of infected host cells were plated on agar plates containing appropriate selective antibiotics, and incubated at 37°C over night. The colonies were counted and phage titre (cfu/ml) calculated.

2.2.19 General Enrichment Procedure for Phage Display Libraries

The phage enrichment (biopanning) procedure is based on affinity selection. In general this involves the capture of phage particles that have specific ligands on their surface using a solid surface coated with a specific target. In this case library screening was carried out by immobilized antigen on ELISA wells. The ELISA well was coated overnight at 4°C of coating buffer containing 5 µg of selective ligand (immobilised IgG) or antigen. The following day the well was washed 3 times with 400 µl of PBS/Tween (0.1% v:v) and blocked for 1 h with 400 µl of 3% BSA (w: v) in PBS/Tween 1 h at room temperature. After blocking the wells were washed 3 times with PBS/Tween and 100 µl of phage library was added. The well was incubated for 1 h at room temperature the unbound phage removed by washing 6 to 8 times with 400 µl PBS/Tween. In this step particles showing low affinity for immobilized target are washed away, leaving the strongly bound particles attached to the target. The enriched population, remaining bound to the target after the stringent washing, was then eluted with acidified glycine (0.2 M, pH 2.2). The eluted phage were used to infect host and generate an enriched library. The process was assessed by monitoring the number of phage being eluted each round and in a typical enrichment procedure the elution rate increased some 50,000 fold over 3 to 4 rounds of selection (Fig 2.5).

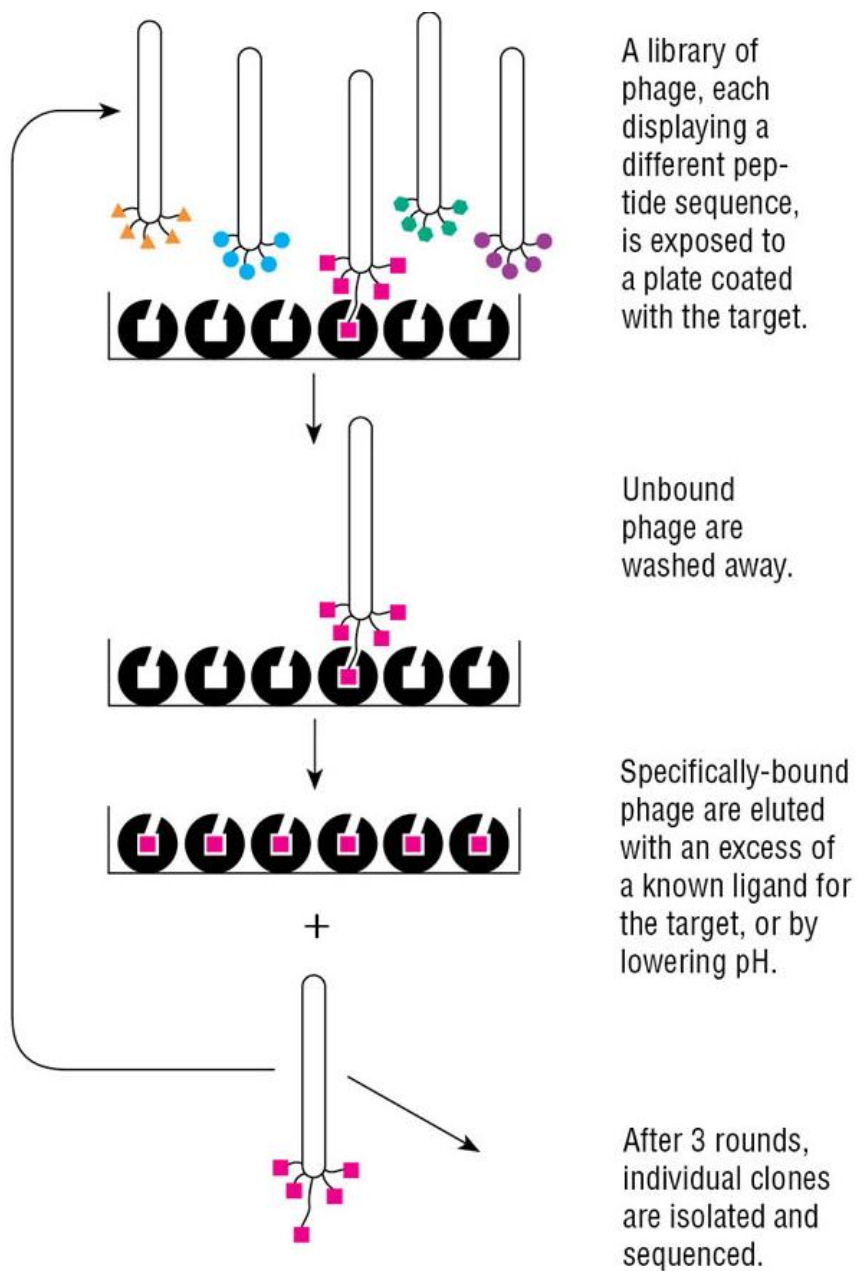


Figure 2.5 Schematic Diagram for Panning Process.

The phage display antibody enriched by affinity selection using immobilized TSH receptor. The non-bound phage washed out and the captured phage eluted and used to re-infect the host and to generate enriched library. This enrichment process was repeated 4-5 times to isolate a high affinity TSAbs.

2.2.18 High Level Expression of Recombinant Protein from pET21a

2.2.18.1 Pilot Scale Expression

Transformation of recombinant proteins was achieved by using Novagen Competent Cells (BL21 (DE3) pLysS) according to manufacturer's instruction, to express plasmid of interest from 10 ml cultures. Briefly, 50 µl of competent cells were transformed with 1 µl of the pET-21a construct and plated onto LB agar plates containing the selective antibiotics (100 µg/ml ampicillin, 34 µg/ml chloramphenicol, 1% glucose (w: v)), and incubated overnight at 37°C. A single colony was picked from freshly agar plate were used to seed 3 ml of fresh LB medium containing 100 µg/ml ampicillin, 34 µg/ml chloramphenicol, and 1% glucose. The culture was grown over 5 h in a 37°C shaking incubator set at 200 rpm. Then 10 µl of the grown culture was transferred into 10 ml of fresh LB medium, leave it grown overnight in a 37°C shaking incubator set at 200 rpm. Next day about 0.5 ml of the grown cells was transferred into 10 ml of fresh LB medium. The cells were grown at 37°C, 200 rpm until $OD_{600nm} \sim 0.4$ and expression was induced with 1 mM final concentration of IPTG (isopropyl β-D-1-thiogalactopyranoside). Cells were incubated at 37°C for 3 s post induction, and harvested by centrifugation at 4000 rpm for 10 min; the pellets were stored at -20°C. The pellets were resuspended in 250 µl of PBS with complete proteases inhibitors cocktail. Cells were then lysed with sodium deoxycholate (Sigma) final concentration of 25 mg/ml and sonicated four times for 10 s each time placed on ice. The cell lysate were then centrifuged at 13,000 rpm for 10 min and the supernatant saved as soluble fraction protein (SFP). The pellet then washed and resuspended in 250 µl of H₂O as an insoluble fraction protein (IFP). The protein fractions were then analyzed by SDS-PAGE and western blotting.

2.2.18.2 Subcellular Fraction Solubilisation Test

The pellets above resuspended 1: 10 w:v in lysis buffer 1 (25 mM Tris, 200 mM NaCl, 20 mM imidazole pH 8.0 with two mini-tablet protease inhibitor cocktail free EDTA in 50 ml), and mixture incubated on ice for 30 min. The mixture was sonicated on ice (4 X 30 sec cycles), then centrifugation at 40,000 g for 30 min and the supernatant saved as soluble protein fraction (SPF1). The pellet was resuspended 1:5 w:v in lysis buffer 2 (10

mM Tris-HCl, 10 mM DTT pH 8.0 with two mini-tablet protease inhibitor cocktail free EDTA in 50 ml), and sonicated on ice (1 x 30 s). Lysozyme was added to a final concentration of 500 µg/ml and mixture incubated on ice for 30 min. The mixture was sonicated on ice (4 x 30 s cycles), and inclusion bodies pelleted by centrifugation at 40,000 g for 30 min. The supernatant saved as soluble protein fraction (SPF 2). The pellet was resuspended in 25 ml wash buffer (10 mM Tris, 10 mM DTT, pH 8.0 with 1% Triton X100 (v:v)), and sonicated on ice (2 x 60 s cycles). Inclusion bodies were pelleted by centrifugation at 40,000 g for 30 min and wash step repeated 4 more times. An additional one washing step using H₂O instead of wash buffer were included to remove excess washing buffer. After the final centrifugation step the pellet was resuspended in 5 ml H₂O. The protein fractions and washes were analyzed by SDS-PAGE with 15% (v:v) polyacrylamide concentration.

2.2.18.3 Large Scale Expression of Recombinant Proteins

A single colony carrying the selected plasmid construct was picked from a fresh agar plate and used to seed 10 ml of fresh LB medium containing 100 µg/ml ampicillin, 34 µg/ml chloramphenicol and 1% glucose. The culture was grown over 5 h in a 37°C shaking incubator set at 200 rpm. Then 100 µl of the grown culture was transferred into 100 ml of fresh LB medium, leave it grown overnight in a 37°C shaking incubator set at 200 rpm. The next day the cultures of 100 ml were centrifuged at 4000 rpm for 3 min and the pellet was transferred in 1 L of TB media in 2.5 L flasks. The cells were grown at 37°C, 200 rpm until OD_{600nm} was approximately 0.4 and the recombinant protein was induced with 1 mM final concentration of IPTG (isopropyl β-D-1-thiogalactopyranoside) for 3 h. Cells were incubated at 37°C for 3 h post induction and harvested by centrifugation at 4000 g for 30 min; the pellets were stored at -80°C.

2.2.19 Solubilisation, Refolding and Purification of Inclusion Body Material

2.2.19.1 Inclusion Body Preparation

Inclusion bodies were prepared by enzymatic lysis: The pellet from 1 L original culture was resuspended in 100 ml ice cold breakage buffer (10 mM Tris-HCl, 10 mM EDTA,

pH 8.0), lysozyme was added to a final concentration of 250 µg/ml and mixture incubated on ice for 30 min. sodium deoxycholate was added to a final concentration of 500 µg/ml and incubated on ice for 30 min. The mixture was sonicated on ice (5 x 10 second cycles) and inclusion bodies pelleted by centrifugation at 13,000 g for 30 min. The pellet was resuspended in 10 ml wash buffer (10 mM Tris, 10 mM EDTA, 2% sodium deoxycholate, pH 8.0) and sonicated on ice (2 x 10 s cycles). Inclusion bodies were pelleted by centrifugation at 13,000 g for 30 min and wash step repeated two more times, the final wash used H₂O instead of wash buffer. Inclusion bodies were pelleted by centrifugation at 13,000 g for 30 min and the final inclusion body prep resuspended in 10 ml H₂O. Inclusion bodies were analysed by 12% SDS-PAGE, following the protocol of Laemmli (Laemmli 1970).

2.2.19.2 Solubilisation and Refolding of Inclusion Body Material

Inclusion bodies were solubilised in 100 ml ice cold solubilisation buffer (40 mM Tris, 4.5 M urea, 10 mM cysteine, pH 11.5) and stirred at 4°C overnight. The next day the solution was diluted in an equal volume of arginine buffer (40 mM Tris, 500 mM L-arginine, 10 mM cysteine, pH 11.5) to give a final arginine concentration of 250 mM. The solution was stirred at 4°C for overnight; the next day the cleared solution dialysed against 30 L of dialysis buffer (10 mM Tris, pH 9.0) at 4°C, with 5 buffer changes over a 48 h period. The success of refolding was assessed at this stage (pre-purification) by the monomeric content of the refolded protein; as determined by Coomassie stained, non-reduced 12% SDS-PAGE (Laemmli 1970).

2.2.20 Preparation of bacterial cell extracts by using osmotic shock method

Periplasmic fractions were prepared by centrifugation of the induced culture at 2000 g for 10 min, the supernatant was retained for further analysis, and the bacterial pellet was used for periplasmic extraction, using osmotic shock method. The bacterial pellet was washed twice with 20 ml of ice cold 10 mM Tris-HCl pH 8, and resuspended in 30 ml of 30 mM Tris-HCl pH 8, 20% sucrose and 60 µl 0.5 M EDTA pH 8. The suspension was stirred slowly for 15 min at room temperature then centrifuged at 13,000 g for 10

min at 4°C. The supernatant was discarded and the pellet was resuspended in 30 ml of ice cold 5 mM MgSO₄ and stirred slowly on ice for 10 min. During this step, the periplasmic proteins are released into the buffer. The mixture was then centrifuged at 13,000 g for 10 min at 4°C, to pellet the shocked cells; the supernatant containing the periplasmic fraction was collected and used for further analysis. The total cell protein was prepared by centrifugation of the culture at 2000 g for 10 min, the supernatant was removed for further analysis and the bacterial pellet resuspended in 0.1 culture volume of PBS containing protease inhibitors (Roche Diagnostic). Cells were disrupted by three freeze and thaw cycles (using liquid nitrogen and 37°C water bath) and between each freezing and thawing the cells sonicated for 8-10 bursts to lyse the cells. The membranes were pelleted by centrifugation at 2000 g for 10 min at room temperature. Supernatant containing soluble protein was retained and stored at -20°C.

All the samples fractions were concentrated under nitrogen pressure in a micro-concentrator (Amicon) and the protein content was estimated by Bradford assay and by measurement of the OD₂₈₀. All samples were stored at -20°C until required for further purification and analysis.

2.2.21 Protein purification

2.2.21.1 Purification of His-Tagged Recombinant Proteins by IMAC

Recombinant proteins were purified by one-step affinity chromatography using a Ni-MAC column (1 ml bed volume and binding up to 30 mg His-Tag fusion protein), equilibrated with 5 column volumes of 1x MAC binding buffer (300 mM NaCl, 50 mM Na phosphate, 10 mM imidazole, pH 8.0). Refolded sample was loaded onto the Ni-MAC column at a flow rate of 1 ml/min and the flow through was collected as FT fraction and stored at -80°C. The column was washed with 10 column volumes of 1 x MAC binding buffer. Then the column was washed with 6 column volumes of 1 x MAC washing buffer (300 mM NaCl, 50 mM Na phosphate, 20 mM imidazole, pH 8.0); collect the binding and washing buffer fractions as W1, W2 and stored at -80°C. Refolded proteins was eluted in a stepwise manner with 1 x MAC elution buffer (300

mM NaCl, 50 mM Na phosphate, 0.25 mM imidazole, pH 8.0), at a flow rate of 1 ml/min, collecting 0.5 ml fractions. Fractions were stored at -80°C. The monomeric and dimeric content of peak fractions was determined by Coomassie stained, non-reduced 15% SDS-PAGE (Laemmli 1970). The cleared purified protein dialyzed again against 2 L of dialysis buffer (300 mM NaCl, 10 mM Tris pH 8.0) at 4°C, with two buffer changes over a 24 h period and then the pure protein concentration was determined by Bradford assay according to manufacturer's instruction and OD_{600nm} recorded.

3.2.21.2 Purification of IgG using Protein G columns

IgG were purified from culture by using a protein G Sepharose column (GE Healthcare Life Sciences). Before applying the sample, the resin was equilibrated with 10 mM sodium phosphate buffer (10 column volumes). After the centrifugation of sample at 15,000g for 10 min or filtration by a 0.22 µm filter. Sample was loaded to the column at an optimised 1 ml/min flow rate. The sample passing throughout the column was collected and labelled. The column was then washed with phosphate buffer (10 column volumes) until the UV trace come again to baseline level. The IgG was eluted by adding 6 ml of 0.1 M glycine, pH 2.7 (elution buffer) at a flow rate of 0.5ml/min. The eluted fractions were collected and neutralised with 1 M Tris/HCl pH 8 to prevent IgG denaturation. The protein content of the eluted fractions were then measured by Bradford assay and dialysed by using dialysis tubing of 8000 M.wt cut off in 5 L of 1 x Tris, with three buffer changes each 12 hours. The column re-equilibrated with phosphate buffer (5 column volumes) and after that the protein G column washed with phosphate buffer (10 column volumes) and stored in 20% ethanol. All purified proteins were stored at -80 °C.

2.2.22 Protein Content Estimation (Bradford assay)

A rapid estimation of the protein content was performed using the Bradford assay. The method employed was adapted from (Bradford 1976) and utilizes the principle of protein-dye binding to measure microgram quantities of protein. A standard curve was

set up with bovine serum albumin (BSA) as follows. A solution of 10 mg/ml BSA was prepared in double distilled water and diluted 100 µg/ml.

Volume of stock	H ₂ O (ml)	BSA Conc. (µg/ml)
2.0 ml of 100 µg/ml	6	25
2.5 ml of 25 µg/ml	2.5	12.5
2.5 ml of 12.5 µg/ml	2.5	6.25
2.0 ml of 6.25 µg/ml	3	2.5
2.0 ml of 2.5µg/ml	2	1.25

From each sample above, 800 µl were mixed with 200 µl of the Bradford reagent in plastic 0.1 cm cuvette and incubated for 5 min at room temperature. The readings were taken for all samples at OD_{595nm} and plotted graphically as the protein standard curve for the assay. Every sample to be measured was mixed with 200 µl Bradford reagent plus the necessary amount of distilled water in order to make up a sample volume of 1 ml in a plastic 0.1 cm cuvette. The reading values were taken as mentioned and they were plotted against the BSA standard curve of measurements. The protein concentration in each sample was calculated by direct comparison of the OD_{595nm} against the standard curve values (Sambrook et.al, 1989).

2.2.23 SDS-PAGE

The samples were fractioned by sodium dodecyl sulphate-polyacrylamide gel electrophoresis (SDS-PAGE). The apparatus used for SDS-PAGE analysis was the protean II and miniprotean II (Bio-Rad). The composition of all solution and reagents is given in Appendix I. Plates were washed and assembled with 1mm spacers for the miniprotean II and 18mm spacers for the protean II. 10% polyacrylamide resolving gel mixture was prepared and poured between the plates. After polymerization, the 4% stacking gel was prepared, poured onto the resolving gel and a comb inserted. After

polymerization, the gel was covered in Laemmli buffer and samples, mixed with sample buffer (1:1) and heated at 85°C for 5 min and loaded along with 5 µl Pre-stained SDS-PAGE standards low range markers (Bio-Rad). The gel was run at a current of 35 mA until the dye front had reached the bottom of the resolving gel. The gel was visualized by covering with Coomassie blue stain overnight, and destaining with several changes of Coomassie blue destain until the bands were clearly visible. Subsequently the gel was dried at 65°C for 1-2 h on a Bio-Rad model 583-slab gel drier.

2.2.24 Western Blotting

Proteins were separated by SDS-PAGE (2.2.20). The gel and 0.45µm nitrocellulose membrane (Bio-Rad) were placed in transfer buffer for 30 min to equilibrate. The transferred unit consisted of 9 sheets of wetted 3MM paper (Whatman) followed by a sheet of nitrocellulose, the gel and 9 more sheets of wetted 3 MM paper, and was set up on a semi-dry electrophoresis apparatus (Genetic Research Instrumentation) at 4°C and proteins were transferred at 25mA overnight. After transfer the nitrocellulose membrane was stained with amido black for 5 min and subsequently destained with amido black destain. The membrane was then cut into strips and stored in foil at -20°C or used immediately. The nitrocellulose strips were blocked for 1 h at room temperature with 5% skimmed milk PBS/0.05% Tween. After blocking, strips were incubated with appropriate primary antibody at appropriate dilution in 1% skimmed milk PBS/0.05% Tween for 2 h at room temperature. The membrane was then washed 4 times with PBS/0.05% Tween and incubated with appropriate dilution of HRP conjugated secondary antibody diluted in 1% skimmed milk PBS/0.05% Tween for 1-2 h at room temperature. After this incubation washed 4 times with PBS/Tween and immersed in ECL substrate solution (Roche Diagnostic) according to manufacturer's instructions for 1 min. Then the nitrocellulose membrane strips were placed on an acetate sheet and covered with Saran wrap. The acetate was exposed to X-ray film (Fujifilm) for a period 1-10, and up to 30 min, and then the film was developed and fixed.

2.2.25 Transfection of Mammalian Cells Using Lipofectamine

Cells to be transfected were seeded at a density of 5×10^4 cells/ml and plated out according to the size of the plate as; 1ml/well was added into 12-well plates and 2 ml/well into 6-well plates and 10 ml/dish when 100 mm culture dishes were used. Cells were then grown in their respective culture media without antibiotics until they reached 90-95% confluence. The Lipofectamine transfection was carried out at 1:2.5 DNA (μg):Lipofectamine (μl) ratios as per manufacturer's instructions. In separate tubes, the DNA and the Lipofectamine reagent were diluted in OptiMEM medium depending on the type of the plate used according to the following table:

Culture vessel	DNA in dilution media	Lipofectamine in dilution media
12-well	1.6 μg in 100 μl	4 μl in 100 μl
6-well	4 μg in 250 μl	10 μl in 250 μl
100mm	24 μg in 1.5ml	60 μl in 1.5ml

Tubes were then incubated at room temperature for 5 min. The DNA and the Lipofectamine tubes then mixed together and incubated for further 25 min at room temperature. The DNA-Lipofectamine complexes then added to the well containing cells and medium. Cells incubated at 37°C in a CO₂ incubator for 24-48 h until they were ready to be tested for the transgene expression.

2.2.26 Development of Stably Transfected Mammalian Cell Lines

To select stable transfected cells at the end of incubation period, the cultures were re-plated in 100 mm dish at 1:20, 1:200 and 1:500 dilutions in culture medium containing 400 $\mu\text{g}/\text{ml}$ 600 $\mu\text{g}/\text{ml}$, 800 $\mu\text{g}/\text{ml}$ and 1000 $\mu\text{g}/\text{ml}$ G418. The cells were incubated at 37°C in a 5% CO₂ incubator for appropriate length of time around 3 weeks before analysis, with changing of media every 2-3 days. When complete cell death had occurred in untransfected CHO-K cells in control dishes, the clumps of transfected cells remaining were removed from dish and transferred to 24 well plates and grown in media containing G-418 at 400 $\mu\text{g}/\text{ml}$, 600 $\mu\text{g}/\text{ml}$, 800 $\mu\text{g}/\text{ml}$ and 1000 $\mu\text{g}/\text{ml}$. Cells were

grown until confluent and split between two 24 well plates. When cells were confluent, one 24 well plate was used to analyse the clones for expression of protein by cells ELISA and FACS, and any clones that were positive were grown and maintained in media containing appropriate concentration of G418.

2.2.27 Flow Cytometry (FACS)

FACS analysis was carried out on a Becton Dickinson FACScan flow cytometry using Cell Quest data acquisition and analysis software. Briefly, the cells were grown in appropriate media until confluence in T75 tissue culture flask. The cells were gently washed with PBS, detached from culture flasks using 3 ml cell dissociation solution (Sigma), and incubate for 3 min. After the cells dissociated, the cells were washed with 5 ml of appropriate media using a syringe and needle, centrifuged at 1000 g for 3 min, and resuspended in 1 ml of media. Cells were counted, resuspended at the density of 1×10^7 cells/ml and 100 μ l aliquoted into LP4 tubes (Becton Dickinson Labware). The appropriate monoclonal antibody, diluted to manufacturer's instructions, or samples was added to the cells, thoroughly mixed and the reaction incubated for 20 min on ice. After washing twice with 2 ml PBS centrifuged at 1000 g for 3 min and resuspended in appropriate diluted FITC-conjugated antibody and incubated on ice for 20 min. After a final wash, cells were analysed using a fluorescence activated cell sorter (FACScan, Becton Dickinson).

2.2.28 Enzyme-linked Immunosorbent Assay (ELISA)

The general ELISA protocol utilised is outlined below and specific modifications are detailed in the appropriate section. The protein required to coat the plate was diluted to the desired concentration in coating buffer and 100 μ l aliquoted into each well of a 96 well flat bottom ELISA plate (Costar), the plate was covered with parafilm and incubated overnight at 4°C. After three times washing with PBS/0.05% Tween, 300 μ l of blocking solution (3% BSA in PBS/0.05% Tween) was added to each well and incubated at 37°C for 1 h. After once washing with PBS/0.05% Tween, 100 μ l of the sample or antibody (diluted as detailed in manufacturer's instructions) was added to

each well and incubated at room temperature for 2 h. Each well was washed three times with PBS/0.05% Tween and 100 µl of the appropriate dilution of alkaline phosphatase conjugated anti-IgG added to each well. After incubation at room temperature for 1 h, each well was washed three times with PBS/0.05% Tween and 100 µl of freshly prepared phosphatase substrate solution (Sigma Fast p-nitrophenyl phosphate) was added to each well. The plate was incubated at room temperature for 15-30 min until colour development occurred and 100 µl of stopping solution was added and the OD_{405nm} was measured in the platereader. All samples were tested in duplicate and results were presented graphically as the mean of absorbance of each sample verses the sample. Known positive or negative controls if available were used in each plate

2.2.29 Cell ELISA

GPI95 and CHO-K1 cell lines media were removed, and the cells were washed in 1 x PBS before incubation with Trypsin-EDTA for 3 min at 37°C. The then cells dislodged by gently tapping the side of the flask and resuspended in 10 ml of the complete medium. Cells then centrifuged at 1000 rpm in a 25 ml universal centrifuge tubes for 5 min. The cell pellets were resuspended in the appropriate medium and cells were counted in a haemocytometer before plating out 75,000 cells per ml, 200 µl in each well of a Poly-D-Lysine 96-well ELISA plate (15,000 cells per well). the plate was incubated overnight at 37°C in a CO₂ incubator. After three times washing with PBS, 300 µl of blocking solution (FCS in cells media) was added to each well and incubated at 37°C for 1 h. After once washing with PBS, 100 µl of the sample or antibody (diluted as detailed in manufacturer's instructions) was added to each well and incubated at room temperature for 1 h. Each well was washed three times with PBS and 100 µl of the appropriate dilution of HRP- conjugated anti-IgG added to each well. After incubation at room temperature for 1 h, each well was washed three times with PBS and 100 µl of freshly prepared substrate solution was added to each well. The plate was incubated at room temperature for 15-30 min until colour development occurred and 100 µl of stopping solution was added and the OD_{450nm} was measured in the platereader. All samples were tested in duplicate and results were presented graphically as the mean of

absorbance of each sample versus the sample. Known positive or negative controls if available were used in each plate

2.2.30 Preparation of Mammalian Cell Extracts

Following incubation for 48-60 h transfected cells were washed 3 times with 5 ml of ice cold PBS and finally scraped off the well in 2 ml of ice cold PBS and transferred to a universal. The cells were pelleted by centrifugation at 3000 rpm for approximately 3 min at 4°C, the supernatant removed, and the cells resuspended in 1 ml of PBS and transferred to an eppendorf. The cells were pelleted by centrifugation at 13,000 rpm for 30 s and a lysate prepared by re-suspending the pellet into 200 µl of 1% SDS denaturing lysis buffer (pre-heated to 90°C and allowed to cool slightly). The resultant solution was passed through a 23G needle 20 times to shear genomic DNA and reduce viscosity, centrifuged at 13,000 rpm for 1 minute to remove any insoluble material and the resulting supernatant stored at -80°C. The cell lysate then concentrated 25 times by using a micro-concentrator (Amicon) and the protein content determined by Bradford assay. Untransfected HEK293 cells as a negative control as well as a positive control cells were subjected to the same protocol.

2.2.31 Triton X-114 Phase Partitioning of GPI-linked Proteins

Triton X-114 phase partition is one of the preferred methods for separation of the GPI-anchored proteins from crude cellular homogenates. This is because these proteins carry a hydrophilic lipid moiety (glycosylphosphatidylinositol) attached to them. Therefore, under temperature-induced phase separation of Triton X-114/water, membrane and GPI-anchored proteins partitioned into the detergent enriched phase. We applied this method to show that our GPI-anchored proteins are able to separate into the detergent phase and thus show evidence of the presence of the lipid moiety. Briefly, The GPI construct transfected cells (1×10^6) were washed in PBS and lysed in 250 µl of lysis buffer (20mM Tris-HCl, 150 mM NaCl, 1 mM EDTA, 2% Triton X-114, 0.1 mM PMSF, protease inhibitor cocktail tablets (1 tablet/10 ml) and 0.0005% bromophenol blue) in an

ependorff tube. Cells were then left on ice with frequent stirring for 20 min. The resulting lysate was centrifuged at 13,000 x g for 5 min at 0°C to remove cellular debris. The coloured supernatant was then collected into a fresh tube and incubated at 30°C for 5 min for phase separation. Tubes were then centrifuged briefly at 4,000 x g for 3 min at room temperature to separate the clear aqueous phase from the detergent phase containing bromophenol blue. The two phases were collected gently and analysed by western blotting for the target proteins.

2.2.32 TSHR Stimulation Bioassay

The cAMP stimulatory activity of the recombinant scFv or Fab antibody fragments were assessed by determining the amount of cAMP produced from CHO-K1 cells transfected with full length of TSHR (JP09 cells) (2.1.3). In brief, the JP09 cells were seeded at 10^5 cells/ml in 24 well plates 48 h before the cAMP assay. These cells were maintained under 5% CO₂ at 37°C and cultured in nutrient mixture F-12 (HAM) medium supplemented with 10% foetal calf serum, 1% 200 mM glutamine, 1% 10 mg/ml penicillin/streptomycin and 400 µg/ml G-418. After the culture medium was removed, cells were pre-incubated with 500 µl of hypotonic Hanks' balanced salt solution (HBSS) containing 1.5% BSA and 0.5 mM 3-isobutyl-1-methylxanthine (IBMX) for 20 min at 37°C. The samples or controls (positive and negative) were then added into each corresponding well, mixed with the 500 µl of HBSS and incubated at 37°C for 2 h. The cell culture supernatant was collected and the amount of extracellular cAMP was determined with a commercial cAMP immunoassay kit (R&D Systems) according to manufacturer's instructions. Briefly, 100 µl of the calibrator diluent was added to the first two wells as the zero standard wells. 100 µl of standards concentrations and unknown samples then added to the corresponding wells in duplicates; 200, 100, 50, 25, 12.5, 6.25 and 3.125 pmol/ml. 50µl of the primary antibody solution was then added to each well followed by 50µl of the cAMP conjugate. The plate was covered with adhesive strip and incubated for 3 h at room temperature on a horizontal orbital microplate shaker set at 500±50 rpm. Each well then aspirated and washed three times with 400 µl of the wash buffer. After the last wash, the remaining wash buffer was removed by inverting the plate and blotting it against clean paper towels. 200 µl of the substrate solution was then added to each well and the plate was

incubated for 30 min at room temperature on a benchtop. The reaction was stopped with 50 μ l of the stop solution and the optical density (OD_{450nm}) of all samples was determined within 30 min, using a microplate reader. Standard absorbance values were subtracted from the average value of the zero standards and plotted graphically against their corresponding concentrations using four parameter log curve-fit generated by Graphpad prism software. The unknown concentrations were determined by direct interpolation using the same software.

2.3.33 Immunisation

Four mice BALB/c were immunised subcutaneously with 300 μ g (75 μ g/ mouse) of M22 scFv in 150 μ l/mouse of Gerbu adjuvant. A second subcutaneous injection of the same concentration of the purified M22 scFv protein (no adjuvant) was given day 14 after the first injection. Ten days after, 100 μ l of boost immune bleed from each mouse was collected and tested at different dilutions for plasma reactivity to the M22 scFv by ELISA. At day 28, mice were injected intraperitoneally with 30 μ g/mouse of antigen (no adjuvant) as a booster dose before killing, and the spleens are collected.

CHAPTER 3

CLONING AND CHARACTERISATION OF TSAB MONOCLONAL M22

3. Cloning of synthetic human monoclonal M22-scFv into phage display vector pAK100

3.1 Introduction

TSHR autoantibodies are the basis of Graves' disease. TSAbs mimic the action of TSH and stimulate thyroid cells, leading to increased thyroid hormone synthesis and goiter. The therapeutic options for Graves' disease are still limited. Understanding of the autoantibody response would provide novel therapeutic strategies and diagnostic tools. Analysis of TSAbs monoclonal and corresponding TSHR epitopes would allow the design of specific peptide antagonists or the development of anti-idiotypic reagents. However, attempts to isolate anti-TSHR antibodies from patients by conventional methods have proven technically very challenging due to the inherent limitations of human B cell cloning, relatively low number of specific B cells in GD patients, and with difficulties in obtaining purified TSHR capable of interacting with patient antibodies. So far only two human TSAbs monoclonals have been reported (Smith, Sanders et al. 2009). Phage display techniques have been used to investigate the autoimmune repertoire in a number of diseases, and offer the potential to recover more examples of TSHR autoantibodies. However, the only published attempt to recover TSH receptor antibodies using phage display was unsuccessful (Van Der Heijden, De Bruin et al. 1999). The reasons for this failure are not clear and before embarking on phage selection experiments in this study it was decided to first produce an appropriate control to optimise the conditions for binding and enrichment. Using the public domain patent document describing the properties of mAb M22 we chemically synthesised the appropriate immunoglobulin heavy and light chain Fv DNA sequences and cloned these as scFv fragments into a phage display vector. The aim of this part of the study was to clone the recombinant human M22 scFv into a phage vector and verify that we had synthesised the correct antibody by characterising the binding and thyroid stimulatory activities of the construct. Based on the patent description we will synthesise the corresponding VH and VL sequences. By using overlap PCR we will assemble the M22 scFv DNA and clone it into phage display and expression vectors. Recombinant protein will be produced and identity confirmed by analysis of TSHR binding and TSAbs activity.

3.2 Methods and Results

3.2.1 Gene Synthesis of M22 VH and VL Genes

The DNA sequence of human monoclonal TSAb M22 was published in patent application WO2004/050708A2 (Sanders, Smith et al. 2004). This information was used to extract the sequences of M22 variable heavy and variable light chain genes. These sequences were synthesised commercially by Eurofins GmbH. One advantage of DNA synthesis is that the codon usage could be adjusted to match that of the projected *E. coli* expression hosts and this optimise protein expression. The VH and VL plasmids provided by the manufacturer were sequenced, and the identity confirmed by comparison to published sequences (Sanders, Smith et al. 2004). DNA sequences were analysed using the VBASE2 web tool which aligns antibody sequences with all known immunoglobulin gene sequences and identifies CDR regions (Retter, Althaus et al. 2005). The heavy chain used was of the IgG1 subclass and used the VH32 germline gene, a member of the comparatively rarely used human VH5 gene family, the D region gene was D6-13, and the J region gene was JH5. The light chain was of the lambda class and used the VL1-11 germline gene and the J region gene JL3b (Fig. 3.1 and Fig. 3.1). The protein sequence was confirmed as identical to that of the published M22 mAb.

3.2.2 PCR Amplification of Heavy and Light Chain Genes

The synthetic VH and VL chain plasmids were diluted 1:1000 in TE to produce template suitable for PCR amplification. The M22 heavy and light Fv coding regions were amplified in separate PCR reactions using 2 µl of the corresponding template and the TSAB-VH-S, TSAB-VH-AS, TSAB-VL-S, TSAB-VL-AS primers (Table 3.1) (2.2.3). A negative control containing no template was included to make sure there was no contamination of the PCR reagents. Amplifications were carried out using the following conditions; initial denaturation 94°C 1 min; 30 cycles of 92°C for 1 min, 55°C for 1 min, 72°C for 1 min. A 10 min final extension at 72°C was carried out and

the reactions cooled to 4°C. PCR products were resolved by gel electrophoresis on 1% agarose minigels (2.2.4). The agarose gel visualized on a UV illuminator and photographed, and product sizes verified by comparison to a 100 bp ladder. The results showed the amplification of products with the appropriate size, and these were used to assemble the final scFv construct (Fig. 3.3). PCR products were excised and purified from agarose using the QIAquick PCR prep kit (2.2.5).

GAATTCGCCCTTATTCTCGAGCAAGTGCAGCTGGTGCAGTCTGGAGCAGAGGTGAAAAAGCCCGGGGAGTCTCTGAAGATCTCCTGTAGG
 ++++++
 CTTAAGCGGGAATAAGAGCTCGTTCACGTCGACCACGTACAGACCTCGTCTCCACTTTTTTCGGGCCCTCAGAGACTTCTAGAGGACATCC
 E F A L I L E Q V Q L V Q S G A E V K K P G E S L K I S C R 90

GGTTCGGATACAGGTTTACCAGCTACTGGATCAACTGGGTGCGCCAGCTGCCCGGAAAGGCTTAGAGTGGATGGGCAGGATTGATCCT
 ++++++
 CCAAGACCTATGTCCAAATGGTCGATGACCTAGTTGACCCACGCGGTGACGGGCCCTTCCGGATCTCACCTACCCGTCCTAACTAGGA
 G S G Y R F T S Y W I N W V R Q L P G K G L E W M G R I D P 180

CDR 1

ACTGACTCTTATACCAACTACAGTCCATCCTTCAAAGGCCACGTACCCGTCCTCAGCTGACAAGTCCATCAACACTGCCTACCTGCAGTGG
 ++++++
 TGACTGAGAATATGGTTGATGTGAGTAGGAAGTTCCGGTGCAGTGGCAGAGTCTGACTGTTGAGGTAGTTGTGACGGATGGACGTACC
 T D S Y T N Y S P S F K G H V T V S A D K S I N T A Y L Q W 270

CDR 2

AGCAGCCTGAAGGCCTCGGACACCGGCATGTATTACTGTGCGAGGCTCGAACCGGGCTATAGCAGCACCTGGTCCGTAATGGGGCCAG
 ++++++
 TCGTCGGACTTCCGGAGCCTGTGGCCGTACATAATGACACGCTCCGAGCTTGGCCCGATATCGTCGTGGACCAGGCATTAACCCCGGTC
 S S L K A S D T G M Y Y C A R L E P G Y S S T W S V N W G Q 360

CDR 3

GGAACCTGGTCACCGTCTCCTCAGCCTCCACCAAGGGCCCATCGGTCTTCCCCCTGGCACCCCTCCTCCAAGAGCACCTCTGGGGGCACA
 ++++++
 CCTTGGGACCAGTGGCAGAGGAGTCCGAGGTGGTTCCTCCGGTAGCCAGAAGGGGACCGTGGGAGGAGTTCCTGTTGGAGACCCCGTGT
 G T L V T V S S A S T K G P S V F P L A P S S K S T S G G T 450

GCGGCCCTGGGCTGCCTGGTCAAGGACTACTTCCCGAACCGGTGACGGTGTGTTGGAAGTCAAGGCGCCCTGACCAGCGGCGTGCACACC
 ++++++
 CGCCGGGACCCGACGGACAGTTCCTGATGAAGGGGCTTGGCCACTGCCACAGCACCTTGAAGTCCGGGGACTGGTCCGCCACAGTGTGG
 A A L G C L V K D Y F P E P V T V S W N S G A L T S G V H T 540

TTCCCGGCTGTCTACAGTCTCAGGACTCTACTCCCTCAGCAGCGTGGTGACCGTGCCTCCAGCAGCTTGGGCACCCAGACCTACATC
 ++++++
 AAGGGCCGACAGGATGTCAGGAGTCTGAGATGAGGGAGTCTGCGCACCACTGGCACGGGAGTCTGCGAACCCGTTGGTCTGGATGTAG
 F P A V L Q S S G L Y S L S S V V T V P S S S L G T Q T Y I 630

TGCAACGTGAATCACAAGCCAGCAACACCAAGGTGGACAAGAAAGTTGAGCCCAAATCTTGTACTAGTAATAAGGGCGAATTC
 ++++++
 ACGTTGCACTTAGTGTTCGGGTCGTTGTGGTCCACCTGTTCTTCAACTCGGGTTTAGAATGATCATTATTCCTGCTTAAG
 C N V N H K P S N T K V D K K V E P K S C T S N K G E F

Figure 3.1 Sequence of Synthetic M22-VH Construct.

Complementarities determining regions are shown highlighted.

GAATTCGCCCTTATTGAGCTCCTTACGGTTCTGACCCCAACCACCCTCTGTGAGTGGTGCTCCGCGTCAACGCGTCACGATCAGTTGTAGC
 E F A L I E L L T V L T Q P P S V S G A P R Q R V T I S C S 90

GGCAATCCAGCAACATTGGCAACAATGCCGTGAAGTGGTATCAGCAGTTGCCGGGTAAAGCACCGAAACTGCTGATCTACTATGACGAT
 G N S S N I G N N A V N W Y Q Q L P G K A P K L L I Y Y D D 180
 CDR 1 CDR 2

CAGCTGCCTTCAGGCGTATCGGATCGCTTCTCGGGGTCCCGTAGTGGCACTTCAGCGAGCTTAGCGATTTCGGGGCTTACAGTCGGAGGAT
 Q L P S G V S D R F S G S R S G T S A S L A I R G L Q S E D 270

GAAGCCGACTACTATTGCACCTCTTGGGACGATAGCCTCGATAGCCAGCTGTTGGCGGTGGTACACGCTTGACCGTTCTGGGTCAGCCC
 E A D Y Y C T S W D D S L D S Q L F G G G T R L T V L G Q P 360
 CDR 3

AAGGCTGCCCCCTCGGTCACTCTGTTCACCCCTCCTCTGAGGAGCTTCAAGCCAACAAGCCACACTGGTGTGTCTATAAGTGACTTC
 K A A P S V T L F P P S S E E L Q A N K A T L V C L I S D F 450

TACCCGGGAGCCGTGACAGTGGCCTGGAAGGCAGATAGCAGCCCCGTCAAGGCGGGAGTGGAGACCACCACCCCTCCAACAAGCAAC
 Y P G A V T V A W K A D S S P V K A G V E T T T P S K Q S N 540

AACAAAGTACGCGCCAGCAGCTACCTGAGCCTGACGCCTGAGCAGTGGAAAGTCCACAAAAGCTACAGCTGCCAGGTCACGCATGAAGGG
 N K Y A A S S Y L S L T P E Q W K S H K S Y S C Q V T H E G 630

AGCACCGTGGAGAAGACAGTGGCCCTACAGAATGTTCTGTAATCTAGAAATAAGGGCGAATTC
 S T V E K T V A P T E C S . S R N K G E F

Figure 3.2 Sequence of Synthetic M22-VL Construct.

Construct. Complementarity determining regions are shown highlighted.

Table 3.1 Primers used for the amplification and cloning of M22-scFv fragments into pAK100.

TSAB-VH-S	5' GGC GGC GGC GGC TCC GGT GGT GGT GGA TCC CAG GTA CAG CTG GTC CAG AGT GGT GCT 3'
TSAB-VH-AS	5' G GAA TTC GGC CCC CGA GGC CGC GCT TGA CAC TGT CAC TAA CGT ACC TTG 3'
TSAB-VL-S	5' GCC ATG GCG GAC TAC AAA GAC CTT ACG GTT CTG ACC CAA CCA CCC TCT 3'
TSAB-VL-AS	5' GGA GCC GCC GCC GCC AGA ACC ACC ACC ACC AGA ACC ACC ACC ACC CAG AAC CGT CAA GCG TGT ACC ACC GCC AAA CAG CTG GCT ATC 3'
SC-back	5'CTA CAG CAG GCC CAG CCG GCC ATG GCG GAC TAC AAA G
SC-for	5'CGG AGT CAG GCC CCC GAG

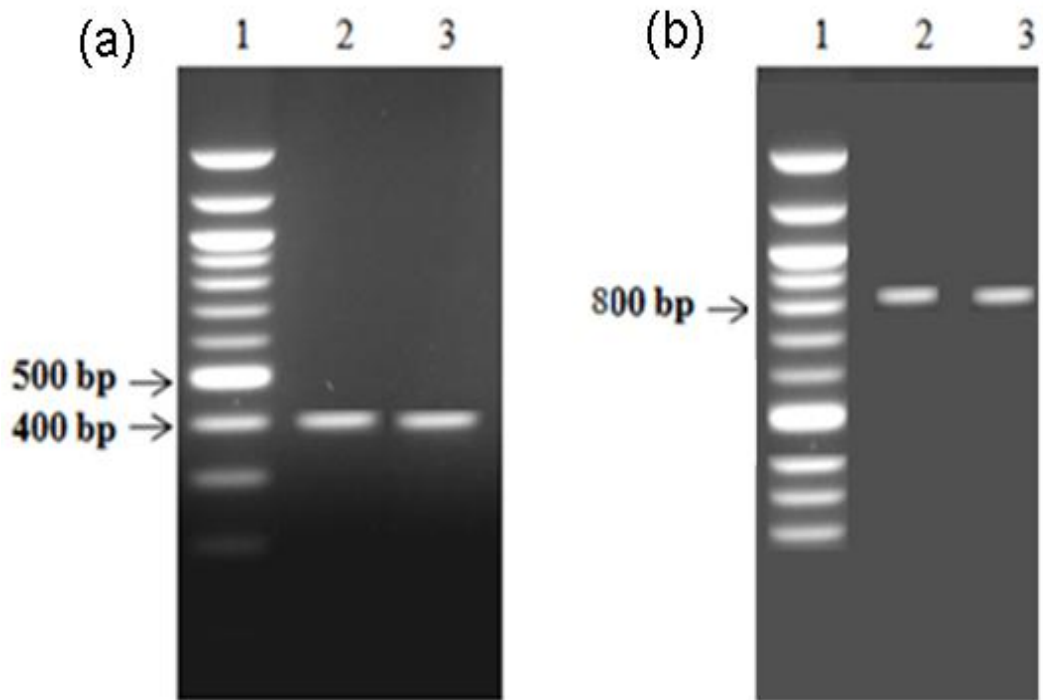


Figure3.3 PCR products of M22 VH and VL Regions and their Overlap Assembly.

(a) Amplified VH and VL DNAs appeared on the 1% agarose gel as sharp bands at 400 bp. Lane 1: 100bp ladder. Lane 2: PCR product of M22 VH-chain (400bp). Lane 3: PCR product of M22 VL-chain (400bp). (b) Lane 1: 100bp ladder; Lane 2-3: The yield of the assembly reaction of VH and VL (800bp). The assembled PCR products (complete M22 scFv) digested and recovered from agarose gel slices prior to ligation into pAK100.

3.2.3 Assembly PCR and Cloning into PAK100 and PAK400

Approximately 30 ng of purified VH and VL PCR products was combined by SOE-PCR (splicing by overlap extension). Complementary regions in the linker sequence annealed to the 3' and 5' end respectively of the VL and VH PCR products, four assembly SOE-PCR reactions were performed using the SC-BACK and SC-FOR primers (Table 3.1) which joined VL and VH products, adding the coding sequence for a flexible G4S linker between them and *Sfi* I site at the 5' and 3' ends of the overlap product. A negative control containing no template was included to ensure there was no contamination of the PCR reagents. Amplification was performed 3 cycles of 1 min. at 92°C, 30 sec. at 63°C, 50 sec. at 58°C and 1 min. at 72°C, followed by 25 cycles of 1 min. at 92°C, 30 sec at 63°C, and 1 min at 72°C, and a 10 min final extension at 72°C was carried out before the samples were cooled to 4°C. PCR products were resolved by gel electrophoresis on 1% agarose minigels. PCR products were excised and purified from agarose using the QIAquick PCR prep kit (2.2.5). The purified scFv products were dissolved in 40 µl of H₂O and 5 µl of buffer 4 (NEB), and digested with 10 units of *Sfi* I restriction enzyme for 2 h at 50°C. At the same time 5 µg of pAK100 vector DNA was cut in a 100 µl reaction containing 10 µl of Buffer 4 and 10 units of *Sfi* I (NEB). The digested scFv DNA and pAK400 were slot gel purified and extracted with the Wizard DNA Cleanup kit. Approximately 200 ng of digested pAK100 and 100 ng of digested M22-scFv were mixed together in a 20 µl ligation reaction containing 2 µl of ligation buffer and 1 unit of T4 DNA ligase (Promega). The reaction was incubated overnight at 15°C. The scheme for cloning M22-scFv into pAK100 is shown in Fig. 3.4.

The pAK100 expresses scFv as fusions to phage coat protein cpIII to enable phage display and selection. In order to increase the functional yield of antibody fragments the M22 scFv gene was sub-cloned into vector pAK400. This construct enabled the increased expression of scFv and added a 6 His tag at the carboxy terminus to allow rapid purification by metal affinity chromatography. A single M22-pAK100 clone was verified by sequencing and after confirmation was grown as a midiprep to provide sufficient DNA for subcloning. Briefly 5 µg of pAK100-scFv plasmid prepared from glycerol stock of a single M22-PAK100 clone was digested with *Sfi* I enzyme as

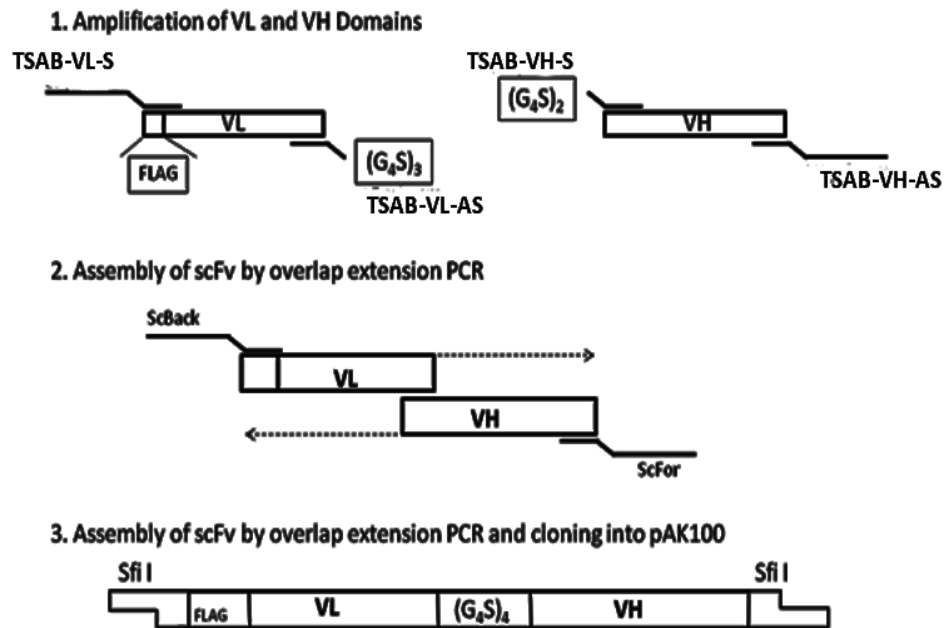


Figure 3.4 Schematic Diagram of Synthesis of M22-scFv Construct.

Immunoglobulin heavy and light chain variable regions were amplified from synthetic M22 template using primers TSAB-VL-S, TSAB-VL-AS, TSAB-VH-S, and TSAB-VH-AS (Table 3.1). Amplicons were gel purified and joined by overlap extension PCR using primers SC-FOR and SC-BACK (Table 3.1) to produce an scFv coding fragment which was cloned into the Sfi I sites of phage vector pAK100 (Krebber, Bornhauser et al. 1997).

described (2.2.7) and the resulting DNA fragments resolved using an agarose slot gel (2.2.4) (Fig. 3.5).

Approximately 800 bp scFv antibody fragment was excised from the gel and purified using the Wizard DNA Cleanup kit (2.2.5). Two μg of pAK400 vector was also restricted with *Sfi* I enzyme and purified, following agarose gel electrophoresis. The purified digested M22-scFv fragment was ligated into *Sfi* I sites of the pAK400 to create M22-pAK400 (Fig. 3.6). The ligation reaction was purified by ethanol precipitation and resuspended in 20 μl TE. 5 μl of ligated mixture was electroporated into 60 μl of a non-suppressor *E.coli* BL21 (2.2.10), 2 μl was plated out onto an agar plate containing 30 $\mu\text{g/ml}$ chloramphenicol and incubated at 37°C overnight. Positive clones were confirmed by restriction digest and glycerol stocks prepared and stored at -80°C to be used for expression and purification of M22 scFv protein.

3.2.4 Expression of M22-scFv

The induction procedure of scFv expression was carried out as described in 2.2.20. Briefly, 10 ml of LB medium containing, 10 μl of 30 $\mu\text{g/ml}$ chloramphenicol was inoculated with 10 μl of glycerol stock of M22-pAK400 and grown overnight in a shaking incubator at 37°C. This culture was used to inoculate 1L of LB (30 $\mu\text{g/ml}$ chloramphenicol) and grown at 25°C with shaking until the OD_{600nm} reached 0.6. At this point gene expression was induced by the addition of IPTG to a final concentration of 1 mM, and the culture was grown overnight in a shaking incubator at 25°C. The following day the induced culture was centrifuged at 2,000 g for 10 min, the supernatant was removed for further analysis, and the bacterial pellet was used for periplasmic extraction, using osmotic shock method as previously described (2.2.20). The periplasmic extract and the supernatant were then concentrated ten-fold using a micro-concentrator (Amicon). The protein content was estimated by Bradford assay (2.2.22) or by measurement the OD₂₈₀ and analysed by SDS-PAGE (2.2.23).

3.2.5 SDS-PAGE and Western Blot Analysis of Bacterial Extracts

SDS-PAGE and western blotting were performed essentially as previously described (2.2.23 and 2.2.24). Extracts of pAK100 approximately 20 µg of supernatants and periplasmic extracts were analysed by SDS-PAGE (Fig. 3.7), stained with Coomassie Blue staining as described in 2.2.23, and following transfer western blotted using a 1:1000 dilution of anti-his in 1% skimmed milk PBS/0.05% Tween for 2 h at room temperature.

After washing 4 times with PBS/0.05% Tween, 1:5000 goat anti-mouse IgG-HRP conjugate (Southern Biotech) in 1% skimmed milk PBS/0.05% was added and incubated for 1 h at room temperature. The blot was then visualised using an enhanced chemiluminescent (ECL) system (Roche Diagnostics) according to manufacturer's instructions (Fig. 3.8).

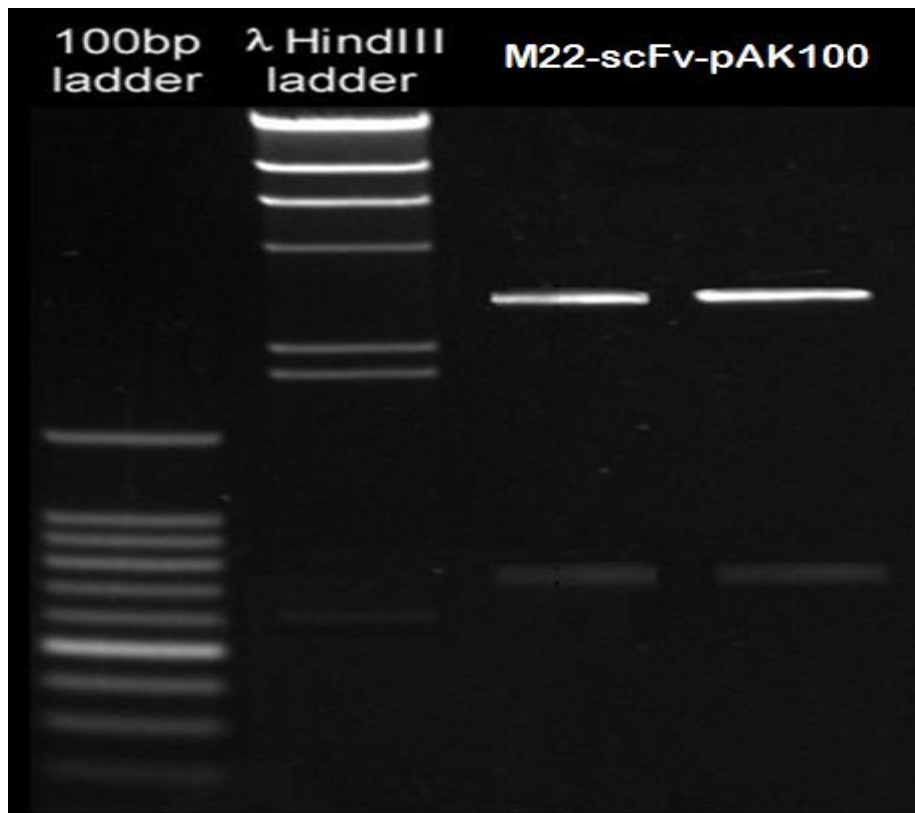


Figure3.5 Restriction digest screening of M22-scFv-pAK100.

Approximately 5 μg of midprep DNA from the M22-pAK100 was digested with *Sfi* I restriction enzyme and run on a 0.8% agarose gel. Lane1: 100bp DNA ladder, lane 2: λ Hind III ladder, lane 3: and 4: digested plasmid from mini-prep1 and 2. Inserts were recovered for cloning into pAK400.

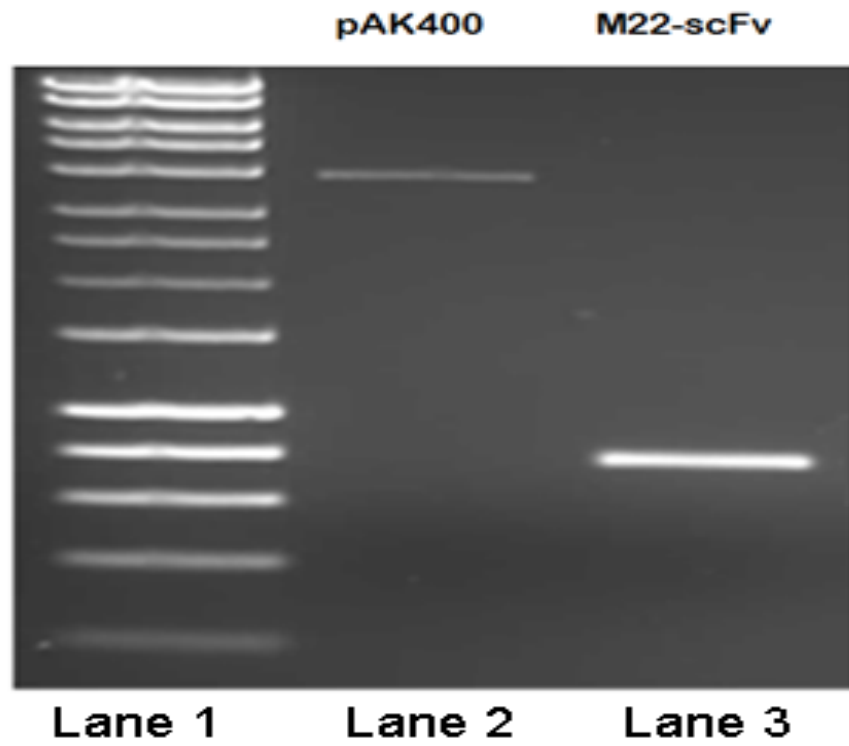


Figure3.6 Purification of digested pAK400 and M22 scFv.

Recovery of digested pAK400 and M22-scFv, samples (4 μ l) of each purified DNA were analysed by gel electrophoresis prior to ligation.

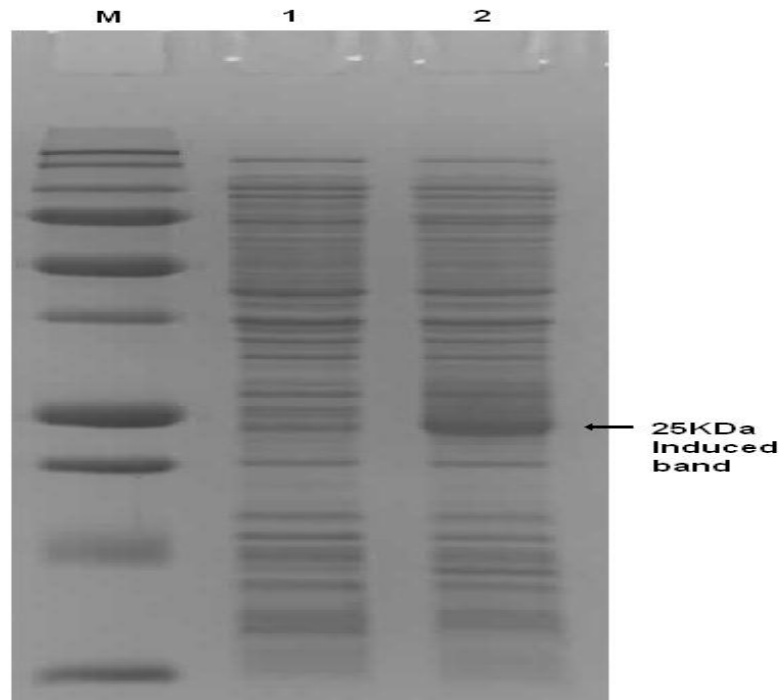


Figure3.7 SDS-PAGE analyses of unpurified M22 scFv periplasmic extracts.

A 15% (w/v) reducing SDS-PAGE gel was used with to visualise expressed proteins by staining with Coomassie blue. The gels, shows E.coli expression of M22 scFv. Lane M: molecular weight marker; precision plus protein marker (Bio-Rad, UK), bands starting at the bottom: 10, 15, 20, 25, 37, 50, 75, 100, 150, and 250 kDa. Lane 1:- Non-induced total cell extract (T0). Lane 2:- IPTG induced total cell extract (T4) after 4 hours, distinct bands at 25 kDa (arrow), corresponding to M22 scFv observed upon induction with 1mM IPTG.

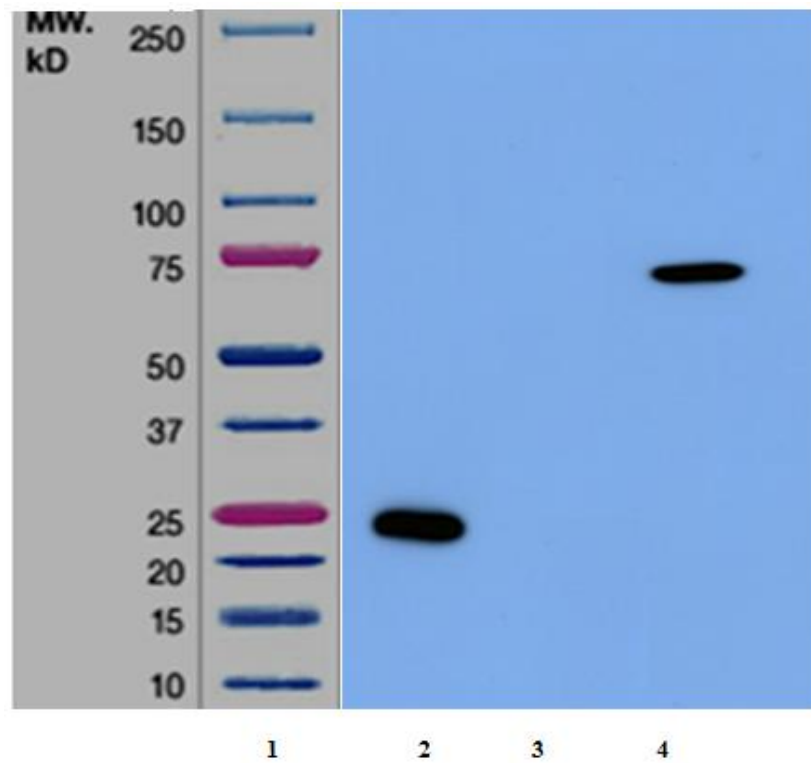


Figure3.8 Western blot analysis of His-tagged purified M2 scFv periplasmic extracts.

Lane 1: Molecular weight marker; precision plus protein marker (Bio-Rad, UK), bands starting at the bottom: 10, 15, 20, 25, 37, 50, 75, 100, 150, and 250 kDa, lane 2: sample of eluted M22-scFv fragments were stained with anti-His mAb and detected by ECL, lane 3: negative control, lane 4: His-tagged TG2 as a positive control.

3.2.6 Purification of Histidine Tagged M22-scFv from Bacterial Periplasmic Extracts

The purification of histidine tagged proteins was achieved by metal chelate resin using TALON Metal Affinity Resins (BD Biosciences) according manufacturer's instructions (2.2.21). Protein loading, washing, and elution were monitored using a UV absorbance detector (Fig. 3.9). The eluted fractions were then collected, neutralized, dialysed against PBS and concentrated ten-fold using a micro-concentrator (Amicon), the protein content were assessed by Bradford assay (2.2.22).

3.2.7 FACS Analysis of M22-scFv

To investigate the binding and specificity of purified M22-scFv to TSHR, the purified antibody was analysed by flow cytometry analysis using GPI-95 cells (2.1.6). GPI-95 cells were derived by stable transfection of CHO-K1 cells with human TSHR cDNA, and express approximately 300,000 copies of TSHR per cell (Metcalf, Jordan et al. 2002). The flow cytometry analysis was performed as described in section 2.2.27. Conventional secondary antibodies are not suitable for detecting scFv, and an aliquot of M22-scFv was biotinylated using EZ-Link Sulfo-NHS-Biotin (Thermo Scientific, Rockford, IL, USA). Cells were counted, resuspended at the density of 1×10^7 cells/ml and 100 μ l aliquoted into LP4 tubes (Becton Dickinson). Two μ g/ml of biotinylated M22-scFv as well as 2 μ g/ml (1:50) of mouse anti-human TSHR monoclonal antibody 2C11 (Serotec) and A10 monoclonal antibody (gift from Prof JP Banga) as positive controls or 2 μ g/ml (1:50) of irrelevant biotinylated scFv (anti-TG2 antibody) were added to the cells, thoroughly mixed and the reaction incubated for 20 min on ice. After washing twice with 2 ml of PBS, cells were centrifuged at 1,000 g for 3 min and resuspended in 1:100 (2 μ g/ml) Extravidin -FITC (Serotec) and incubated on ice for 20 min. After a final wash, cells were analysed using a fluorescence activated cell sorter (FACScan, Becton Dickinson) (Fig.3.9 (a-d)).

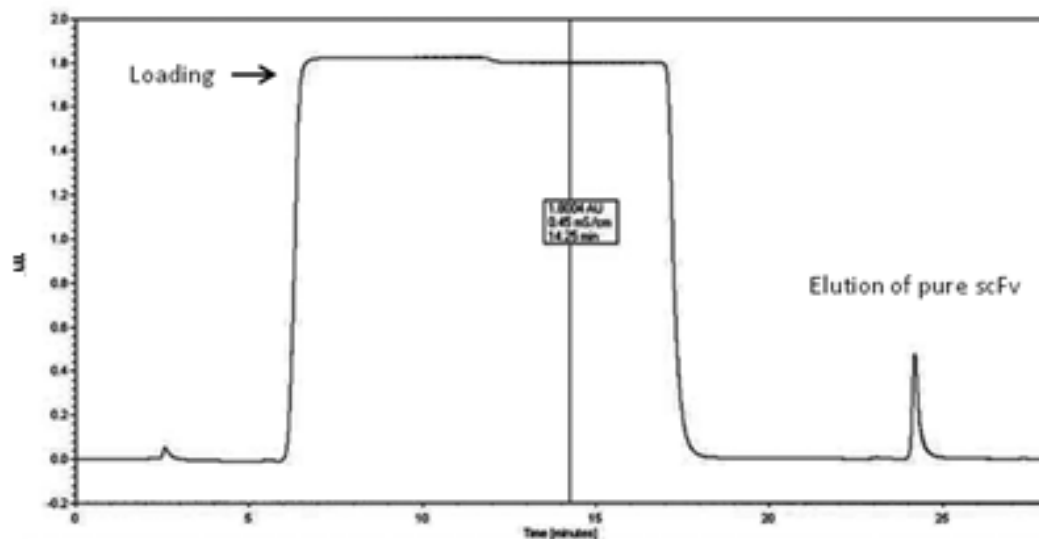


Figure3.9 Elution of purified M22-scFv protein from Ni- column.

Bacterial extract was loaded onto a nickel affinity column and washed with 5 column volumes of Wash Buffer. Pure scFv was eluted with Elution Buffer containing 300 mM imidazole. Protein loading, washing, and elution were monitored using a UV absorbance detector fitted in series with the affinity column.

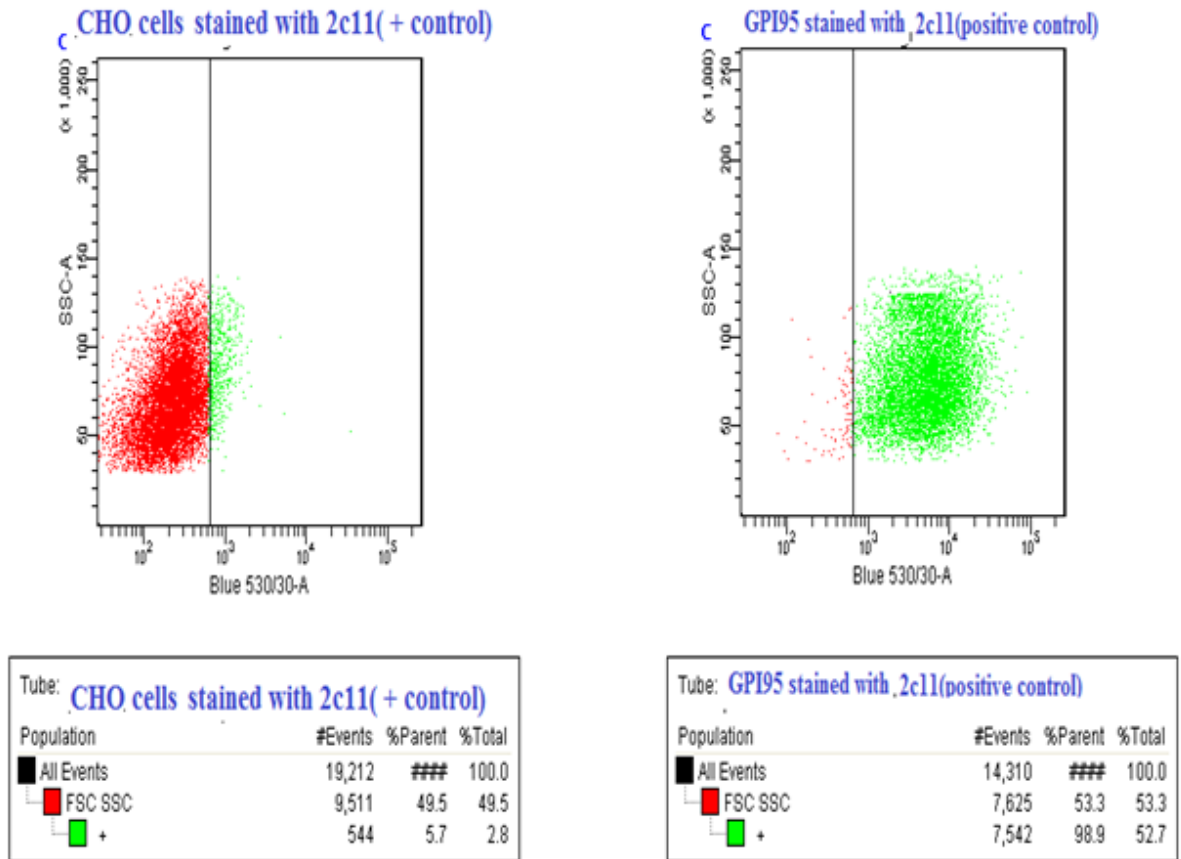


Figure3.10.a: FACS of the binding of 2c11 to CHO-K and GPI-95 cells.

Histograms of fluorescence intensity are showing inability of 2c11 (commercial anti TSH receptor antibody) (Serotec) to bind untransfected CHO-K cells as a negative control versus to significant binding of 2c11 to GPI-95 (CHO-K transfected with TSH receptor ectodomain) as a positive control.

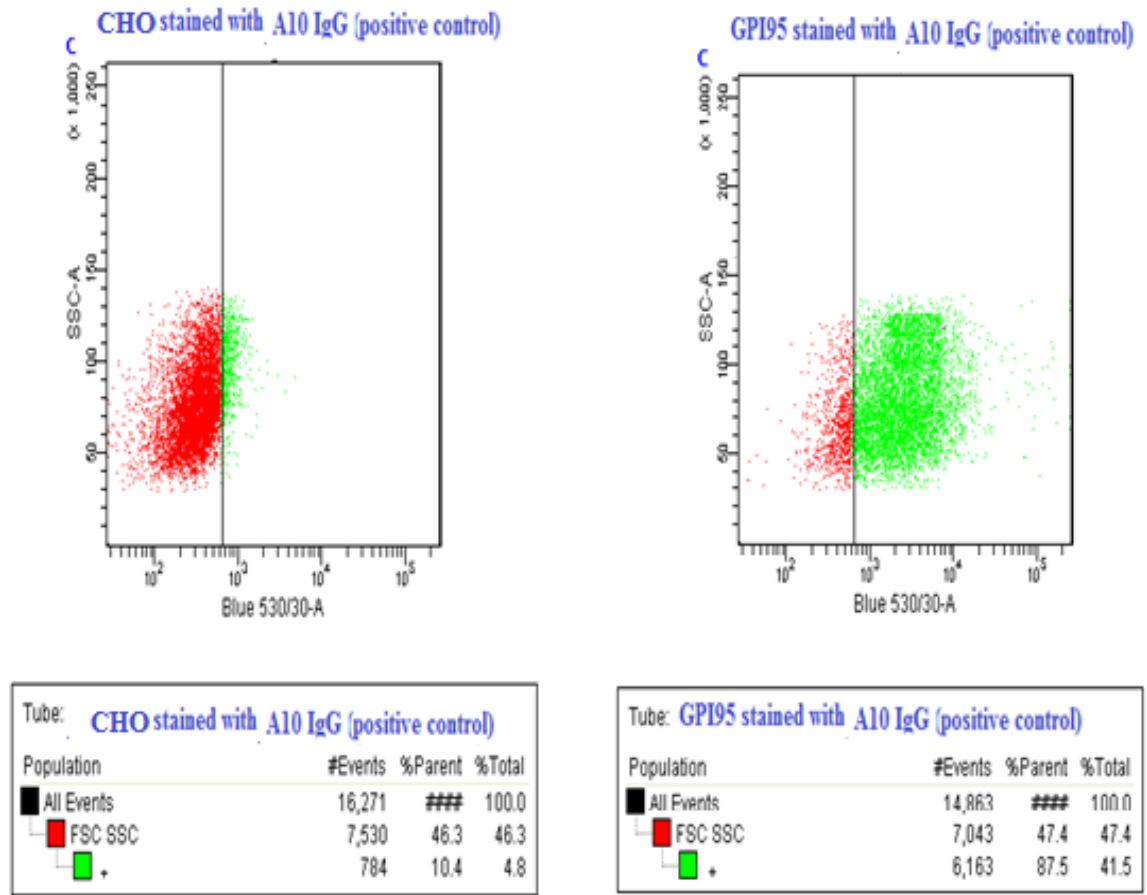


Figure3.10.b: FACS of the binding of A10 IgG to CHO-K and GPI-95 cells.

Histograms of fluorescence intensity are showing inability of A10 (mouse anti TSH receptor antibody) to bind untransfected CHO-K cells as a negative control versus to significant binding of A10 ((mouse anti TSH receptor antibody) to GPI-95 (CHO-K transfected with TSH receptor ectodomain) as a positive control.

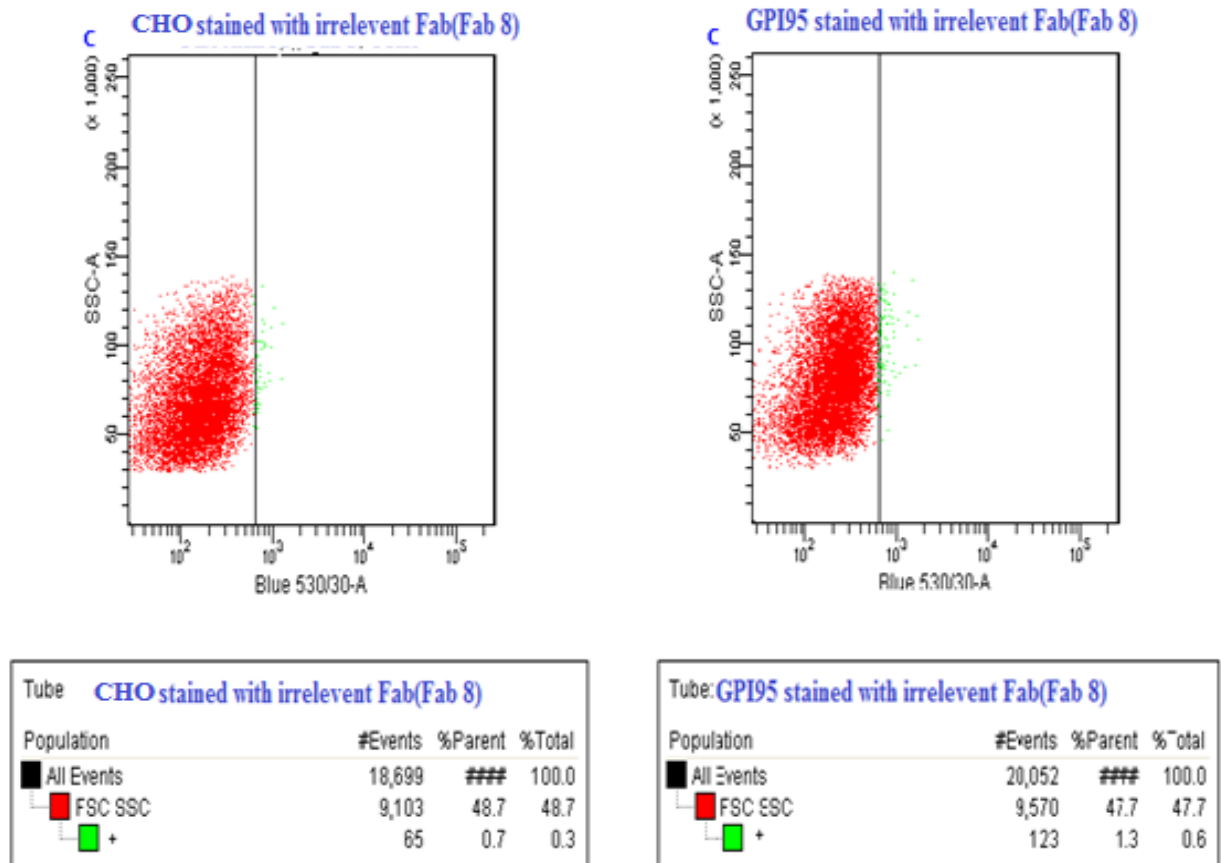


Figure 3.10.c: FACS of the binding of Fab 8 to CHO-K and GPI-95 cells.

Histograms of fluorescence intensity are showing inability of Fab 8 (TG2 antibody) as a negative control to bind untransfected CHO-K cells and GPI95 (CHO-K transfected with TSH receptor ectodomain).

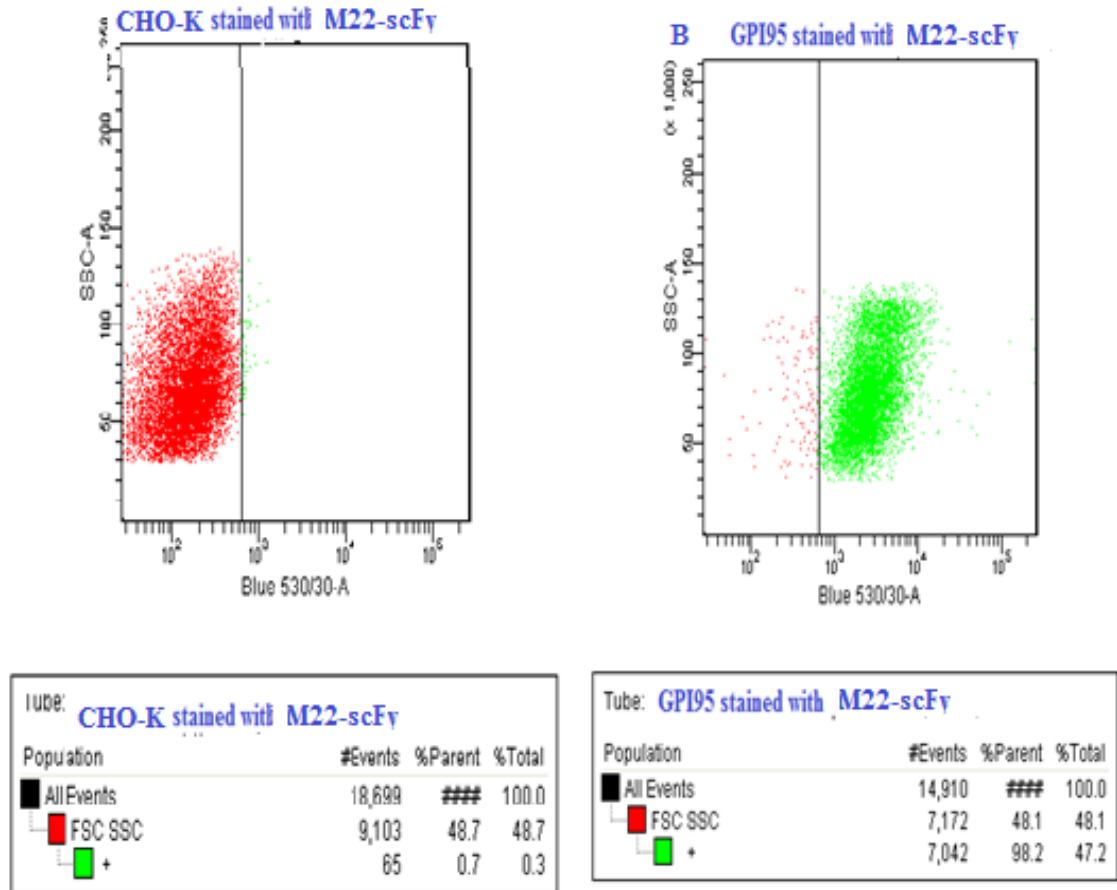


Figure 3.10.d FACS of the binding of Biotinylated M22-scFv to CHO-K and GPI-95 cells.

Histograms of fluorescence intensity showing significant binding of Biotinylated M22-scFv to GPI-95(CHO-K transfected with TSH receptor ectodomain) versus to inability of Biotinylated M22-scFv to bind untransfected CHO-K cells.

3.2.8 Stimulation of cAMP Production by M22 scFv

TSHR agonist activity was assessed by measurements of cAMP induction using the CHO-K1 cell line JP09 (Persani, Tonacchera et al. 1993). This cell line expresses approximately 20,000 copies of TSHR per cell and responds to TSH and TSAAb by producing cAMP. Purified M22 scFv was tested in the JP09 bioassay using a range of dilutions. JP09 cells were grown to confluence in 24-well plates and 20 μ l of each sample were added to the standard assay mix (500 μ l of Hanks BSS) (2.2.32) and incubated for 2 h. TSH and PBS were added as positive and negative controls respectively (Fig. 3.11). Cell extracts were produced by lysis and cAMP concentrations determined by ELISA using a commercial kit (cAMP Parameter Assay Kit, R and D Systems, Oxford UK).

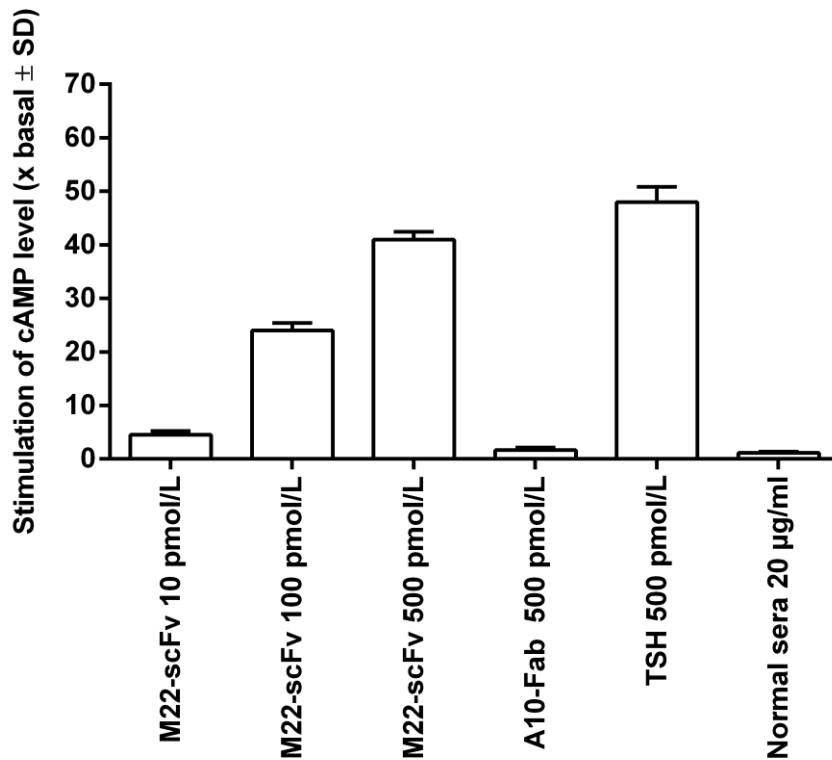


Figure3.101 JP09 Bioassay of TSHR Stimulation by Recombinant M22 scFv.

Stimulation of cyclic AMP to JP09 cells (Chinese hamster ovary cells (CHO-K) cells transfected with thyrotropin receptor (TSHR) by M22 scFv (10 pmol/L, 100 pmol/L, 500 pmol/L), non-stimulatory mAb A10 (500 pmol/L), bovine thyrotropin (bTSH) 500 pmol/L, and pooled normal human sera (20 µg/ml). Results shown are mean ± standard deviation (n=3). Basal cAMP production was determined in the presence of assay buffer only. Controls were mAb A10 was a non-stimulatory TSHR antibody (Nicholson, Vlase et al. 1996), bovine TSH, and pooled normal human sera. M22 scFv at 500 pmol/L increased cAMP production approximately 42-fold over basal, and bTSH at 500 pmol/L increased cAMP production approximately 50-fold. Negative controls showed no significant increase of cAMP production compared to basal levels. The overall *F*-test gave a *p*-value of 0.006; Results shown are the mean of at least two independent experiments.

3.3 Discussion

In this stage of the project we were able to successfully synthesise and clone the immunoglobulin gene sequences of the human monoclonal thyroid stimulating antibody M22. The antibody was successfully expressed and characterised. We were able to express useful quantities of the scFv antibody and confirm its binding and stimulating properties. The recombinant antibody bound to the TSHR in FACS, and more importantly it possessed agonist activity against the receptor. We were able to induce cAMP production in the JP09 bioassay at ng/ml concentrations - evidence of a true TSAb. Thyroid stimulating activity has been previously described for Fab fragments of M22 (Sanders, Evans et al. 2003), but this was the first time that stimulating activity has been documented for an scFv fragment. This was an important step for our project as examples of true TSAb monoclonals are very difficult to obtain, and are still considered commercially sensitive reagents.

The only reported attempt to use phage display to recover TSHR antibodies was unsuccessful, for reasons that were unclear (Van Der Heijden, De Bruin et al. 1999). To date there has been no published account of how potential TSAb antibodies behave when expressed on the surface of phage particles. Phage display has been successfully used to isolate patient autoantibodies in autoimmune thyroid disease (Hexham, Partridge et al. 1994; McIntosh, Tandon et al. 1994; McIntosh, Asghar et al. 1996; McIntosh, Asghar et al. 1997; McIntosh and Weetman 1997) and if this technique could be applied to the TSHR it would offer the potential to recover more examples of TSAb monoclonals from Graves' patient antibody phage libraries.

Construction of the M22-scFv phage provided for the first time a representative example of a TSAb in a phage display format, and could be used to investigate the binding properties of these antibodies, thus enabling the development of enrichment strategies that could be applied to recovery of other TSHR phage antibodies. The next stage of the project involved an investigation of this reagent, and attempts to demonstrate specific binding of M22 phage to different preparations of recombinant TSH receptor.

CHAPTER 4

SELECTIVE ENRICHMENT OF M22 PHAGE ON THE THYROTROPIN RECEPTOR

4.1 Introduction

In the previous section we described the construction of a phage antibody positive control based on the published human monoclonal TSAb M22 (Sanders, Evans et al. 2003). The identity of the antibody was confirmed by sequence analysis, and characterisation of its receptor binding properties, and ability to stimulate cAMP production in TSHR transfected CHO-K1 cells. The next stage of the project involved an investigation of the ability of this phage construct, and other variants, to recognise and bind preparations of the TSH receptor. The power of the phage display technique resides in the ability to select specific antibodies from diverse libraries through an iterative of enrichment on antigen, in which irrelevant antibodies are discarded to leave a population of specific recombinant monoclonal. The key to this process is the availability of pure or relatively pure antigen and an appropriate selective enrichment procedure. The phage antibody approach has been shown to be highly effective in autoimmune thyroid disease, and a range of monoclonal antibodies have been cloned in this way using other thyroid antigens such as thyroid peroxidase (TPO) and thyroglobulin (TG) (Hexham, Partridge et al. 1994; McIntosh, Asghar et al. 1996; McIntosh, Asghar et al. 1997). A stumbling block for attempts to isolate TSHR antibodies using this approach has been the lack of sources of pure TSH receptor. This protein is difficult to purify in native form (1.2.2), and binding of TSHR antibodies are exquisitely dependent on protein conformation (Rapoport, Chazenbalk et al. 1998). Recent advances in the field have seen the development of novel forms of TSH receptor expression, and have set the scene for renewed attempts to isolate TSHR monoclonals using recombinant antibody approaches.

The development of the BRAHMS TRAK assay for TSHR antibodies (Costagliola, Morgenthaler et al. 1999) was the result of advances in the recombinant expression of the TSH receptor. New cell lines were developed that expressed approximately 2 million copies of receptor per cell, and this breakthrough enabled the production of receptor on an industrial scale in bioreactors (Stiens, Buntmeyer et al. 2000). Attaching the recombinant receptor to solid support in plastic tubes provided the basis of the first commercial assay for direct binding of antibodies to the thyrotropin receptor and was marketed as the BRAHMS TRAb TRAK assay (BRAHMS GmbH, Hennigsdorf,

Germany). The BRAHMS kit provided a useful alternative source of native receptor to investigate binding of antibody phage constructs.

Alternative sources of high density cell surface expression of TSH receptor were produced by exploitation of glycosyl-phosphatidylinositol (GPI) anchors (Da Costa and Johnstone 1998; Metcalfe, Jordan et al. 2002). GPI anchors are found in a number of natural proteins, and comprise a glycolipid moiety that is attached to the carboxyl terminus during post-translational processing (Low 1989). This glycolipid structure intercalates between the lipids of the outer membrane and anchors the protein to the cell surface. Expression of the TSHR extracellular domain (TSHRecd) via a GPI anchor leads to high levels of protein expression and in the GPI-95 cell line produced in our laboratory this yields approximately 300,000 copies of the TSHRecd per cell, providing a useful reagent for the analysis of receptor binding (Metcalfe, Jordan et al. 2002). Another useful feature of GPI-linked proteins is that they can be extracted by partitioning with detergents such as Triton X-114, enabling the preparation of semi-pure protein extracts (Patton, Dhanak et al. 1989)

In this section of the project we will investigate the binding of the M22 antibody phage construct to different preparations of the TSHR. We will use this control reagent to attempt to develop an enrichment strategy for the recovery of TSHR antibodies using phage display techniques. In addition, in line with the aims of the project, we will attempt the enrichment of TSHR antibodies from a phage antibody library that was previously synthesised in our laboratory using B lymphocytes extracted from the thyroid gland of a Graves' patient (McIntosh and Weetman 1997). Lymphocytic infiltration of the thyroid gland is a feature of AITD patients and intra-thyroidal lymphocytes are known to be a rich source of autoantibody producing B cells (Dalan and Leow 2012). Phage antibody libraries made from this source represent the most promising starting material for attempts to recover specific receptor antibodies.

4.2 Initial Phage Binding Experiments

4.2.1 Investigation of M22-scFv Phage

4.2.1.1 Methods

Phage displaying M22 scFv antibody was produced by phage rescue using the method described in section 2.2.16. In brief, a glycerol stock of M22-pAK100 was inoculated into 10 ml of LB medium, and after a period growth in which the turbidity approximately doubled it was superinfected with VCSM13 helper phage (Stratagene) and grown overnight with high aeration (2.2.16). Phage particles were precipitated by the addition of PEG 6000 and 5 M NaCl, followed by centrifugation at 2,500 g for 30 min. Precipitated phage were resuspended in PBS/Tween (0.1% v:v) and titered (2.2.18). Phage particles were re-suspended to a density of approximately 10^{11} plaque forming units (pfu) per ml. TSHR-coated immunotubes, hereafter referred to as BRAHMS tubes, were obtained from a commercial anti-TSHR antibody assay kit (BRAHMS, GmbH, Hennigsdorf, Germany). BRAHMS tubes are coated with native recombinant TSHR protein which is captured and stabilised on the assay tube using a mouse mAb which is pre-coated onto the tube surface (Costagliola, Morgenthaler et al. 1999). This monoclonal (BA8) was carefully selected not to interfere with the assay process, and does not interfere with the blocking or stimulatory epitopes of the TSH receptor. The tubes were blocked with 400 μ l of PBS/BSA 3% (w:v) for 1 hour at 37°C. The blocking solution taken out and 100 μ l of phage library was added (typically 10^{10} pfu) and incubated for 1 hour at room temperature. Unbound phage were removed, and the tubes washed eight times with 2 ml PBS/Tween (0.1% v: v) at room temperature. Adherent phage were eluted by the addition of 100 μ l of glycine buffer and incubation at room temperature for 10 min. Eluted phage were, and neutralised with 6 μ l of 2 M of Tris. Eluted phage were used to infect 1 ml of log phase culture of fresh XL1-Blue host for 20 min at 37°C. The pAK100 vector is a phagemid and after infecting host bacteria it produces a conventional plasmid which carries antibiotic resistance and will give rise to a conventional colony, in contrast to other bacteriophage such lambda, which is limited to plaque formation. Exploiting this this feature, the number of eluted phage were monitored by plating 10 μ l samples of infected host onto LB agar plates containing (30 μ g/ml chloramphenicol 10 μ g/ml tetracycline), followed by overnight

incubation at 37°C to allow colony growth. The resulting colonies were used to calculate the number of eluted phage. To provide a suitable negative control irrelevant antibody phage were prepared from an anti-tissue transglutaminase antibody (TG2-8). A positive control phage construct was produced using TSHR mAb A10. This antibody recognises a linear TSHR epitope remote from the key binding sites for TSHR autoantibodies, and does not require native protein conformation for recognition (Nicholson, Vlase et al. 1996). Both TG2-8 and A10 immunoglobulin genes were cloned into pAK100 and used to generate phage particles (data not shown). As an additional control identical uncoated immunotubes, lacking TSH receptor, were also used in binding-elution experiments.

4.2.1.2 Results

The results of the binding-elution experiments are shown in Fig. 4.1. Surprisingly, there was no significant difference between the binding and elution of the M22-scFv phage and both positive and negative control phage. Approximately $8-10 \times 10^4$ phage were eluted in each case. In this one-step elution experiment no difference in phage binding to TSH receptor was observed.

4.2.2 Enrichment of Graves' Patient Antibody Library on BRAHMS Tubes

4.2.2.1 Methods

The experiment described in the previous section was a one-step elution design, in which phage were simply bound to antigen coated tubes, washed to remove unbound phage and then eluted. This methodology is appropriate when dealing with single defined phage clones with specificity for the antigen target. More commonly phage antibody libraries are highly diverse and repeated rounds of enrichment, or panning, are used to select single monoclonal reagents from a non-specific background. A conventional phage enrichment protocol sees an increase in the number of eluted phage at each round of selection, typically leading to an increase of the order of 10,000 fold between the first and last round. In this stage of the project the library used, HT127 was derived from intrathyroidal lymphocytes was highly diverse, comprising approximately

2×10^6 individual clones (McIntosh, Asghar et al. 1996). The aim of this experiment was to take advantage of the pure TSH receptor protein provided by the BRAHMS tubes to attempt the enrichment of the HT127 library by sequential rounds of panning, and to recover receptor specific monoclonal antibodies.

BRAHMS tubes were blocked with 400 μ l of 3% BSA in PBS/Tween for 1 hour at 37°C. The tubes were washed five times with 2 ml (approximately 0.5 tube volumes) of PBS/Tween and 100 μ l of HT127 phage library (10^{10} phage particles) was added and incubated for 1 hour at room temperature. The phage library was removed, and the tube washed ten times with 2 ml of PBS/Tween to remove unbound particles. Adherent phage were eluted by the addition of 100 μ l of Glycine Buffer and incubation at room temperature for 10 min. was added and the tube incubated on ice for 10 min. The eluted phage were neutralized with 6 μ l of 2 M Tris and used to infect 1 ml of log phase culture of fresh XL1-Blue host. Aliquots of infected host were plated onto selective medium and following overnight the resulting colonies were used to calculate the number of phage eluted from the coated tubes at each round. The remaining infected host was added to 100 ml of LB medium (30 μ g/ml chloramphenicol, 20 μ g/ml tetracycline) and grown for 1 hour in a 37°C shaking incubator. The culture was superinfected with 50 μ l of helper phage VCSM13 (10^{11} pfu/ml), adjusted to 30 μ g/ml kanamycin, and grown overnight in a 37°C shaking incubator. The rescued phage libraries were recovered as described (2.2.16), titered and used for the next round of enrichment.

4.2.2.2 Results

The HT127 phage library was enriched for 5 rounds on the BRAHMS tubes and on control uncoated tubes. As a negative control TG2-8 phage were also subjected to enrichment to probe the effects of any non-specific binding. The results for TSHR coated tubes are shown in Fig. 4.2. Both the HT127 library and negative control libraries showed only a moderate, approximately 3 fold increase in the number of eluting phage over 5 rounds of enrichment. There no apparent evidence of selective binding or enrichment for either Graves' patient or negative control phage antibodies. Similar data were obtained for the non-coated tubes (Fig. 4.3). Overall the number of

eluting phage was slightly less than seen with the TSH receptor coated tubes, but suggested that there was no specific binding to the TSH receptor.

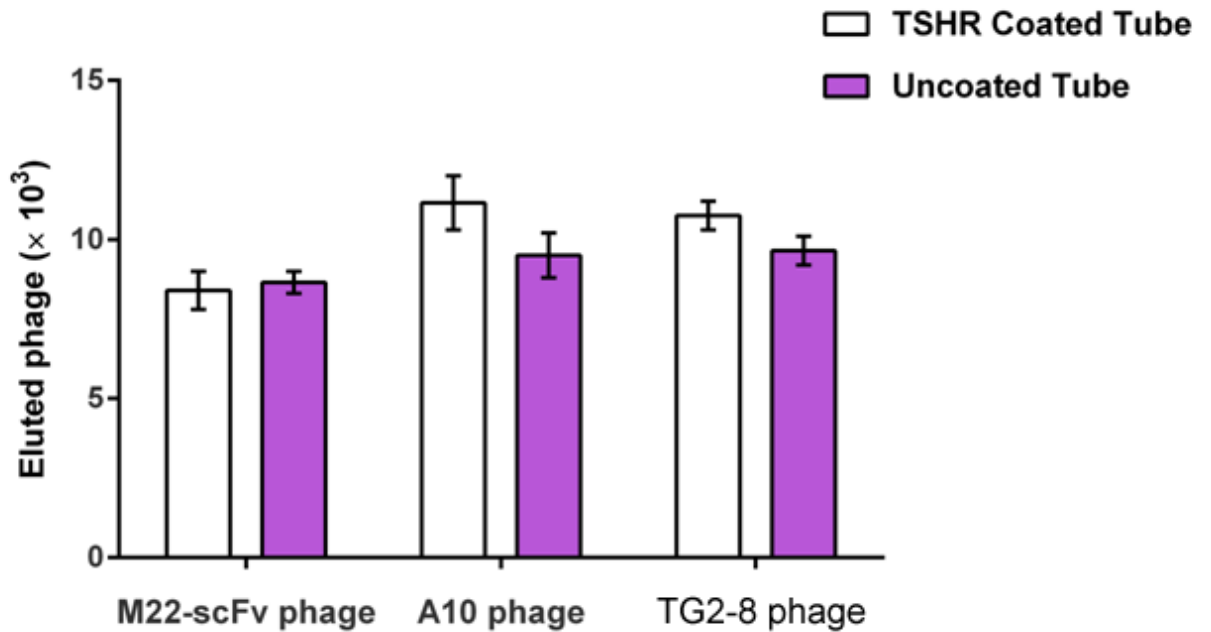


Figure 4.1 Binding of M22-scFv to TSHR-coated BRAHMS tubes.

The number of phage eluted from TSHR-coated and non-coated tubes. The number was estimated by plating of aliquots of infected host cells. Binding was determined for phage displaying M22 scFv, positive control phage displaying an anti-TSHR antibody A10, and irrelevant phage displaying an anti-transglutaminase antibody TG2-8. Data are the mean \pm SD (n=3), results shown are the mean of at least three independent experiments.

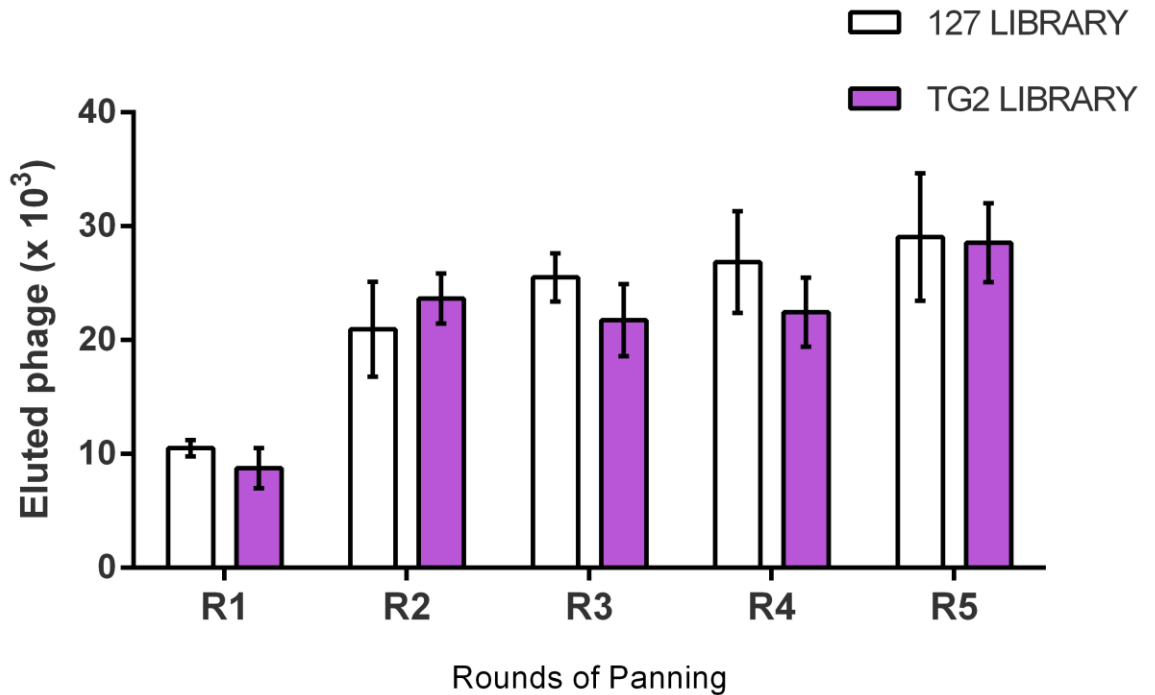


Figure4.2:- Enrichment of 127-scFv library to TSHR-coated BRAHMS tubes.

The number of phage eluted from TSHR coated tubes following binding of HT127-scFv and TG2-8 (negative control) libraries. A moderate increase in the number of bound phage was observed with both HT127 and TG2-8(anti-transglutaminase antibody) phage over 5 rounds of selection. There was no evidence of selective enrichment of the HT127 Graves' patient antibody library. The number was estimated by plating of aliquots of infected host cells. Data are the mean \pm SD (n=3), results shown are the mean of at least three independent experiments.

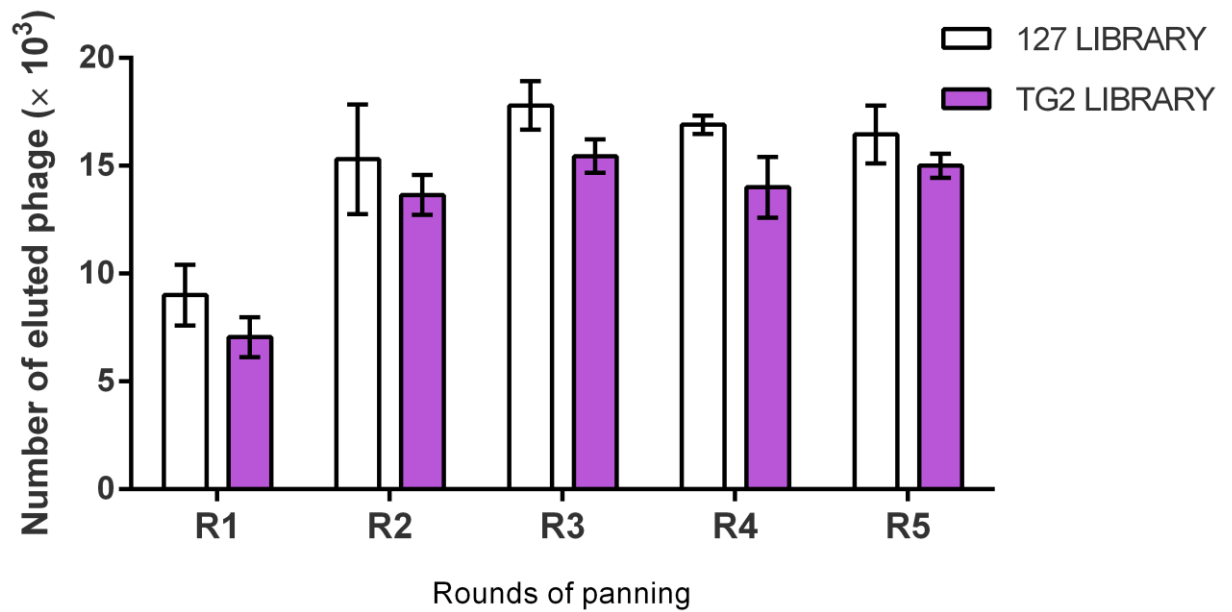


Figure4.3:- **Enrichment of 127-scFv library to non-coated tubes.**

The number of phage eluted from non-coated tube from HT127 and TG2-8(anti-transglutaminase antibody as negative control) libraries. The number was estimated by plating of aliquots of infected host cells. Data are the mean \pm SD (n=3), results shown are the mean of at least three independent experiments.

4.2.3 Results Summary

The binding and elution results obtained for the positive control M22-scFv phage showed no evidence for specific binding to BRAHMS tubes coated with purified TSH receptor. Both positive control A10 and negative control TG2-8 phage eluted with approximately similar numbers indicating a level of non-specific binding of all phage constructs. The M22 scFv antibody was previously shown to be specific for the TSH receptor and possessed the predicted agonist activity as determined by the induction of cAMP production in a TSHR transfected cell line. Monoclonal A10 is also specific for the TSHR and recognises a distinct linear epitope distal to the disease-related blocking or stimulatory antibody binding sites (Nicholson, Vlase et al. 1996). The eluted phage from M22 and A10 may have bound to the receptor in this experiment but the non-specific background binding of negative control TG2-8 phage indicated that it would not be possible to select receptor targeting phage antibodies using this approach. The attempted enrichment of the Graves' patient antibody library HT127 seemed to support this conclusion. There was no evidence of selective enrichment of this library when compared to irrelevant control phage. This result contrasted strongly with previous experiments carried out in our laboratory using the HT127 library, in which selective enrichment on two other thyroid antigens, thyroid peroxidase and thyroglobulin, lead to an increase in elution frequency of approximately 100,000 fold over 5 rounds of panning, and the recovery of high affinity antibody clones (McIntosh and Weetman 1997).

A number of possible reasons could account for the results obtained and these were considered under two main headings:

TSHR as an antigen

Potential differences between the M22 antibody and M22 phage fusion

Firstly, the receptor coated tubes may not have contained sufficient receptor to provide an efficient binding surface. The exact coating density of the BRAHMS tubes is proprietary information to which we did not have access. However, communication with a representative of the company suggested that the TSHR coating was of the order of micrograms, and well within the range necessary for phage enrichment. Indeed, the

coating density is such that the tubes can be used in a conventional ELISA format (Dr. Andreas Bergmann, BRAHMS GmbH, personal communication). A second consideration was the fact that the TSHR extracellular domain is heavily glycosylated, approximately 40% by weight (Rapoport, Chazenbalk et al. 1998). Heavy glycosylation around antigenic sites can sterically disrupt antibody binding, and this phenomenon of "glycan shielding" is well established in the field of viral immunology (Wanzeck, Boyd et al. 2011). In this case the M22 scFv antibody has already been shown to recognise the receptor, and possible interference with binding in this case seems to be a problem only when the antibody is used as a phage construct. An important consideration is that phage antibodies are really quite different in physical terms from their corresponding phage fusions. A typical IgG class antibody has a molecular weight of approximately 150 kDa, in Fab form this becomes 50 kDa, and scFv antibodies are approximately 25 kDa. M13 filamentous phage has a molecular weight of approximately 55 MDa, or more than 2,000 times bigger than an scFv antibody. A typical Fab fragment is approximately 8 nm in length, and an scFv antibody around 3-4 nm. In phage display either Fab or scFv are fused to the minor coat protein cpIII, which is approximately 4 nm in length. M13 phage is essentially a long cylinder, capped at one end with cpIII (or cpIII fusions). The phage capsid is 6 nm in diameter and 900 nm long (Fig. 4.4). It is possible that in some cases the physical form of antibody phage may sterically hinder access to the corresponding target epitope.

Based on the initial results of phage panning it was decided to investigate the possible effects of both glycosylation and the phage antibody structure in a series of experiments. TSHR glycosyl groups were enzymically removed, and panning experiments repeated to investigate any effect on binding. In a second series of experiments different antibody phage constructs were made to modify the arrangement of antibody and capsid. Fab fragments are approximately double the size of scFv constructs, and a Fab version of M22 was synthesised and investigated. Finally, a long flexible linker was inserted between the antibody and cpIII coding regions to further extend the distance of the antigen binding domains from the virus capsid.

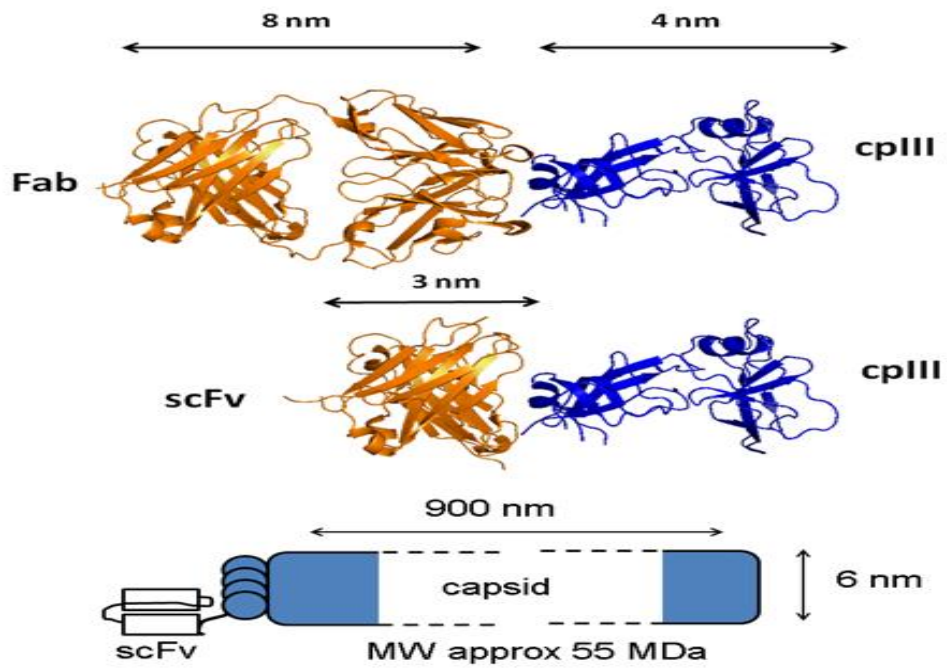


Figure 4.4 Schematic diagram showing the components of phage antibody structures. Relative sizes of antibody fragments, phage coat protein cplIII, and the M13 viral capsid.

4.3 M22 Fab Binding Experiments

Phage binding experiments with the M22-scFv construct failed to give any results for specific binding of M22 scFv to tubes coated with TSH receptor while the soluble form of M22 scFv was shown the ability to bind to the TSH receptor in FACS analysis, and stimulated cAMP production. The possible reason for this may be the involvement of some steric factor. The structure of phage may be the cause that prevents the binding.

In this part of experiments, different antibody phage constructs were made to modify the arrangement of antibody and phage and solve the binding problem between the phage expressing M22 and TSH receptors.

Linking of Fab fragments to phage surfaces has been reported by a number of groups. In the pComb3 vector system, immunoglobulin heavy chain Fab fragments are expressed as fusion proteins covalently linked to the minor phage coat protein III (cpIII). Immunoglobulin light chain Fab fragments are expressed from a second promoter in the same plasmid. Secretion leader sequences direct both chains to the periplasmic space where the redox conditions enable the formation of disulfide bonds and generation of cpIII-Fab fusion protein (Fig. 4.5) (Barbas 1991).

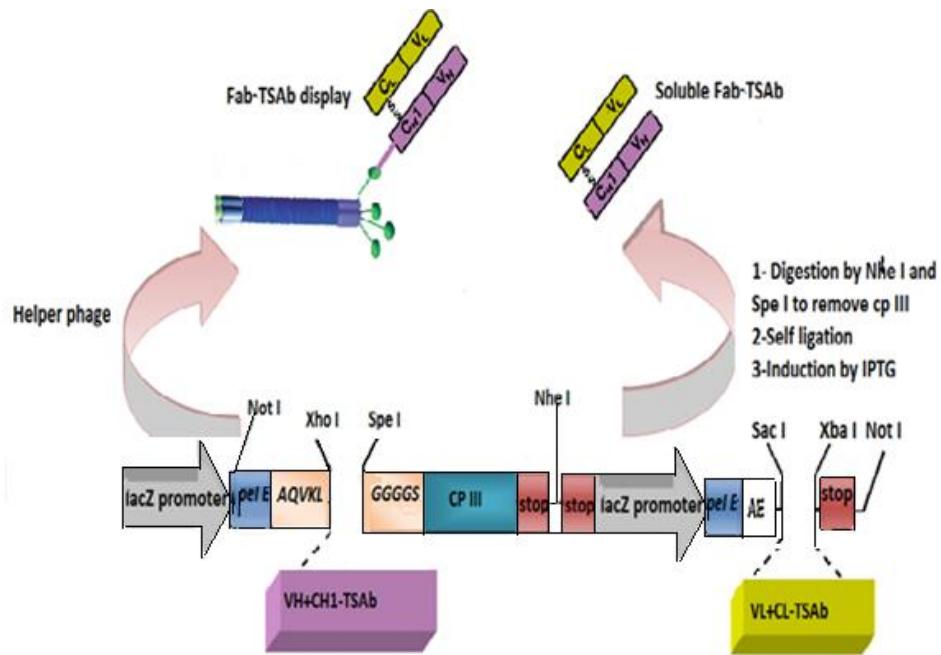


Figure 4. 5 Cloning sites of phage display vector pComb3.

Immunoglobulin heavy chains were cloned into the *Xho* I and *Spe* I sites of pComb3 and expressed as amino terminal fusions with minor phage protein cpIII. Light chains were cloned into the *Sac* I and *Xba* I sites. Expression of both chains is driven by a separate *lacZ* promoter and secretion into the periplasm is directed by a *pelB* secretion leader upstream of the 5' cloning site.

4.3.1 Methods

4.3.1.1 Cloning of M22 Immunoglobulin Chains into pComb3

The synthetic M22 heavy and light chains (section x.x.x) were diluted 1:1000 in H₂O and used for template for PCR amplification. The M22 VH chain was amplified (25 cycles) using the primers RS-VH1 and RS-VH2 containing Xho I and Spe I restriction sites for cloning into the pComb3 heavy chain site (Table 4.1), and the M22 VL chain was amplified (25 cycles) using the primers RS-VL1 and RS-VL2 (Table 4.1) containing Sac I and Xba I restriction sites for cloning into the pComb3 light chain site. M22 VH Fab PCR products were purified using Wizard DNA Cleanup kit. Purified VH PCR product was digested with 10 units of *Spe* I and *Xho* I and 10 µl of 10 x restriction buffer (Buffer B), in 100 µl reaction mixture at 37°C for 3 hours.

5 µg of pComb3 was digested with 10 units of *Spe* I and *Xho* I and 10 µl of 10 x restriction buffer (buffer B), in 100 µl reaction mixture at 37°C for 3 hours, and the cut vector gel purified by the Wizard DNA Cleanupkit. 60 ng of digested VH PCR products were ligated to 100 ng of pComb3 plasmid at 15°C overnight in a 20 µl ligation reaction containing 2 µl of ligation buffer and 5 units of T4 ligase (Promega). The next day the ligation mixture was transformed into XL1-Blue and plated out onto LB agar plates (100 µg/ml ampicillin). Colonies were picked and the construct confirmed by sequencing and identified as pCOMB3-VH.

DNA was prepared from pComb3-VH and digested for 3 hours at 37°C with Sac I and Xba I in a 100 µl reaction containing 10 µl of Multicore Buffer and 10 units of each enzyme (Promega). The recombinant pComb3-VH band was purified by slot gel electrophoresis and used for cloning of M22 light chains.

Purified M22 VL PCR products were digested with *Xba* I and *Sac* I restriction in a 100 µl reaction containing 10 µl of Multicore Buffer and 10 units of each enzyme (Promega). Digested VL products were gel purified by the Wizard DNA Cleanup kit. M22 VL PCR products (approximately 100 ng) were ligated to 200 ng of digested pComb3+VH in a 20 µl ligation reaction containing 2 µl of ligation buffer and 5 units of T4 ligase (Promega) (2.2.9). The ligation mixture was incubated overnight at 15°C, transformed into XL1-

Blue (2.2.210), and plated out onto LB agar plates (100 µg/ml ampicillin). Random colonies were selected for confirmation by restriction digest and sequencing.

4.3.1.2 Expression and Purification of M22 Fab

To verify the cAMP stimulatory activity of the recombinant M22 Fab it was necessary to express and purify soluble Fab from the M22-pComb3 construct. The original pComb3 plasmid was modified by insertion of a histidine tag to facilitate Fab purification. A pair of phosphorylated complementary oligonucleotides were designed to encode a 6 histidine tag, a stop codon and included cohesive ends compatible with the *Spe* I and *Nhe* I sites of pComb3. These oligonucleotides, His-1 (5'- CT AGT CAT CAT CAT CAT CAT TAA GCT AGC -3') and His-2 (5'-C TAG GCT AGC TTA ATG ATG ATG ATG ATG ATG A -3'), were combined in TE buffer at a concentration of 10 pmol/µl and heated to 90°C for 1 minute and cooled over a period of 20 mins to 0°C to allow annealing. Annealed oligonucleotides were diluted 1:100 to a final concentration of 0.1 pmol/µl in. M22-pComb3 DNA (2 µg) was restricted for 3 hours at 37°C with 10 units each of *Spe* I and *Nhe* I in a 100 µl reaction contained 10 µl of Buffer B (Promega)(2.2.7). The digested DNA was purified by slot gel electrophoresis and the Wizard DNA Cleanup kit (2.2.5). Annealed oligonucleotides (40 pmole) were ligated overnight with 200 ng of digested M22-pComb3 plasmid in a 20 µl ligation reaction. Ligated DNA was electroporated into XL1-Blue and transformed cells plated onto LB agar plates (100 µg/ml of ampicillin (2.2.10).

The induction procedure of M22 Fab expression was carried out as described in 2.2.22. Briefly, 10 ml of LB medium (60 µg/ml ampicillin) was inoculated with 10 µl of glycerol stock of M22-pComb3His and grown overnight in 37°C shaking incubator. This culture was used to inoculate 1L of LB (60 µg/ml ampicillin) and grown in presence of 1 mM IPTG for overnight in a 25°C shaking incubator.

The induced culture was centrifuged at 2000 g for 10 min, the supernatant was removed for further analysis and the bacterial pellet was used for periplasmic extraction, using osmotic shock method as previously described (2.2.22). The periplasmic extract and the

supernatant were then concentrated ten-fold using a micro-concentrator (Amicon). The protein content was estimated by Bradford assay (2.2.22) or by measurement the OD₂₈₀ and used for SDS-PAGE, western blotting analysis and purification. The M22 Fab content was estimated by ELISA to be approximately 200 µg/ml.

Periplasmic extracts were loaded onto the TALON IMAC column (2.2.23.1) and washed with 3 times with Equilibration/Wash buffer. His-tagged M22 Fab was eluted with 100 µl aliquots of elution buffer containing increasing concentrations of imidazole (50 mM, 100 mM, 200 mM, and 500 mM). Small aliquots (10 µl) of eluted fractions were mixed directly with 100 µl of Bradford reagent and protein elution monitored directly by visual inspection. Positive fractions were pooled, dialyzed overnight against PBS and resuspended at approximately 50 µg/ml. Purified M22 Fab was analyzed by SDS-PAGE and Coomassie staining (2.2.25).

4.3.1.3 FACS Analysis of M22 Fab

To investigate the binding and specificity of purified M22 Fab to TSHR, the purified M22 Fab was analysed by flow cytometry analysis using GPI-95 cells (2.1.6). The flow cytometry analysis was performed as described in section 2.2.27 After cells were counted, resuspended at the density of 1×10^7 cells/ml and 100 µl aliquoted into LP4 tubes (Becton Dickinson). Mouse anti-human TSHR monoclonal antibody 2C11 (Serotec) was used as a positive control, and irrelevant transglutaminase antibody TG2-8 was used a negative control. Antibody was added to the cells, thoroughly mixed and the reaction incubated for 20 min on ice. After washing twice with 2 ml PBS cells were centrifuged at 1,000 g for 3 min, and resuspended in 1:100 (2 µg/ml) goat-anti-human immunoglobulin FITC conjugate (Serotec) for M22 Fab, and 1:100 (2 µg/ml) goat-anti-mouse immunoglobulin FITC conjugate (Serotec) for the 2C11 and TG2-8 controls. Samples were incubated on ice for 20 min. After a final wash, cells were analysed using a fluorescence activated cell sorter.

4.3.1.4 cAMP Bioassay of M22 Fab

To confirm the identity of the purified M22 Fab samples were tested in the JP09 bioassay (2.2.32). Three samples of each, 10 µl, 20 µl, and 50 µl were added to the standard assay mix (500 µl of Hanks BSS) (2.2.24) and incubated for 2 h. TSH and PBS were added as positive and negative control respectively.

4.3.1.5 Rescue of M22 Fab Phage and Binding Experiments

To perform phage binding experiments the M22-pComb3 plasmid was used to produce phage particles by superinfection with VCSM13 helper phage (2.2.15). Briefly, a log phase 10 ml culture of M22-pComb3 was infected with 50 µl of VCSM13 helper phage and incubated at 37°C for 15 min. Then infected culture was put in 100 ml LB media (100 µg/ml of ampicillin, 20 µg/ml of kanamycin, and 20 µg/ml of tetracycline) and incubated overnight at 37°C with shaking. The culture was then centrifuged at 2,000 g for 15 min to remove all bacterial cells. 40% PEG 800 (5 ml) and 5 M NaCl (5 ml) were added to the resulting supernatant and incubated at 4°C overnight to precipitate phage particles. These were centrifuged at 2,000 g for 30 min and the pellet resuspended in 1 ml of PBS. The phage suspension was tittered (2.2.18) and suspended at a density of approximately 10^{11} pfu/ml.

4.3.1.6 Panning of M22 Fab Phage

BRAHMS tubes were blocked by 400 µl of 3% (w: v) BSA for 1 hour at 37°C. The blocking solution taken out, and 100 µl of M22 Fab phage was added (10^{10} pfu) and incubated for 1 hour at room temperature. Unbound phage were removed, and the tube washed eight times with 2 ml PBS/Tween at room temperature. The adherent phage were eluted by the addition of 100 µl of glycine buffer and incubation on ice for 10 min, and neutralised with 6 µl of 2 M of Tris. Eluted phage were used to infect 1 ml of a log phase culture of XL1-Blue host for 15 min at room temperature to allow infection take place. The number of eluted phage were monitored by plating 10 µl of infected host onto LB agar plates (100 µg/ml ampicillin 10 µg/ml tetracycline) and growing overnight at 37°C. The resulting colonies were used to calculate the number of bound phage.

4.3.2 Results

4.3.2.1 M22 cloning into pComb3

Synthetic M22 VH and VL genes were used as template for PCR amplification of heavy and light chain Fab fragments. PCR products were analysed by agarose gel electrophoresis. Figure 4.6 shows the yield of VH and VL from the amplification. Both products were clean with no evidence of side bands and the negative control did not contain any products.

M22 VH products were digested with *Xho* I and *Spe* I and ligated into pComb3 to give pComb3-VH. This construct was linearised by *Spe* I digestion and compared to the original pComb3 vector by gel electrophoresis. Figure 4.7 shows that pComb3-VH contained the M22 VH chain and was approximately 800 bp larger than pComb3. M22 VL chains were digested with *Sac* I and *Xba* I and ligated into pComb3-VH to give the final construct M22-pComb3. Samples of M22-pComb3 were linearised by *Spe* I digestion and compared to pComb3 and pComb3-VH (Fig. 4.7). The results showed the expected size of the final construct and sequencing confirmed the presence of M22 VH and VL chains.

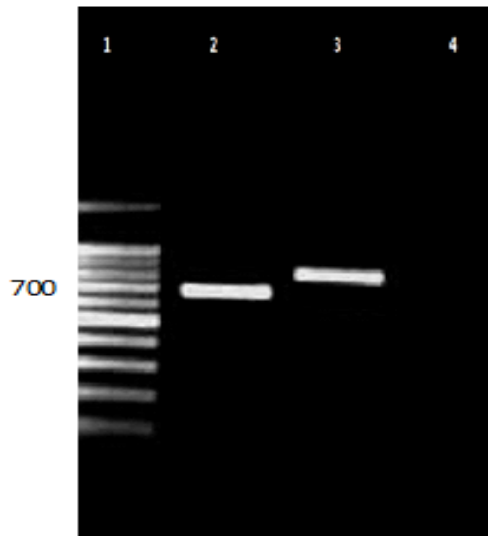


Figure 4.6 PCR products of VL and VH M22 Fab.

Lane 1: 100bp ladder. Lane 2: The yield of M22 VL (approx. 700bp). Lane 3: The yield of variable M22 VH (approx. 800bp). The PCR products purified digested and ligated to pComb3. Lane 4: Negative control.

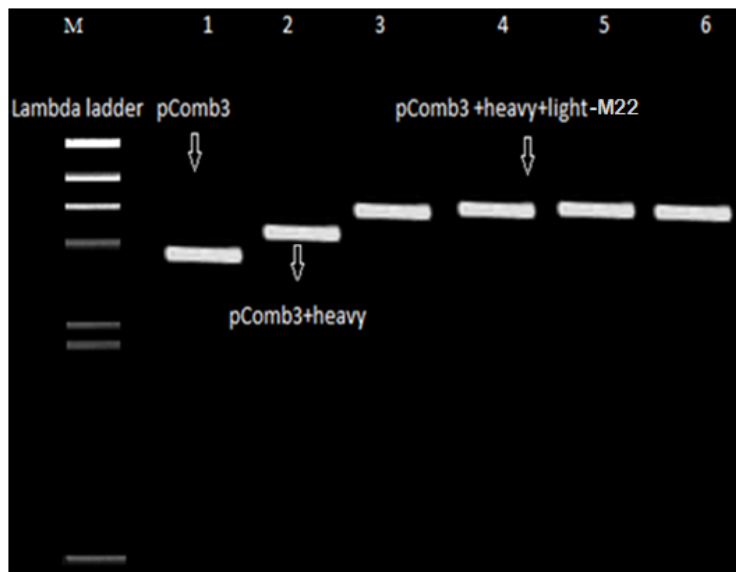


Figure 4.7 Cloning of M22 VH and VL genes into pComb3.

Comparison between Size of pComb3, pComb3-VH, and M22-pComb3. DNA samples were linearised by Spe I digestion and analysed by agarose gel electrophoresis. Lane M: λ HindIII ladder, Lane 1: pComb3 (4023 bp), Lane 2: pComb3-VH (4023+800 bp), Lane 3-6: M22-pComb3 (4023+800+700 bp).

4.3.2.2 Expression and Purification of M22 Fab

To enable the production and purification of M22 Fab the M22-pComb3 construct was digested with *Spe* I and *Nhe* I to remove the cpIII coding region. Approximately 5 µg of M22-pComb3 was digested and purified by slot gel electrophoresis. Figure 4.8 shows the separation of the parent vector, containing M22 VH and VL genes, and the cpIII region. The vector was extracted from the gel using the Wizard DNA Cleanup kit. To produce soluble Fab a histidine tag and stop codon was introduced at the C-terminal coding region of the M22 heavy chain. Complementary oligonucleotides (His-1 and His-2) were annealed and ligated into the digested M22-pComb3 vector to produce M22-pComb3-His. The ligation was transformed and five random colonies were picked and grown in 10 ml LB (100 µg/ml ampicillin), and plasmid DNA purified by miniprep. The clones were screened for recombinance by sequencing using primer pc-prim2, and Figure 4.9 shows a partial sequence of the verified clone. The M22 heavy chain was placed in-frame with a 6 histidine coding sequence, followed by a stop codon.

A 1 L culture of XL1-Blue containing the M22-pComb3-His construct was grown at 37°C until the turbidity reached approximately 0.4 OD_{600nm}. At this point gene expression was induced by the addition of IPTG to 1 mM and the culture was continued for a further 12 hours. 10 ml samples of the culture were taken immediately before the addition of IPTG (T₀) and following the 12 hour induction (T₁₂), these were used to produce cell extracts and analysed by non-reducing SDS-PAGE to monitor gene expression. Figure 4.10 shows the gel analysis of M22 Fab expression. A clear band of induced protein can be seen at in the T₁₂ sample at approximately 50 kDa, corresponding to the predicted size of recombinant Fab molecule. A second smaller band (25 kDa) is also present in the induced sample and probably corresponds to monomeric heavy or light antibody chain. Recombinant Fab is maintained in dimer form by a single disulphide bond and the appearance of monomers is common phenomenon under SDS-PAGE conditions. The remaining induced culture was used to prepare bacterial extracts (2.2.22) and concentrated ten fold before the M22 Fab was purified via the 6xHis tag by metal affinity chromatography on a TALON nickel column. Pure Fab was eluted with 300 mM imidazole and dialysed overnight against 20

mM Tris pH 7.0 before being concentrated to approximately 200 mg/ml. A sample of the pure M22 Fab was analysed by non-reducing SDS-PAGE (Fig. 4.11) and showed a clear pure band of Fab at approximately 50 kDa.

4.3.2.3 FACS Analysis of M22 Fab

Direct binding to the TSHR was assessed by flow cytometric analysis using GPI-95 cells, a stably CHO-K1 cell line that expresses the TSHR extracellular domain on the cell surface attached to a GPI anchor (Metcalf, Jordan et al. 2002). An anti-TSHR mouse monoclonal A10 was used as a positive control. An anti-transglutaminase Fab TG2-8 was included as a negative control, and in addition binding was measured using control untransfected CHO-K1 cells. All antibodies were used at a concentration of 25 µg/ml and the secondary antibody was FITC-conjugated anti-mouse . Fig. 4.12 shows the binding of M22 Fab

4.3.2.4 cAMP Bioassay

TSHR stimulatory activity was analysed using a bioassay based on CHO-K1 cells expressing the receptor. Cellular cAMP levels were determined using a commercial ELISA assay. Figure 4.13 shows the ability of M22 Fab to stimulate cAMP production at a range of concentrations from 10 to 1000 pmol/L. Maximal cAMP stimulation (30 x basal) was achieved with M22 Fab at approximately 300 pmol/L. Bovine TSH was used as a positive control and gave maximal cAMP production (30 - 40 x basal) at a concentration of approximately 1400 pmol/L. Negative controls Fab TG2-8 and pooled normal human serum showed no significant increase in cAMP production across the dose range. The results showed that recombinant M22 Fab exhibited TSHR stimulatory activity at nanomolar concentrations and confirmed the identity of the M22 Fab construct.

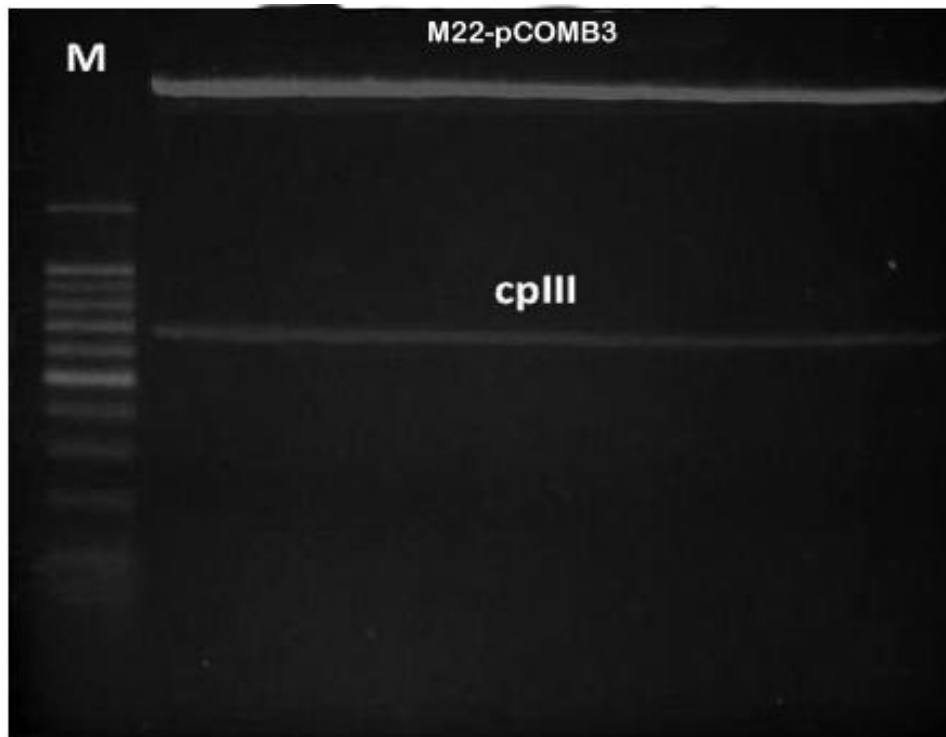


Figure 4.8 Digestion and gel purification of M22-pComb3.

0.8% agarose gel showing the digested M22-pComb3. Lane M: 100bp DNA ladder, and slot showing the M22 pComb3 construct digested with *Spe I* and *Nhe I* to release the phage coat protein (cpIII coding region) which is approximately 700bp and create compatible ends for the ligation of the His linker.

```

CTGGGCTGCCTGGTCAAGGACTACTTCCCCGAACCGGTGACGGTGTCTCGTGGAACTCAGGCGCCCTGACCA
L G C L V K D Y F P E P V T V S W N S G A L T

GCGGCGTGCACACCTTCCCGGCTGTCCTACAGTCCCTCANGACTCTACTCCCTCGGCAGCGTGGTGACCGT
S G V H T F P A V L Q S S X L Y S L G S V V T V

                               Spe I
GCCCTCCAGCAGCTTGGGCACCCAGACCTACATCTGCACTAGTCATCATCATCATCATCATTAAGCTAGC
P S S S L G T Q T Y I C T S H H H H H H . A S

```

Figure 4.9 Partial sequence of the M22 VH region of construct M22-pComb3-His.

The sequence shows the C-terminal portion of the M22 Fab heavy chain. The 6 His tag coding sequence and stop codon is highlighted in purple.

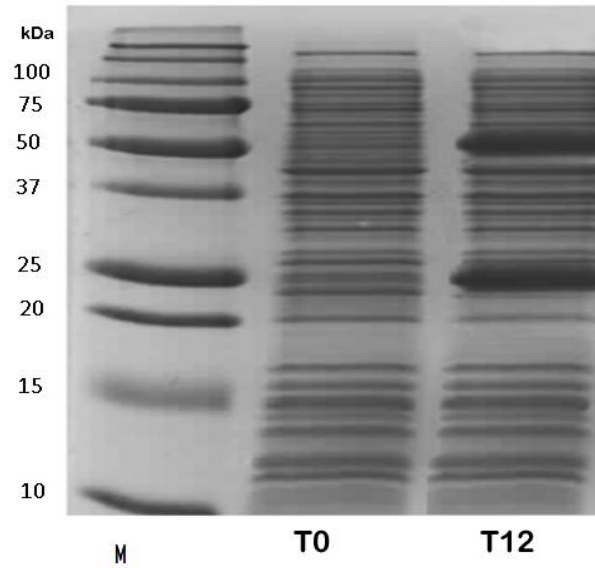


Figure4.10: Non-reducing SDS-PAGE analysis of induced cultures of M22-pComb3-His.

Cell extracts were prepared from XL1-Blue containing plasmid M22-pComb3-His at 0 hours (T0) and 12 hours (T12) after the induction of gene expression by the addition of 1 mM IPTG. Lane M shows a molecular weight ladder. After 12 hours of induction cell extracts contained a significant level of M22 Fab (approx. 50 kDa). There was also evidence of some monomeric chains in the extract (heavy or light) which appear at approx. 25 kDa.

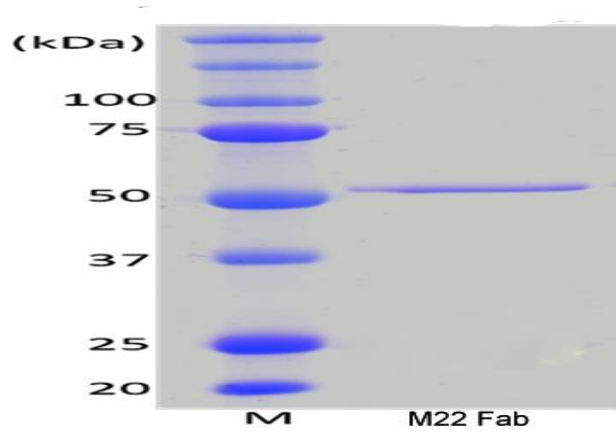


Figure 4.11: SDS-PAGE analysis of purified M22 Fab.

A sample of M22 Fab obtained from metal affinity chromatography was analysed by non-reducing SDS-PAGE. The gel shows a band of pure Fab at approx. 50 kDa.

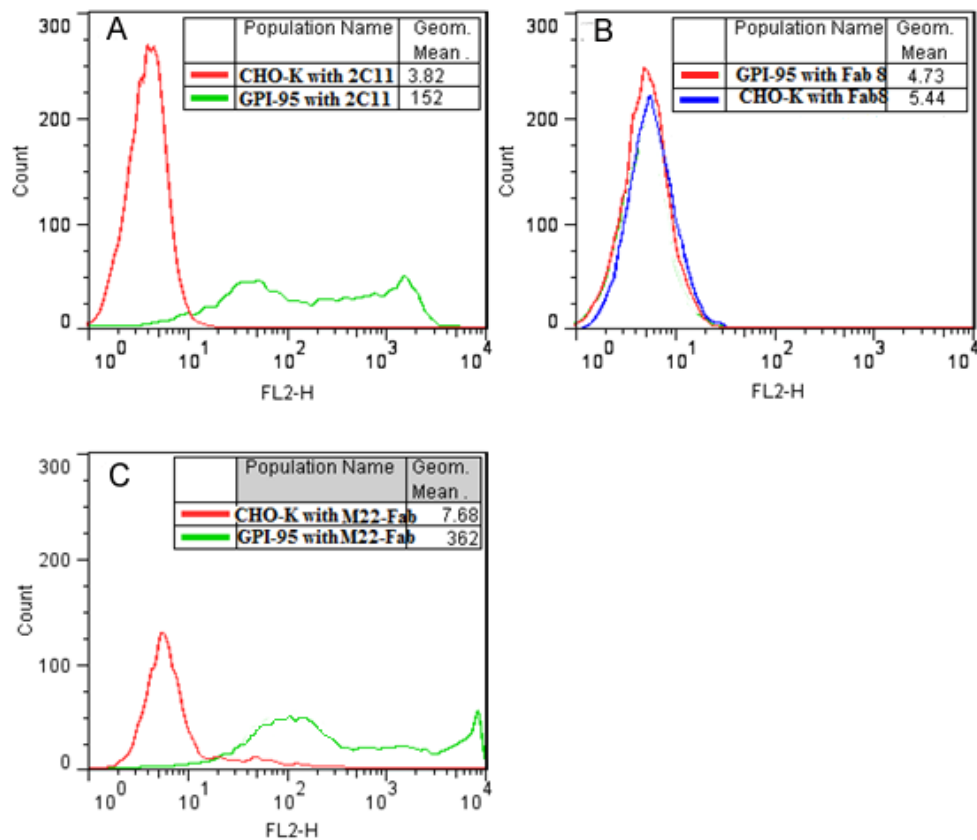


Figure 4.12 Flow cytometric analysis of M22 Fab binding to TSHR expressed on GPI-95 cells.

Antibody binding to the TSHR was assessed by FACS analysis using GPI-95 cells, a stable CHO-K1 cell line expressing TSHR extracellular domain at a high density on the cell surface. Binding was assessed for M22 Fab, positive control antibody 2C11, a commercial monoclonal against TSHR, and TG2-8 (Fab 8) an irrelevant monoclonal against tissue transglutaminase. Untransfected CHO-K1 cells were used as an additional control. Significant fluorescence was observed for positive control antibody 2C11 against GPI-95 cells (A), but not TG2-8 (B), neither showed significant fluorescence with CHO-K1 cells. M22 Fab gave significant fluorescence with GPI-95 cells, and low background signal against CHO-K1 (C) results shown are at least two independent experiments.

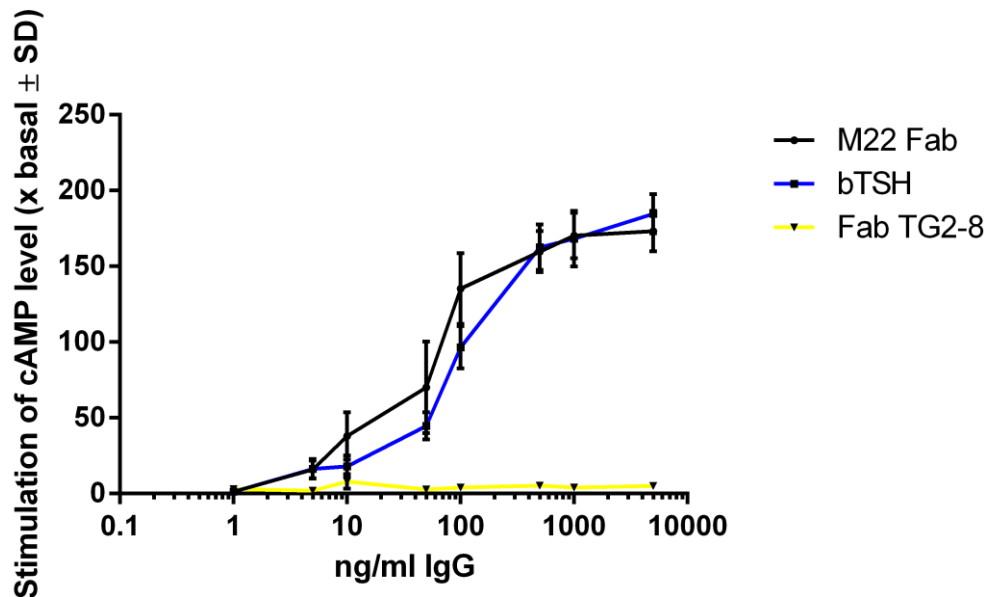


Figure 4.13 JP09 Bioassay of TSHR Stimulation by Recombinant M22 scFv.

Stimulation of cyclic AMP production in TSHR-transfected Chinese hamster ovary cells by M22 Fab, irrelevant mAb TG2-8, and bovine thyrotropin (bTSH). Results shown are mean \pm standard deviation (n=3). Basal cAMP production was determined in the presence of assay buffer only. M22 Fab at 100 pmol/L increased cAMP production approximately 140-fold over basal, and bTSH at 100 pmol/L increased cAMP productions approximately 100-fold. The EC_{50} of M22 Fab was approximately 80 ng/ml which was in the nanomolar range. Negative control Fab TG2-8 showed no significant increase of cAMP production compared to basal levels, the overall *F*-test gave a p-value of 0.016

4.3.2.5 M22 Fab Phage Binding

The M22-pComb3 construct expresses the TSAb monoclonal in Fab form on the surface of phage. The Fab moiety is approximately twice the size of the original scFv construct and should allow the antigen binding domain to project further from the phage surface. We investigated the binding of this M22 phage construct to commercial BRAHMS tubes coated with purified human TSHR. Binding was compared to phage derived from the original M22 scFv, a positive control Fab phage produced from a TSHR monoclonal A10 that recognise a different epitope of TSHR, and irrelevant Fab phage derived from an anti-transglutaminase monoclonal TG2-8.

The results of phage binding experiments are shown in Fig. 4.14. Measurements of eluted phage determined by counting the number of colonies produced indicated no significant difference between the binding of M22 Fab phage and any of the controls. Fab A10 is known to be specific for human TSHR, and recognises a linear determinant that does not require the receptor to be in a native conformation. Negative control phage TG2-8 does not recognise the TSHR at all. There was significant difference in binding and elution between M22 Fab phage, A10 phage, or TG2-8. The results suggested that there was a non-specific background that prevented discrimination between the different M22 phage and controls. The reason for this lack of specificity was unclear. The TSHR itself could be the source of non-specific binding and is known feature "stickiness" in binding assays (Rapoport, Chazenbalk et al. 1998). An alternative possibility is that it is some component of the BRAHMS kit or the tubes themselves that are masking any specific binding.

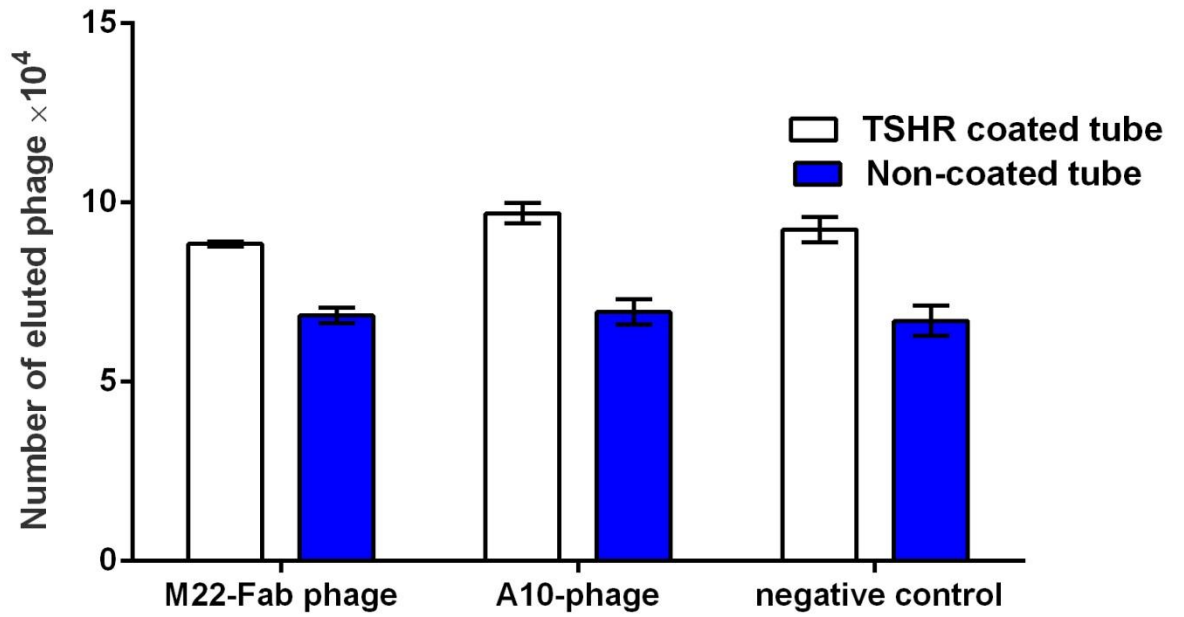


Figure 4.14: Binding of M22 Fab-phage to BRAHMS tubes.

The number of phage eluted from TSHR-coated tubes. The number was estimated by plating of aliquots of infected host cells. Binding was determined for phage displaying M22 scFv, positive control phage displaying an anti-TSHR antibody A10, and irrelevant phage displaying an anti-transglutaminase antibody TG2-8. Data are the mean \pm SD (n=3), the one-way analysis of variance (ANOVA) with Bonferroni's post-hoc comparison was performed on the data to confirm the statistical insignificant, p=0.062.

4.4 Construction of M22 Long Linker pComb3 Plasmid

Aim:

In an effort to address these potential steric problems after the use of a Fab construct, a long flexible linker was inserted between the phage capsid and the antigen binding site to increase the distance between the phage particle and the epitope.

To investigate the possible effect of steric hindrance from the phage-antibody structure a long linker was introduced between the M22 Fab heavy chain and the phage coat protein cpIII. To test this possibility, we inserted a flexible peptide linker between the M22 heavy chain and the cpIII coat protein gene. This linker was based on a design that was optimised to produce a flexible peptide sequence with no secondary structure (Hennecke, Krebber et al. 1998). The linker comprised 20 aa residues and was inserted in duplicate into the M22 Fab phage construct to increase the existing distance of the M22 Fab from the phage capsid by approximately 80-100 Å.

4.4.1 Methods

4.4.1.1 Insertion of Peptide Linker into M22-pComb3 Construct

The coding sequence of the peptide linker was constructed as two complementary oligonucleotides and inserted into the *Spe* I site of the M22-pComb3 Fab construct (Fig. 4.15). Annealing of the oligonucleotides produced overhangs at the 5' and 3' end of the resulting DNA fragment that were compatible with the *Spe* I sites. Ligation of the linker DNA recreated the *Spe* I site upstream of the in-frame linker coding sequence but removed the potential second *Spe* I site at the 3' end of the insert (Fig 4.15). Using this remaining *Spe* I site it was possible to digest the intermediary construct containing one copy of the linker and insert a second, thus doubling the linker length to approximately 40 amino acids and increasing the peptide tether length to approximately 50-100 Å (Fig. 4.15). Using this construct we produced M22 phage featuring the long linker and investigated the effect of this structural alteration on receptor binding properties.

M22-pComb3 (5 µg) was digested with 10 units of *Spe* I and phosphatased by the addition of 2 units of alkaline phosphatase (Promega) for 10 min at 37°C. We visualized

the digested products on a 0.6% agarose gel, and the linearised M22-pComb3 was recovered from an agarose slot gel the Wizard DNA Cleanup kit (2.2.5).

Digested M22-pComb3 was ligated to annealed oligonucleotide linker primers. The ligation mixture was then electroporated into XL1-Blue and plated out onto LB agar plates (100 µg/ml ampicillin). Five random colonies were picked and grown in 10 ml LB (100 µg/ml ampicillin), and plasmid DNA purified by miniprep. The clones were screened for recombinance by sequencing using primer pc3-prim2. A verified clone was isolated and confirmed by sequencing. This plasmid was digested with *Spe* I and purified by slot gel electrophoresis (2.2.4). The cloning was repeated to produce a second linker insert and following ligation and plating random colonies were picked for miniprep and sequencing. The final construct M22-pComb3-LL was confirmed by sequence analysis (Fig. 4.16).

4.4.1.2 Generation of M22 Long Linker Phage

A 10 ml culture of M22-pComb3-LL plasmid was superinfected with VCSM13 helper phage (2.2.16) and incubated at 37°C for 15 min. To generate phage particles the infected culture was put in 100 ml LB media (100 µg/ml of ampicillin, 20 µg/ml of kanamycin, and 20 µg/ml of tetracycline) and incubated overnight at 37°C with shaking. The culture was then centrifuged at 2,000 g for 15 min and the supernatant removed to a 50 ml tube and 40% PEG 800 (5 ml) and 5 M NaCl (5 ml) were added and incubated at 4°C overnight to precipitate phage particles. These were centrifuged at 2,000 g for 30 min and the pellet resuspended in 1 ml of PBS. The phage suspension was titered (2.2.17) and suspended at a density of approximately 10^{11} pfu/ml.

4.4.1.3 Phage Binding Experiments

BRAHMS tubes were blocked with 400 µl of PBS/BSA 3% (w:v) for 1 hour at 37°C. The blocking solution removed and 100 µl of phage suspension added (typically 10^{10} pfu) and incubated for 1 hour at room temperature. Unbound phage were removed, and the tubes washed eight times with 2 ml PBS/Tween (0.1% v:v) at room temperature. Adherent phage were eluted by the addition of 100 µl of glycine buffer and incubation at room temperature for 10 min. Eluted phage were, and neutralised with 6 µl of 2 M of

Tris. Eluted phage were used to infect 1 ml of log phase culture of fresh XL1-Blue host for 20 min at 37°C. The number of eluted phage were monitored by plating 10 µl samples of infected host onto LB agar plates followed by overnight incubation at 37°C to allow colony growth. The resulting colonies were used to calculate the number of eluted phage. To provide a suitable negative control irrelevant antibody phage were prepared from a mouse anti-transglutaminase antibody (TG2-8). A positive control phage construct was produced using mouse anti-TSHR mAb A10. This antibody recognises a linear TSHR epitope remote from the key binding sites for TSHR autoantibodies, and does not require native protein conformation for recognition (Nicholson, Vlase et al. 1996). Binding of long linker M22 phage were also compared to M22 scFv and M22 Fab phage. Data shown was the result of three independent experiments.

4.4.2 Results

The results from BRAHMS tube binding experiments are shown in Fig. 4.17. There was no significant difference in binding to the receptor-coated tubes in any of the phage samples. All samples eluted approximately 10^4 phage from the BRAHMS tubes, indicative of a significant degree of non-specific binding. The long linker M22 Fab construct bound to a similar extent as the other M22 antibody constructs and the negative control TG2-8 eluted approximately the same number of phage. It was apparent that either the TSH receptor-coated BRAHMS tubes did not represent a selective surface, or for some reason the M22 antibody binding sites were not able to access the stimulatory epitope on the receptor. Possible reasons for this could include steric hindrance between the phage-antibody structure and the receptor, or the orientation of the receptor in the coated tubes. BRAHMS tubes are coated with a specific monoclonal antibody that serves to capture the recombinant receptor onto the surface. This would suggest that the orientation of receptor in the tubes is not random but determined by this capture antibody. It is possible that this particular arrangement prevents binding due to the large molecular size of the antibody-phage fusion. One possible way to explore this would be to study phage binding using alternative forms of the TSH receptor.

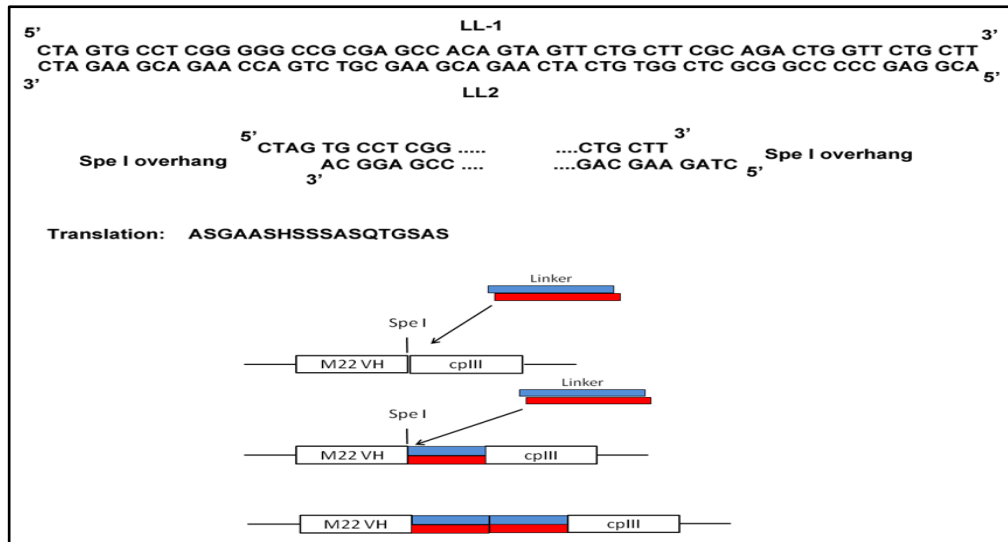


Figure 4.15 Strategy for introducing a flexible peptide linker into M22 Fab construct.

A pair of complementary oligonucleotides LL1 and LL2 was designed to encode a peptide linker. When annealed the oligonucleotides produced a DNA fragment with overhangs suitable for cloning into the *Spe I* site of the M22-pComb3 plasmid. The new construct introduces two copies of a flexible peptide linker in-frame between the M22 heavy chain and phage coat protein cpIII.

```

CTGGGCTGCCTGGTCAAGGACTACTTCCCCGAACCGGTGACGGTGTTCGTGGAACTCAGGCGCCCTGACCA
L G C L V K D Y F P E P V T V S W N S G A L T
GCGGCGTGACACCTTCCCGGCTGTCCTACAGTCCCTCANGACTCTACTCCCTCGGCAGCGTGGTGACCGT
S G V H T F P A V L Q S S X L Y S L G S V V T V
GCCCTCCAGCAGCTTGGGCACCCAGACCTACATCTGCACTAGTGCCCTCGGGGGCCGCGAGCCACAGTAGT
P S S S L G T Q T Y I C T S A S G A A S H S S
TCTGCTTCGCAGACTGGTTCTGCTTCTAGTGCCTCGGGGGCCGCGAGCCACAGTAGTTCTGCTTCGCAGA
S A S Q T G S A S S A S G A A S H S S S A S Q
CTGGTTCTGCTTCTAGTGGTGGCGGTGGCTCTCCATTTCGTTTGTGAATATCAAGGCCAATCGTCTGACCT
T G S A S S G G G G S P F V C E Y Q G Q S S D L
GCCTCAACCTCCT
P Q P P

```

Figure 4.16 Partial sequence of M22-pComb3-LL.

The long linker construct was sequenced to confirm insertion of the two copies of the linker coding sequence between the C-terminus of the M22 VH chain and the N-

terminus of phage coat protein cpIII, and to verify the reading frame. M22 VH sequence is highlighted in purple, and the linker coding sequence is highlighted in pink.

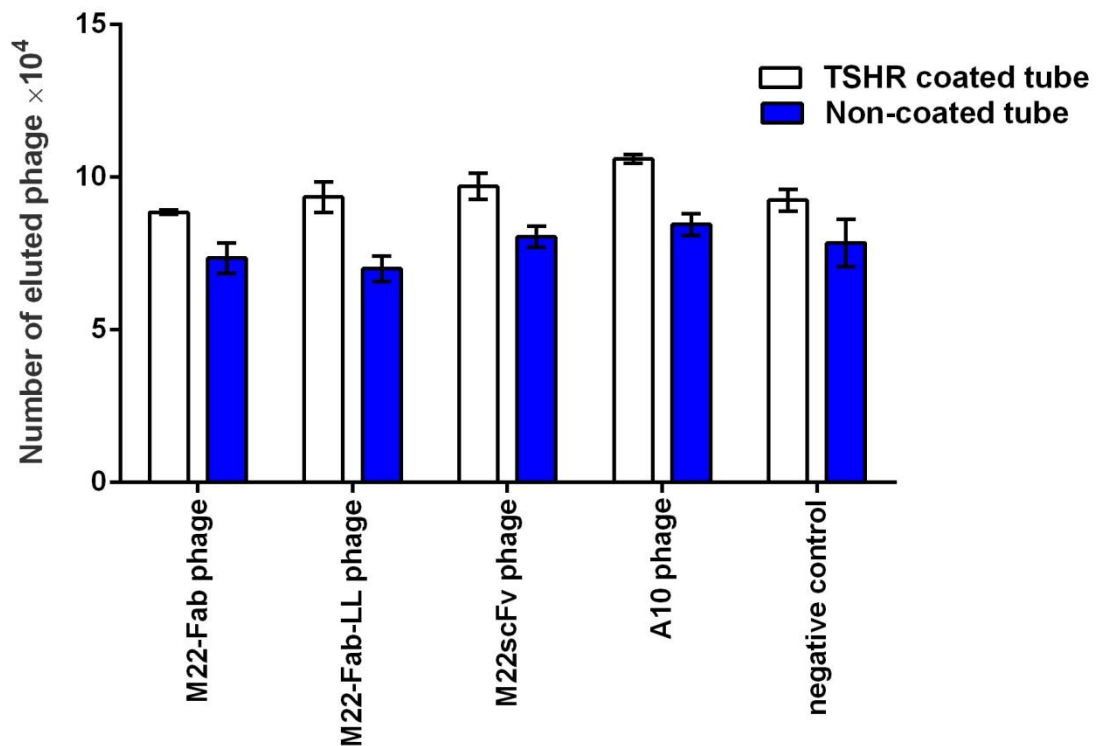


Figure 4.17 Binding of M22 LL-Fab-phage to BRAHMS tubes.

The number of phage eluted from TSHR-coated tubes. The number was estimated by plating of aliquots of infected host cells. Binding was determined for phage displaying M22 long linker Fab phage, M22 Fab phage, and M22 scFv phage. Positive control phage displaying an anti-TSHR antibody A10, and irrelevant phage displaying an anti-transglutaminase antibody TG2-8 were also included as a negative control. Data are the mean \pm SD (n=3).

4.5 Using different form of TSH receptors

Switching from the M22 scFv construct to the Fab form did not produce any change in phage binding properties. If the TSH receptor or the assay tubes were the source of this non-specific background then further experiments, using receptor in a different form may provide the solution to the enrichment problem. Steric hindrance may also still be an issue if the antibody in Fab form is still sufficiently close to the phage capsid that binding to the antibody paratope is physically prevented. A modified phage antibody construct may serve to investigate this possibility.

4.5.1 Triton X114 Extraction of TSHRecd-GPI

Phage binding experiments using a range of different M22 antibody constructs had consistently failed to show evidence for specific binding to recombinant TSH receptor using the commercial receptor-coated immunotubes. The reasons for this were unclear but could include steric interactions between the receptor, in this tube format, and the various phage antibody constructs. An alternative source of receptor was available in the form of the GPI-95 cell line. This cell line expresses a high density of TSH receptor extracellular domain on the cell surface via a glycosylphosphatidylinositol (GPI) anchor (Metcalf, Jordan et al. 2002). The receptor density has been estimated to be approximately 300,000 per cell and represents a potential source of native receptor for binding studies. A useful feature of GPI-anchored proteins is that they can be simply extracted using selected detergents. Triton X114 has been used previously to efficiently separate and purify GPI-anchored proteins (Ko and Thompson 1995). In this section of the study we will use GPI-95 cells to provide a enriched source of TSH receptor. GPI-95 cells will be extracted using Triton X114, and the GPI-linked receptor domain partitioned as a semi-purified extract for use in binding assays.

4.5.1.1 Method of Detergent Extraction of TSHR Extracellular Domain

Triton X114 phase partitioning was used to separate GPI-anchored proteins from crude cellular homogenates as described in section 2.2.31. Briefly, approximately 5 million GPI-95 were grown to 75% confluence in 75 cm flasks in RBMI medium. The cell monolayers were washed in 10 ml of PBS, pelleted by centrifugation, and incubated in

400 µl of lysis buffer for 20 min on ice with frequent stirring. The detergent and aqueous phases were separated at 30°C for 5 min into aqueous and detergent phases and centrifuged at 4,000 g for 10 min. The Triton X114 fraction was recovered in approximately 1 ml and stored at -80°C until use. Both phases were analysed by SDS-PAGE and western blotting to confirm recovery of receptor.

4.5.1.2 Binding of M22 Fab to Extracted TSHRecd-GPI

To determine the binding activities and the specificity of M22 Fab, an ELISA plate was coated with 100 µl of 100 µg/ml of detergent extracted TSHR in coating buffer using additional wells coated with PBS (no TSHR) as a negative control and incubated overnight at 4°C. After four washes with 400 µl of PBS/Tween, 300 µl of blocking solution (5% skimmed milk in PBS/0.05% Tween) was added to each well and incubated at 37°C for 1 hour. After washing twice with PBS/Tween, samples of antibody were added at the appropriate dilution in 5% skimmed milk in PBS/Tween and incubated at 37°C for 2 h. The wells were washed five times with 400 µl of PBS/Tween, and 100 µl of secondary antibody added. M22 Fab binding was detected with alkaline phosphatase conjugated Fab-specific goat anti-human antibody (A8542; Sigma; 1:2000), and alkaline phosphatase conjugated Fab-specific goat anti-mouse antibody was used for the control Fabs, A10, an anti-TSHR monoclonal, and TG2-8, an irrelevant antibody against tissue transglutaminase. Following incubation for 1 hour at room temperature the wells were washed 10 times with PBS/Tween and developed using pNPP alkaline phosphatase substrate (Sigma) and read in a plate reader at 405 nm.

4.5.1.3 Binding of M22 Phage to Extracted TSHRecd-GPI

To determine the binding of M22 Fab phage and controls to TSHR extracts, ELISA plates were coated with 50 µl of TSHR detergent extract (100 µg/ml total protein) mixed with 50 µl of coating buffer (2.1.8) and incubated overnight at 4°C. After five washes with PBS/Tween, 300 µl of blocking solution (5% skimmed milk in PBS/Tween) was added to each well and incubated at 37°C for 1 hour. After five washes with PBS/Tween, 100 µl of test phage (approximately 10^9 particles) in PBS/Tween containing 5% (w:v) skimmed milk was added to the wells and incubated at 37°C for 2 hours. Each well was washed eight times with PBS/Tween and 100 µl of 1:2000 of horseradish peroxidase conjugated anti-M13 monoclonal antibody (GE Healthcare) in PBS/Tween 5% skimmed milk (w:v) was added. After incubation at

37°C for 1 hour, wells were washed ten times with PBS/Tween and bounded phage detected by addition of 50 µl of TMB substrate (Sigma). The reaction was stopped by addition of 50 µl of stopping solution and the absorbance at 450 nm measured.

4.5.2 Results

4.5.2.1 Extraction of TSHRecd from GPI-95

Detergent extracts of TSHR extracellular domain from GPI-95 cells were analysed by SDS-PAGE (Fig. 4.18). Total protein content of the extract was determined using measurements of OD280nm using a Nanodrop and was approximately 100 ug/ml. Based on SDS-PAGE we estimated that approximately 75% of this protein was in the size range corresponding to the TSHR domain, but it was not possible to precisely determine this ratio. Analysis by western blotting using a specific anti-TSHR antibody (A10) showed that the recombinant protein migrated at its predicted molecular weight (approximately 50 kDa) and the vast majority had partitioned into the detergent-enriched phase with no detectable protein visible in the aqueous phase (Fig. 4.19).

4.5.2.2 Binding of M22 Fab to Extracted TSHRecd

Binding of recombinant M22 Fab to the TSHR extract was analysed by ELISA. Binding was compared to that of a positive control anti-TSHR Fab A10, and an irrelevant Fab TG2-8. All Fabs were used at a concentration of 1 µg/ml. The results showed a high level of binding by M22 Fab, indicating that the recombinant antibody was able to recognise the receptor in GPI-95 extracts (Fig. 4.20). As M22 recognition is dependent on native conformation this result also demonstrates that the extract contained properly folded receptor. Positive control antibody A10 also gave a strong signal against the receptor-coated wells. Both M22 Fab and A10 showed a low level of binding to uncoated wells, and negative control antibody TG2-8 gave no binding to either receptor-coated or uncoated wells.

4.5.2.3 Binding of M22 Phage to Extracted TSHRecd

Following demonstration of M22 Fab binding to receptor extract the experiment was repeated using the antibodies in phage format. M22 antibody phage in both Fab and scFv format were assessed for binding to the receptor by ELISA. Positive control phage were derived from anti-TSHR monoclonal A10. Negative controls were provided by irrelevant phage derived from transglutaminase antibody TG2-8, and VCSM13 helper phage. The results showed no evidence for receptor binding by any of the M22 phage constructs (Fig. 4.21). In contrast, A10 phage showed very strong binding to the receptor extract. Negative control phage TG2-8 and helper phage did not exhibit binding to receptor. None of the phage tested gave a signal on the uncoated wells.

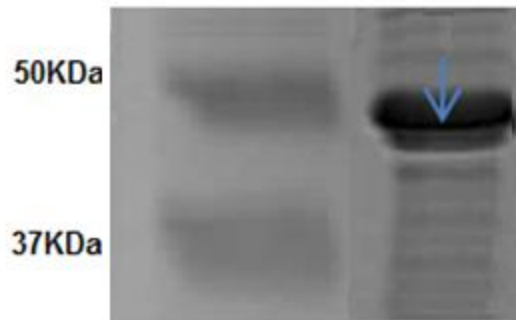


Figure 4.18: SDS PAGE for the GPI-anchored TSHRecd extracted by triton X-114

Detergent partitioned extracts of GPI-95 cells were analysed by SDS-PAGE Lane 1: Molecular weight markers; Lane 2: 30 μ l of Triton X-114 phase.

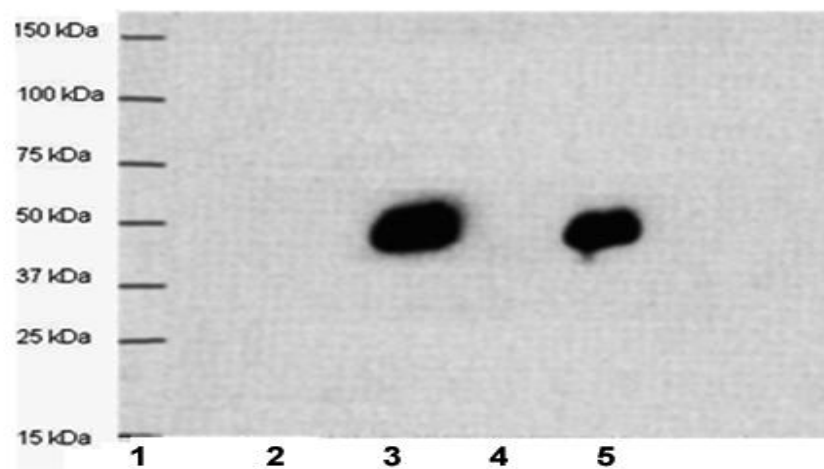


Figure 4.19 Western blot for the GPI-anchored TSHRecd extracted by triton X-114

Detergent partitioned extracts of GPI-95 cells were analysed by SDS-PAGE and transferred to PVDF membrane before blotting with anti-TSHR monoclonal A10. Receptor protein was detected at the predicted molecular weight in the detergent extracts only. Lane 1: Molecular weight markers; Lane 2: 30 μ l of aqueous phase; Lane

3: 30 μ l of Triton X-114 phase; Lane 4: 10ul of aqueous phase; Lane 5: 10ul of Triton X-114 rich phase.

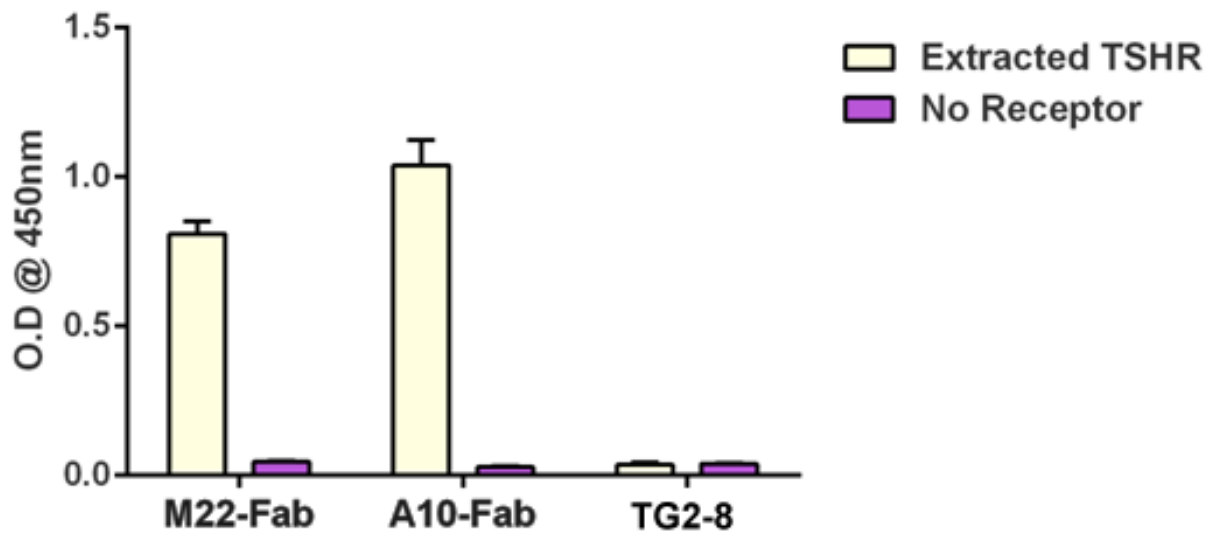


Figure4.20 Binding of M22 Fab to detergent extracts of TSHR.

M22 Fab binding to detergent extracted TSHR was determined by ELISA. Wells were coated with TSHR extract (0.5 μ g/well). Anti-TSHR antibody A10 was used as positive control, and irrelevant antibody TG2-8 was included. Data shown are the mean \pm SD and were derived from three independent experiments. One-way analysis of variance (ANOVA) was performed on the data to confirm the statistical significant different between the binding of M22-Fab, A10 Fab to wells coated with the extracted TSHR and uncoated wells, $p=0.002-0.003$.

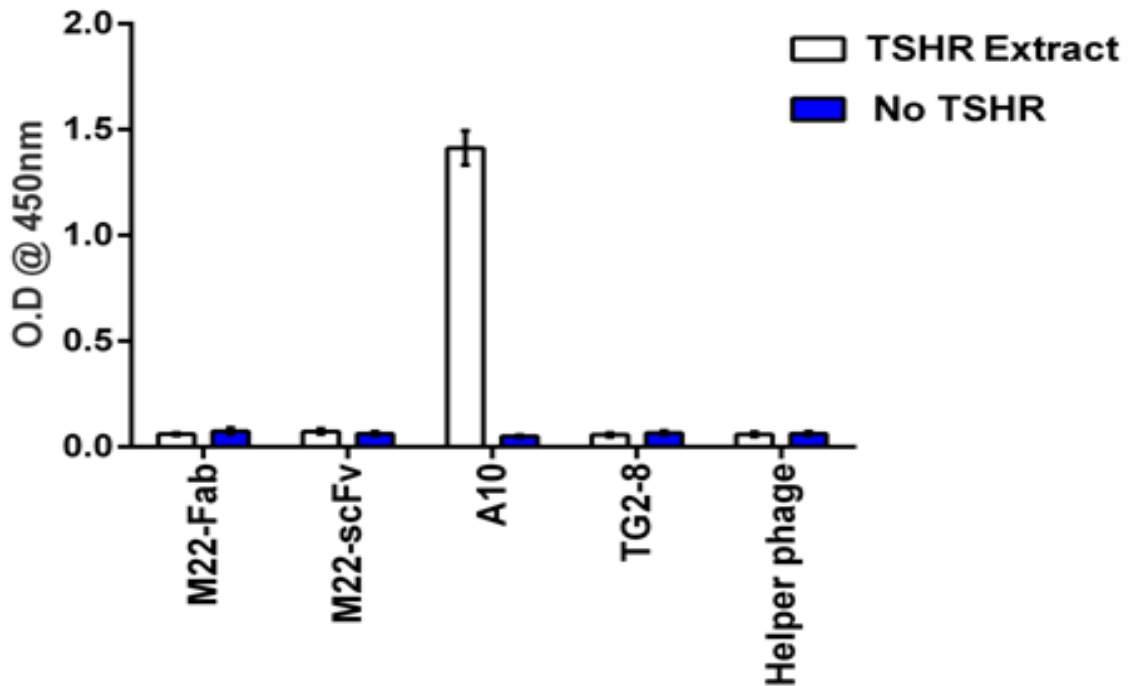


Figure 4.21 Binding of M22 Fab-phage to detergent extracts of TSHR.

Phage binding to detergent extracted TSHR was determined by ELISA. Equal numbers of phage (10^9) were added to ELISA wells coated with TSHR extract ($0.5 \mu\text{g}/\text{well}$). M22 scFv and Fab phage constructs were tested. Positive control phage were derived from anti-TSHR antibody A10. Irrelevant antibody TG2-8 and VCMS13 helper phage were used as negative controls. Binding was compared to uncoated wells. Data shown are the mean \pm SD and were derived from three independent experiments. One-way analysis of variance (ANOVA) was performed on the data to confirm the statistical insignificant difference between the binding of M22-Fab phage to wells coated with the extracted TSHR and uncoated wells, $p=0.0820$ and significant difference between the binding of A10 Fab to wells coated with the extracted TSHR and uncoated wells, $p=0.002$

4.6 Binding to GPI-95 Cells

4.6.1 Binding of M22 Fab to GPI95 Cells

Both FACS analysis and the detergent extract experiments described above demonstrated that stable cell line GPI-95 was a useful source of high level expression of native TSH receptor. In this section we investigated the use of this cell line in a direct binding assay in a cell ELISA format. As an alternative source of antigen we investigated the use of TSHR expressing cell line GPI-95. It is well established that thyroid stimulating antibodies only recognise native receptor, and that as a protein the TSHR is rather unstable and prone to spontaneous unfolding and denaturation upon purification (Rapoport, Chazenbalk et al. 1998). If it was possible to use a stable cell line for phage binding experiments this would offer the opportunity to access native antigen as a binding surface.

4.6.1.1 Methods

GPI-95 and control CHO-K1 cells were seeded into a Poly-D-lysine 96-well ELISA plate at a density of 1,500 cells per well in 300 μ l of XXX medium. The plates were incubated overnight at 37°C in a CO₂ incubator. When the wells reached 75% confluence they were washed three times with 400 μ l of PBS, and 300 μ l of blocking solution (10% FCS in RBMI media) added to each well and incubated at 37°C for 1 hour. After one wash with 400 μ l of PBS, 100 μ l of test antibody (50 μ g/ml) was added. The antibodies used were recombinant M22 Fab, positive control mouse anti-TSHR antibody A10, and irrelevant anti-transglutaminase antibody TG2-8 as negative control. Plates were sealed and incubated at room temperature for 1 hour. Each well was washed five times with 400 μ l of PBS, and 100 μ l of anti-mouse or anti-human HRP-conjugated anti-IgG added to each well. After incubation at room temperature for 1 hour, each well was washed five times with PBS. Plates were examined under the microscope to confirm cells were still attached and then 100 μ l of freshly prepared substrate solution was added to each well. The plate was incubated at room temperature for 15-30 min until colour development occurred and 100 μ l of stopping solution was added and the OD_{405nm} was measured in the plate reader. All samples were tested in triplicate (Fig. 4.22).

4.6.2 Binding of M22 Phage to GPI95 Cells

Following demonstration of M22 Fab binding to GPI95 cells, the experiment was repeated using the antibodies in phage format. M22 antibody phage in both Fab and scFv format were assessed for binding to the receptor by ELISA. Positive control phage were derived from anti-TSHR monoclonal A10. Negative controls were provided by irrelevant phage derived from transglutaminase antibody TG2-8, and VCSM13 helper phage. The results showed no evidence for receptor binding by any of the M22 phage constructs (Fig. 4.23). In contrast, A10 phage showed very strong binding to the GPI95 cells. Negative control phage TG2-8 and helper phage did not exhibit binding to receptor. None of the phage tested gave a signal on the uncoated wells.

4.6.2 Results

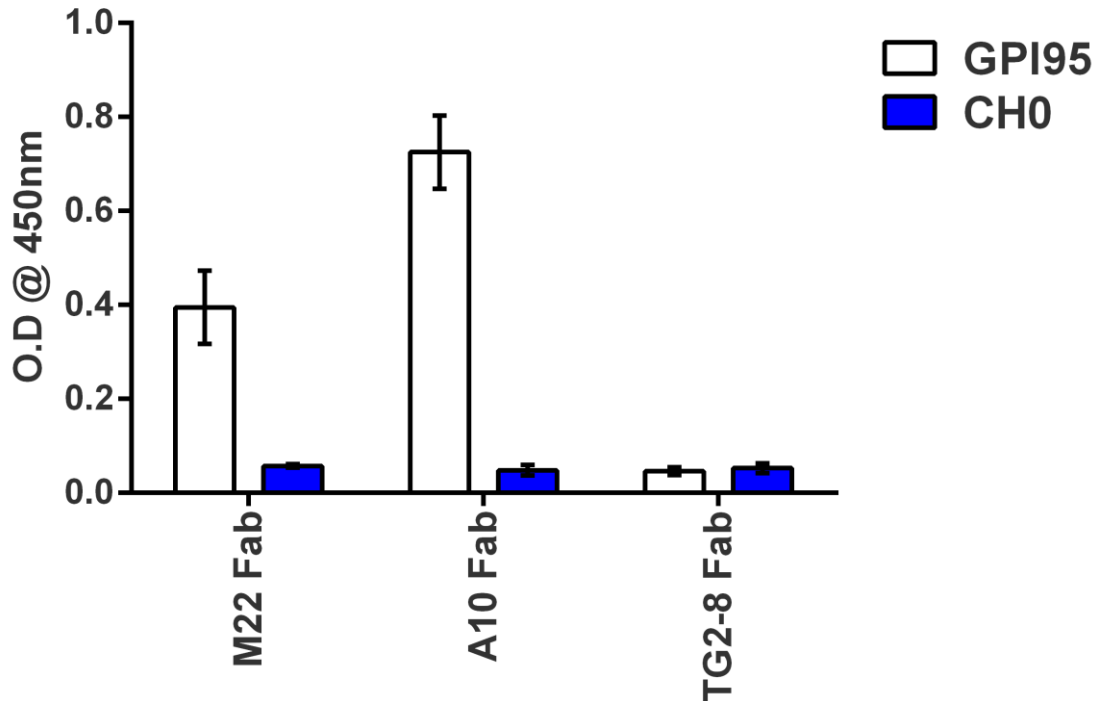


Figure 4.22 M22 Antibody Binding to GPI-95 cells.

M22 binding to GPI-linked TSHR was determined by cell ELISA using the GPI-95 cell line. The Fab, scFv (M22 scFv), A10 Fab and TG2-8 Fab as a negative control were assessed for binding to ELISA wells coated with monolayers of GPI-95 cells. Positive control phage were derived from anti-TSHR antibody A10, and TG2-8 was the negative control. Binding to untransfected CHO-K1 cells was also assessed. Data shown are the mean \pm SD and were derived from three independent experiments. Statistical analysis was performed using a one way analysis of variance (ANOVA), showed significant difference between the bindings of M22 Fab, A10 Fab to TSH-R transfected and untransfected CHO cells ($p= 0.002-0.005$)

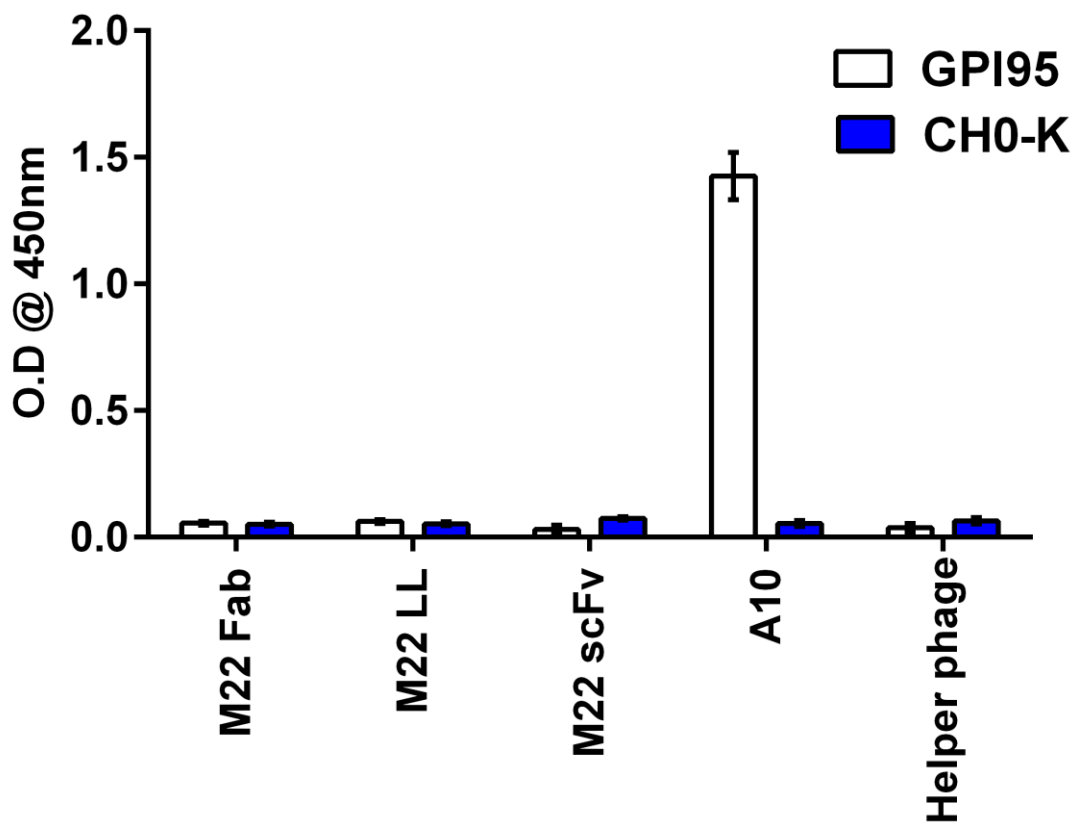


Figure 4.23 Phage binding to GPI-95 cells.

Phage binding to GPI-linked TSHR was determined by cell ELISA using the GPI-95 cell line. The Fab , Fab long linker (M22 LL) and scFv (M22 scFv) M22 antibody phage constructs were assessed for binding to ELISA wells coated with monolayers of GPI-95 cells. Positive control phage were derived from anti-TSHR antibody A10, and helper phage VCSM13 was the negative control. Binding to untransfected CHO-K1 cells was also assessed. Data shown are the mean \pm SD and were derived from three independent experiments. Statistical analysis was performed using a one way analysis of variance (ANOVA), showed insignificant difference between the bindings of M22

phage to TSH-R transfected and untransfected CHO cells ($p= 0.09-0.15$) and significant difference between the binding of A10 phage to TSH-R transfected and untransfected CHO cells ($p= 0.001$)

4.7 Discussion

Initial phage binding experiments with the M22-scFv construct failed to demonstrate any evidence for specific binding of the recombinant antibody to tubes coated with TSH receptor. This result was rather surprising given that the antibody construct had been shown to contain the functional sequence of the human TSHR monoclonal M22. The soluble form of the recombinant antibody was shown to bind to the TSH receptor in FACS analysis, and stimulated cAMP production in the JP09 TSHR bioassay. These results showed that the antibody itself possessed the required specificity, but the phage display antibody was unable to bind its corresponding epitope on the TSH receptor when attached to the BRAHMS tubes.

The most probable reason for this failure was involvement of some steric factor. It is clear that the M13 phage capsid is a relatively huge structure when compared to the displayed antibody. With approximate dimensions of 6 nm x 900 nm phage particles is effectively a long cylinder with a small antibody moiety of between 4-8 nm attached to the end (Fig xx). It seems logical that this structure may prevent binding to some epitopes if they were partially obstructed by domains of the antigen.

In an effort to address these potential steric problems we investigated the use of a first a Fab construct, effectively doubling the size of the antibody fragment, and a Fab variant in which a long flexible linker was inserted between the phage capsid and the antigen binding site. Disappointingly neither of these approaches resolved the binding difficulties, and no evidence of specificity for the receptor was observed in phage binding experiments.

A second consideration was the orientation of the target antigen and physical access to the target epitope. The initial experiments relied on the commercial TSHR-coated BRAHMS tubes. In this system the receptor is captured onto the tube surface using a

specific monoclonal antibody. There is at least the potential for the antigen to be coated in a uniform fashion in relation to its orientation. The data we obtained could be explained if this arrangement was unfavourable for phage antibody binding. In an effort to address this possibility we attempted to extract native receptor from a transfected cell line GPI-95, which expresses a high level of TSHR extracellular domain on the cell surface. Partitioning the GPI-anchored receptor using detergent enabled the recovery of useful quantities of antigen, and this material was used in a series of ELISA experiments. Soluble M22 Fab was able to recognise this material, which was an important result as it showed that the material contained receptor in native form, a prerequisite for the binding of TSAbs. M22 in single chain form also bound the receptor extract. However, the M22 antibody phage fusions, including the long linker variant, failed to recognise the receptor in these ELISA assays. M22 phage antibodies were also unable to recognise the receptor on the surface of the transfected cell line GPI-95. These were significant findings as it can be assumed that the receptor would be bound to the ELISA wells in, essentially, a random arrangement. This suggested that the failure of M22 phage to bind TSHR was unlikely to be due to the arrangement of antigen on the supporting surface, but due to the intrinsic nature of the receptor itself, an observation supported by the failure of M22 phage antibodies to bind receptor on the surface of GPI-95 cells in ELISA. Accumulating evidence suggested that modifications to the structure of the TSH receptor may be necessary to overcome the apparent inability of antibody phage fusions to access the key target epitope.

CHAPTER 5

CONSTRUCTION OF CHO TSHR260-GPI

5.1 Introduction

The preceding chapters have described my attempts to selectively bind a recombinant phage expressing a human TSAb monoclonal antibody to various preparations of recombinant TSH receptor. Although we were able to demonstrate that the recombinant antibody, in soluble form, could bind the receptor and possessed the characteristic agonistic activity behaviour, we were unable to show specific binding of the phage antibody. This was a surprising result given that M22, and other TSAb antibodies, have been shown to have a very high affinity for the receptor, in the order of 10^{-11} nM. The reasons for these results were unclear but given the functional activity of soluble antibody it appeared attachment to the phage viral coat was the problematic issue, suggesting a role for steric interference.

X-ray analysis of the TSHR-M22 complex for first time produced structural data for the TSH receptor, confirming the predicted structure of the "horseshoe" shaped ligand binding LRR domain (Sanders, Chirgadze et al. 2007), and showing similarities to the previously crystallised FSH receptor (Fan and Hendrickson 2005). Interestingly, the recombinant receptor construct used for the M22 crystal only comprised the first 260 amino acid residues of the TSHR. This subunit had been previously shown to be sufficient for both ligand and receptor binding and in recombinant form was stable in solution, enabling crystallisation. Sequence homology shows that the TSH receptor is similar to other glycoprotein receptors, including the hCG, FSH, LH receptors. This similarity is most pronounced in the region between amino acids 58-288, which includes the LRR domain (Rapoport, Chazenbalk et al. 1998). The sequence of the TSHR differs from the other glycoprotein receptors in having an "extra" 50 amino acids inserted in the region downstream of the LRR (Rapoport, Chazenbalk et al. 1998), the so-called "hinge" region. The function of this significant stretch of amino acids is unknown. Evidence suggests that the TSHR seems to be unique among the glycoprotein hormone receptors in that it undergoes intramolecular cleavage at the cell surface to create two subunits A and B, the A subunit comprising the ligand binding domain, and subunit B containing the transmembrane domains (Hamidi, Chen et al. 2011). The "extra" 50 amino acid residues, or C peptide, are removed in this cleavage reaction, and in vitro experiments have shown that the C peptide residues can be removed without

affecting antibody or ligand binding (Rapoport, Chazenbalk et al. 1998). The published TSHR structural data was limited to the LRR domain and X-ray information was only available for amino acids up to position 260 (Sanders, Chirgadze et al. 2007). A possible hypothesis for the observed failure of antibody-phage binding is that amino acid residues beyond position 260 are in some way forming a structure that interferes with phage binding by steric hindrance. Evidence supporting this hypothesis comes from the recent structural data regarding the entire FSHR and its ligand (Jiang, Liu et al. 2012). In this study it was shown that residues from the hinge region actually project into the anterior face of the LRR domain and contribute to ligand binding. The GPI-95 cell line expresses the entire TSHR extracellular domain from amino acid position 1 to 412 (Metcalf, Jordan et al. 2002), which was the conventional approach to TSHR_{Recd} at the time the cell line was produced.

The aim of this section of the project was to construct a novel cell line in which a smaller region of the TSHR, extending from amino-acids 1-260, was expressed on the cell surface at high density using a GPI anchor. The effect of removing the receptor "hinge" region on phage antibody binding will be investigated.

5.2 Methods and Results

5.2.1 Cloning of TSHR 1-260 as a GPI Anchored Membrane Protein (TSHR260-GPI)

Primers were designed to amplify the TSHR coding sequence corresponding to Met-1 at the start of the secretion leader, and Leu-260, and included BamHI and XhoI restriction sites at the 5' and 3' end of the amplicon respectively (Table 5.1). To produce a DNA template for amplification the original TSHR-GPI construct (Metcalf, Jordan et al. 2002) was diluted 1:1000 in H₂O. This was subject to 30 cycles of PCR amplification (2.2.3) using the TSHR260-1 and TSHR260-2 primers and the following conditions; 94°C for 35 s, 52°C for 1 min, 72°C for 2 min and 72°C for 10 min for termination. An amplification product of approximately 800 bp was obtained (Fig. 5.1), and cloned into the pCR3.1 vector using the TOPO TA cloning kit (Invitrogen). The ligation was transformed into TOP10 competent cells (Invitrogen) and plated onto LB agar (100 µg/ml ampicillin). Five random clones were used to produce minipreps, and the

identity of the clone verified by sequencing. This construct was designated pCR3.1/TSHR260.

A DNA fragment encoding the GPI attachment motif was produced by annealing a series of seven complementary oligonucleotides (Table 5.1). The attachment motif used was based on the sequence of domain 3 and 4 of rat CD4, which has been previously shown to contain a fortuitous recognition sequence for the glycosylphosphatidylinositol processing pathway (Johnstone, Cridland et al. 1994). The annealed oligos were designed to produce *Xho* I compatible DNA overhangs at the 5' and 3' end. The sequence of the 5' overhang was designed to eliminate the *Xho* I site after ligation so that this site could be re-used for sub-cloning of the final receptor construct into an expression vector. The oligonucleotides were prepared at a concentration of 10 pmol/μl and heated to 90°C for 1 min and cooled slowly to 0°C to allow annealing. The annealed oligonucleotides were diluted 1:100 to final concentration (0.1 pmol/μl) in the annealing buffer (10 mM Tris, pH 7.5-8.0, 50 mM NaCl and 1 mM EDTA). The pCR3.1/TSHR260 TOPO clone DNA was digested with *Xho*I, treated with 2 units of alkaline phosphatase (Promega) for 20 min at 37°C. Results of the digest were analysed by gel electrophoresis (Fig. 5.2), and the linearised vector DNA purified by slot gel electrophoresis. Annealed oligonucleotides (4 μl) were ligated to 200 ng of digested pCR3.1/TSHR260 plasmid. An aliquot of the ligation mixture (3 μl) was electroporated into XL1-Blue (2.2.11) and transformed cells plated onto LB agar plates (100 μg/ml ampicillin) (2.2.10). Four random colonies were picked and grown in 10 ml LB (100 μg/ml ampicillin) and plasmid DNA purified by miniprep (2.2.12). The identity of the construct was confirmed by DNA sequencing and this intermediate construct designated pCR3.1/TSHR260-GPI

The final step was excision of the TSHR260-GPI assembly and subcloning into mammalian expression vector pcDNA3.1. The verified pCR3.1/TSHR260-GPI construct (5 μg) was digested with *Bam* HI and *Xho* I and the insert, approximately 800 bp, recovered by slot gel electrophoresis. The expression vector pcDNA3.1 was digested with *Bam* HI and *Xho* I and purified by slot gel electrophoresis. Both DNA fragments were recovered using the Wizard DNA Cleanup kit. Vector DNA, approximately 200 ng, was mixed with 100 ng of TSHR260-GPI insert and ligated in a

20 µl ligation reaction containing 2 µl of ligase buffer and 1 unit of T4 DNA ligase (Promega). The reaction was incubated overnight and transformed into competent XL1-Blue cells. The transformed cells were plated onto LB agar (100 µg/ml ampicillin). Five random colonies were picked and used to prepare miniprep DNA. The correct construct was verified by DNA sequencing and designated pTHSR260-GPI, the sequence is shown in Fig. 5.3.

5.2.2 Expression of TSHR 1-260 on CHO-K cells

To verify functional expression of the truncated TSH receptor transient transfections were performed and the expressed protein analysed by SDS-PAGE and western blotting with TSH receptor antibodies.

5.2.2.1 Transient Expression of TSHR260 and Protein Analysis

CHO-K1 cells lines (2.1.6) were used for DNA transfection. These cells were grown in DMEM-medium (Dulbecco's MOD Eagle medium) (2.1.6). A calcium phosphate transfection technique (2.2.28) was used to transiently transfect CHO-K cell lines with pCR3.1/1-260TSHR-GPI. In brief, for small-scale expression of pCR3.1/TSHR1-260-GPI protein the cells were plated out at a density 2×10^5 cells/ml in T75 tissue culture flask and grown until 50-60% confluent. The cells were split to approximately 20-30% confluence in a 6-well plate in DMEM medium and incubated for at least 2 hours prior to transfection. Transfectant solutions were prepared, solution A was consist of: 10 µg of pCR3.1/TSHR260-GPI, 12.2 µl of 2 M CaCl₂ and 88.0 µl distilled water, and solution B contained HEPES buffered saline (HBS). Solution A and B were then combined dropwise by adding the solution B into solution A, whilst bubbling air through solution B and mixed gently. The suspension was incubated at room temperature for 30 min and then used for transfection by adding slowly and evenly into medium of each well, trying to cover as much of the plate as possible. Plates were then incubated at 37°C in a 5% CO₂ incubator for 48-60 hours before harvesting. After 60 hours of incubation 3 dishes of cells were washed 3 times with ice cold PBS, scraped and combined for protein extraction and purification.

Following incubation for 48-60 hours after transfection, the proteins were extracted from transfected cells as described previously in 2.2.33. Untransfected CHO-K1 cells as a negative control as well as GPI-95 cells (2.1.3) as a positive control were subjected to the same protocol. All the samples were stored at -20°C prior to further analysis.

5.2.2.2 SDS-PAGE and Western Blotting

SDS-PAGE and western blotting were performed essentially as described in (2.2.26). The crude cell extracts and the purified protein prepared from transfected cells as well as from positive and negative control cells were separated by SDS-PAGE and subjected to western blotting analysis. For western blotting, proteins separated by SDS-PAGE were electrophoretically transferred onto nitrocellulose membrane and stained with 5µg/ml mouse anti-human TSHR monoclonal antibody 2C11 (Serotec) as a primary antibody and 1:2000 (2 µg/ml) of horseradish peroxidase-conjugated goat-anti-mouse antibody (DAKO) as secondary. The blots were visualised using an enhanced chemiluminescent (ECL) system (Roche Diagnostics).

The results showed the presence of the predicted truncated receptor protein in cell extracts (Fig. 5.5). Cells transfected with the pTSHR260-GPI plasmid gave a band of approximately 37 kDa. This was compared to extracts from the original TSHRecd-GPI cell line GPI-95 gave a band of approximately 50 kDa.

5.2.2.3 Production of Stable CHO-K1 Transfectants

Following successful confirmation of the construct by western blotting of cell extracts we transfected CHO-K1 cells once more and produced stable clones expressing the truncated TSH receptor GPI construct. Duplicate dishes were seeded out at low density and grown in DMEM medium containing 800 µg/ml of G-418. This dose of G-418 killed untransfected or transiently transfected CHO-K1 cells over a period of two weeks of incubation. By visual inspection culture dishes containing 50-100 isolated clumps of growing cells were selected and the clonal cell clumps picked under the microscope using a 20 µl pipette and placed in separate wells of a 24-well plate containing 300 µl of DMEM medium (800 µg/ml G-418). Following another two weeks of incubation the cells were of sufficient density to be screened for TSHR260 expression by FACS analysis. From 40 picked clones we were able to isolate 3 cell lines which showed a significant fluorescent shift in FACS when stained for TSHR260 expression.

We selected a stable CHO-K1 cell line transfected with pTSHR260-GPI and investigated cell surface expression of receptor using a specific murine anti-TSHR antibody A10. Untransfected CHO-K1 cells were used as a negative control. Flow cytometric analysis was performed as described in section 2.2.30. After cells were counted, resuspended at a density of 1×10^7 cells/ml and 100 µl aliquoted into LP4 tubes (Becton Dickinson). Mouse monoclonal A10 (2 µg/ml) was added to the cells, thoroughly mixed and the reaction incubated for 20 min on ice. After washing twice with 2 ml PBS centrifuged at 1,000 g for 3 min and resuspended in 1:100 (2 µg/ml) goat-anti-mouse immunoglobulin FITC conjugate (Serotec) and incubated on ice for 20 min. After a final wash, cells were analysed using a fluorescence activated cell sorter (FACScan, Becton Dickinson).

The results showed a significant fluorescent signal from the CHO/TSHR260 cells with A10 antibody (Fig. 5.6), indicating a high density of receptor expression on the cell surface. Untransfected control CHO-K1 cells displayed an insignificant level of fluorescence. This cell line was sub-cultured in DMEM (800 µg/ml G-418) and re-

tested by FACS to confirm stability. CHO/TSHR260 cells were used for subsequent antibody and antibody-phage binding studies.

Primers for TSHR260-GPI synthesis	
TSHR260-1	GCGCGCGGATCCATGAGGCCGGCGGACTTGCTGCA
TSHR260-2	GCGCGCCTCGAGAAGAGTCCAGCTGTTTCTTGCTATCA
GPI Oligos	
Sense	
GPI#1	TCGAGCTGGTGCCAAGAGGCTCTATCGAGGGCAGA
GPI#3	GGCACATCCATCACGGCCTATAAGAGTGAG
GPI#5	GGGGAGTCAGCGGAGTTCTTCTTCCTACTC
GPI#7	ATCCTTCTGCTCCTGCTCGTGCTCGTCTAAT
Antisense	
GPI#2	CGTGATGGATGTGCCTCTGCCCTCGATAGAGCCTCTTGGCACCAGC
GPI#4	CTCCGCTGACTCCCCCTCACTCTTATAGGC
GPI#6	TCGAATTAGACGAGCACGAGCAGGAGCAGAAGGATGAGTAGGAAGAAGAA

Table 5.1 Oligonucleotides used in construction of GPI-anchored TSHR1-260 with [His]10 tag. Sense and antisense oligonucleotides were designed to anneal and generate the [His]10 and GPI motif coding region. The double stranded product was cloned into the *Xho* I site of pCR3.1/TSHR260.

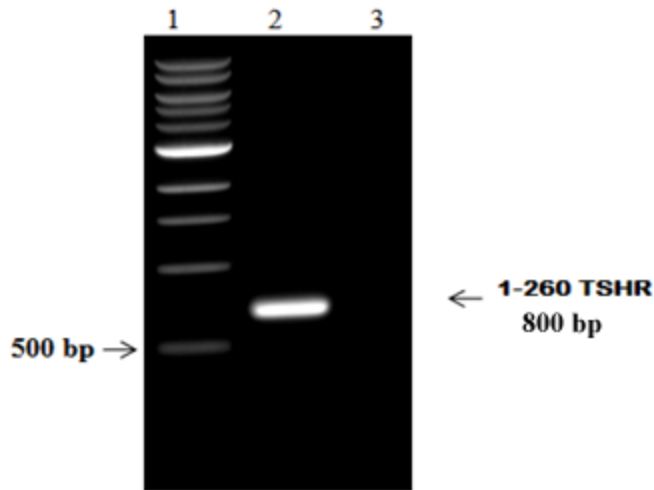


Figure 5.1 PCR amplification of TSHR 1-260

PCR (25 cycles) was performed using a high fidelity polymerase and primers contain *Bam* HI and *Xho* I restriction sites. The PCR products were run on a 1% agarose gel, Lane1: 1kb DNA ladder, Lane2: TSHR 1-260 PCR product of the expected size (~700bp). Lane3: PCR negative control (primers only without template).

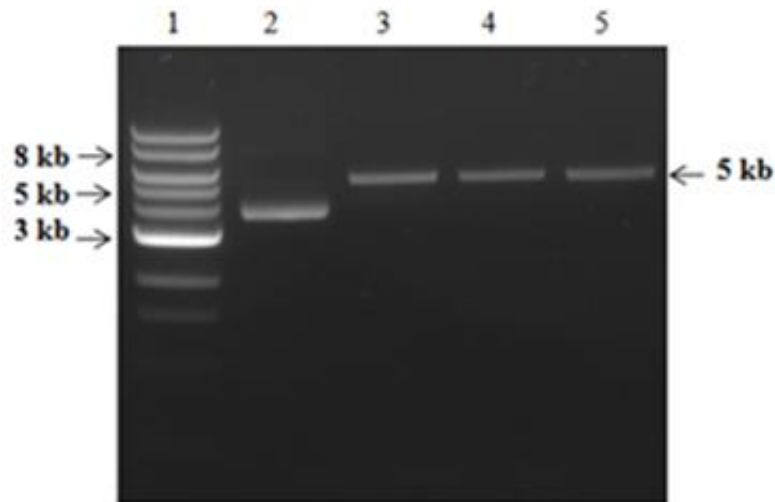


Figure 5.2 Enzymatic digestions of the pCR3.1/GPI and the TSHR1-260 PCR products.

pCR3.1/GPI plasmid and TSHR1-260 PCR product were digested with *Xho* I and *Bam* HI and run on 1.0 % agarose gels. In 3.5 (a) lane1: 100bp DNA ladder, lane2: undigested TSHR1-260 PCR product, lane3: digested TSHR1-260 PCR product. In 3.5 (b) lane1: the 1kb DNA ladder, lane 2: undigested vector, lane 3: *Xho* I single digest vector, lane 4; *Bam* HI single digest vector, lane5: double digested vector.

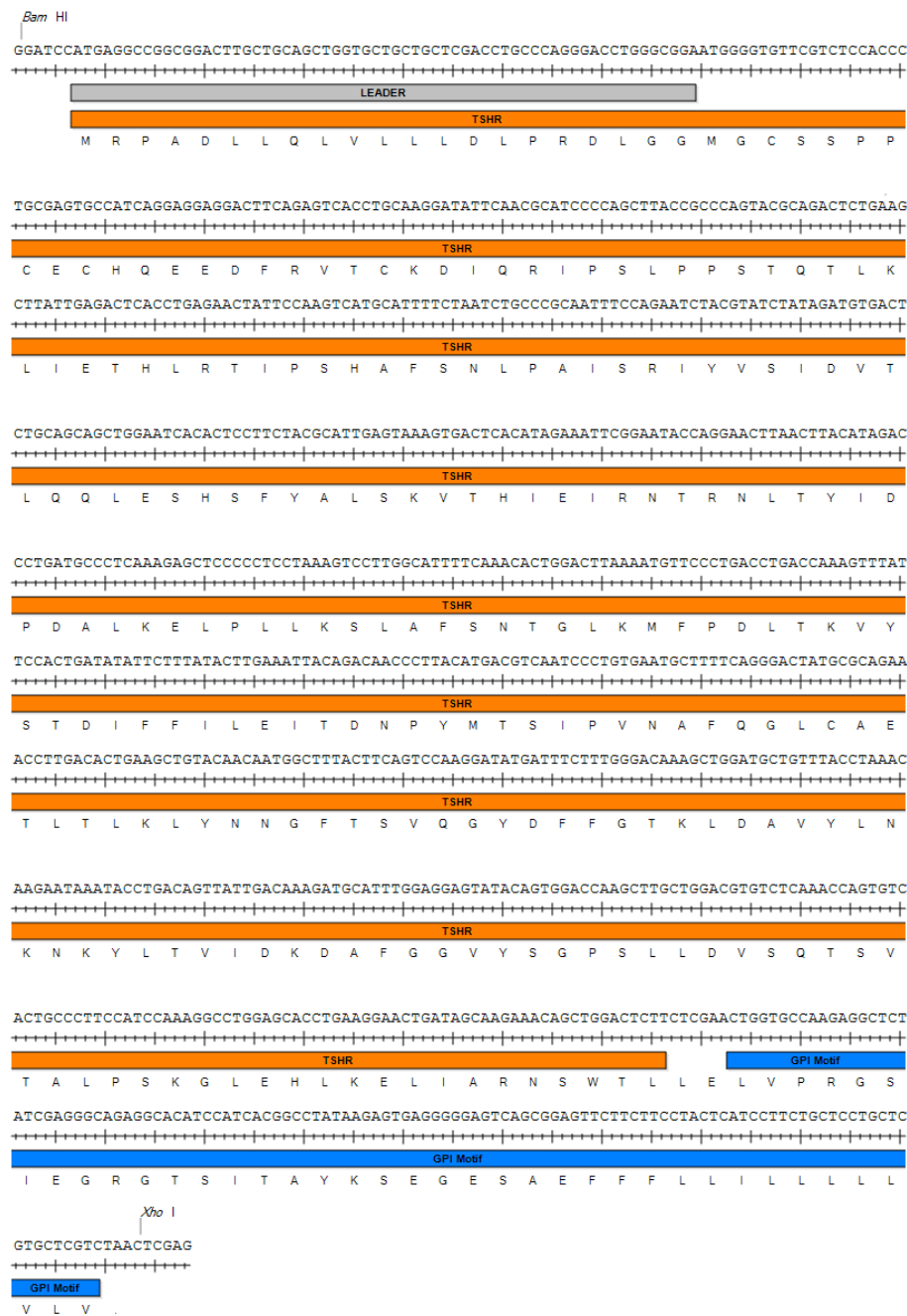


Figure 5.3 Sequencing data and translation for pTSHR260-GPI construct.

GPI motif is shown in red. The selected construct was sequenced in both directions and verified by BLAST comparison to the human TSHR cDNA sequence.

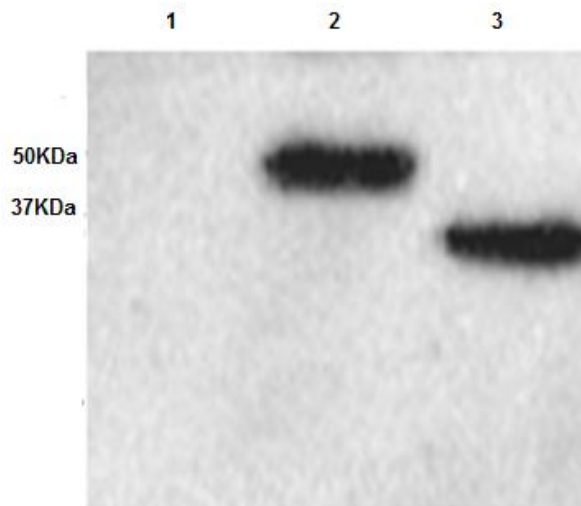


Figure 5.4 Western blots of TSHR260-GPI and GPI-95.

CHO cells were either untransfected or transiently transfected with either TSHR-ecd (GPI-95) as positive control or TSHR260-GPI. Cells were then lysed and the cellular lysates were run on 15% SDS-PAGE and probed with A10 IgG mAb antibody. Lane 1 shows no detectable antigen in untransfected cells, lane 2 GPI-95 and lane 3 TSHR260-GPI transfected cells show positive detection of the proteins.

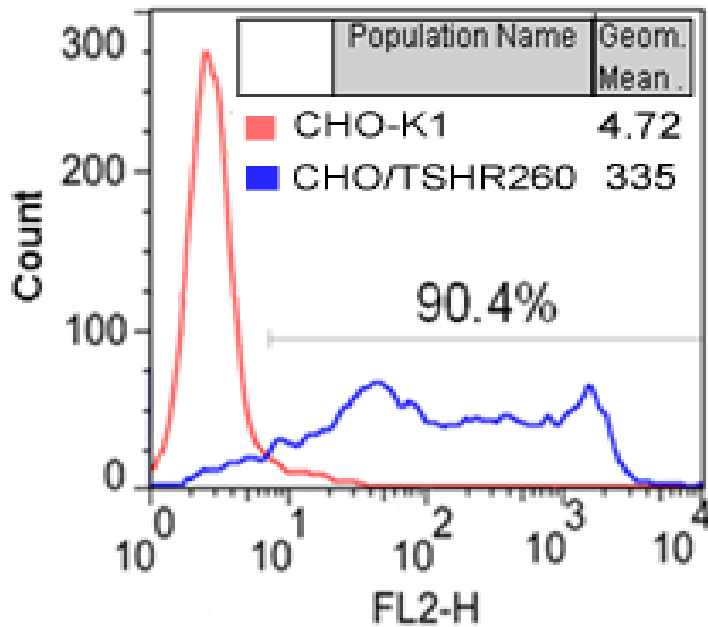


Figure 5.5 Flow Cytometric analysis of constructed TSHR-260.

The expression of TSHR260-GPI on the cell surface of stably transfected CHO-K1 cells was demonstrated by flow cytometry. Stable cell line CHO/TSHR260 was stained with murine anti-TSHR mAb A10. As a control untransfected CHO-K1 were also stained. Binding was detected by FITC-conjugated goat-anti-mouse immunoglobulin (40 µg/ml). FACS analysis showing a significant fluorescence shift with mAb A10 for the stable CHO/TSHR260 cell line (blue line) versus untransfected CHO-K1 cells (red line)

5.2.4 Binding of M22-Fab to CHO/TSHR260 Cells

The stable CHO/TSHR260 cell line was used to setup a cell ELISA methodology to demonstrate binding of the recombinant M22 Fab and confirm that, as reported, this receptor subunit was sufficient to bind TSAbs. CHO/TSHR260-GPI cells, 70,000 per ml in DMEM medium, were aliquoted into each well of a Poly-D-Lysine 96-well ELISA plate, 200 μ l per well. The original TSHR-GPI cell line GPI-95 (expressing amino acid residues 1-412), and control untransfected CHO-K1 cells were plated in identical fashion. The plates were incubated overnight at 37°C in a CO₂ incubator. After five washes with 400 μ l of PBS, 300 μ l of blocking solution (10% FCS in DMEM media) was added to each well in both plates and incubated at 37°C for 1 hour. After five washes with PBS, 100 μ l of the M22 Fab, mouse anti-TSHR control A10 IgG, and irrelevant Fab (TG2-8) as negative control, were added to the plates. All antibodies were at 2 μ g/ml. Plates were incubated at room temperature for 1 hour and then washed five times with 400 μ l of PBS. 100 μ l of the appropriate dilution of HRP-conjugated anti-IgG secondary antibody (human for M22-Fab and mouse for A10 and TG2-8) added to each well. After incubation at room temperature for 1 hour, each well was five times with PBS, and, after visually checking cell adherence under the microscope, 100 μ l of freshly prepared substrate solution was added to each well. Plates were incubated at room temperature for 15-30 min until colour development occurred, 100 μ l of stopping solution added, and the OD₄₅₀ was measured in the plate reader. All samples were tested in triplicate and results were presented graphically as the mean of absorbance of each sample \pm SD.

The results are shown in Fig. 5.6. Both M22 Fab and mouse mAb A10 samples showed high binding signals against the CHO/TSHR260 cell line, confirming that the receptor configuration was suitable as a target for TSAbs. Control untransfected CHO-K1 cells showed a low level of background staining, as did the negative control antibody TG2-8. Antibody binding was also assessed for both the CHO/TSHR260 cell line and the original TSHR cell line GPI-95, which expressed the large TSHR_{recd} domain. Both the recombinant M22 Fab and the control mouse TSHR antibody A10 showed comparable binding to the two TSHR expressing cell lines. The signal from mouse mAb

A10 was rather higher against the GPI-95 cell line, and the reason for this is not clear. Negative control antibody TG2-8 showed a low level of background binding.

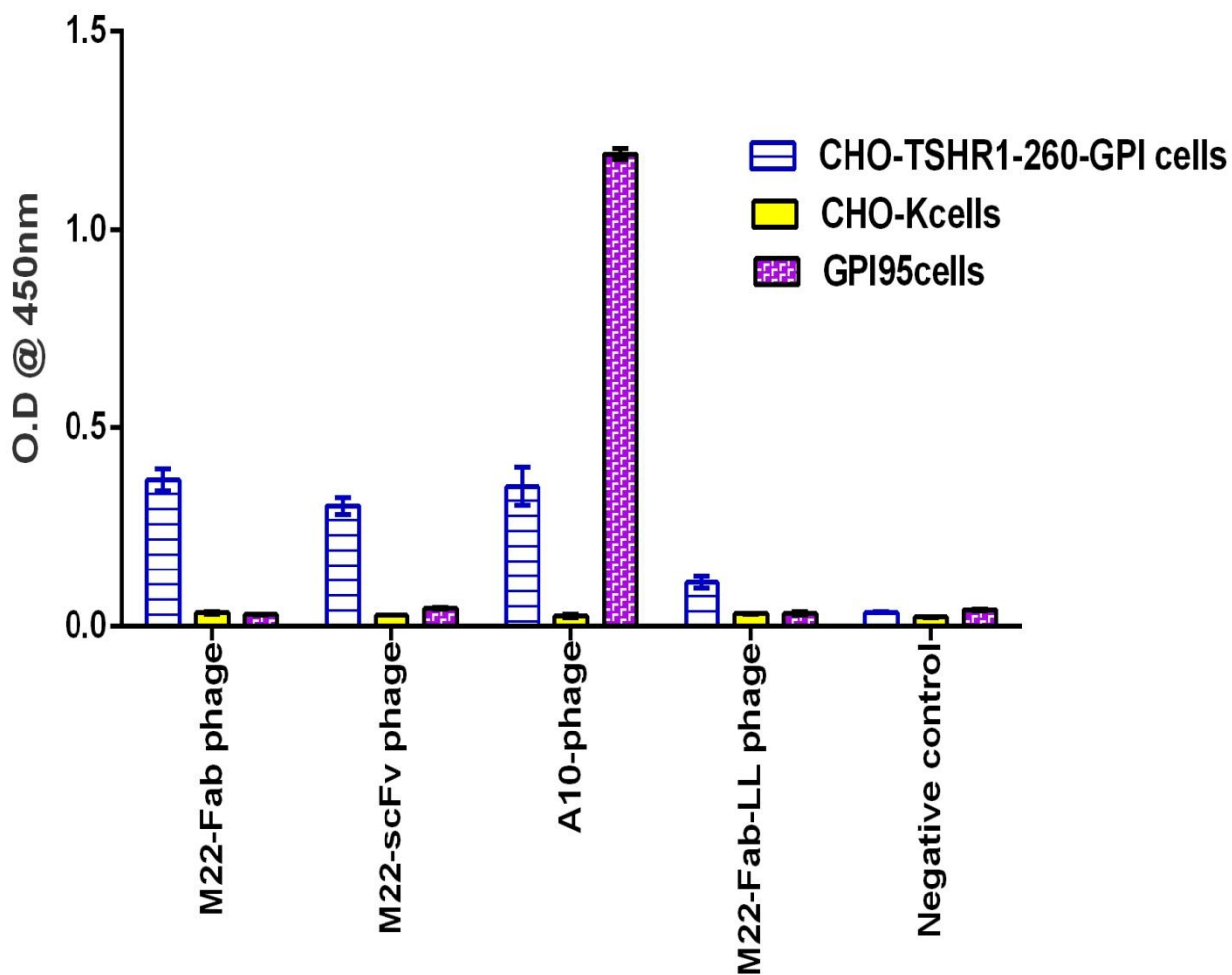


Figure 5.6 ELISA Fab binding of recombinant M22 Fab antibody to the CHO/TSHR260.

The binding of recombinant M22 Fab antibody to the CHO/TSHR260 was measured by cell ELISA. Positive control antibody was the mouse anti-TSHR antibody A10, and the negative control antibody was an irrelevant antibody TG2-8. Binding was also assessed also for GPI95 and untransfected CHO-K1 cells. Data shown are the mean \pm SD and were derived from three independent experiments. Statistical analysis was performed using a one way analysis of variance (ANOVA), showed significant difference for the bindings of M22-Fab, M22-scFv, A10 Fab to CHO/TSHR260 in comparison to untransfected CHO-K cells, $p=0.03$.

5.2.5 M22 phage binding to CHO/TSHR260-GPI

Having established that the CHO/TSHR260-GPI cell line presented suitable antigen for antibody binding we then investigated the binding of antibody-phage fusions to these cells using a cell ELISA approach. CHO/TSHR260 cells (70,000 per ml) in DMEM medium, were aliquoted into each well of a Poly-D-Lysine 96-well ELISA plate, 200 μ l per well. The original TSHR-GPI cell line GPI-95 (expressing amino acid residues 1-412), and control untransfected CHO-K1 cells were plated in identical fashion. The plates were incubated overnight at 37°C in a CO₂ incubator. After five washes with 400 μ l of PBS, 300 μ l of blocking solution (10% FCS in DMEM media) was added to each well in both plates and incubated at 37°C for 1 hour. After five washes with PBS, 100 μ l of the M22-phage, M22 scFv, M22 Fab-LL, A10 phage, and helper phage VCSM13 was added to each well in both plates (CHO-TSHR1-260-GPI and CHO-K1). Each well was washed eight times with PBS/0.05% Tween and 100 μ l of 1:10,000 of horseradish peroxidase conjugated anti-M13 monoclonal antibody (GE Healthcare) in 5% skimmed milk in PBS/0.05% Tween was added to each well. After incubation at 37°C for 1 hour, each well was washed ten times with PBS/0.05% Tween and bounded phage detected by addition of 100 μ l TMB peroxidase substrate (Promega).

The ELISA was developed by incubation at room temperature for 10-15 mins and the reaction was stopped by addition of 100 μ l/well of stopping solution and the absorbance at 450 nm was measured in the iEMS platereader.

The results for the comparison of binding to CHO/TSHR260 versus untransfected CHO-K1 are shown in Fig. 5.7. The various M22 phage constructs all showed significant binding to the CHO/TSHR260 cell line, as did positive control phage A10. The negative control helper phage VCSM13 showed low level binding to both cell lines, and the binding of all phage to untransfected CHO-K1 cells was insignificant.

Phage antibody binding was next assessed for the CHO/TSHR260 cell line in comparison to the original TSHR GPI-95 cell line which expresses amino acid residues

1-412 on a GPI linkage. The results are shown in Fig. 5.8. Once again all the M22 phage antibody constructs, and positive control A10, showed significant binding against the CHO/TSHR260 cell line, but this contrasted with the results for the GPI-95 cell line. The positive control A10 phage also showed significant binding to the GPI-95 cell line, as previously observed, but no binding was observed for any of M22 phage antibody constructs, that is the Fab, scFv, and long linker Fab variants. The negative control TG2-8 phage did not show binding to either cell line.

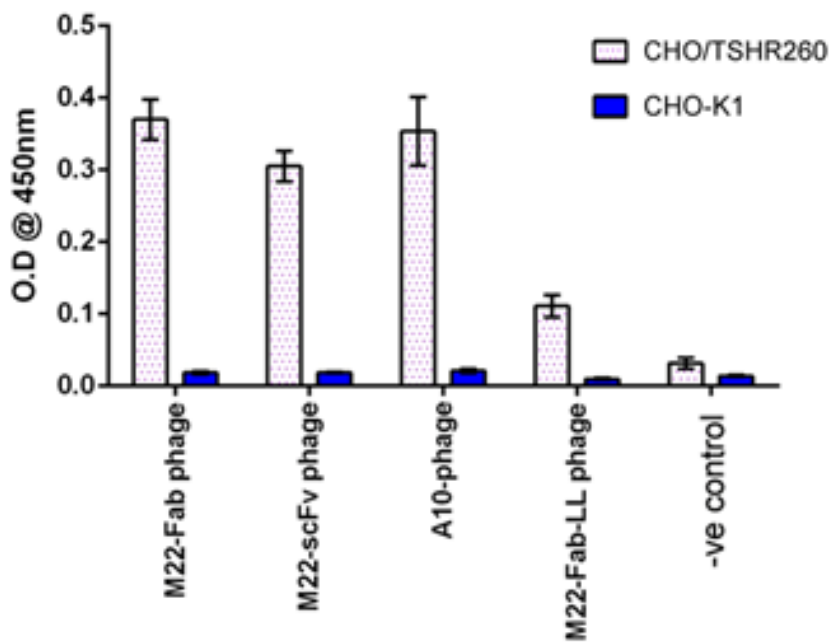


Figure 5.7 Binding of Antibody Phage Constructs to TSHR260 Determined by Cell ELISA.

Phage binding to GPI-linked TSHR was determined by cell ELISA using the CHO/TSHR260 cell line. The M22 Fab, Fab long linker (M22 LL) and scFv (M22 scFv) M22 antibody phage constructs were assessed for binding to ELISA wells coated with monolayers of CHO/TSHR260 cells. Positive control phage were derived from anti-TSHR antibody A10, and helper phage VCSM13 was the negative control. Binding to untransfected CHO-K1 cells was also assessed. Data shown are the mean \pm SD and were derived from three independent experiments.

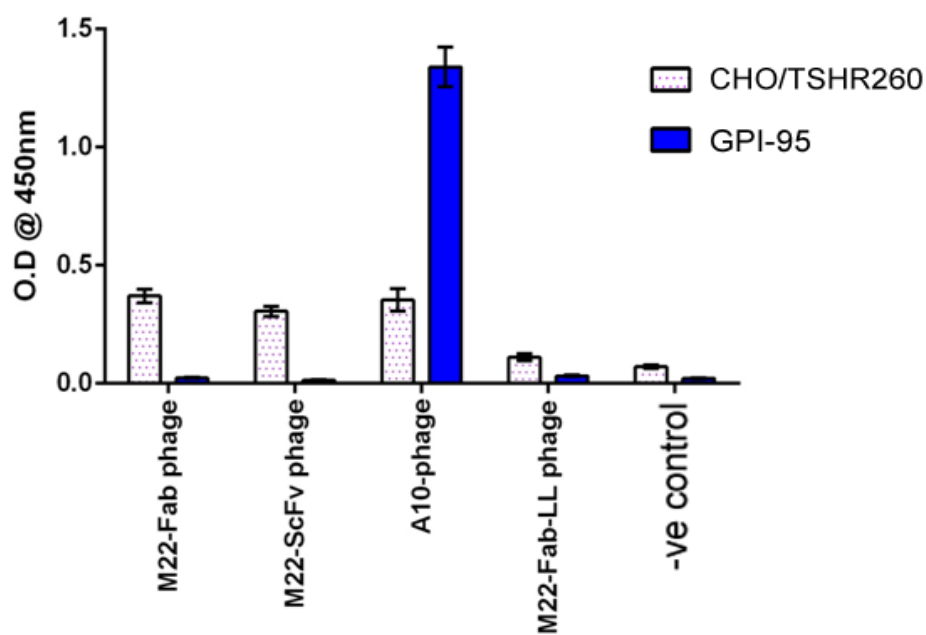


Figure 5.8 Binding of M22 phage antibody constructs to CHO/TSHR260 and GPI-95 cells determined by cell ELISA.

Comparison of antibody-phage binding to GPI-linked TSHR using the CHO/TSHR260 and original GPI-95 cell lines. The M22 Fab, Fab long linker (M22 LL) and scFv (M22 scFv) M22 antibody phage constructs were assessed for binding to ELISA wells coated with monolayers of CHO/TSHR260 cells. Positive control phage were derived from anti-TSHR antibody A10, and helper phage VCSM13 was the negative control. Data shown are the mean \pm SD and were derived from three independent experiments.

5.3 Discussion

The aim of this stage of the project was to investigate the possible basis for the failure of M22 antibody phage to bind the various forms of TSH receptor investigated in our initial studies. Using commercial TSH receptor-coated tubes we were able to demonstrate binding for the recombinant form of the M22 antibody, and this was also observed using detergent extracted receptor from the GPI-95 cell line, and cell ELISA assays using the same GPI-95 cell line. We were also able to demonstrate stimulation of cAMP production in cell lines transfected with the full length receptor, showing the agonist properties of the recombinant antibody, and demonstrating its identity with the original human monoclonal.

Analysis of the preliminary binding data suggested that antibody binding was eliminated when the antibody was physically attached to the phage surface. The large difference in molecular size between the antibody domain and the phage capsid suggested an explanation based on steric hindrance. This phenomenon is not unknown and it has been previously reported that for other antigens certain epitopes may prove inaccessible to phage-antibody fusions (Hoogenboom, Lutgerink et al. 1999). Accordingly we investigated the possibility that the relatively large “hinge” region of the TSHR extracellular domain may adopt a conformation that physically prevents close approach of the phage capsid to the key receptor epitope contained in the LRR ligand binding domain. X-ray data has been published for the TSH receptor but was limited to amino acid residues 1-260, which encompasses the LRR domain. The conformation of “hinge” region thus remains unknown.

As TSH receptor residues 1-260 are sufficient to bind TSAAb and is known to form a stable structure in recombinant form (Sanders, Jeffreys et al. 2004) we produced a stable cell line expressing this domain on the plasma membrane via a GPI linkage. After confirming the properties of the cell line by flow cytometry, antibody and phage binding studies were carried out using a cell ELISA approach. The results showed that, in contrast to the results obtained with the original GPI-95 cell line, we were able to demonstrate significant binding of M22 phage antibody constructs to the new TSHR260 cell line. The results confirmed that the full length TSHR extracellular domain, expressed by GPI-95, was unable to bind the phage but truncation of the receptor to the

minimal LRR domain appeared to remove some form of steric hindrance and antibody phage binding was observed. This was a significant result as phage selection of novel TSAbs from phage libraries can only be possible if an appropriate binding surface is available. The new CHO/TSHR260 cell line represents an important advance and should enable progress in this field.

CHAPTER 6

ISOLATION OF ANTI-IDIOTYPIC ANTIBODIES AGAINST

M22

6.1 Introduction

In Graves' disease thyroid stimulating antibodies (TSAb) are the basis of patient symptoms, producing chronic overactivity of the thyroid gland and excessive levels of thyroid hormone. Evidence suggests that this important class of autoantibodies has a restricted origin and are produced by a small subset of human immunoglobulin genes (Williams, Marshall et al. 1988; Weetman, Yateman et al. 1990; Rapoport, Chazenbalk et al. 1998). Evidence for this restriction has been limited to biochemical characterisation of patient sera as the lack of examples of monoclonal TSAb have prevented extensive DNA analysis. Genetic restriction of these antibodies is not simply of academic interest, knowledge of the variable gene usage may shed light on the immunological origins of thyroid stimulating antibodies, and could highlight novel and specific therapeutic approaches.

Phage display is a powerful technique for the rapid isolation of specific monoclonal antibodies, and has been applied with success to the study of autoimmune thyroid disease (Hexham, Partridge et al. 1994; McIntosh, Asghar et al. 1997; McIntosh and Weetman 1997). The larger part of this current study has been an attempt to develop a selection for the recovery of TSHR antibodies using patient phage libraries. Clearly, as has been described, the use of recombinant TSH receptor, in a variety of forms, presents challenges to this approach. TSAb require a native receptor for binding and the TSH receptor is a difficult protein to produce in recombinant form without loss of conformation (Rapoport, Chazenbalk et al. 1998). In an attempt to overcome these limitations an entirely novel strategy was devised involving the use of anti-idiotypic antibodies.

Anti-idiotypic antibodies have been known and studied for some time, both naturally occurring and artificially produced (Pan, Yuhasz et al. 1995). By definition an anti-idiotypic antibody is one that recognises and binds sites on a second antibody. If the target epitope on the second antibody is the antigen binding variable regions (or paratope) then the anti-idiotypic antibody may possess interesting properties, including the ability to neutralise the binding of the target antibody. In this case we aimed to generate an anti-idiotypic antibody against the monoclonal human TSAb M22. This reagent, if specific for the antigen binding domain, would provide us with a selective surface for

the enrichment of phage antibodies with an identical or similar variable region. This would be a powerful approach for the enrichment of further examples of TSAb from patient antibody libraries and would not be susceptible to the steric difficulties we encountered with recombinant TSH receptor itself. Other applications of this anti-i reagent could include the staining and enumeration of circulating TSAb-producing B cells in samples of Graves' patient blood. These B cells could also be recovered using magnetic bead techniques, or through flow cytometric cell sorting. These experiments would provide a great deal of novel data concerning the frequency of TSAb-producing B cells in patients, and may assist in the cloning of further monoclonals. Finally, a TSAb-specific anti-i with the ability to block antigen binding should eliminate thyroid stimulating activity and thus provide a novel approach to Graves' disease therapy.

To generate anti-idiotypic reagents we will immunise mice with recombinant M22 scFv. This is the smallest subunit of immunoglobulin that retains the antigen specific domain and was chosen to minimise the availability of alternative epitope targets for the immunised mouse immune response. The immune mice spleens will be used to generate a recombinant antibody library, and phage selection will be used to rapidly isolate a series of scFv antibodies that target M22. These will be characterised by ELISA.

6.2 Cloning of M22 scFv into pET21a (+)

M22-scFv-pAK100 construct (described in chapter 3) was diluted 1:1000 in dH₂O as template and amplified by PCR using the primers M22-Pet-1 5' GCGCGC GCT AGC CTT ACG GTT CTG ACC CAA CCA 3', and M22-Pet-2 5' GCGCGC AAG CTT GCT AGA CAC CGT CAC AAG AGT GCC T 3'. The primers introduced NheI and HindIII sites at the 5' and 3' end of the amplification product respectively for sub-cloning into expression vector pET21a. The PCR product was purified using the Wizard PCR Prep kit (2.2.5) and digested for 5 hours at 37°C with 10 units each of NheI and HindIII in 100 µl reaction with 10 µl of Buffer B (Promega). The digested PCR product was purified by gel electrophoresis and purified using the Wizard PCR Prep kit before ligation into pET21a digested with NheI and Hind III. The double digestion of the M22-scFv PCR products and the pET21a vector with NheI and HindIII restriction enzymes can be seen in Fig. 6.1(b). Following transformation, a number of clones were picked, minipreps prepared and the construct confirmed by double digestion with NheI and

HindIII (Fig. 6.1(c)) and by sequencing. The sequencing data of the construct M22-scFv/pET21a revealed the presence of the M22-scFv sequence, His-tag in addition to NheI and HindIII restriction enzymes sites.

6.3 Expression of M22 scFv

6.3.1 Preliminary E.coli Expression of M22-scFv Proteins

The M22-scFv/pET21a plasmid has been transformed into BL21 [DE3] pLysS, a specialised *E. coli* expression host for T7 vectors, containing the T7 RNA polymerase gene under the control of the lacZ operon (Novagen). Initial small scale cultures were carried out to assess expression of the M22-scFv construct (2.2.18.1). Briefly, a fresh colony was picked and grown in 10 ml culture of LB medium (100 µg/ml ampicillin, 30 µg/ml chloramphenicol, 1% glucose) in a shaking incubator at 37°C. Following overnight growth 500 µl of the 10 ml culture was added to 10 ml of LB medium containing 100 µg/ml ampicillin, 30 µg/ml chloramphenicol and grown at 37°C in a shaking incubator with high aeration until the OD_{600nm} was 0.4. IPTG added to a final concentration of 1 mM to induce expression. Culture samples were taken at initiation, and at intervals up to 6 h of induction. Bacterial were pelleted by centrifugation and protein extracted by sodium deoxycholate treatment and sonication (2.2.18) (Fig. 6.2). Samples were analysed by SDS-PAGE and western blotting (2.2.23; 2.2.24). The preliminary induction of BL21 cells using 1 mM IPTG in 2YT medium at 37°C has shown a significant band being produced with molecular weight about 25 kDa visualized by coomassie blue staining in PEG (Fig. 6.3). The solubility test has shown a predominant presence of the protein in the insoluble fraction rather than the soluble proteins fraction.

6.3.2 Large Scale Expression of M22 scFv Protein

pET-21a containing the M22 scFV was transformed into BL21 (DE3) pLysS cells and inoculate to a 1L of 2YT media. Induction of transformed BL21 cells with 1 mM IPTG stimulated expression of a 25 kDa band on a 15% reducing SDS PAGE. This band corresponds to the M22-scFv. The step of extraction was modified to included 500 µg/ml of lysozyme to break the cells (Fig. 6.4). Detergent extraction by 1% Triton x100 was performed and the fractions were loaded on to a SDS-PAGE (Fig. 6.5). Analysis of those fractions showed M22 scFv was in the insoluble fraction.

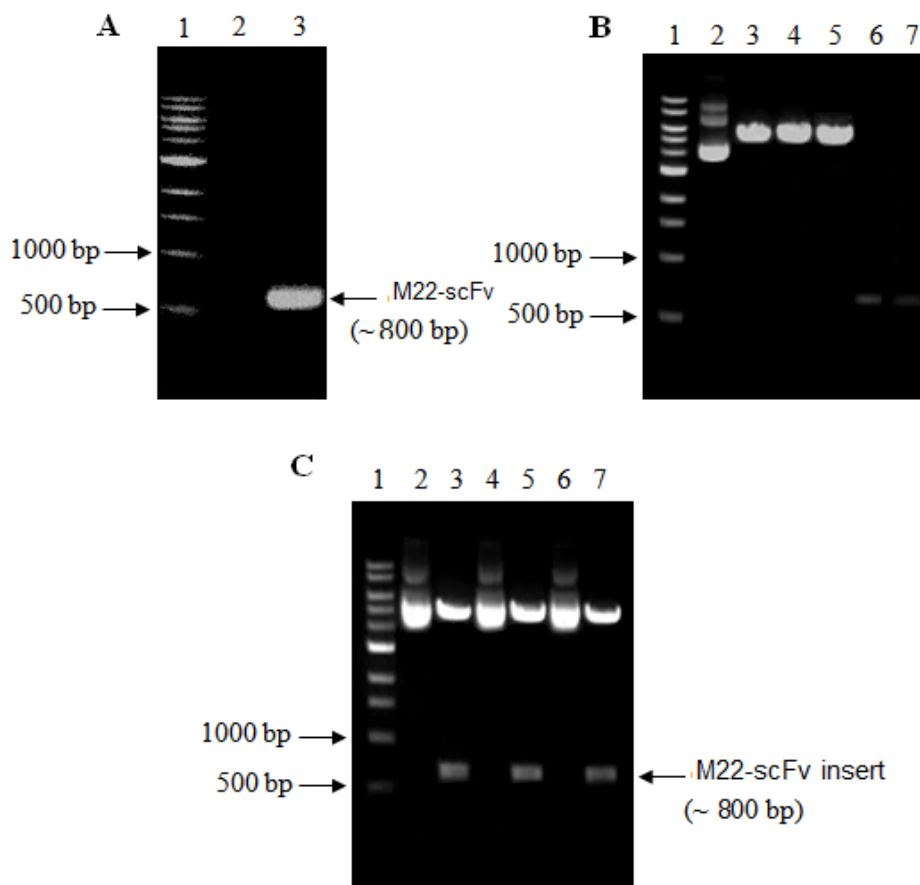


Figure 6.1: Cloning of M22 scFv into pET21a gel images

6.1(a), the figure represents the amplified M22-scFv using PCR. The figure shows the 1% agarose gel with the 1kb DNA ladder in lane 1, PCR negative control in lane 2 and the (~800bp) M22-scFv PCR product in lane 4. 6.1(b), the pET21a plasmid and the M22-scFv PCR product were double digested before they can be ligated and run on 1% agarose gel. The pET21a plasmid was either undigested (Lane 2), single digested with NheI (Lane 3), HindIII (Lane 4) or double digested (Lane 5). The undigested next to double digested M22-scFv products are shown in Lanes 6&7 respectively. 6.1(c), double digestion check was performed on three plasmid mini-preps and confirmed the presence of the correct insert (~800bp) in all of them. Lanes 2-7 represents the undigested next to the double digested plasmid of the three minipreps.

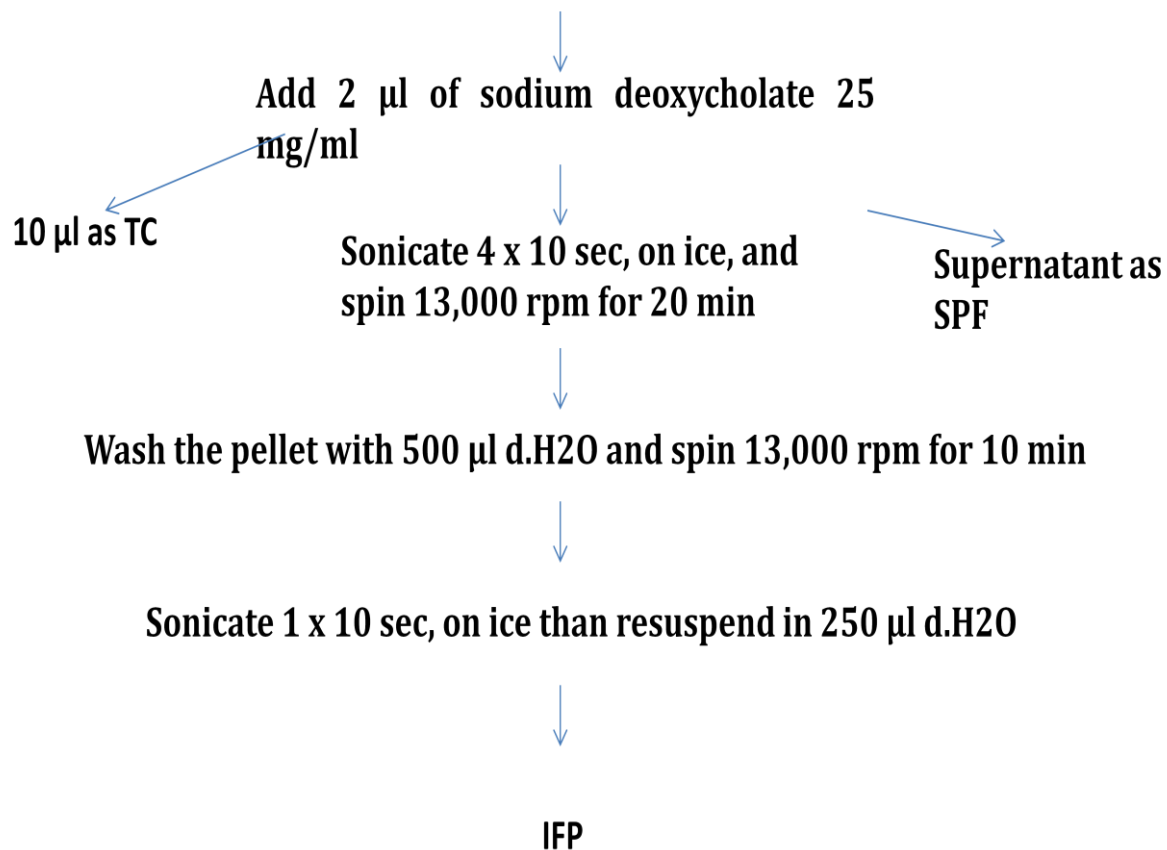


Figure 6.2: Flow diagram of preliminary fractionation of M22-scFv protein.

TC = Total cell protein expression, SPF = Soluble protein fraction, IPF = Insoluble protein fraction (i.e. Inclusion body)

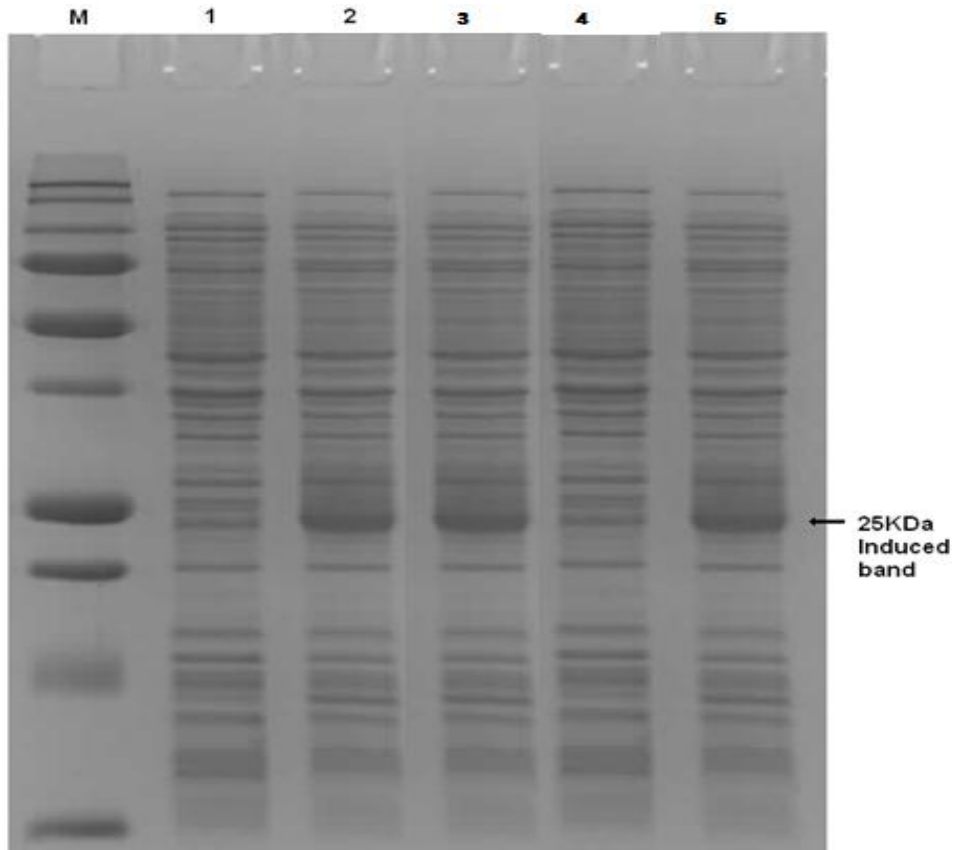


Figure 6.3 SDS PAGE for the induction of M22-scFv.

15% SDS-PAGE, stained with Coomassie blue shows the separated proteins from BL21 (DE3)-RIPL cells after the preliminary induction of M22 scFv (1-2) and the solubility test (3-5). Lane 1 shows the proteins from the BL21 cells before induction of the expression with IPTG, Lane 2 represents the proteins after 4 hours of induction, the expected size of M22 scFv can be seen at about 25 kDa in lane 2. The solubility test was performed is indicated in the last three lanes. Lane 3 represents total cell proteins fractions, lane 4; soluble proteins fraction, Lane 5; insoluble proteins fraction. M22 scFv band was lost in lane 4; indicating that M22 scFv protein was insoluble.

Pellet from E coli expression of M22-scFv resuspended in 1:10 w/v lysis buffer 1

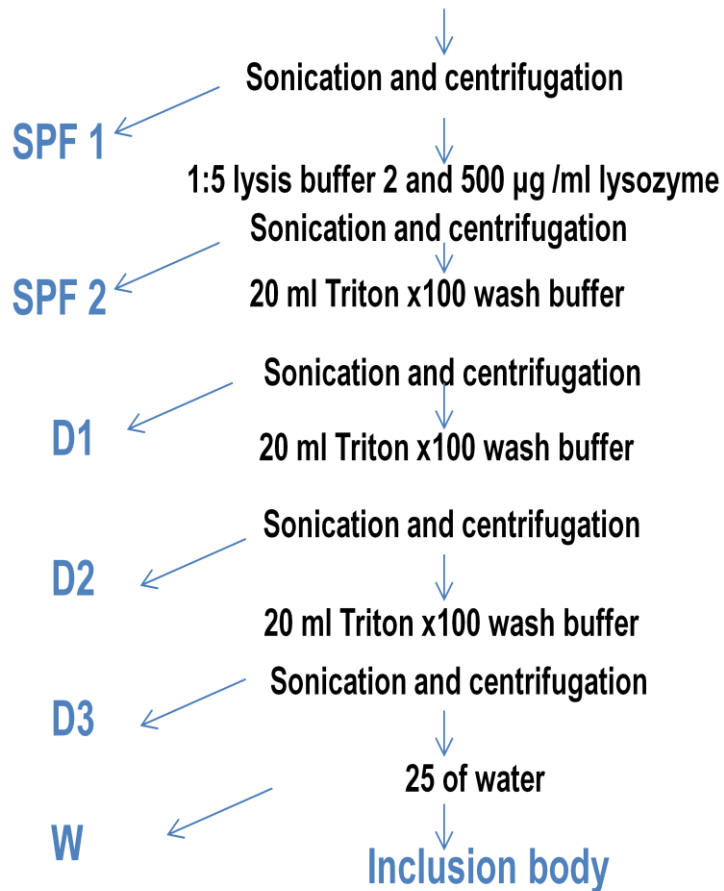


Figure 6.4 Fractionation protocol for large scale expression of M22-scFv protein.

SPF1 = Soluble protein fraction 1; SPF2 = Soluble protein fraction 2; D1 = Detergent extraction fraction wash 1; D2 = Detergent extraction fraction wash 2; D3 = Detergent extraction fraction wash 3; W1 = Water fraction wash 1

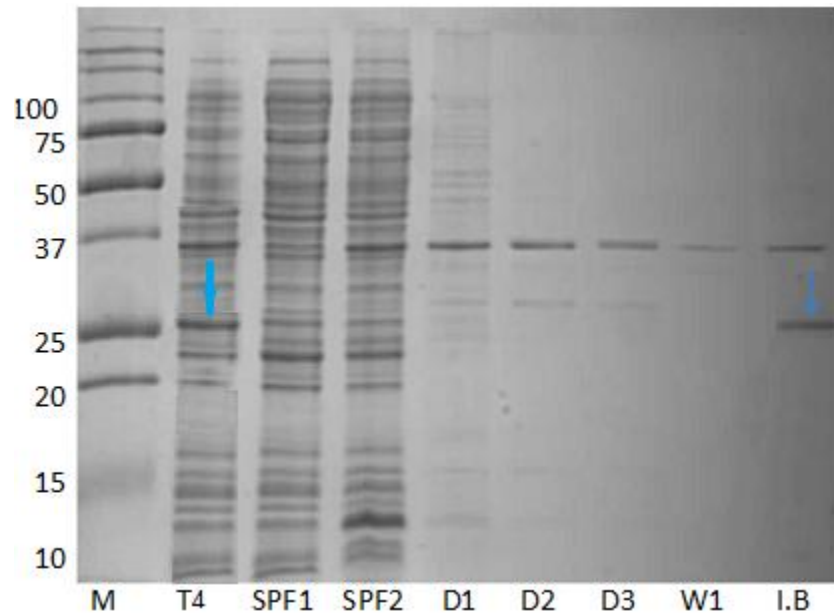


Figure 6.5 SDS-PAGE for protein fractions of M22 scFv expression.

Protein fractions and washes were loaded onto a 15% reducing SDS-PAGE. The gel is showing *E. coli* expression of the M22 scFv in various cell fractions. M = Molecular weight of precision plus protein marker, lane T4: IPTG induced total cell extract after 4 hours, lane SPF1: soluble protein fraction 1, lane SPF2: soluble protein fraction 2, lane D1: Detergent extraction fraction wash 1: lane D2: detergent extraction fraction wash 2 lane D3: detergent extraction fraction wash 3, lane W1: water fraction washes 1, lane I.B = Inclusion body. A 15 kDa band, corresponding to the M22 scFv, was observed upon induction with 1 mM IPTG (arrow 1), which was strongly seen in inclusion bodies (arrow 2).

6.3.3 Solubilisation of Aggregated M22 scFv Insoluble Fraction

M22-scFv was predominantly found in inclusion bodies and thus required solubilisation and refolding in an appropriate buffer. The protein aggregate of M22 scFv was solubilised in 40 mM Tris-HCl plus 6M guanidine hydrochloride. The DTT (dithiothreitol) was also used as a reducing agent to aid solubilisation of inclusion body protein.

6.3.4 Post- M22 scFv Solubilisation Buffer Exchange

Having soluble protein it was then required to put it in a suitable buffer to assist the purification process by nickel column chromatography, but also need natural protein folding to increase the immunogenic response (2.2.19). Soluble M22-scFv was buffer exchanged by dialysis in dialysis tubing with 10,000 kDa cut-off, against 2 L of 10 mM Tris, pH 8.0 and 300 mM NaCl at 4°C with 2 x buffer exchanges over 24 hrs.

6.3.5 Purification of M22 scFv Protein

M22-scFv protein was purified after dialysis by Ni MACTM purification chromatography. Ni column selectively binds the histidines tag at the C-terminus of the M22 scFv proteins immobilising it on the column. After washing of the Ni column, the protein is eluted with 400 mM imidazole (Fig. 6.6). M22-scFv proteins in each elution fraction were measured by Bradford assay. Eluted M22-scFv was dialysed against 2 L of 40 mM Tris-HCl, and 150 mM NaCl, pH 8.0 at 4°C, to remove imidazole. Purification was tested by SDS-PAGE (Fig. 6.7), and Bradford assay. The total amount of purified M22 scFv was measured by Nanodrop and Bradford and it gave an average concentration of 0.522 mg/ml. This material was analysed by SDS-PAGE to confirm the size of the protein, and identity also confirmed by western blotting, using anti-His conjugated with HRP (Fig. 6.8).

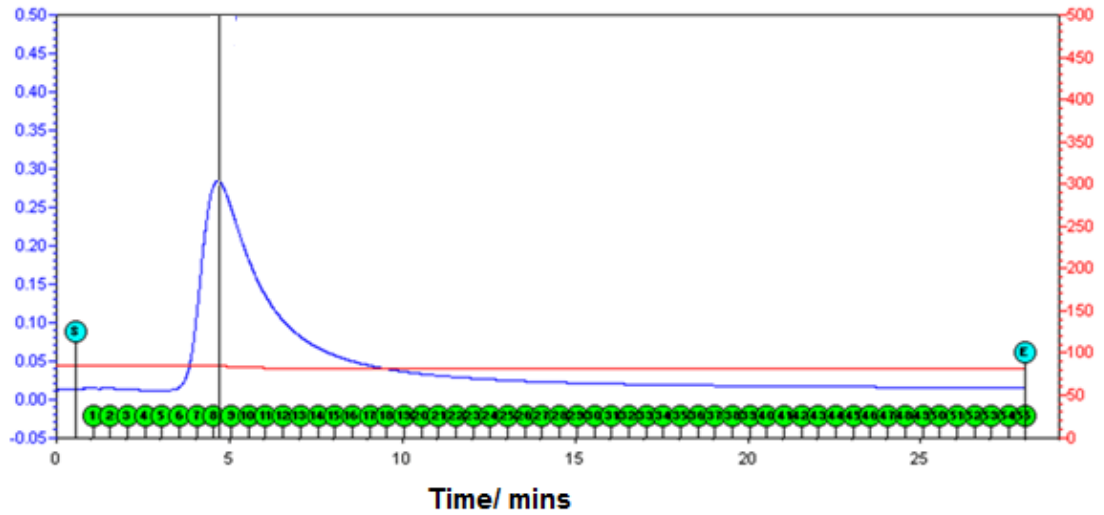


Figure 6.6 Elution of purified M22 scFv.

Following washing the HIS-tagged M22 scFv material was eluted using elution buffer containing 400 mM imidazole. The UV absorbance was monitored and the peak elution fraction collected in a series of 400 μ l samples to be tested by Bradford assay.

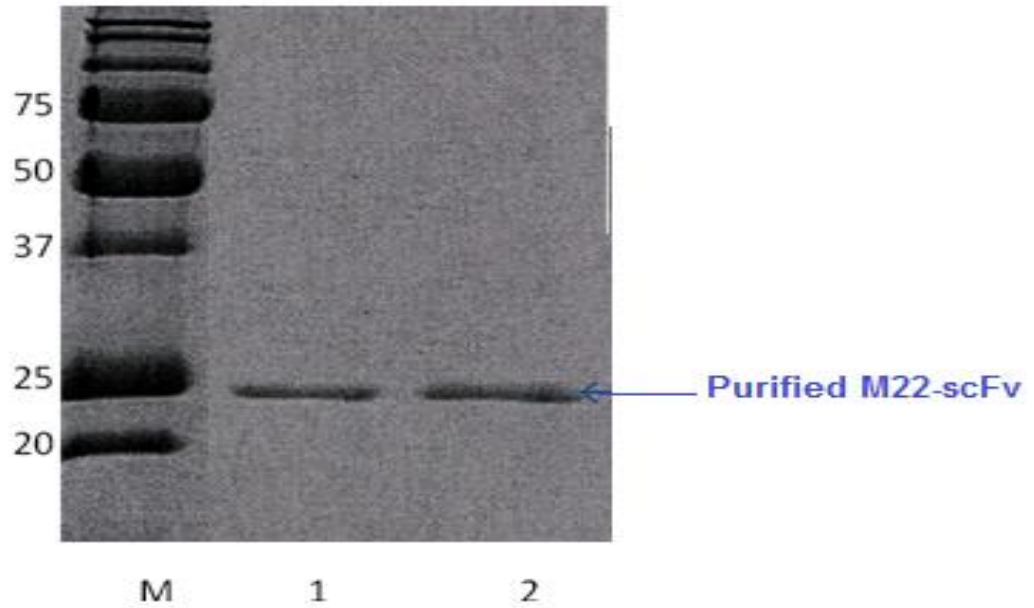


Figure 6.7 SDS-PAGE of Purified M22 scFv.

SDS-PAGE (15%) showing purified M22 scFv before and after dialysis, lane 1: protein marker, lane 2: purified M22 scFv before dialysis and lane 3 purified concentrated M22 scFv after dialysis.

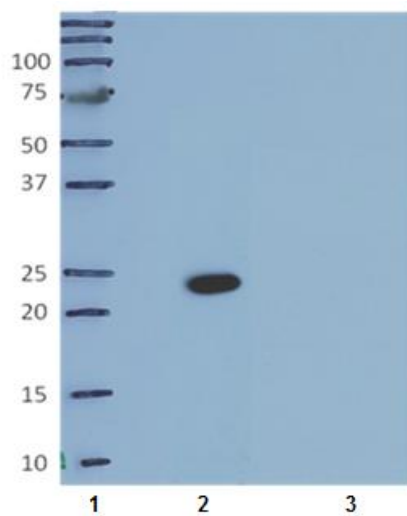


Figure 6.8 Western blot analysis of purified M22 scFv.

Recombinant human M22 scFv was resolved by SDS-PAGE (20 ng per well) and transferred to PVDF membrane. Detection was by HRP-conjugated anti-His antibody and enhanced chemiluminescence and was recorded on X-ray film (2.2.24).

6.4 Immunisation

Four BALB/c mice were immunised with the recombinant M22 scFv as described in materials and methods (2.2.33). Ten days after the final booster immunisation sera from each mouse were collected and serial dilutions screened for M22 scFv reactivity by ELISA. ELISA screening of tail bleeds showed that the immunised mice had developed a high level of IgG response to the recombinant M22 scFv, with high ELISA signal at dilutions up to 1:25,600 (Fig. 6.9). Ten days after the final booster immunisation sera from each mouse were collected for the second time and serial dilutions screened for M22 scFv reactivity by ELISA, which showed high signal at dilutions up to 1:53,000 (Fig. 6.10). The 2 immunised mice with highest ELISA titres (mice 1 and 2) were sacrificed and splenocytes isolated for RNA extraction.

6.5 Cloning of anti-M22-idiotype

6.5.1 Cloning of anti-M22-idiotype scFv

Total RNA was extracted from immunised mouse spleen and reverse transcribed using random primers and reverse transcriptase (2.2.1) (Fig. 6.11). Heavy and light chain variable regions were amplified by PCR (2.2.3) using a large set of primers designed to amplify all murine immunoglobulin variable regions with the minimum level of degeneracy (Krebber, Bornhauser et al. 1997). The upstream light chain primers included a SfiI cutting site and encoded a FLAG tag. The downstream light chain primers included the coding sequence for a flexible Gly₄Ser peptide linker. The upstream heavy chain primers including a portion of this Gly₄Ser coding sequence, and the downstream primers included a second non-complementary SfiI site. The LB primers were combined with the LF primers to produce 5 different primers mixes; LB-1 (LB1-LB4); LB-2 (LB5-LB8); LB-3(LB9-LB12); LB-4 (LB13-LB15); and LB-5 (LB16 & LB18) (Fig. 6.12). The HB primers were combined with the HF primers to produce 5 different primers mixes; HB-1 (HB1-HB4); HB-2 (HB5-HB8); HB-3(HB9-HB13); HB-4 (HB14-HB17); and HB-5 (HB18 & HB19). Heavy and light chain genes of anti M22

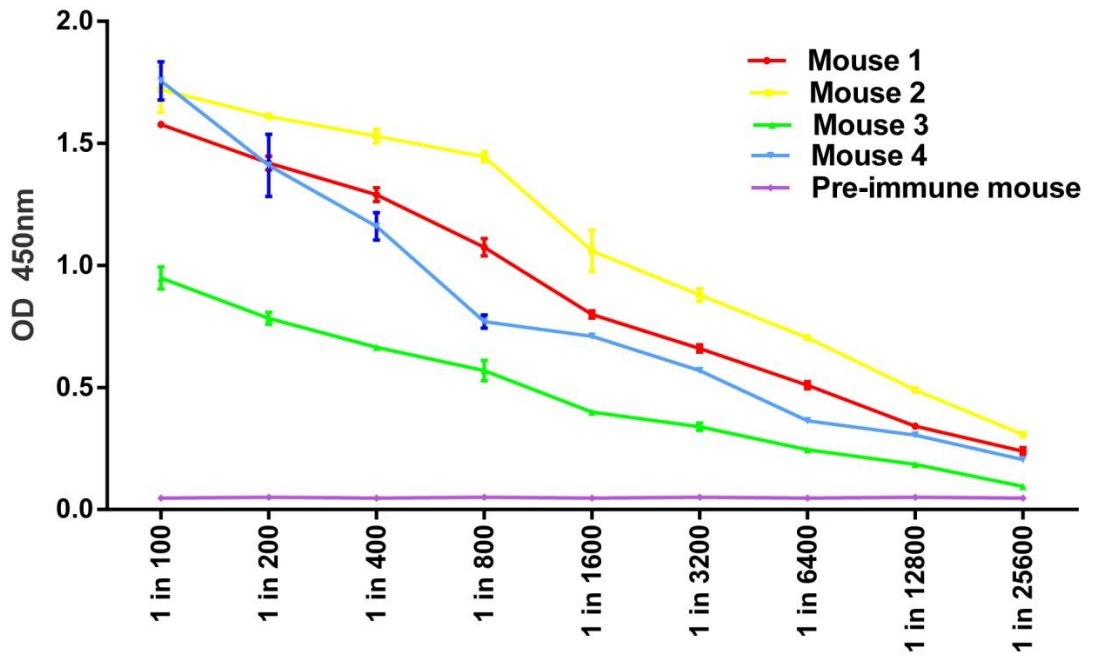


Figure 6.9 Post-immune mouse response to M22 scFv (first boost).

Mouse immune response was assessed by ELISA ten days post first immunisation. Plasma was obtained from the four mice, diluted serially and screened by ELISA against M22 scFv. Plasma from a non-immunised mouse was included as a negative control and detected by Y chain specific secondary antibody (2.2.28), all samples were tested in duplicate and mean absorbance calculated

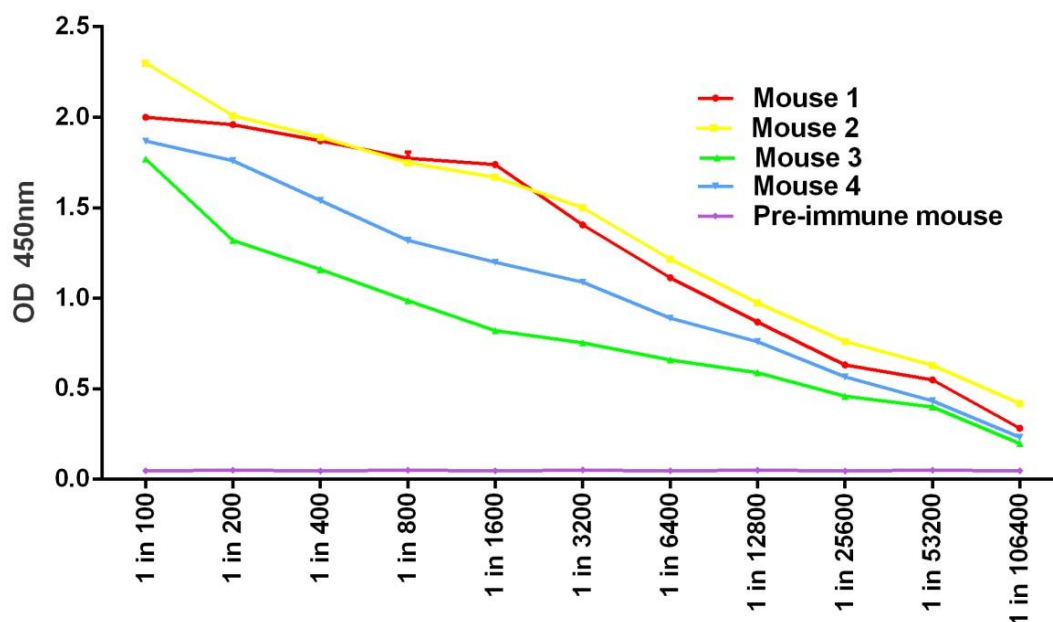


Figure 6.10 Post-immune mouse response to M22 scFv (final boost).

Mouse immune response was assessed by ELISA ten days post final immunisation. Plasma was obtained from the four mice, diluted serially and screened by ELISA against M22 scFv. Plasma from a non-immunised mouse was included as a negative control and detected by gamma chain specific secondary antibody (2.2.28), all samples were tested in duplicate and mean absorbance calculated

obtained were approximately 400 bp (Fig 6.13 (a) and (b)). The PCR products were gel purified (2.2.5) and used in a PCR overlap extension reaction, with primers SCFOR and SCBACK, to generate the final scFv product. The scFv products were cloned into the SfiI cloning sites of phage display vector pAK100. The assembly reaction was successful and yielded an approximately 800 bp product, and the negative control reaction did show a band (Fig. 6.13(c)). Ten assembly reactions were carried out and these were pooled, cleaned up with the Wizard PCR prep kit and eluted in 50 µl of dH₂O. Restrictions digest by 20 units of SfiI (NEB) The reaction was mixed and incubated for 3-4 hours at 50°C, after covered with a drop of mineral oil. The digest was loaded onto a 1% agarose gel (Fig. 6.14), and purification of digested scFv antibody gene and vector were carried out from agarose gel using Wizard PCR prep kit (2.2.5). A ligation reaction was prepared as described previously in 2.2.8. The reaction was mixed and incubated overnight at 16°C. Ligation were ethanol precipitation and resuspended in 20 µl TE buffer, The ligation reaction was electroporated XL1-Blue cells (Stratagene) (2.2.10), and aliquots plated onto solid media to assess ligation quality while the remaining cells were stored on ice overnight. Library quality was confirmed by counting of the number of transformants with 200,000 independent clones being considered the cut-off point for a successful library. The percentage of recombinants was determined by PCR amplification of random colonies using the *scback* and *scfor* primers and by sequencing.

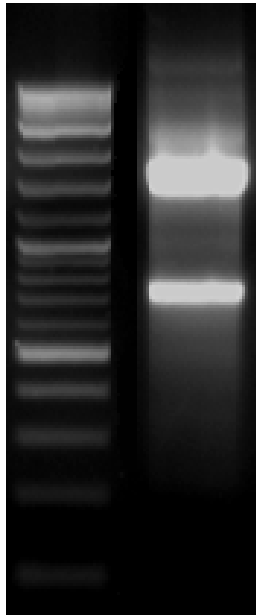


Figure 6.11Total RNA of mouse spleen after immunisation with M22 scFv.

Samples of total RNA recovered from immunised mouse spleen, analysed by agarose gel electrophoresis. RNA was recovered by using Trizol (Gibco).

	Sfi I	FLAG	
SCBACK	TTA CTC GCG GCC CAG CCG GCC ATG	GCG GAC TAC AAA G	
LB1		GCC ATG GCG GAC TAC AAA GAY	ATC CAG CTG ACT CAG CC
LB2		GCC ATG GCG GAC TAC AAA GAY	ATT GTT CTC WCC CAG TC
LB3		GCC ATG GCG GAC TAC AAA GAY	ATT GTG MTM ACT CAG TC
LB4		GCC ATG GCG GAC TAC AAA GAY	ATT GTG YTR ACA CAG TC
LB5		GCC ATG GCG GAC TAC AAA GAY	ATT GTR ATG ACM CAG TC
LB6		GCC ATG GCG GAC TAC AAA GAY	ATT MAG ATR AMC CAG TC
LB7		GCC ATG GCG GAC TAC AAA GAY	ATT CAG ATG AYD CAG TC
LB8		GCC ATG GCG GAC TAC AAA GAY	ATY CAG ATG ACA CAG AC
LB9		GCC ATG GCG GAC TAC AAA GAY	ATT GTT CTC AWC CAG TC
LB10		GCC ATG GCG GAC TAC AAA GAY	ATT GWG CTS ACC CAA TC
LB11		GCC ATG GCG GAC TAC AAA GAY	ATT STR ATG ACC CAR TC
LB12		GCC ATG GCG GAC TAC AAA GAY	RTT KTG ATG ACC CAR AC
LB13		GCC ATG GCG GAC TAC AAA GAY	ATT GTG ATG ACB CAG KC
LB14		GCC ATG GCG GAC TAC AAA GAY	ATT GTG ATA ACY CAG GA
LB15		GCC ATG GCG GAC TAC AAA GAY	ATT GTG ATG ACC CAG WT
LB16		GCC ATG GCG GAC TAC AAA GAY	ATT GTG ATG ACA CAA CC
LB17		GCC ATG GCG GAC TAC AAA GAY	ATT TTG CTG ACT CAG TC
LB18		GCC ATG GCG GAC TAC AAA GAT	GCT GTT GTG ACT CAG GAA TC
(Gly₄Ser)₃-linker			
LF1	GGA GCC GCC GCC GCC (AGA ACC ACC ACC ACC) ₂		ACG TTT KAT TTC CAG CTT GG
LF4	GGA GCC GCC GCC GCC (AGA ACC ACC ACC ACC) ₂		ACG TTT TAT TTC CAA CTT TG
LF5	GGA GCC GCC GCC GCC (AGA ACC ACC ACC ACC) ₂		ACG TTT CAG CTC CAG CTT GG
(Gly₄Ser)₃-linker			
HB1	GGC GGC GGC GGC TCC GGT GGT GGT GGA TCC	GAG GTR MAG CTT CAG GAG TC	
HB2	GGC GGC GGC GGC TCC GGT GGT GGT GGA TCC	GAG GTB CAG CTB CAG CAG TC	
HB3	GGC GGC GGC GGC TCC GGT GGT GGT GGA TCC	CAG GTG CAG CTG AAG SAR TC	
HB4	GGC GGC GGC GGC TCC GGT GGT GGT GGA TCC	GAG GTC CAR CTG CAA CAR TC	
HB5	GGC GGC GGC GGC TCC GGT GGT GGT GGA TCC	CAG GTY CAG CTB CAG CAR TC	
HB6	GGC GGC GGC GGC TCC GGT GGT GGT GGA TCC	CAG GTY CAR CTG CAG CAR TC	
HB7	GGC GGC GGC GGC TCC GGT GGT GGT GGA TCC	CAG GTC CAC GTG AAG CAR TC	
HB8	GGC GGC GGC GGC TCC GGT GGT GGT GGA TCC	GAG GTG AAS STG GTG GAR TC	
HB9	GGC GGC GGC GGC TCC GGT GGT GGT GGA TCC	GAV GTG AWG STG GTG GAG TC	
HB10	GGC GGC GGC GGC TCC GGT GGT GGT GGA TCC	GAG GTG CAG STG GTG GAR TC	
HB11	GGC GGC GGC GGC TCC GGT GGT GGT GGA TCC	GAK GTG CAM CTG GTG GAR TC	
HB12	GGC GGC GGC GGC TCC GGT GGT GGT GGA TCC	GAG GTG AAG CTG ATG GAR TC	
HB13	GGC GGC GGC GGC TCC GGT GGT GGT GGA TCC	GAG GTG CAR CTT GTT GAR TC	
HB14	GGC GGC GGC GGC TCC GGT GGT GGT GGA TCC	GAR GTR AAG CTT CTC GAR TC	
HB15	GGC GGC GGC GGC TCC GGT GGT GGT GGA TCC	GAA GTG AAR STT GAG GAR TC	
HB16	GGC GGC GGC GGC TCC GGT GGT GGT GGA TCC	CAG GTT ACT CTR AAA SAR TC	
HB17	GGC GGC GGC GGC TCC GGT GGT GGT GGA TCC	CAG GTC CAA CTV CAG CAR CC	
HB18	GGC GGC GGC GGC TCC GGT GGT GGT GGA TCC	GAT GTG AAC TTG GAA SAR TC	
HB19	GGC GGC GGC GGC TCC GGT GGT GGT GGA TCC	GAG GTG AAG GTC ATC GAR TC	
HF1	GGA ATT CCG CCC CCG AGG CCG	AGG AAA CGG TGA CCG TGG T	
HF2	GGA ATT CCG CCC CCG AGG CCG	AGG AGA CTG TGA GAG TGG T	
HF3	GGA ATT CCG CCC CCG AGG CCG	CAG AGA CAG TGA CCA GAG T	
HF4	GGA ATT CCG CCC CCG AGG CCG	AGG AGA CGG TGA CTG AGG T	
SCFOR	GGA ATT CCG CCC CCG AG		

Figure 6.12List of primers for cloning mouse scFv fragments.

Sequence degeneracy is indicated using the IUPAC system, R=A/G; Y=C/T; M=A/C; K=G/T; S=C/G; W=A/T; H=A/C/T; B=C/G/T; V=A/C/G; D=A/G/T. The LB primers encode the short form of the FLAG tag (Knappik and Pluckthun, 1994) and anneal to 20 bp of mature mouse immunoglobulin κ chains. The LF primers are complementary to the J κ regions and include three repeats of the Gly₄Ser sequence. HB primers include two copies of the Gly₄Ser sequence and anneal to 20 bp of mouse immunoglobulin κ chains. The HF primers are complementary to mouse JH regions and include an SfiI restriction site. Primers SCBACK and SCFOR annealed to the 5'

terminus of the light chain Fv sequence and the 3' terminus of the heavy chain Fv sequence, and were used to amplify the final assembled scFv product.

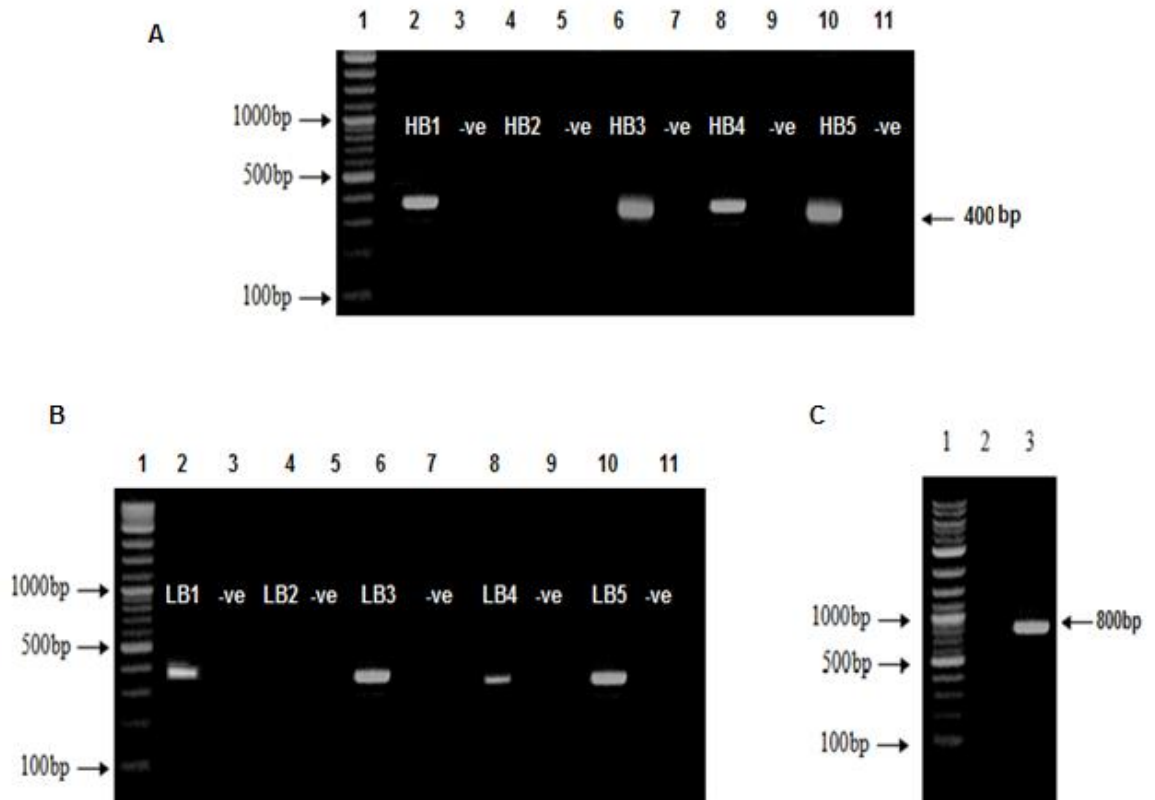


Figure 6.13 Cloning of anti M22 idiotype scFv into pAK100 gel images.

In 6.13(a), the figure represents the amplification of heavy variable gene from anti-M22 scFv cDNA. Samples of cDNA were amplified for 30 cycles and included non-template negative controls. Lane 1 was a 100 bp ladder (Promega) and indicated that products were approximately 400 bp. In 6.13(b) the figure represents the amplification of kappa variable genes from anti-M22 scFv cDNA. Samples of cDNA were amplified for 30 cycles and included non-template negative controls. Lane 1 was a 100 bp ladder and indicated that products were approximately 400 bp. In 6.13(c), the figure represents the assembly PCR of scFv fragments of anti M22 scFv. Purified VL and VH PCR products were mixed together and amplified for 25 cycles with primers ScFor and ScBack. Assembled scFv products were obtained and by comparison to the 100 bp DNA markers (1) had the expected size of 800 bp.

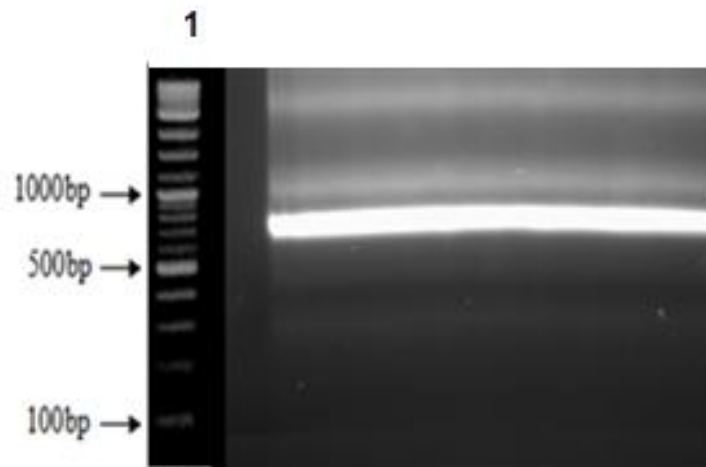


Figure 6.14 Gel purification of digested scFv fragments of anti-M22 scFv.

Assembled M22 scFv fragment was digested for 5 h with SfiI and purified by slot gel electrophoresis. The marker lane (1) was 100 bp ladder (Promega) and the appropriate bands (approximately 800 bp) were excised and purified for cloning into vector pAK100.

6.5.2 Sequence Analysis of Anti M22-scFv Library

Random colonies of anti M22 idiotype scFv library were picked and grown in 10 mls of LB (30µg/ml chloramphenicol, 10µg/ml tetracycline). Miniprep plasmid DNA was prepared (2.2.11) and templates sequenced by fluorescent dye terminator method on an ABI310 machine in the Sheffield University Core Sequencing Facility. The sequencing primer was *scback*. Immunoglobulin gene sequences were analysed using the DNAPLOT software suite and matched to a database of all known germline gene sequences.

6.5.3 Anti M22-scFv Library Rescue

Immediately following electroporation of pAK100 ligations the transformed cells were stored on ice until the assessment of ligation efficiency was completed. The transformed cells were cultured in 100 ml of LB (30µg/ml chloramphenicol, 10µg/ml tetracycline) for 1h in a 37°C shaking incubator. VCSM13 helper phage was added (50 µl of 10¹¹ pfu/ml) and the culture incubated for 15 min at 37°C. Kanamycin was added (10 µg/ml) and the 100 ml culture was grown overnight in a 37°C shaking incubator. The next day library phage particles were recovered as described in 2.2.15 and resuspended at approximately 10¹¹ cfu/ml.

6.5.4 Enrichment of anti-M22-scFv library on M22 scFv

Briefly ELISA wells coated with the recombinant M22-scFv, the wells were blocked by 400 µl of 3% bovine serum albumin (BSA) in phosphate buffer saline (PBS) with 0.05% (v/v) Tween 20 (PBS/Tween) for 1 hour at 37°C. The blocking solution was taken out, and 100 µl of phage library was added (typically equivalent to 10¹⁰ phage particles) and incubated for one hour at room temperature. The phage library was removed, and the tube washed ten times with 400 µl PBS/Tween at room temperature. To elute adherent phage 100 µl of glycine buffer (0.1 M glycine/HCl, pH 2.2) was added and the tube incubated on ice for 10 min. The eluted phage were neutralized with 6 µl of 2 M Tris and used to infect

1 ml of log phase culture of fresh XL1-Blue host. Aliquots of infected host were plated onto selective medium and following overnight the resulting colonies were used to calculate the number of phage eluted from the coated tubes at each round. The remaining infected host was added to 100 ml of LB medium (30 µg/ml chloramphenicol, 10 µg/ml tetracycline) and grown for 1h in a 37°C shaking incubator. The culture was superinfected with 50 µl of helper phage VCSM13 (10^{11} pfu/ml), adjusted to 14 µg/ml kanamycin, and grown overnight in a 37°C shaking incubator. The rescued phage libraries were recovered as described (2.2.15), titered and used for the next round of enrichment.

The anti-M22 idiotype phage library was enriched for 5 rounds on the wells coated with M22 scFv. As a negative control an existing laboratory human anti-TG2 antibody phage library was also subjected to enrichment to reveal the effects of any non-specific binding (Fig. 6.15). Each panning experiment was repeated a minimum of three times and in some cases more. Variations in the washing and elution procedure produced no significant change in outcome.

6.5.5 M22 scFv ELISA of Selected Anti-idiotypic Phage Libraries

The phage display anti M22 idiotype scFv library obtained from final rounds of panning (round 1-5) were tested for binding to M22 scFv by ELISA. The phage display scFv library selected from final round of panning (round 5) shows a higher binding to M22 scFv than phage display scFv library selected from other rounds (Fig. 6.16). The result suggested that the phage display scFv selected from final round of panning could specifically bind to M22 scFv. ELISA plates were coated with µl of M22 scFv mixed with 50 µl of coating buffer (2.1.8) and incubated overnight at 4°C. After five washes with PBS/Tween, 300 µl of blocking solution (5% skimmed milk in PBS/Tween) was added to each well and incubated at 37°C for 1 hour. After five washes with PBS/Tween, 100 µl of round 1-5 phage (approximately 10^9 particles) in PBS/Tween containing 5% (w:v) skimmed milk was added to the wells and incubated at 37°C for 2 hours. Each well was washed eight times with PBS/Tween and 100 µl of 1:5000 of horseradish peroxidase conjugated anti-M13 monoclonal antibody (GE Healthcare) in PBS/Tween 5% skimmed milk (w:v) was added. After incubation at 37°C for 1 hour, wells were washed ten times with PBS/Tween and bounded phage detected by addition of 50 µl of TMB substrate (Sigma). The reaction

was stopped by addition of 50 μ l of stopping solution and the absorbance at 450 nm measured.

6.5.6 ELISA Analysis of Random M22 scFv Anti-Idiotypic Clones

According to rounds ELISA result, 50 colonies of round 5 were cultured each in 10 ml of LB (30 μ g/ml chloramphenicol, 10 μ g/ml tetracycline) for 3 hours in a 37°C shaking incubator. VCSM13 helper phage was added (50 μ l of 10^{11} pfu/ml) and the culture incubated for 15 min at 37°C. Kanamycin was added (10 μ g/ml) and the 100 ml culture was grown overnight in a 37°C shaking incubator. The next day phage particles in each clone were recovered as described in 2.2.15 and resuspended at approximately 10^{11} cfu/ml. On wells coated with M22 scFv. Phage ELISA was done as described in 2.2.28, (Fig. 6. 17).

6.6 Production of Anti M22 scFv protein

6.6.1 Cloning of anti M22 Idiotypic scFv From pAK 100 to pAK 400

In order to increase the functional yield of antibody fragments the anti M22 gene was sub-cloned into vector pAK400. This construct enabled the increased expression of scFv and added a 6 His tag at the carboxy terminus to allow rapid purification by metal affinity chromatography. The highest signal clone in the previous ELISA which reacts with M22 scFv (ID-43) was grown as a midiprep to provide sufficient DNA for subcloning. Briefly 8 μ g of pAK100 ID-43-scFv plasmid prepared from glycerol stock of this clone was digested with SfiI enzyme as described (2.2.7) and the resulting DNA fragments resolved using an agarose slot gel (2.2.4).

Approximately 800 bp scFv antibody fragment was excised from the gel and purified using the Wizard DNA Cleanup kit (2.2.5). Two μ g of pAK400 vector was also restricted with SfiI enzyme and purified, following agarose gel electrophoresis. The purified digested ID-43 fragment was ligated into SfiI sites of the pAK400 to create ID-43-pAK400. The ligation reaction was purified by ethanol precipitation and resuspended in 20 μ l TE. 5 μ l of ligated mixture was electroporated into 60 μ l of a non-suppressor *E. coli* BL21 (2.2.10), 2 μ l was plated out onto an agar plate containing 30 μ g/ml chloramphenicol and incubated at 37°C overnight. Positive clones were

confirmed by restriction digest and glycerol stocks prepared and stored at -80°C to be used for expression and purification of ID-43 scFv protein.

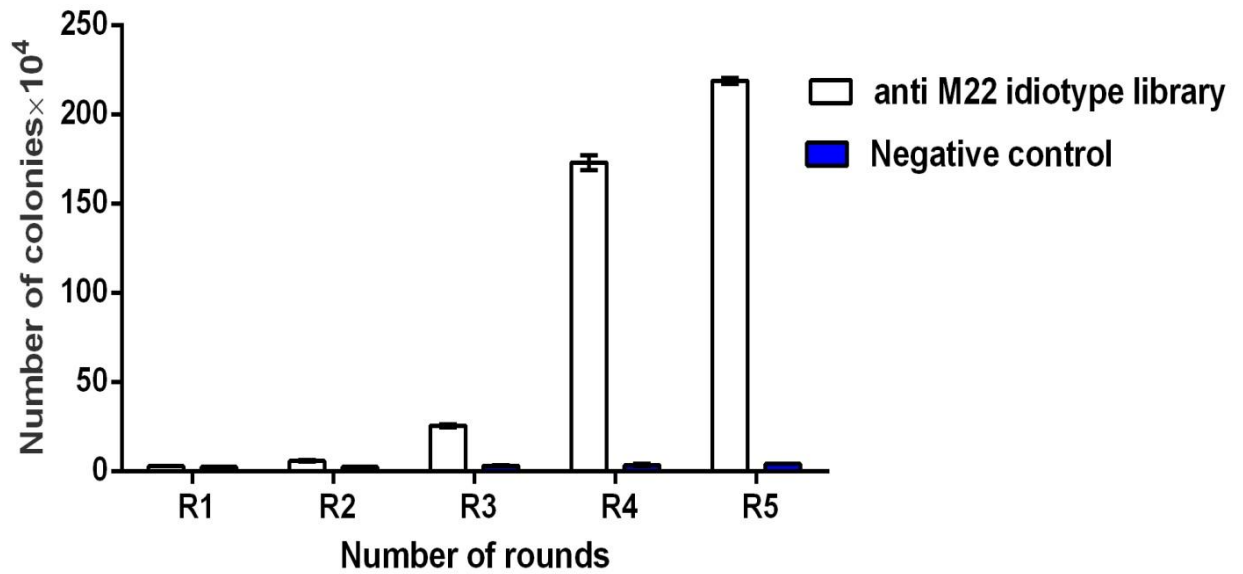


Figure 6.15 Panning of anti-M22 scFv library to M22 scFv-coated wells.

A significant increase in the number of bound phage was observed over 5 rounds of selection. There was evidence of selective enrichment of the anti M22 scFv library. The number of phage eluted from M22 scFv coated wells and negative control was estimated by plating of aliquots of infected host cells. Data are the mean of three independent experiments \pm SD (n=3).

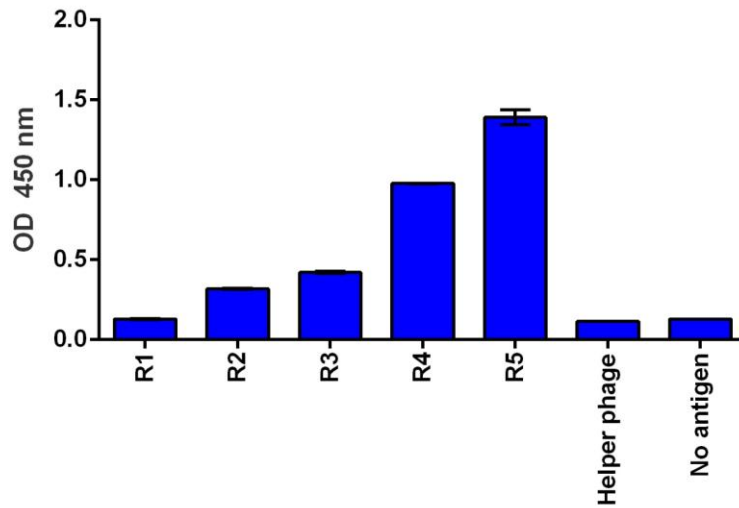


Figure 6.16 Binding of selected anti-M22 idiotypic scFv libraries to M22 scFv.

The phage display scFv library were rescued from different rounds and tested by ELISA for their ability to bind to M22 scFv. The ELISA wells were coated with M22 scFv. The phage rounds display scFv were added to each corresponding wells after eight time washing, 1:5000 of horseradish peroxidase conjugated anti-M13 monoclonal antibody. Data are the means of three independent experiments \pm SD.

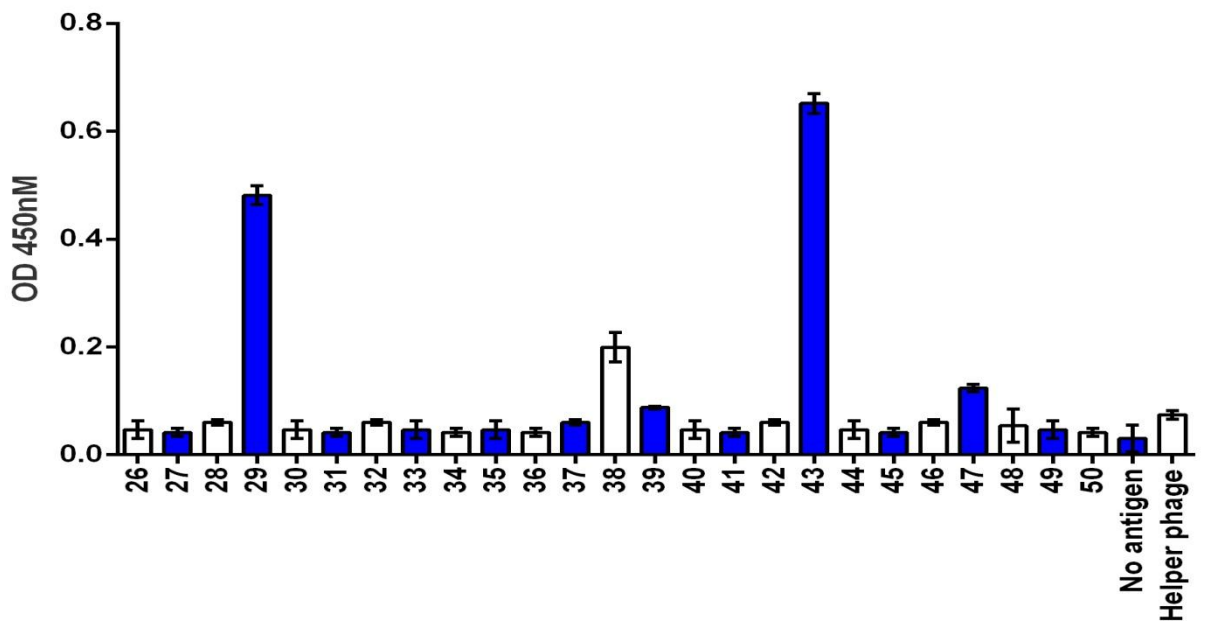
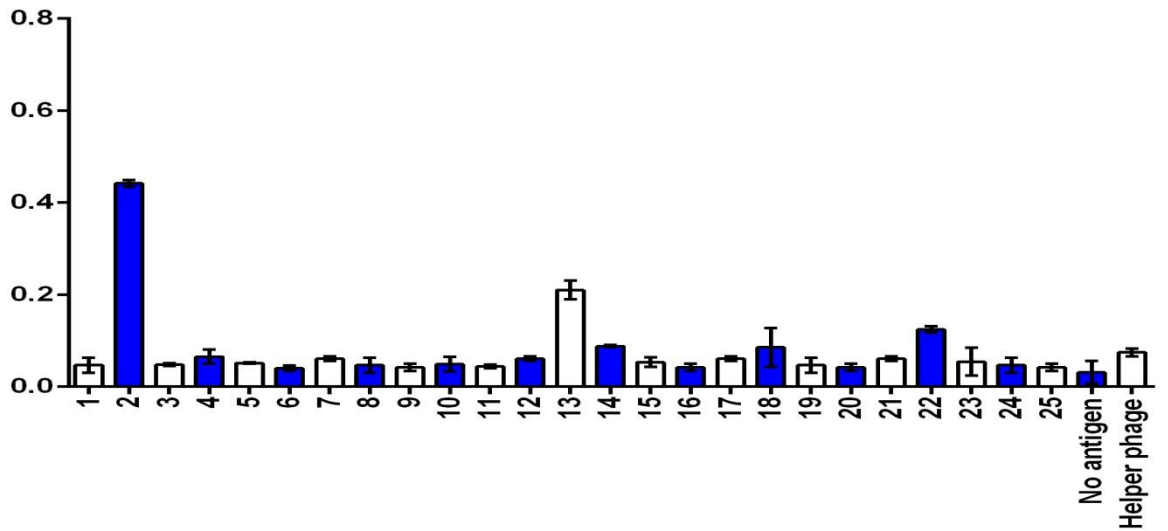


Figure 6.17 ELISA screening of random phage clones for binding to M22 scFv.

Random colonies from the final selected phage antibody library were picked and grown and rescued to produce phage. Phage supernatants were screened for binding to M22 scFv by ELISA. Phage binding was detected using horseradish peroxidase conjugated anti-M13 (GE Healthcare). Uncoated wells were included as a negative control and VCSM13 helper phage. Data are the means of three independent experiments \pm SD.

6.6.2 Expression of ID-43-scFv

The induction procedure of scFv expression was carried out as described in 2.2.20. Briefly, 10 ml of LB medium containing, 10 µl of 30 µg/ml chloramphenicol was inoculated with 10 µl of glycerol stock of ID-43-pAK400 and grown overnight in a shaking incubator at 37°C. This culture was used to inoculate 1L of LB (30 µg/ml chloramphenicol) and grown at 25°C with shaking until the OD_{600nm} reached 0.6. At this point gene expression was induced by the addition of IPTG to a final concentration of 1 mM, and the culture was grown overnight in a shaking incubator at 25°C. The following day the induced culture was centrifuged at 2,000 g for 10 min, the supernatant was removed for further analysis, and the bacterial pellet was used for periplasmic extraction, using osmotic shock method as previously described (2.2.20). The periplasmic extract and the supernatant were then concentrated ten-fold using a micro-concentrator (Amicon). The protein content was estimated by Bradford assay (2.2.22) or by measurement the OD₂₈₀ and analysed by SDS-PAGE (2.2.23).

6.6.3 SDS-PAGE and Western Blot Analysis of Bacterial Extracts

SDS-PAGE and western blotting were performed essentially as previously described (2.2.23 and 2.2.24). Extracts of pAK400 approximately 20 µg of supernatants and periplasmic extracts were analysed by SDS-PAGE, stained with Coomassie blue staining as described in 2.2.23, and following transfer western blotted using a 1:1000 dilution of anti-His in 1% skimmed milk PBS/0.05% Tween for 2 hours at room temperature. After washing 4 times with PBS/0.05% Tween, 1:5000 goat anti-mouse IgG-HRP conjugate (Southern Biotech) in 1% skimmed milk PBS/0.05% was added and incubated for 1 hour at room temperature. The blot was then visualised using an enhanced chemiluminescent (ECL) system (Roche Diagnostics) according to manufacturer's instructions, Fig. 6.18.

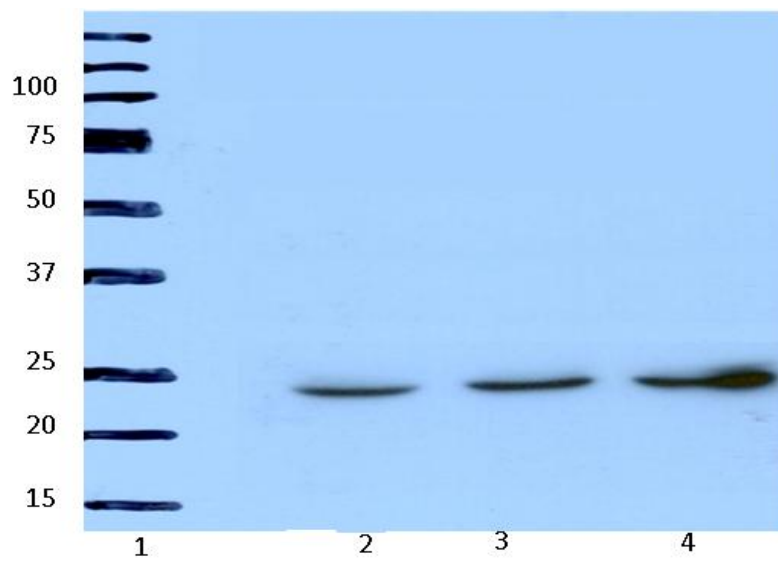


Figure 6.18 SDS-PAGE analysis of purified ID-43 scFv protein.

Lane 1: Protein markers; Lane 2: 10 µg; Lane 3: 20 µg; Lane 4: 30 µg. Purified ID-43 scFv ran at the appropriate molecular weight of approximately 25 kDa.

6.6.4 Purification of Histidine Tagged ID-43 from Bacterial Extracts

The purification of histidine tagged ID-43 protein was achieved by metal chelate resin using TALON Metal Affinity Resins (BD Biosciences) according manufacturer's instructions (2.2.21.1). The eluted fractions were then collected, neutralized, dialysed against PBS and concentrated ten-fold using a micro-concentrator (Amicon), the protein content were assessed by Bradford assay (2.2.22).

6.6.5 Confirmation of Binding Properties

To confirm the predicted binding properties of the ID-43 ELISA assays were carried out using different concentrations of purified ID-43 scFv. ELISA wells were coated with 10 µg of M22 scFv in coating buffer (2.2.14). The wells were blocked for 1 hour with PBS/5% milk (w:v), washed five times with 400 µl of PBS/Tween. A control well of M22 scFv was incubated with anti-FLAG-M1 alone (1:1000) and irrelevant mouse mAb IgG control was included. 50 µl of anti-FLAG M1 (Sigma) diluted in PBS/Tween (1 mM CaCl₂) was added to the wells. The plate was incubated for 1 hour at room temperature and then washed five times with PBS/Tween. 50 µl of anti-mouse IgG HRP conjugate (Sigma) 1:5000 in PBS/Tween was added and the plates incubated for 1 hour at room temperature. The plates were washed five times and developed with 50 µl of HRP substrate for 20 min. The reaction was stopped with 20 µl of 0.1 M H₂SO₄ and the absorbance readings determined at 450nm using an Multiskan Ascent spectrophotometer.

The results are shown in Fig. 6.20. Significant binding was obtained with ID-43 concentrations ranging from 8 µg/ml down to 0.5 µg/ml. No significant signal was obtained from negative control wells containing no M22 scFv and from antigen coated wells incubated with PBS alone.

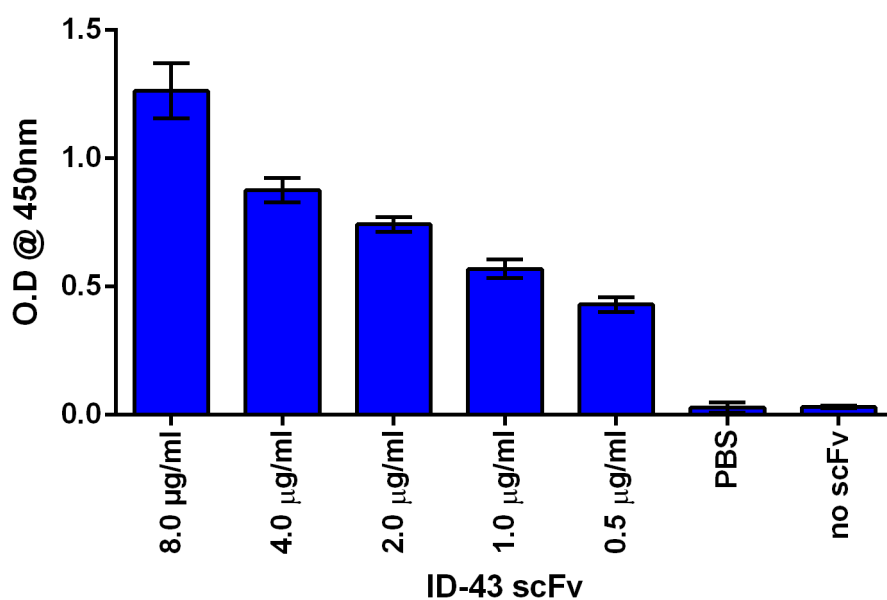


Figure 6.19 Binding of anti-idiotypic mAb ID-43 to purified M22 scFv.

Binding of ID-43 to M22 scFv was confirmed by ELISA. Wells were coated with M22 scFv and ID-43 scFv added in a range of concentrations. Binding was detected using anti-FLAG M1 (Sigma). Negative controls were wells with only coating buffer (no scFv) and antigen coated wells incubated with PBS. Data are the means of three independent experiments \pm SD.

6.6.6 Inhibitory Effect of ID-43 on M22-scFv Phage Binding to TSHR

To investigate the paratope binding properties of ID-43 a phage binding experiment was designed using M22-scFv phage and CHO/TSHR260 cells in an ELISA format. If ID-43 recognised the antigen binding domain of M22 then it can be predicted that ID-43 would block binding of M22 scFv phage to the TSH receptor.

CHO/TSHR260 cells (70,000 per ml) in DMEM medium, were aliquoted into each well of a Poly-D-Lysine 96-well ELISA plate, 200 μ l per well. CHO-K1 cells were plated similarly as a negative control. The plates were incubated overnight at 37°C in a CO₂ incubator. After five washes with 400 μ l of PBS, 300 μ l of blocking solution (10% FCS in DMEM media) was added to each well in both plates and incubated at 37°C for 1 hour. 100 μ l aliquots of M22-scFv phage (10^{10} pfu/ml) were pre-incubated for 30 min at room temperature with different concentrations of ID-43 scFv (2.5-40 μ g/ml). The phage suspensions were then added to the blocked wells and incubated for 1 hour at room temperature. Wells were washed eight times with PBS/0.05% Tween and 100 μ l of 1:10,000 of horseradish peroxidase conjugated anti-M13 monoclonal antibody (GE Healthcare) in 5% skimmed milk in PBS/0.05% Tween added to each well. After incubation at 37°C for 1 hour, each well was washed ten times with PBS/0.05% Tween and bounded phage detected by addition of 100 μ l TMB peroxidase substrate (Promega). The reaction was stopped with 20 μ l of 0.1 M H₂SO₄ and the absorbance readings determined at 450nm using an Multiskan Ascent spectrophotometer. The results are shown in Fig. 6.21. The data were the results from three independent experiments.

M22-scFv phage gave a significant binding signal against stable cell line CHO/TSHR260. Pre-incubation with purified ID-43 reduced M22 phage binding across the concentration range. Inhibition of M22-scFv binding was observed at the lowest concentration of ID-43 2.5 μ g/ml. No binding was seen with control wells coated with CHO-K1 cells and maximal binding of M22 scFv phage was observed with no pre-incubation with ID-43.

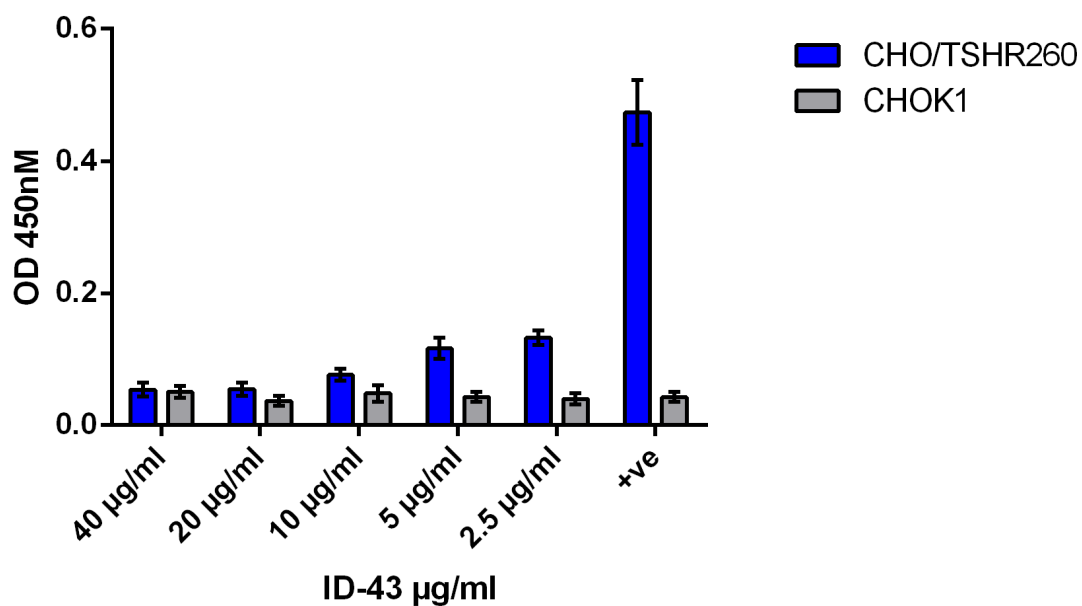


Figure 6.20 Inhibition of M22-scFv-phage binding by anti-idiotypic mAb ID-43.

Binding of M22-scFv phage was measured using a cell ELISA format. Wells were coated with cell line CHO/TSHR260. Phage binding was inhibited by pre-incubation of M22 phage with a range of concentrations (2.5–40 µg/ml) of purified anti-idiotypic antibody ID-43. Positive control wells were M22 phage without preincubation with ID-43. Data are the means of three independent experiments \pm SD.

6.7 Discussion

The recombinant synthesis of TSAb monoclonal M22 presented a number of novel opportunities for the analysis of this interest class of autoantibodies. For the first time we were able to produce a range of phage antibody constructs and investigate their binding characteristics. The difficulties we encountered with the phage selection experiments served to highlight the technical challenges that arise when using the thyrotropin receptor as an antigen binding surface. In an attempt to circumvent these problems we devised an alternative strategy based on the development of an anti-idiotypic antibody that targeted the antigen binding domains of M22. A ready supply of recombinant M22, verified by both binding and cAMP stimulation assays, enabled the immunisation of a series of mice with the monoclonal TSAb. To rapidly isolate a series of anti-M22 monoclonals we employed a phage antibody library approach. After several rounds of biopanning we succeeded in isolating an enriched library and scFv antibodies and clones from this library were screened by ELISA against purified M22. The result of this approach was the characterisation of a monoclonal anti-idiotypic antibody ID-43 that showed specific binding against M22. ID-43 was also able to neutralise the binding properties of M22 scFv phage against cell lines expressing TSHR260. These data suggest that ID-43 was reacting against the antigen binding region of M22 and so blocking antigen recognition, indicative of a true anti-idiotypic antibody. This is the first documented isolation of an anti-idiotypic reagent that targets a thyroid stimulatory antibody and opens the way for a series of novel experiments that will provide insights into the nature of this autoreactive immune response.

The novel antibody should provide an alternative selective surface for the enrichment of anti-TSHR antibodies from phage libraries that is both more stable and easier to produce than the native receptor itself. In addition, it will selectively capture antibodies that share identical or similar antigen binding variable gene re-arrangements that recognise the thyroid stimulatory epitope of the TSHR. Aside from phage antibody experiments this novel reagent could also be used to label and capture circulating B cells from Graves' disease patients, leading to the isolation of new examples of patient monoclonal TSAbs. Finally, an anti-idiotypic antibody may prove an exciting new departure from conventional therapeutic approaches to Graves' disease, that is the

ability to specifically bind and neutralise circulating thyroid stimulating antibodies that are the basis of disease symptoms.

CHAPTER 7

DISCUSSION

7 Discussion

Together, autoimmune hypothyroidism and autoimmune hyperthyroidism, or Graves' disease, represent the most common form of organ specific autoimmunity in the population with a frequency of approximately 1-2% (Tunbridge, Evered et al. 1977). Graves' disease is particularly interesting as the condition is driven almost exclusively by a humoral, antibody mediated process, in contrast to many other autoimmune conditions in which the pathological mechanisms are dominated by cell mediated immunity and tissue destruction. The symptoms of Graves' disease, chronic overstimulation of the thyroid gland and excess production of thyroid hormones, are caused by a specific sub-class of autoantibodies, TSAb, that act as agonists towards the thyrotropin receptor. As such they belong to a subset of autoantibodies with biological action separate and distinct from their role in the immune system.

Since their discovery in 1956 (Adams 1956) these antibodies have been the subject of intense study. Important questions included: what was the origin of these antibodies? Was there a genetic basis underlying the risk of an individual developing TSAb. What were the target epitopes recognised by TSAb? In addition to the academic importance of understanding these properties, insights into the nature of these stimulatory antibodies may suggest novel therapeutic approaches to the treatment of Graves' disease. Initially, technical limitations of available methods restricted analysis of these antibodies to the bulk properties of patient sera. Nonetheless it became clear that in some patients TSAb immunoglobulins were at least partially restricted to the lambda subclass of IgG (Weetman, Yateman et al. 1990), and possibly oligoclonal. With the molecular cloning of the human thyrotropin receptor (TSHR) cDNA in 1989 (Libert, Lefort et al. 1989; Nagayama, Kaufman et al. 1989) it became possible to confirm the identity of the TSH receptor as the target antigen for TSAb and also allowed the development of recombinant sources of antigen and bioassays to routinely measure the stimulatory activity of patient sera. With these advances it quickly became clear that TSAb, in contrast to other autoantibodies, were present at very low, nanogram per ml, levels in patient sera, a further hindrance to detailed analysis (Rapoport, Chazenbalk et al. 1998). With the cloning of the human TSHR attention turned to the development of recombinant expression of the receptor, and attempts to use this material to produce

animal models of Graves' disease, the hope being that this approach would prove less intractable than the analysis of patient antibodies.

For a period of some ten years following the initial publication of the TSHR sequence, a series of studies were reported describing immunisation of animals with recombinant forms of TSH receptor, and the recovery of monoclonal antibodies (Rapoport, Chazenbalk et al. 1998). There were repeated claims of monoclonals possessing the thyroid stimulatory activity observed in Graves' disease but none could be repeated, and indeed on closer inspection none of the published antibodies achieved agonist activity at the nanogram per ml concentrations seen with true TSAbs (McLachlan and Rapoport 1996).

What did become clear from these and other studies was that the TSH receptor itself was a complex and difficult antigen to manipulate experimentally. Human receptor antibodies failed to recognise TSHR expressed in bacteria or in other non-native forms. Binding of TSAbs to the receptor has a strict requirement for a native conformation (Rapoport, Chazenbalk et al. 1998). Expression in mammalian cells was achieved and stable cell lines proved useful in both bioassays and for direct binding studies, though the levels achieved initially did not lend themselves to high level production and purification (Rapoport, Chazenbalk et al. 1998). The eventual isolation of cell lines with high level expression was a major technical breakthrough (Stiens, Buntmeyer et al. 2000) and for the first time allowed the development of high throughput assays for direct antibody binding to native TSHR that lent themselves to a degree of automation (Costagliola, Morgenthaler et al. 1999).

By 2002 the development of novel immunisation strategies, including cell immunisation and DNA transfection (McLachlan and Rapoport 1996) led to the first successful animal models of Graves' disease, and the first recovery of TSAbs monoclonals that at least partially fulfilled previously accepted criteria for success i.e. thyroid stimulation at nanogram per ml levels (Costagliola and Vassart 2002; Sanders, Jeffreys et al. 2002; Ando, Imaizumi et al. 2003). Shortly afterwards the use of the novel high throughput TSHR direct binding assays contributed to the isolation of the first example of a human TSAbs monoclonal M22 (Sanders, Evans et al. 2003). This represented a mammoth task, and indeed some 16,000 culture supernatants had to be screened to obtain this

monoclonal, an effort that would have been impossible without the use of novel binding assays, and testimony to the low level of circulating B cells producing TSAAb in Graves' patients.

These technical breakthroughs were impressive but have not lead to an avalanche of further reports. Indeed, there are still only two examples of monoclonal human TSHR antibodies in the literature, and a handful of rodent antibodies. Thus the questions initially posed about the nature of patient TSAAb remain to be answered. How diverse are they? Are they oligoclonal? Do they arise in different patients from a similar subset of immunoglobulin germline genes? The answers to these questions will only come from the analysis of further examples of clonal TSAAb from a large number of patients. Given the efforts required to isolate the two current examples of patient TSHR antibodies, it is unlikely that this approach will lead to a rapid resolution of these key questions. Alternative approaches are required and one of these could be the use of phage display, a powerful technique for the expression and antigen-specific recovery of monoclonal antibodies (McCafferty, Griffiths et al. 1990; Burton and Barbas 1994).

Antibody phage display techniques offer the potential for greatly facilitating the generation and characterization of recombinant antibodies originating from humans and mice (Graus, de Baets et al. 1997; Ditzel, Masaki et al. 2000). In this system the antibody heavy and light chain are cloned and expressed in bacteriophage, the antibody genes can be expressed as the scFv or Fab antibodies fragments form using suitable vectors and cloning systems. Recombinant antibodies are expressed on the surface of the phage in functional form and able to bind their corresponding antigen. Capture of antibodies by an antigen surface also leads to capture of the attached phage and this the genes used to express the antibody. Sub-culture of these selected clones and repeated rounds of enrichment by antigen capture allow the rapid isolation of high affinity monoclonal antibodies.

Requiring only the availability of B cell RNA, the phage antibody display technique offers the potential for rapid enrichment of specific recombinant antibodies from cloned patient repertoires, and has proven particularly successful in the analysis of patient autoantibodies in autoimmune thyroid disease (Portolano, Chazenbalk et al. 1992; Hexham, Partridge et al. 1994; Jaume, Portolano et al. 1994; McIntosh and Weetman

1997). All these studies centered on antibodies to two major thyroid antigens: thyroid peroxidase and thyroglobulin. As described above the successful expression of native TSHR has always presented something of a technical challenge, and was thus unavailable as a selective binding surface until the advent of modern commercial binding assays. The only reported attempt to use phage display to recover TSHR antibodies was unsuccessful, for reasons that were unclear (Van Der Heijden, De Bruin et al. 1999).

Clearly if the technical challenges for the enrichment of phage antibodies on TSHR could be overcome then this approach may lead to the recovery of many more examples of patient TSAbs monoclonal and provide invaluable data regarding the nature and origin of this important class of autoantibodies. Accordingly this project was designed to investigate the potential of phage display techniques to enable the recovery of novel TSAbs monoclonals.

The availability of the human TSAb M22 DNA sequence provided the starting point for this project; the development of a positive control reagent that would allow an investigation of the binding conditions for TSAbs in phage antibody format. In this project we were able to successfully synthesise and clone the immunoglobulin gene sequences of the human monoclonal thyroid stimulating antibody M22, and we could express and characterise the antibody. We expressed valuable quantities of the scFv antibody and confirm its binding and stimulating properties. The recombinant antibody bound to the TSHR in FACS, and more importantly it possessed agonist activity against the receptor. We were able to induce cAMP production in the JP09 bioassay at ng/ml concentrations; evidence of a true TSAb. Thyroid stimulating activity has been previously described for Fab fragments of M22 (Sanders, Evans et al. 2003), but this was the first time that stimulating activity has been documented for an scFv fragment. This was an important step for our project as examples of true TSAbs monoclonals are very difficult to obtain, and are still considered commercially sensitive reagents.

Construction of the M22-scFv phage provided for the first time a representative example of a TSAb in a phage display format, and could be used to investigate the binding properties of these antibodies, thus enabling the development of enrichment strategies that could be applied to recovery of other TSHR phage antibodies.

Initial phage binding experiments with the M22-scFv construct failed to demonstrate any evidence for specific binding of the recombinant antibody to tubes coated with TSH receptor. This result was rather surprising because the soluble form of the antibody was shown to bind to the TSH receptor in FACS analysis, and stimulated cAMP production in the JP09 TSHR bioassay. These results showed that the antibody itself possessed the required specificity, but the phage-antibody fusion was unable to bind its corresponding epitope on the TSH receptor when it was attached to coated tubes from the commercial TSHR antibody assay kit (BRAHMS tubes). These observations represented a significant setback for the project, and what mechanism lay behind this phenomenon was not clear. The most likely explanation was that the phage-antibody fusion was behaving fundamentally different from the soluble antibody and that this difference was the result of some unforeseen steric interaction between the phage capsid and the receptor.

In chapter 4 we sought to investigate the mechanism of phage antibody binding by producing a range of different phage-antibody fusions and probing the binding of each to the TSHR. From a purely physical standpoint it seemed likely that the relatively large molecular size of the phage-antibody fusion was playing a role in the antigen binding process. The M13 phage capsid is a relatively huge structure when compared to the displayed antibody. With approximate dimensions of 6 nm x 900 nm, phage particles are effectively a very long thin cylinder with a small antibody moiety of between 4-8 nm attached to the end. It seems logical that this structure may prevent binding to some epitopes if they were partially obstructed by domains of the antigen.

In this part of the study we synthesised a series of M22 variants in which the Fab version of the antibody was expressed as a phage fusion. This effectively doubled molecular distance of the antigen binding domains from the phage coat protein fusion partner. An additional construct was made in which the Fab structure was extended by a flexible peptide linker to be allowed to move further away from the phage capsid. The physical access of the antibody to the target epitope was also a consideration. The initial tube binding experiments depended on the commercial TSHR-coated BRAHMS tubes. In this system the TSH receptor is captured onto the tube surface using a specific

monoclonal antibody. There is at least the potential for the antigen to be coated in a uniform fashion in relation to its orientation. To address this possibility we extracted native receptor from a transfected cell line GPI-95, which expresses a high level of TSHR extracellular domain on the cell surface. Partitioning the GPI-anchored receptor using detergent (Ko and Thompson 1995) enabled the recovery of useful quantities of antigen, and this material was used in a series of ELISA experiments. As before only soluble M22 antibody was able to recognise this material, which was an important result as it showed that the recovered material contained receptor in native form, a prerequisite for the binding of TSAb. M22 in single chain form also bound the receptor extract. However, the M22 antibody phage fusions, including the long linker variant, failed to recognise the receptor in neither the BRHAMS tube format, nor in these ELISA assays. This effectively eliminated the hypothesis that it was the orientation of the antigen that was preventing antibody-phage binding, or indeed proximity to the plasma membrane. At this point we began to consider that the explanation may be found within the nature of the antigen itself.

In chapter 5 we considered the conformation of the TSH receptor and the possibility that in some way the 3-dimensional shape of the receptor extracellular domain was preventing phage-antibody binding by some steric mechanism. By convention many groups had expressed the extracellular domain in a form that included the amino acid residues from 1 to 412. This sub-domain had been shown to be sufficient for both TSH and TSHR antibody binding (Rapoport, Chazenbalk et al. 1998). However, the TSHR is unique among glycoprotein hormone receptors in having an extra stretch of 50 amino acids inserted into so-called “hinge” region immediately preceding the seven transmembrane domains (Rapoport, Chazenbalk et al. 1998). There is no structural data to offer insights into the conformation of this hinge region, and it is possible that some residues may be positioned in the space immediately anterior to the ligand binding site and thus may interfere with phage-antibody binding. Evidence from studies of the FSHR suggested that some carboxy terminal regions of the receptor do participate in ligand binding and may adopt positions close to the LRR ligand binding site (Jiang, Liu et al. 2012). The only published crystallographic studies of the TSHR expressed a stable LRR domain comprising only residues 1-260, approximately half the size of the extracellular domain expressed in our GPI-95 cell line. Accordingly we created a new

GPI cell line in which expressed residues 1-260 in order that we could investigate the possible effect on phage antibody binding.

Surprisingly the results showed a dramatic change in phage-antibody binding. For the first time we were able to demonstrate different M22 phage constructs could bind to the TSHR in this form. The results suggested that the hypothesis was correct and regions of the receptor distal to the LRR domain were in some way preventing access of phage-antibodies to the target epitope. This was an important breakthrough and for the first time should allow the use of the new cell line to selectively enrich phage antibody libraries for TSHR antibodies.

Chapter 6 described our efforts to pursue a radically different approach to phage-antibody enrichment. Having encountered significant problems in our attempts to bind M22 phage constructs to the TSH receptor in various forms we designed an alternative approach that moved away from the direct use of TSH receptor as a selective surface. Having made recombinant M22 antibody, and verified its properties, we decided to exploit this resource more fully than simply using it as a control reagent. Access to the clonal TSAb enabled us to produce an anti-idiotypic antibody against M22 that would specifically recognise the antigen-binding CDR domains. We immunised a series of mice with recombinant M22 scFv and were able to produce a significant immune response. We selected scFv for this experiment rather than Fab as the variable CDR domains represent a greater proportion of total protein in scFv and would assist in restricting the murine immune response to the desired target. We synthesised a phage antibody library from the immunised mouse spleens and successfully enriched an anti-idiotypic monoclonal antibody that recognised human TSAb M22. Using ELISA we were able to confirm the specificity of this reagent, and went on to demonstrate that the antibody could indeed bind the M22 CDR regions and block binding of the human TSAb to the TSHR. To our knowledge this is the first time an anti-idiotypic antibody has been raised to a human TSAb and should prove an invaluable reagent for future studies.

Future Work

- Use the new CHO/TSHR260 cell line to selectively enrich antibody libraries generated from Graves' patients and animal models of Graves' disease and recover novel examples of thyroid stimulatory antibodies.
- Investigate the use of the anti-idiotypic antibody ID-43 to stain circulating patient B cells and identify those producing antibodies with similar CDR regions. These will be recovered and studied for thyroid stimulating activity.
- Study the ability of ID-43 to neutralise the stimulating activity of a range of Graves' patient sera. This would allow us to estimate the frequency of "M22-like" TSAbs in a large number of Graves' patients, and provide a measure of TSAbs diversity.

8 References

References

- Adams, D. D., Purves H.D. (1956). "Abnormal responses in the assay of thyrotropins." Proc Univ Otago Sch Med **34**: 11-12.
- Adams, D. D. and H. D. Purves (1956). "The assessment of thyroid function by tracer tests with radioactive iodine." New Zealand Medical Journal **55**(305): 36-41.
- Ajjan, R. A., C. Findlay, et al. (1998). "The modulation of the human sodium iodide symporter activity by Graves' disease sera." J Clin Endocrinol Metab **83**(4): 1217-1221.
- Amoroso, A., P. Garzia, et al. (1997). "Hashimoto's thyroiditis associated with urticaria and angio-oedema: disappearance of cutaneous and mucosal manifestations after thyroidectomy." J Clin Pathol **50**: 254-256.
- Ando, T., M. Imaizumi, et al. (2003). "Induction of thyroid-stimulating hormone receptor autoimmunity in hamsters." Endocrinology **144**(2): 671-680.
- Antonelli, A., M. Rotondi, et al. (2005). "Increase of interferon-gamma inducible alpha chemokine CXCL10 but not beta chemokine CCL2 serum levels in chronic autoimmune thyroiditis." Eur J Endocrinol **152**(2): 171-177.
- Arcott, P., E. D. Rosen, et al. (1992). "Immunoreactivity to Yersinia enterocolitica antigens in patients with autoimmune thyroid disease." J Clin Endocrinol Metab **75**: 295-300.
- Badenhoop, K., G. Schwarz, et al. (1992). "Tumor necrosis factor beta gene polymorphisms in Graves' disease." J Clin Endocrinol Metab **74**: 287-291.
- Baker, G., G. Mazziotti, et al. (2005). "Reevaluating thyrotropin receptor-induced mouse models of graves' disease and ophthalmopathy." Endocrinology **146**(2): 835-844.

- Barbas, C. (1991). "Combinatorial immunoglobulin libraries on the surface of phage (Phabs): Rapid selection of antigen-specific Fabs." Methods: A companion to Methods in Enzymology **2**: 119-127.
- Barbas, C. F., 3rd, A. S. Kang, et al. (1991). "Assembly of combinatorial antibody libraries on phage surfaces: the gene III site." Proc Natl Acad Sci U S A **88**: 7978-7982.
- Barbas, C. F., 3rd, A. S. Kang, et al. (1991). "Assembly of combinatorial antibody libraries on phage surfaces: the gene III site." Proc Natl Acad Sci U S A **88**(18): 7978-7982.
- Bartels, E. D. (1941). Heredity in Graves' disease. Copenhagen, Denmark, Munksgaard.
- Berger, M., V. Shankar, et al. (2002). "Therapeutic applications of monoclonal antibodies." Am J Med Sci **324**: 14-30.
- Better, M., C. P. Chang, et al. (1988). "Escherichia coli secretion of an active chimeric antibody fragment." Science **240**: 1041-1043.
- Boas, M., U. Feldt-Rasmussen, et al. (2012). "Thyroid effects of endocrine disrupting chemicals." Mol Cell Endocrinol **355**(2): 240-248.
- Bogdanos, D. P., D. S. Smyk, et al. (2012). "Twin studies in autoimmune disease: genetics, gender and environment." J Autoimmun **38**(2-3): J156-169.
- Bradford, M. M. (1976). "A rapid and sensitive method for the quantitation of microgram quantities of protein utilizing the principle of protein-dye binding." Anal Biochem **72**: 248-254.
- Braley-Mullen, H. and S. Yu (2000). "Early requirement for B cells for development of spontaneous autoimmune thyroiditis in NOD.H-2h4 mice." J Immunol **165**(12): 7262-7269.
- Burton, D. R. and C. F. Barbas, 3rd (1994). "Human antibodies from combinatorial libraries." Adv Immunol **57**: 191-280.

- Cabilly, S., A. D. Riggs, et al. (1984). "Generation of antibody activity from immunoglobulin polypeptide chains produced in *Escherichia coli*." Proc Natl Acad Sci U S A **81**: 3273-3277.
- Chazenbalk, G. D., J. C. Jaume, et al. (1997). "Engineering the human thyrotropin receptor ectodomain from a non-secreted form to a secreted, highly immunoreactive glycoprotein that neutralizes autoantibodies in Graves' patients' sera." J Biol Chem **272**(30): 18959-18965.
- Chen, C. R., P. Pichurin, et al. (2003). "The thyrotropin receptor autoantigen in Graves disease is the culprit as well as the victim." J Clin Invest **111**(12): 1897-1904.
- Christoph, T. and U. Krawinkel (1989). "Physical linkage of variable, diversity and joining gene segments in the immunoglobulin heavy chain locus of the mouse." Eur J Immunol **19**: 1521-1523.
- Ciampolillo, A., V. Marini, et al. (1989). "Retrovirus-like sequences in Graves' disease: implications for human autoimmunity." Lancet **1**: 1096-1100.
- Coles, A. J., M. Wing, et al. (1999). "Pulsed monoclonal antibody treatment and autoimmune thyroid disease in multiple sclerosis." Lancet **354**: 1691-1695.
- Costagliola, S., L. Alcalde, et al. (1994). "Overexpression of the extracellular domain of the thyrotrophin receptor in bacteria; production of thyrotrophin-binding inhibiting immunoglobulins." J Mol Endocrinol **13**(1): 11-21.
- Costagliola, S., N. G. Morgenthaler, et al. (1999). "Second generation assay for thyrotropin receptor antibodies has superior diagnostic sensitivity for Graves' disease." J Clin Endocrinol Metab **84**(1): 90-97.
- Costagliola, S., P. Rodien, et al. (1998). "Genetic immunization against the human thyrotropin receptor causes thyroiditis and allows production of monoclonal antibodies recognizing the native receptor." J Immunol **160**(3): 1458-1465.
- Costagliola, S. and G. Vassart (2002). "Monoclonal antibodies with thyroid stimulating activity, at last." Thyroid **12**(12): 1039-1041.

- Czarnocka, B., J. Ruf, et al. (1985). "[Antigenic relation between thyroid peroxidase and the microsomal antigen implicated in auto-immune diseases of the thyroid]." C R Acad Sci III **300**(15): 577-580.
- Da Costa, C. R. and A. P. Johnstone (1998). "Production of the thyrotrophin receptor extracellular domain as a glycosylphosphatidylinositol-anchored membrane protein and its interaction with thyrotrophin and autoantibodies." J Biol Chem **273**(19): 11874-11880.
- Dalan, R. and M. K. Leow (2012). "Immune manipulation for Graves' disease: re-exploring an unfulfilled promise with modern translational research." Eur J Intern Med **23**(8): 682-691.
- Davies, T. F. (2008). "Infection and autoimmune thyroid disease." J Clin Endocrinol Metab **93**(3): 674-676.
- de Forteza, R., C. U. Smith, et al. (1994). "Visualization of the thyrotropin receptor on the cell surface by potent autoantibodies." J Clin Endocrinol Metab **78**(5): 1271-1273.
- de Lloyd, A., J. Bursell, et al. (2010). "TSH receptor activation and body composition." J Endocrinol **204**(1): 13-20.
- de Luis, D. A., C. Varela, et al. (1998). "Helicobacter pylori infection is markedly increased in patients with autoimmune atrophic thyroiditis." J Clin Gastroenterol **26**: 259-263.
- DeGroot, L. J. and J. Quintans (1989). "The causes of autoimmune thyroid disease." Endocr Rev **10**: 537-562.
- Dinareello, C. A. (1991). "Interleukin-1 and interleukin-1 antagonism." Blood **77**: 1627-1652.
- Ditzel, H. J., Y. Masaki, et al. (2000). "Cloning and expression of a novel human antibody-antigen pair associated with Felty's syndrome." Proc Natl Acad Sci U S A **97**: 9234-9239.

- Edwards, J. C. and G. Cambridge (2006). "B-cell targeting in rheumatoid arthritis and other autoimmune diseases." Nat Rev Immunol **6**(5): 394-403.
- El Fassi, D., C. H. Nielsen, et al. (2007). "B lymphocyte depletion with the monoclonal antibody rituximab in Graves' disease: a controlled pilot study." J Clin Endocrinol Metab **92**(5): 1769-1772.
- Endo, K., K. Kasagi, et al. (1978). "Detection and properties of TSH-binding inhibitor immunoglobulins in patients with Graves' disease and Hashimoto's thyroiditis." J Clin Endocrinol Metab **46**(5): 734-739.
- Eschler, D. C., A. Hasham, et al. (2011). "Cutting edge: the etiology of autoimmune thyroid diseases." Clin Rev Allergy Immunol **41**(2): 190-197.
- Fan, Q. R. and W. A. Hendrickson (2005). "Structure of human follicle-stimulating hormone in complex with its receptor." Nature **433**(7023): 269-277.
- Fountoulakis, S. and A. Tsatsoulis (2004). "On the pathogenesis of autoimmune thyroid disease: a unifying hypothesis." Clin Endocrinol (Oxf) **60**(4): 397-409.
- Fox, K. M., J. A. Dias, et al. (2001). "Three-dimensional structure of human follicle-stimulating hormone." Mol Endocrinol **15**(3): 378-389.
- Franklyn, J. A. and K. Boelaert (2012). "Thyrotoxicosis." Lancet **379**(9821): 1155-1166.
- Garrity, J. A. and R. S. Bahn (2006). "Pathogenesis of graves ophthalmopathy: implications for prediction, prevention, and treatment." American Journal of Ophthalmology **142**(1): 147-153.
- Ghosh, P., M. Amaya, et al. (1995). "The structure of an intermediate in class II MHC maturation: CLIP bound to HLA-DR3." Nature **378**(6556): 457-462.
- Gilbert, J. A., S. Salehi, et al. (2004). "Contrasting properties of induced hyperthyroidism with thyrotropin receptor DNA delivery by adenovirus or

immunogenic liposomes." Proc 30th Annual Meeting of the European Thyroid Association, Istanbul, 2004. Turkish J Endocrinol Metab **8**(27).

Graus, Y. F., M. H. de Baets, et al. (1997). "Human anti-nicotinic acetylcholine receptor recombinant Fab fragments isolated from thymus-derived phage display libraries from myasthenia gravis patients reflect predominant specificities in serum and block the action of pathogenic serum antibodies." J Immunol **158**: 1919-1929.

Gripenberg, M., A. Miettinen, et al. (1978). "Humoral immune stimulation and anti-epithelial antibodies in Yersinia infection." Arthritis Rheum **21**: 904-908.

Guo, T., Y. Huo, et al. (2013). "Genetic association between IL-17F gene polymorphisms and the pathogenesis of Graves' Disease in the Han Chinese population." Gene **512**(2): 300-304.

Hamidi, S., C. R. Chen, et al. (2011). "Relationship between thyrotropin receptor hinge region proteolytic posttranslational modification and receptor physiological function." Mol Endocrinol **25**(1): 184-194.

Harfst, E., A. P. Johnstone, et al. (1992). "The use of the amplifiable high-expression vector pEE14 to study the interactions of autoantibodies with recombinant human thyrotrophin receptor." Mol Cell Endocrinol **83**(2-3): 117-123.

Harfst, E., A. P. Johnstone, et al. (1992). "Characterization of the extracellular region of the human thyrotrophin receptor expressed as a recombinant protein." J Mol Endocrinol **9**(3): 227-236.

Harfst, E., M. S. Ross, et al. (1994). "Production of antibodies to the human thyrotropin receptor and their use in characterising eukaryotically expressed functional receptor." Mol Cell Endocrinol **102**(1-2): 77-84.

Hasemann, C. A. and J. D. Capra (1990). "High-level production of a functional immunoglobulin heterodimer in a baculovirus expression system." Proc Natl Acad Sci U S A **87**: 3942-3946.

- Hasham, A. and Y. Tomer (2012). "Genetic and epigenetic mechanisms in thyroid autoimmunity." Immunol Res **54**(1-3): 204-213.
- Hasselbalch, H. C. (2003). "B-cell depletion with rituximab-a targeted therapy for Graves' disease and autoimmune thyroiditis." Immunol Lett **88**(1): 85-86.
- Hennecke, F., C. Krebber, et al. (1998). "Non-repetitive single-chain Fv linkers selected by selectively infective phage (SIP) technology." Protein Eng **11**(5): 405-410.
- Hexham, J. M., J. Furmaniak, et al. (1992). "Cloning of a human autoimmune response: preparation and sequencing of a human anti-thyroglobulin autoantibody using a combinatorial approach." Autoimmunity **12**: 135-141.
- Hexham, J. M., L. J. Partridge, et al. (1994). "Cloning and characterisation of TPO autoantibodies using combinatorial phage display libraries." Autoimmunity **17**: 167-179.
- Hexham, J. M., L. J. Partridge, et al. (1994). "Cloning and characterisation of TPO autoantibodies using combinatorial phage display libraries." Autoimmunity **17**(3): 167-179.
- Hexham, J. M., M. A. Persson, et al. (1991). "Cloning and expression of a human thyroglobulin autoantibody." Autoimmunity **11**: 69-70.
- Hiatt, A., R. Cafferkey, et al. (1989). "Production of antibodies in transgenic plants." Nature **342**: 76-78.
- Hoekman, K., B. M. von Blomberg-van der Flier, et al. (1991). "Reversible thyroid dysfunction during treatment with GM-CSF." Lancet **338**: 541-542.
- Holliger, P. and H. Bohlen (1999). "Engineering antibodies for the clinic." Cancer Metastasis Rev **18**: 411-419.
- Hoogenboom, H. R., J. T. Lutgerink, et al. (1999). "Selection-dominant and nonaccessible epitopes on cell-surface receptors revealed by cell-panning with a large phage antibody library." Eur J Biochem **260**(3): 774-784.

- Hoogenboom, H. R. and G. Winter (1992). "By-passing immunisation. Human antibodies from synthetic repertoires of germline VH gene segments rearranged in vitro." J Mol Biol **227**: 381-388.
- Huang, G. C., M. J. Page, et al. (1993). "The thyrotrophin hormone receptor of Graves' disease: overexpression of the extracellular domain in insect cells using recombinant baculovirus, immunoaffinity purification and analysis of autoantibody binding." J Mol Endocrinol **10**(2): 127-142.
- Huse, W. D., L. Sastry, et al. (1989). "Generation of a large combinatorial library of the immunoglobulin repertoire in phage lambda." Science **246**: 1275-1281.
- Iyer, S. and R. Bahn (2012). "Immunopathogenesis of Graves' ophthalmopathy: The role of the TSH receptor." Best Practice & Research Clinical Endocrinology & Metabolism **26**(3): 281-289.
- Janeway, C. A. and P. Travers (1997). "Immunobiology." 3rd ed. Current Biology Ltd, London.
- Jaume, J. C., A. Kakinuma, et al. (1997). "Thyrotropin receptor autoantibodies in serum are present at much lower levels than thyroid peroxidase autoantibodies: analysis by flow cytometry." J Clin Endocrinol Metab **82**(2): 500-507.
- Jaume, J. C., S. Portolano, et al. (1994). "Molecular cloning and characterization of genes for antibodies generated by orbital tissue-infiltrating B-cells in Graves' ophthalmopathy." J Clin Endocrinol Metab **78**: 348-352.
- Jiang, X., H. Liu, et al. (2012). "Structure of follicle-stimulating hormone in complex with the entire ectodomain of its receptor." Proc Natl Acad Sci U S A **109**(31): 12491-12496.
- Johnstone, A. P., J. C. Cridland, et al. (1994). "Monoclonal antibodies that recognize the native human thyrotropin receptor." Mol Cell Endocrinol **105**(2): R1-9.
- Kaithamana, S., J. Fan, et al. (1999). "Induction of experimental autoimmune Graves' disease in BALB/c mice." J Immunol **163**(9): 5157-5164.

- Kamath, C., M. A. Adlan, et al. (2012). "The role of thyrotrophin receptor antibody assays in graves' disease." J Thyroid Res **2012**: 525936.
- Kang, A., R. Burton, et al. (1991). "Combinatorial immunoglobulin library in phage lambda." Methods: A companion to Methods in Enzymology **2**: 111.
- Kimura, H., M. Kimura, et al. (2005). "Expression of class II major histocompatibility complex molecules on thyrocytes does not cause spontaneous thyroiditis but mildly increases its severity after immunization." Endocrinology **146**(3): 1154-1162.
- Knappik, A. and A. Pluckthun (1994). "An improved affinity tag based on the FLAG peptide for the detection and purification of recombinant antibody fragments." Biotechniques **17**(4): 754-761.
- Ko, Y. G. and G. A. Thompson, Jr. (1995). "Purification of glycosylphosphatidylinositol-anchored proteins by modified triton X-114 partitioning and preparative gel electrophoresis." Anal Biochem **224**(1): 166-172.
- Kobe, B. and A. V. Kajava (2001). "The leucine-rich repeat as a protein recognition motif." Curr Opin Struct Biol **11**(6): 725-732.
- Kodama, K., H. Sikorska, et al. (1984). "Use of monoclonal antibodies to investigate a possible role of thyroglobulin in the pathogenesis of Graves' ophthalmopathy." J Clin Endocrinol Metab **59**(1): 67-73.
- Kohler, G. and C. Milstein (1975). "Continuous cultures of fused cells secreting antibody of predefined specificity." Nature **256**(5517): 495-497.
- Kotsa, K., P. F. Watson, et al. (1997). "A CTLA-4 gene polymorphism is associated with both Graves disease and autoimmune hypothyroidism." Clin Endocrinol **46**: 551-554.

- Krebber, A., S. Bornhauser, et al. (1997). "Reliable cloning of functional antibody variable domains from hybridomas and spleen cell repertoires employing a reengineered phage display system." J Immunol Methods **201**(1): 35-55.
- Kreisler, A., J. de Seze, et al. (2003). "Multiple sclerosis, interferon beta and clinical thyroid dysfunction." Acta Neurol Scand **107**: 154-157.
- Laemmli, U. K. (1970). "Cleavage of structural proteins during the assembly of the head of bacteriophage T4." Nature **227**(5259): 680-685.
- Lapthorn, A. J., D. C. Harris, et al. (1994). "Crystal structure of human chorionic gonadotropin." Nature **369**(6480): 455-461.
- Latif, R., K. Michalek, et al. (2010). "A tyrosine residue on the TSH receptor stabilizes multimer formation." PLoS One **5**(2): e9449.
- Lazarus, J. H. (1998). "The effects of lithium therapy on thyroid and thyrotropin-releasing hormone." Thyroid **8**: 909-913.
- Lenzner, C. and N. G. Morgenthaler (2003). "The effect of thyrotropin-receptor blocking antibodies on stimulating autoantibodies from patients with Graves' disease." Thyroid **13**(12): 1153-1161.
- Li, T., K. D. Janda, et al. (1994). "Antibody catalyzed cationic cyclization." Science **264**: 1289-1293.
- Libert, F., A. Lefort, et al. (1989). "Cloning, sequencing and expression of the human thyrotropin (TSH) receptor: evidence for binding of autoantibodies." Biochem Biophys Res Commun **165**(3): 1250-1255.
- Low, M. G. (1989). "Glycosyl-phosphatidylinositol: a versatile anchor for cell surface proteins." FASEB J **3**(5): 1600-1608.
- Ludgate, M., S. Costagliola, et al. (1992). "Recombinant TSH-receptor for determination of TSH-receptor-antibodies." Exp Clin Endocrinol **100**(1-2): 73-74.

- Lum, L. G., E. Burns, et al. (1990). "IgG anti-tetanus toxoid antibody synthesis by human bone marrow. I. Two distinct populations of marrow B cells and functional differences between marrow and peripheral blood B cells." J Clin Immunol **10**: 255-264.
- Luo, G., J. L. Fan, et al. (1993). "Immunization of mice with *Yersinia enterocolitica* leads to the induction of antithyrotropin receptor antibodies." J Immunol **151**: 922-928.
- Marino, M., R. Ricciardi, et al. (1997). "Mild clinical expression of myasthenia gravis associated with autoimmune thyroid diseases." J Clin Endocrinol Metab **82**: 438-443.
- Mariotti, S., E. L. Kaplan, et al. (1980). Circulating thyroid antigen antibody immune complexes. Proceedings of the Eighth International Thyroid Congress, Sydney, Australia, February 3-8.
- Matsuura, N., Y. Yamada, et al. (1980). "Familial neonatal transient hypothyroidism due to maternal TSH-binding inhibitor immunoglobulins." N Engl J Med **303**(13): 738-741.
- McCafferty, J., A. D. Griffiths, et al. (1990). "Phage antibodies: filamentous phage displaying antibody variable domains." Nature **348**: 552-554.
- McIntosh, R. S., M. S. Asghar, et al. (1997). "Analysis of immunoglobulin G kappa antithyroid peroxidase antibodies from different tissues in Hashimoto's thyroiditis." J Clin Endocrinol Metab **82**(11): 3818-3825.
- McIntosh, R. S., M. S. Asghar, et al. (1996). "Cloning and analysis of IgG kappa and IgG lambda anti-thyroglobulin autoantibodies from a patient with Hashimoto's thyroiditis: evidence for in vivo antigen-driven repertoire selection." J Immunol **157**(2): 927-935.

- McIntosh, R. S., N. Tandon, et al. (1994). "Cloning and analysis of IgM anti-thyroglobulin autoantibodies from patients with Hashimoto's thyroiditis." Biochim Biophys Acta **1227**(3): 171-176.
- McIntosh, R. S., P. F. Watson, et al. (1997). "Analysis of the T cell receptor V alpha repertoire in Hashimoto's thyroiditis: evidence for the restricted accumulation of CD8+ T cells in the absence of CD4+ T cell restriction." J Clin Endocrinol Metab **82**: 1140-1146.
- McIntosh, R. S. and A. P. Weetman (1997). "Molecular analysis of the antibody response to thyroglobulin and thyroid peroxidase." Thyroid **7**(3): 471-487.
- McKenzie, J. M. (1958). "The bioassay of thyrotropin in serum." Endocrinology **63**(3): 372-382.
- McKenzie, J. M. (1958). "Delayed thyroid response to serum from thyrotoxic patients." Endocrinology **62**(6): 865-868.
- McLachlan, S. M., Y. Nagayama, et al. (2005). "Insight into Graves' hyperthyroidism from animal models." Endocr Rev **26**(6): 800-832.
- McLachlan, S. M. and B. Rapoport (1996). "Monoclonal, human autoantibodies to the TSH receptor--the Holy Grail and why are we looking for it?" J Clin Endocrinol Metab **81**(9): 3152-3154.
- McLachlan, S. M. and B. Rapoport (2013). "Thyrotropin-blocking autoantibodies and thyroid-stimulating autoantibodies: potential mechanisms involved in the pendulum swinging from hypothyroidism to hyperthyroidism or vice versa." Thyroid **23**(1): 14-24.
- Meek, J. C., A. E. Jones, et al. (1964). "CHARACTERIZATION OF THE LONG-ACTING THYROID STIMULATOR OF GRAVES' DISEASE." Proc Natl Acad Sci U S A **52**: 342-349.

- Metcalf, R., N. Jordan, et al. (2002). "Demonstration of immunoglobulin G, A, and E autoantibodies to the human thyrotropin receptor using flow cytometry." J Clin Endocrinol Metab **87**(4): 1754-1761.
- Michalek, K., S. A. Morshed, et al. (2009). "TSH receptor autoantibodies." Autoimmun Rev **9**(2): 113-116.
- Michelangeli, V. P., D. S. Munro, et al. (1994). "Measurement of thyroid stimulating immunoglobulins in a new cell line transfected with a functional human TSH receptor (JPO9 cells), compared with an assay using FRTL-5 cells." Clin Endocrinol (Oxf) **40**(5): 645-652.
- Mochizuki, H., K. Nakamura, et al. (2011). "Multiplex PCR and Genescan analysis to detect immunoglobulin heavy chain gene rearrangement in feline B-cell neoplasms." Vet Immunol Immunopathol **143**(1-2): 38-45.
- Nagataki, S., Y. Shibata, et al. (1994). "Thyroid diseases among atomic bomb survivors in Nagasaki." Jama **272**: 364-370.
- Nagayama, Y., K. D. Kaufman, et al. (1989). "Molecular cloning, sequence and functional expression of the cDNA for the human thyrotropin receptor." Biochem Biophys Res Commun **165**(3): 1184-1190.
- Nagayama, Y., M. Kita-Furuyama, et al. (2002). "A novel murine model of Graves' hyperthyroidism with intramuscular injection of adenovirus expressing the thyrotropin receptor." J Immunol **168**(6): 2789-2794.
- Nanba, T., M. Watanabe, et al. (2009). "Increases of the Th1/Th2 cell ratio in severe Hashimoto's disease and in the proportion of Th17 cells in intractable Graves' disease." Thyroid **19**(5): 495-501.
- Neuberger, M. S. (1983). "Expression and regulation of immunoglobulin heavy chain gene transfected into lymphoid cells." Embo J **2**: 1373-1378.
- Neuberger, M. S. and C. Milstein (1995). "Somatic hypermutation." Curr Opin Immunol **7**: 248-254.

- Neumann, S., B. M. Raaka, et al. (2009). "Human TSH receptor ligands as pharmacological probes with potential clinical application." Expert Rev Endocrinol Metab **4**(6): 669.
- Nicholson, L. B., H. Vlase, et al. (1996). "Monoclonal antibodies to the human TSH receptor: epitope mapping and binding to the native receptor on the basolateral plasma membrane of thyroid follicular cells." J Mol Endocrinol **16**(2): 159-170.
- Nielsen, C. H., L. Hegedus, et al. (2004). "Autoantibodies in autoimmune thyroid disease promote immune complex formation with self antigens and increase B cell and CD4+ T cell proliferation in response to self antigens." Eur J Immunol **34**(1): 263-272.
- Nielsen, C. H., R. G. Leslie, et al. (2001). "Natural autoantibodies and complement promote the uptake of a self antigen, human thyroglobulin, by B cells and the proliferation of thyroglobulin-reactive CD4(+) T cells in healthy individuals." Eur J Immunol **31**(9): 2660-2668.
- Nunez Miguel, R., J. Sanders, et al. (2009). "Thyroid stimulating autoantibody M22 mimics TSH binding to the TSH receptor leucine rich domain: a comparative structural study of protein-protein interactions." J Mol Endocrinol **42**(5): 381-395.
- Ochi, Y. and L. J. DeGroot (1969). "Vitiligo in Graves' disease." Ann Intern Med **71**: 935-940.
- Ochi, Y., Y. Kajita, et al. (2012). "A novel hypothesis for the etiology of Graves' disease: TSAb may be thyroid stimulating animal IgG-like hormone and TBAb may be the precursor of TSAb." Med Hypotheses **78**(6): 781-786.
- Onaya, T., M. Kotani, et al. (1973). "New in vitro tests to detect the thyroid stimulator in sera from hyperthyroid patients by measuring colloid droplet formation and cyclic AMP in human thyroid slices." J Clin Endocrinol Metab **36**(5): 859-866.

- Orgiazzi, J., D. E. Williams, et al. (1976). "Human thyroid adenyl cyclase-stimulating activity in immunoglobulin G of patients with Graves' disease." J Clin Endocrinol Metab **42**(2): 341-354.
- Orlandi, R., D. H. Gussow, et al. (1989). "Cloning immunoglobulin variable domains for expression by the polymerase chain reaction." Proc Natl Acad Sci U S A **86**: 3833-3837.
- Pan, Y., S. C. Yuhasz, et al. (1995). "Anti-idiotypic antibodies: biological function and structural studies." FASEB J **9**(1): 43-49.
- Parmley, S. F. and G. P. Smith (1988). "Antibody-selectable filamentous fd phage vectors: affinity purification of target genes." Gene **73**: 305-318.
- Paschke, R., J. Van Sande, et al. (1996). "The TSH receptor and thyroid diseases." Baillieres Clin Endocrinol Metab **10**(1): 9-27.
- Pastan, I., J. Roth, et al. (1966). "Binding of hormone to tissue: the first step in polypeptide hormone action." Proc Natl Acad Sci U S A **56**(6): 1802-1809.
- Patton, W. F., M. R. Dhanak, et al. (1989). "Differential partitioning of plasma membrane proteins into the triton X-100-insoluble cytoskeleton fraction during concanavalin A-induced receptor redistribution." J Cell Sci **92** (Pt 1): 85-91.
- Paul, W. E. (2003). Immunoglobulins and B lymphocytes. Fundamental Immunology. Philadelphia, Lippincott Williams and Wilkins: 47-68.
- Persani, L., M. Tonacchera, et al. (1993). "Measurement of cAMP accumulation in Chinese hamster ovary cells transfected with the recombinant human TSH receptor (CHO-R): a new bioassay for human thyrotropin." J Endocrinol Invest **16**(7): 511-519.
- Persson, M. A., R. H. Caothien, et al. (1991). "Generation of diverse high-affinity human monoclonal antibodies by repertoire cloning." Proc Natl Acad Sci U S A **88**: 2432-2436.

- Petersen, V. B., P. J. Dawes, et al. (1977). "The interaction of thyroid-stimulating antibodies with solubilised human thyrotrophin receptors." FEBS Lett **83**(1): 63-67.
- Pichurin, P., X. M. Yan, et al. (2001). "Naked TSH receptor DNA vaccination: A TH1 T cell response in which interferon-gamma production, rather than antibody, dominates the immune response in mice." Endocrinology **142**(8): 3530-3536.
- Portolano, S., G. D. Chazenbalk, et al. (1992). "Recognition by recombinant autoimmune thyroid disease-derived Fab fragments of a dominant conformational epitope on human thyroid peroxidase." J Clin Invest **90**: 720-726.
- Portolano, S., P. Seto, et al. (1991). "A human Fab fragment specific for thyroid peroxidase generated by cloning thyroid lymphocyte-derived immunoglobulin genes in a bacteriophage lambda library." Biochem Biophys Res Commun **179**: 372-377.
- Posch, P. E., H. A. Araujo, et al. (1995). "Microvariation creates significant functional differences in the DR3 molecules." Hum Immunol **42**(1): 61-71.
- Preziati, D., L. La Rosa, et al. (1995). "Autoimmunity and thyroid function in patients with chronic active hepatitis treated with recombinant interferon alpha-2a." Eur J Endocrinol **132**: 587-593.
- Prummel, M. F. and P. Laurberg (2003). "Interferon-alpha and autoimmune thyroid disease." Thyroid **13**: 547-551.
- Rapoport, B. and R. J. Adams (1978). "Bioassay of TSH using dog thyroid cells in monolayer culture." Metabolism **27**(12): 1732-1742.
- Rapoport, B., G. D. Chazenbalk, et al. (1998). "The thyrotrophin (TSH) receptor: interaction with TSH and autoantibodies." Endocr Rev **19**(6): 673-716.
- Rapoport, B. and S. M. McLachlan (2001). "Thyroid autoimmunity." J Clin Invest **108**(9): 1253-1259.

- Rapoport, B., S. M. McLachlan, et al. (1996). "Critical relationship between autoantibody recognition and thyrotropin receptor maturation as reflected in the acquisition of complex carbohydrate." J Clin Endocrinol Metab **81**(7): 2525-2533.
- Rees Smith, B., S. M. McLachlan, et al. (1988). "Autoantibodies to the thyrotropin receptor." Endocr Rev **9**(1): 106-121.
- Retter, I., H. H. Althaus, et al. (2005). "VBASE2, an integrative V gene database." Nucleic Acids Res **33**(Database issue): D671-674.
- Romagnani, P., M. Rotondi, et al. (2002). "Expression of IP-10/CXCL10 and MIG/CXCL9 in the thyroid and increased levels of IP-10/CXCL10 in the serum of patients with recent-onset Graves' disease." Am J Pathol **161**(1): 195-206.
- Rose, N. R., R. Bonita, et al. (2002). "Iodine: an environmental trigger of thyroiditis." Autoimmun Rev **1**(1-2): 97-103.
- Rose, N. R. and E. Witebsky (1956). "Studies on organ specificity. V. Changes in the thyroid glands of rabbits following active immunization with rabbit thyroid extracts." J Immunol **76**(6): 417-427.
- Sanders, J., D. Y. Chirgadze, et al. (2007). "Crystal structure of the TSH receptor in complex with a thyroid-stimulating autoantibody." Thyroid **17**(5): 395-410.
- Sanders, J., M. Evans, et al. (2008). "A human monoclonal autoantibody to the thyrotropin receptor with thyroid-stimulating blocking activity." Thyroid **18**(7): 735-746.
- Sanders, J., M. Evans, et al. (2003). "Human monoclonal thyroid stimulating autoantibody." Lancet **362**(9378): 126-128.
- Sanders, J., J. Jeffreys, et al. (2004). "Characteristics of a human monoclonal autoantibody to the thyrotropin receptor: sequence structure and function." Thyroid **14**(8): 560-570.

- Sanders, J., J. Jeffreys, et al. (2002). "Thyroid-stimulating monoclonal antibodies." Thyroid **12**(12): 1043-1050.
- Sanders, J., B. R. Smith, et al. (2004). Antibody for the thyrotropin receptor and uses thereof, Rsr Ltd
- Sanders, JFurmaniak, JSmith, BR. **WO2004050708 A2**.
- Sanders, P., S. Young, et al. (2011). "Crystal structure of the TSH receptor (TSHR) bound to a blocking-type TSHR autoantibody." J Mol Endocrinol **46**(2): 81-99.
- Scott, J. K. and G. P. Smith (1990). "Searching for peptide ligands with an epitope library." Science **249**: 386-390.
- Seetharamaiah, G. S., R. K. Desai, et al. (1993). "Induction of TSH binding inhibitory immunoglobulins with the extracellular domain of human thyrotropin receptor produced using baculovirus expression system." Autoimmunity **14**(4): 315-320.
- Seetharamaiah, G. S., N. M. Wagle, et al. (1995). "Generation and characterization of monoclonal antibodies to the human thyrotropin (TSH) receptor: antibodies can bind to discrete conformational or linear epitopes and block TSH binding." Endocrinology **136**(7): 2817-2824.
- Shimojo, N., Y. Kohno, et al. (1996). "Induction of Graves-like disease in mice by immunization with fibroblasts transfected with the thyrotropin receptor and a class II molecule." Proc Natl Acad Sci U S A **93**(20): 11074-11079.
- Shu, L., C. F. Qi, et al. (1993). "Secretion of a single-gene-encoded immunoglobulin from myeloma cells." Proc Natl Acad Sci U S A **90**: 7995-7999.
- Simmonds, M. J. and S. C. Gough (2011). "The search for the genetic contribution to autoimmune thyroid disease: the never ending story?" Brief Funct Genomics **10**(2): 77-90.

- Simons, G. F., R. N. Konings, et al. (1981). "Genes VI, VII, and IX of phage M13 code for minor capsid proteins of the virion." Proc Natl Acad Sci U S A **78**: 4194-4198.
- Skerra, A. and A. Pluckthun (1988). "Assembly of a functional immunoglobulin Fv fragment in Escherichia coli." Science **240**: 1038-1041.
- Smith, B. R. (2003). "Human monoclonal thyroid stimulating autoantibody." Lancet **362**(july 12).
- Smith, B. R. and R. Hall (1981). "Measurement of thyrotropin receptor antibodies." Methods Enzymol **74 Pt C**: 405-420.
- Smith, B. R., J. Sanders, et al. (2009). "TSH receptor - autoantibody interactions." Horm Metab Res. 2009 Jun;**41**(6):448-5 **41**(6): 448-455.
- Smith, G. P. (1985). "Filamentous fusion phage: novel expression vectors that display cloned antigens on the virion surface." Science **228**: 1315-1317.
- Song, Y. H., Y. Li, et al. (1996). "The nature of autoantigens targeted in autoimmune endocrine diseases." Immunol Today **17**(5): 232-238.
- Sospedra, M., X. Ferrer-Francesch, et al. (1998). "Transcription of a broad range of self-antigens in human thymus suggests a role for central mechanisms in tolerance toward peripheral antigens." J Immunol **161**: 5918-5929.
- Spitzweg, C., W. Joba, et al. (1999). "Expression of thyroid-related genes in human thymus." Thyroid **9**: 133-141.
- Stiens, L. R., H. Buntmeyer, et al. (2000). "Development of serum-free bioreactor production of recombinant human thyroid stimulating hormone receptor." Biotechnol Prog **16**(5): 703-709.
- Sun, P. D. and D. R. Davies (1995). "The cystine-knot growth-factor superfamily." Annu Rev Biophys Biomol Struct **24**: 269-291.

- Swain, M. S., T. and Mohanty, BK (2005). "AUTOIMMUNE THYROID DISORDERS - AN UPDATE." Indian Journal of Clinical Biochemistry **20**(1): 9-17.
- Szkudlinski, M. W., V. Fremont, et al. (2002). "Thyroid-stimulating hormone and thyroid-stimulating hormone receptor structure-function relationships." Physiol Rev **82**(2): 473-502.
- Takai, O., R. K. Desai, et al. (1991). "Prokaryotic expression of the thyrotropin receptor and identification of an immunogenic region of the protein using synthetic peptides." Biochem Biophys Res Commun **179**(1): 319-326.
- Tang, D. C., M. DeVit, et al. (1992). "Genetic immunization is a simple method for eliciting an immune response." Nature **356**(6365): 152-154.
- Toccafondi, R. S., S. Aterini, et al. (1980). "Thyroid-stimulating antibody (TSab) detected in sera of Graves' patients using human thyroid cell cultures." Clin Exp Immunol **40**(3): 532-539.
- Tomer, Y. (2010). "Genetic susceptibility to autoimmune thyroid disease: past, present, and future." Thyroid **20**(7): 715-725.
- Tomer, Y. and T. F. Davies (1993). "Infection, thyroid disease, and autoimmunity." Endocr Rev **14**: 107-120.
- Tomer, Y., A. Hasham, et al. (2013). "Fine mapping of loci linked to autoimmune thyroid disease identifies novel susceptibility genes." J Clin Endocrinol Metab **98**(1): E144-152.
- Tunbridge, W. M., D. C. Evered, et al. (1977). "The spectrum of thyroid disease in a community: the Whickham survey." Clinical Endocrinology **7**(6): 481-493.
- Unal, H., R. Jagannathan, et al. (2012). "Mechanism of GPCR-directed autoantibodies in diseases." Adv Exp Med Biol **749**: 187-199.

- Van Der Heijden, J. H., T. W. De Bruin, et al. (1999). "Limitations of the semisynthetic library approach for obtaining human monoclonal autoantibodies to the thyrotropin receptor of Graves' disease." Clin Exp Immunol **118**(2): 205-212.
- Wanzeck, K., K. L. Boyd, et al. (2011). "Glycan Shielding of the Influenza Virus Hemagglutinin Contributes to Immunopathology in Mice." American Journal of Respiratory and Critical Care Medicine **183**(6): 767-773.
- Webber, K. O., Y. Reiter, et al. (1995). "Preparation and characterization of a disulfide-stabilized Fv fragment of the anti-Tac antibody: comparison with its single-chain analog." Mol Immunol **32**: 249-258.
- Weetman, A., F. Creagh, et al. (1981). "Lithium increases immunoglobulin and thyroid autoantibody production. *Annales Endocrinologie* 42, A45."
- Weetman, A. P. (1991). Autoimmune endocrine disease. Cambridge, Cambridge University Press.
- Weetman, A. P. (1996). Infection and endocrine autoimmunity. Microorganisms and autoimmune diseases H. Friedman, Rose, N.R. and Bendinelli, M: 257-275.
- Weetman, A. P. (2003). "Autoimmune thyroid disease: propagation and progression." Eur J Endocrinol **148**: 1-9.
- Weetman, A. P. (2010). "Diseases associated with thyroid autoimmunity: explanations for the expanding spectrum." Clinical Endocrinology.
- Weetman, A. P., P. G. Byfield, et al. (1990). "IgG heavy-chain subclass restriction of thyrotropin-binding inhibitory immunoglobulins in Graves' disease." Eur J Clin Invest **20**(4): 406-410.
- Weetman, A. P. and A. M. McGregor (1984). "Autoimmune thyroid disease: developments in our understanding." Endocr Rev **5**(2): 309-355.
- Weetman, A. P. and A. M. McGregor (1994). "Autoimmune thyroid disease: further developments in our understanding." Endocr Rev **15**: 788-830.

- Weetman, A. P., A. M. McGregor, et al. (1984). "Extrathyroidal sites of autoantibody synthesis in Graves' disease." Clin Exp Immunol **56**(2): 330-336.
- Weetman, A. P., M. E. Yateman, et al. (1990). "Thyroid-stimulating antibody activity between different immunoglobulin G subclasses." J Clin Invest **86**(3): 723-727.
- Welti, H. (1968). "Skin manifestations associated with severe forms of Basedow's disease." Bull Schweiz Akad Med Wiss **23**: 476-482.
- White, R. G., B. H. Bass, et al. (1961). "Lymphadenoid goitre and the syndrome of systemic lupus erythematosus." Lancet **1**: 368-373.
- Williams, R. C., Jr., N. J. Marshall, et al. (1988). "Kappa/lambda immunoglobulin distribution in Graves' thyroid-stimulating antibodies. Simultaneous analysis of C lambda gene polymorphisms." J Clin Invest **82**(4): 1306-1312.
- Wood, C. R., M. A. Boss, et al. (1985). "The synthesis and in vivo assembly of functional antibodies in yeast." Nature **314**: 446-449.
- Wood, C. R., A. J. Dorner, et al. (1990). "High level synthesis of immunoglobulins in Chinese hamster ovary cells." J Immunol **145**: 3011-3016.
- Yamashita, K. and J. B. Field (1970). "Preparation of thyroid plasma membranes containing a TSH-responsive adenyl cyclase." Biochem Biophys Res Commun **40**(1): 171-178.
- Yamazaki, K., K. Tanigawa, et al. (2010). "Iodide-induced chemokines and genes related to immunological function in cultured human thyroid follicles in the presence of thyrotropin." Thyroid **20**(1): 67-76.
- Yanagawa, T., Y. Hidaka, et al. (1995). "CTLA-4 gene polymorphism associated with Graves' disease in a Caucasian population." J Clin Endocrinol Metab **80**: 41-45.
- Yoshida, A., I. Hisatome, et al. (2009). "Pendrin is a novel autoantigen recognized by patients with autoimmune thyroid diseases." J Clin Endocrinol Metab **94**(2): 442-448.

Zaghouani, H., R. Steinman, et al. (1993). "Presentation of a viral T cell epitope expressed in the CDR3 region of a self immunoglobulin molecule." Science **259**: 224-227.

Zophel, K., D. Roggenbuck, et al. (2010). "TSH receptor antibody (TRAb) assays based on the human monoclonal autoantibody M22 are more sensitive than bovine TSH based assays." Horm Metab Res **42**(1): 65-69.